SUSTAINABLE BIOREFINERY SCHEMES FOR THE RECOVERY OF ENERGY, MATERIAL AND NUTRIENT OF RESIDUAL BIOMASS

Documento elaborado por

Mónica Liliana Amado Villamizar

UNIVERSIDAD EAN

FACULTA DE INGENIERÍA

SUSTAINABLE BIOREFINERY SCHEMES FOR THE RECOVERY OF ENERGY, MATERIAL AND NUTRIENT OF RESIDUAL BIOMASS

AUTOR:

MONICA LILIANA AMADO VILLAMIZAR

DIRECTOR:

PHD JEFFREY LEÓN PULIDO

BOGOTÁ, D.C, 15 DE NOVIEMBRE DE 2021

Agradecimientos

Agradezco a Dios por esta oportunidad, de crecimiento profesional y personal, por ser mi luz y mi guía.

A mi familia, por ser mi apoyo día a día, a mi padre por ser mi soporte incondicional.

A mis amigos y compañeros, por sus oraciones, por ser mi compañía durante este proceso.

A la Universidad EAN por el apoyo en tiempo y confianza para mi crecimiento profesional.

A mis directores nacionales e internacionales por ser guía y corrección en mi proceso de investigación.

A mis evaluadores por el tiempo para la lectura del documento y mejora en la calidad de su entrega.

Abstract

Agricultural activities are a constant source of residual biomass that does not usually have an added value during the harvesting activities or throughout the raw material processing industry, which affect the environment where these activities are carried out. Residual biomass from the livestock sector (manure) and the agricultural sector (transient and permanent crops) has a high pollutant related to biodegradable organic matter. Colombian economy must evolve to tackle an exit from oil. Biofuels are then an alternative to diminish the dependence in the fossil fuels industry. Additionally, it has been shown that the use of biofuels decreases the negative environmental impact, thus making biorefineries viable. Using waste from agriculture as a main source for bioenergy recovery can contribute to the problem of treating and valorizing them.

The objective of this PhD thesis is to assess the energy recovery potential of three residual biomasses produced in Colombia (coffee mucilage, cocoa mucilage, and swine manure), and to contribute to the development of sustainable biorefineries based on the treatment and valorization of these three residual biomasses. The chosen processes to recover energy from these wastes are the biological processes of anaerobic co-digestion (AD) or dark fermentation (DF). However, the exploitations of these processes are limited by the efficiency of the use of the substrates and the economic recovery of the initial investments. For this reason, it is more striking to complete the conversion with the design of a refinery that takes advantage of the products and byproducts in a complete way. The methodology approach for the biorefinery schemes construction was based on the bibliographic review for processes refining and the development of a super structure. Followed by the process selection according to the input requirements (stream conditions). Process simulation, PINCH analysis evaluation and life cycle analysis were used as evaluation tools for the finally proposed schemes, with methane as a reference, hydrogen and methanol are targeted.

Due to the territorial heterogeny of available substrate, modeling of those processes is done locally, then aggregates at a national scale. The rough potential for the country is then evaluated to 155 ktoe. Overall, biogas production performances of AD and DF processes improve by increasing coffee mucilage/swine manure and/or cocoa mucilage/swine manure ratios of the feed, and by increasing organic load from 2 to 26 $gCOD \cdot l^{-1}$. The results also

indicate that the local availability of different types of residual biomass represents the most influential parameter in assessing the energy recovery potential in Colombia. Subsequently, a Life Cycle Assessment along with an evaluation of the energy balance establish the sustainability of the proposed schemes. The results show energy efficiencies between 37% and 55%, above all it is shown that the total energy supply of the biorefineries is possible with the products obtained and additionally digestate rich in useful elements for the agricultural processes are produced. According to the LCA, the strongest environmental impact is caused on the damage to ecosystems. Overall, the environmental impact of methane, hydrogen and methanol per kg produced are equal or lower than current processes when the schemes are designed including energy integration methodologies and PINCH analysis. Furthermore, it shows the importance of energy and mass integration to increase energy efficiencies and decrease environmental impacts on biorefinery schemes. Efficiencies are quite closed whatever the final product chose, nevertheless CO_2 emission are strongly decreases when methanol production is considered.

Keywords: Biorefinery, Biomass, Anaerobic Digestion, Dark fermentation, Simulation.

Acknowlegements

The authors acknowledge financial support from Minciencias (Ministry of Science, Technology and Innovation of Colombia) - Project number FP44842-38-2017 - – contract 038-2017

Research projects, ONTARE Group, research management. EAN University
Facultad de Ingeniería, Universidad EAN, Bogotá D.C., Colombia

Aix Marseille Univ, CNRS, Centrale Marseille, M2P2, Marseille, France

TABLE OF CONTENTS

LIST OF FIGURES

LIST OF TABLES

GENERAL INTRODUCTION

Nowadays, the development of engineering has been forced to use its efforts and knowledge in the fulfillment of the Sustainable Development Objectives (SDG) proposed by the United Nation in 2015[1]. One of the topics of interest has been energy generation and consumption due to the fact that between 1990 and 2018 the total primary energy supply and total CO_2 emissions have increased by 63%, and although the population has increased significantly, the ratio has not been the same, increasing CO_2 emissions per capita by 14%. Only in 2018 the final worldwide energy consumption was almost 25,000 Mtoe. One of the alternatives is the development and implementation of alternative energies and although the supply of these has increased in recent years, the gap between renewable energies and the supply of non-renewable energies continues to increase annually. However, Colombia's energy exploitation and production currently consists of 93% of primary resources of fossil origin, approximately 4% of hydropower and 3% of biomass, according to the Colombian energy balance (BECO) for 2020[2]. Diversification in the energy matrix has motivated government entities to generate alternative energy projects, including solar, wind, hydro, and the use of residual biomass.

Worldwide, it is estimated that up to one third of food for human consumption is discarded, generating waste from the cultivation of the raw material to its commercialization. In recent years, awareness of re-utilization of these residual biomasses has increased in different areas due to the low cost, high availability, and the need to reduce the impact that they can cause to the environment. Several technologies can be applied to recover energy and/or materials from residual biomasses, including biological (e.g. anaerobic digestion, fermentation) and thermochemical (e.g. gasification, pyrolysis, combustion) processes. Selection of the most suitable valorization process primarily depends on the production amount and on the composition of the residual biomasses. Residual biomass generation depends mainly on the position of each country with respect to average income, gross domestic product, and population consumption, since these influence the amount and type of

[1] https://www.undp.org/sustainable-development-goals
[2] https://www1.upme.gov.co/InformacionCifras/Paginas/BalanceEnergetico.aspx

consumption. In countries such as Colombia, Ecuador, Paraguay, India, Mexico, and Panama, residual biomass is generated mainly from agricultural activities, due to the high economic activity in this sector. According to National Administrative Department of Statistics of 2020 (DANE), agricultural sector has increased by 6.8% compared to the previous year. This 6.8% growth is mainly due to the increase of specific activities such as fishing and aquaculture (31.5%), crops (8.6%), livestock (7.1%), and forestry and timber extraction (2.6%).

The objective of this PhD thesis is to assess the energy recovery potential of three residual biomasses produced in Colombia (coffee mucilage, cocoa mucilage, and swine manure), and to contribute to the development of sustainable biorefineries based on the treatment and valorization of these three residual biomasses. The chosen processes to recover energy from these wastes are the biological processes of anaerobic co-digestion or dark fermentation. However, the exploitations of these processes are limited by the efficiency of the use of the substrates and the economic recovery of the initial investments. For this reason, it is more striking to complete the conversion with the design of a refinery that takes advantage of the products and byproducts in a complete way. With methane as a reference, hydrogen and methanol are targeted.

Residual biomass such as cocoa and coffee mucilage have increased their production in recent years in all departments of Colombia, particularly coffee since it is one of the main economic activities. Therefore, their energy valorization potential is investigated in this study. In addition, cocoa and coffee mucilage usually present a high content of carbohydrates, which are suitable substrates for bioconversion processes that contribute to biogas generation. This study also considers another type of residual biomass, swine manure, which is also part of the increase in the agricultural sector. Swine manure usually presents a high alkalinity and high and protein contents that stabilize the operational conditions of the bioprocesses such as the carbon-nitrogen ratio and pH, this when it is used in co-digestion processes with other types or residual biomasses.

This work is linked to the project "Evaluation of routes for the use of residual biomass under the biorefinery scheme", funded by the Ministry of Science, Technology and Innovation of Colombia (COLCIENCIAS) through the call for proposals 745-2016. This COLCIENCIAS project aims to strengthen the development of Colombian agriculture through the design of biorefinery schemes that aim to maximize the residual biomass

valorization from the Colombian industry, being the biogas production the main product of the treatment.

This PhD thesis is organized in four chapters. Chapter I presents the state of the art on the development of three agricultural sectors (coffee, cocoa, and pig farming) in Colombia, the development of biological and thermochemical processes, and the design, implementation, and assessment of biorefinery scheme. Chapter II presents the materials and the methodologies used for the development of the simulation models, for the energy potential evaluation, and for the environmental and energy assessment of the different biorefinery schemes that were investigated. Chapter III presents the results of the development of biological models to simulate biogas production by anaerobic digestion and dark fermentation, as well as the biogas production potential by anaerobic digestion and dark fermentation of the available amounts of residual biomasses, this at the local departmental scale and at the national scale in Colombia. Then, Chapter IV presents an energy, environmental, and life cycle assessment analysis of the application of three different biorefinery schemes to the Colombian Department of Santander, thus according to its local biomass availability. The first biorefinery scheme that was investigated involves the production of biogas by anaerobic digestion and dark fermentation, followed by biogas purification by a biofilter. The second biorefinery scheme involves the production of biogas by anaerobic digestion and dark fermentation, followed by methane reforming to hydrogen gas. The third biorefinery scheme involves the production of biogas by anaerobic digestion and dark fermentation, followed by methane reforming to methanol. Finally, the document presents the general conclusions, the list of references and annexes.

CHAPTER I STATE OF THE ART

1.BIOMASS STATE OF THE ART

The literature identifies different types of biomass according to the different sources and/or production sectors. Their different composition hinders the replicability of the processes used for treatment and/or valorization, thus varying the final efficiencies. Moreover, the amount of residual biomass and the lack of studies and developments have made landfill the best biomass treatment option for developing countries in recent years. Although different categorizations are reported (Figure 1), they can be divided into forest products (wood, logging residues, trees, shrubs, sawdust, barks, roots, etc.), bio-renewable waste (agricultural waste, crop waste, urban wood, municipal and household solids), energy crops (grasses, starch, forage, oilseed, etc.), aquatic plants (algae, reed and rushes), food waste (grains, oil crops), sugar crops (sugar cane, molasses, sorghum), landfill, organic industrial waste, algae and mosses, and kelps and lichens. This variety puts biomass in fourth place as an energy resource worldwide (Demirbas, 2010).

Among these different biomass types, solid biomasses such as wood and municipal waste have long been used as a heat source through combustion. Animal biomass waste is excellent for biogas production, while solid forestry biomass waste is converted into liquid fuels such as ethanol and biodiesel (Kumar and Dixit, 2021). Also, the worldwide production of lignocellulose biomass is estimated as 1010 million tons. The lignocellulose materials (LCMs) include hardwoods, softwoods, residues from agricultural and forest activity as well as energy crops. LCMs demonstrate several advantages, namely, their lower price in comparison to that of traditional agricultural feedstock’s, not requiring arable land and fertilizers to grow, and not competing with food and feed sectors (Morais et al., 2015).

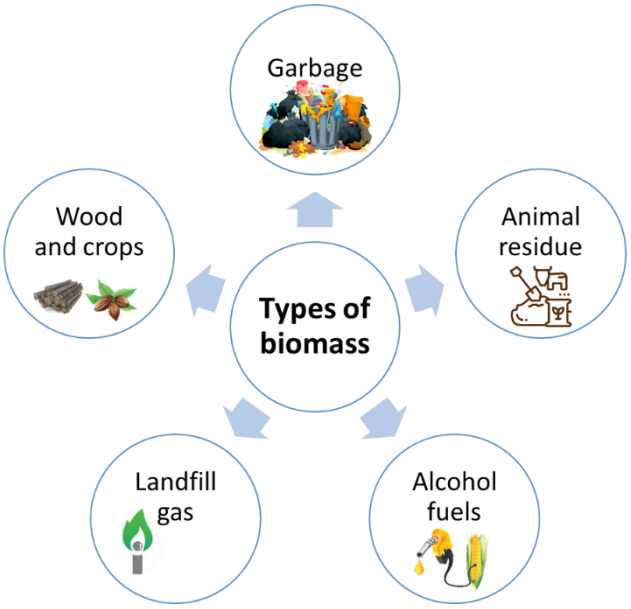

Figure 1 Different types of biomass from daily activities (Energy Information Administration (EIA), 2020). Reproduced from The National Energy Education Project (public domain).

Colombia is highly dependent on the hydrocarbon sector for the supply of energy and chemicals for industry. However, and in spite of its growth[3], the current situation shows an industry affected by: hydrocarbon prices, limiting production activities, the associated environmental impacts, and the processing requirements due to the decrease in the quality of the extracted hydrocarbons. Despite this, hydrocarbons continue to be the primary energy carriers used regardless of the country's efforts to produce biofuels. For example, according to the 2012 UPME report[4], the national exploitation and production of primary energy resources was based on 46% coal and 38% oil, and according to the Colombian energy balance (BECO) in 2020, the extraction of primary energy was mainly composed of oil (40.6%), coal (33.1%) and natural gas (16.7%). The use of biofuels in blending with fossil fuels has contributed to the reduction of environmental impact. The government currently allows blends of 8% bioethanol and 10% biodiesel[5]. On the other hand, the alternative of second-generation biofuels, based on the use of residual biomass, has been poorly developed. Although the production of organic waste in Colombia has been a latent problem due to the fact that agricultural activities are a fundamental part of the country's economy, the production of organic waste has been a major problem (DANE, 2020).

[3] http://www.sipg.gov.co/sipg/Home/Sectores/tabid/105/language/es%ADES/Default.aspx
[4] https://www1.upme.gov.co/InformesGestion/Informe_gestion_2012.pdf
[5] http://www.fedebiocombustibles.com/

1.1 Agriculture Colombian context

Colombian agriculture plays an important role in the economy's development, as it is the main source of income for rural areas, which account for 20% of the population. In addition, the percentage share of Colombian agriculture in the Gross Domestic Product (GDP) was 6.3% between 2011 and 2015. However, the globalization, Free Trade Agreements (FTAs), technological innovations, taxation and market restrictions have significantly slowed down agriculture. Colombia, being a developing country, has a lack of studies and developments in its agricultural processes, which generates two impacts. The first is that the production process costs are very high and therefore the products are not competitive at an international level. The second is the environmental impact generated by the processes due to the lack of rigorous waste treatment. One of the biggest problems is that due to the country's infrastructure it is not easy to access the entire territory to educate, develop and recover products and waste.

The generation of waste can be analyzed from three fundamental components: agricultural, livestock and organic waste from transportation, handling, and consumption of food. The amount of agricultural waste generated was around 1376 ton/day, the livestock sector (poultry, bovine and swine) produced an estimated 5166 ton/day and organic waste from market places, food supply centers and pruning of green areas generated an average of 344 ton/day (Humberto Escalante Hernández et al., 2011; Valderrama, 2013). Regarding the treatment of organic waste in Colombia until 2013, no major progress had been made in terms of integrated waste management due to the fact that the use and recovery of these wastes is deficient. On average, 65% of the organic waste generated is taken together with municipal solid waste (MSW) to a final disposal in landfills, leaving aside the implementation of techniques for the utilization of waste generated in the country. Some of the treatments used for the recovery of organic waste are composting where 49% of organic waste is used, 17% of waste is incinerated for thermochemical recovery, agronomic recovery with a share of 16%, vermiculture with a use of 13% and recycling with a use of 5%.

Despite weaknesses in technical and process development, since 2010, in Colombia, the National Administrative Department of Statistics (DANE) has reported an increase in different agro-industrial activities, which has improved the income and social benefits of the

national economy. According to DANE data (2018), coffee production increased from 0.64 to 0.86 Mton, cocoa production from 34.9 to 101 kton, and pork production from 0.23 to 0.41 Mton between 2011 and 2018 (Figure 2). In addition, according to recent figures from the Ministry of Agriculture, agricultural and agro-industrial exports grew 3.6% in September 2020. Just in September, sectoral exports reached a growth of 22%, marked by coffee, which compared to the same month of 2019, exported US$ 50 million more. This results in an increased production of residual biomass from these agro-industrial sectors (e.g. coffee and cocoa mucilage, and swine manure), residual biomass that requires treatment processes for biological stabilization and/or final disposal, which represent an over cost for the agro-industry.

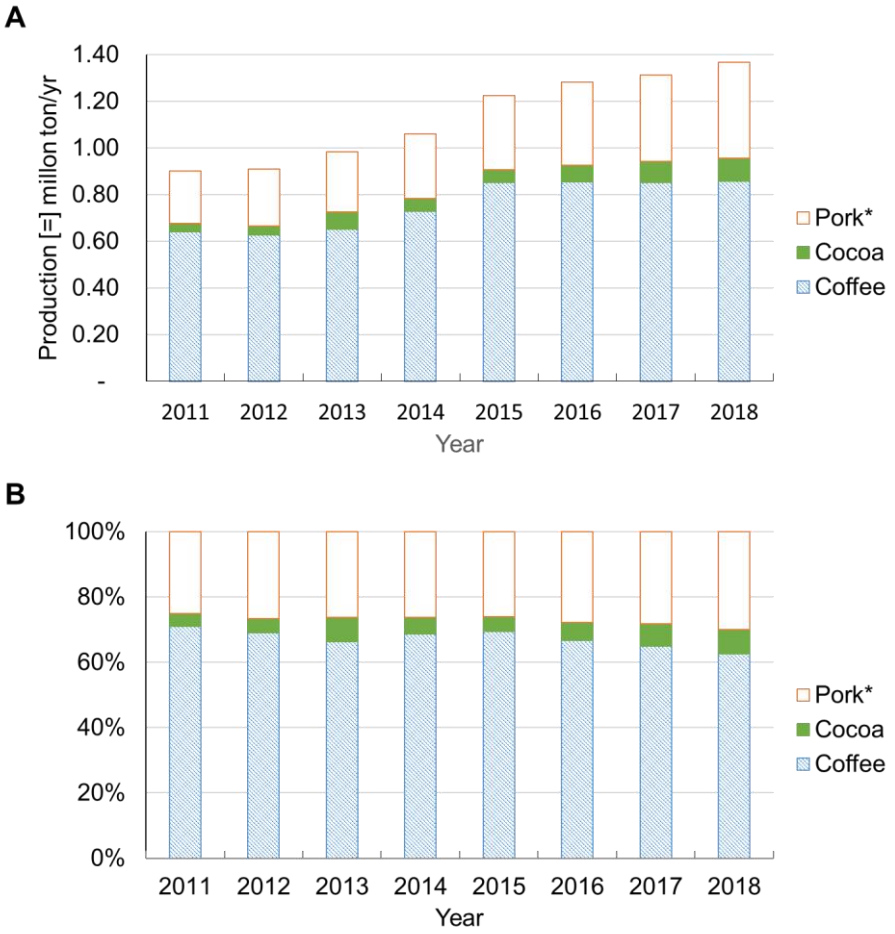

Figure 2 Colombian agro-industry production history. (A) Total production per year. (B) Relative production per year. Coffee and cocoa: Dry grains for sale. *Pork: Pork meat. Adapted from (DANE, 2020; “Fedecacao - Federación Nacional de Cacaoteros,” 2020; “Federación Nacional de cafeteros,” 2020).

The largest agricultural production is located in the Colombian massif, i. e., the region of the Andes mountain range, coffee crops are one of them. The Andean region (Center and

Southwest of the country) produces more than 800 thousand tons of coffee per year produced by three harvests. Table 1 shows that departments such as Tolima and Huila have increased their production between 50 and 150% equaling the production of the department with the highest production (Antioquia). Cocoa production is concentrated in the northeastern part of the country, mainly in the departments of Santander and Arauca, producing 50% of annual production (> 40 thousand tons). The department of Antioquia again stands out for its production, with 10% of the national production. Production in the rest of the country is homogeneously distributed, with Casanare being the department with the lowest production (78 tons/year). The departments of Atlántico, Archipielago de San Andres, Vichada, Amazonas, Guainía, and Vaupes do not report any production. The department of Chocó began reporting coffee and cocoa production as of 2018. Pig farming has developed mainly in the department of Antoquia, with 33% of the pig heads (according to the census of heads of pigs per year). The remaining 67% is evenly distributed in the rest of the country, with an average of 147,000 heads per year per department. The department of Vichada shows the lowest pig production (5351 heads per year according to the 2017 report).

Table 1 Annual agricultural production according to DANE 2017 report by activity

Department	**Cocoa Production (ton/yr)**	**Coffee production ton/yr**	**Swine heads heads/yr**
Antioquia	6073	195594	1733529
Arauca	9132	0	60400
Atlántico	0	0	156692
Bolívar	1248	208	109995
Boyacá	3889	6343	180082
Caldas	1079	102725	140193
Caquetá	368	1972	62655
Casanare	84	488	62642
Cauca	1288	76274	99679
Cesar	1867	3445	62230
Córdoba	6	0	367737
Cundinamarca	1201	14805	484888
Huila	4160	99387	140380
La Guajira	188	19	36129
Magdalena	900	15643	212130
Meta	2026	185	223237
Nariño	113	29251	141986
Norte de Santander	5039	9353	80213
Putumayo	447	0	30967
Quindío	0	22184	68578

Risaralda	36	66528	131529
Santander	28474	54203	92600
Sucre	3	10	213137
Tolima	3333	56468	77913
Valle del Cauca	178	75639	310392
Vichada	11	1	5351

1.1.1 Coffee

With an average annual production of 5.9 Mtons, coffee is one of the most marketed beverages in the world. It is mainly farmed in tropical areas, in particular in Brazil, and is consumed mainly in Europe and in the United States. Arabica (Coffee Arabica) and Robusta (Coffee Canephora) are the two varieties which are traded the most at an international level. Arabica fetches higher prices, due to its more favorable taste characteristics, and it makes up 61% of the world's production (C. von Enden and Calvert, 2010).

Colombia has the most extensive coffee production in the World, after Brazil, Vietnam and Indonesia in 2020[6]. From this crop the coffee mucilage can be separated by mechanical demucilagination of the ripe harvested beans using less water than the traditional separation process. Figure 3 below shows the content of chemical compounds in fresh (wet) coffee mucilage, obtained mechanically with 1.6 L of water per minute according to a study carried out by the National Coffee Research Center CENICAFE[7].

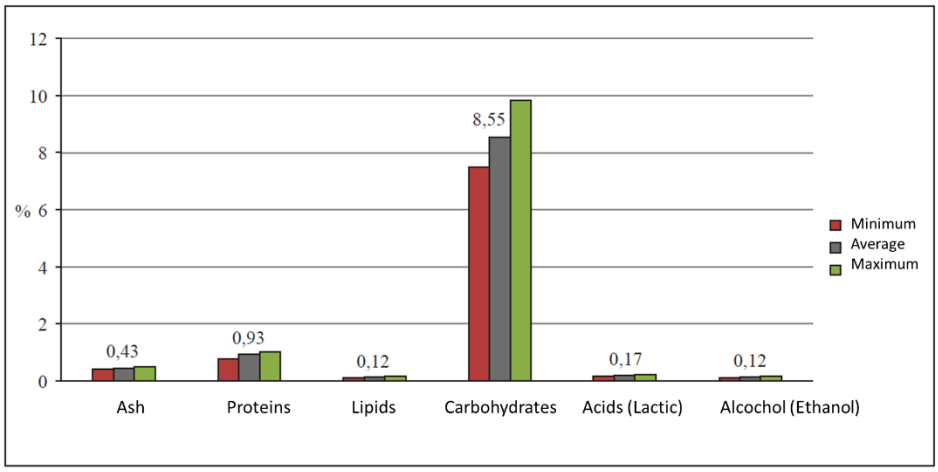

Figure 3 Coffee mucilage chemical composition. Wet basis (Puerta-Quintero and Ríos-Arias, 2011).

[6] https://federaciondecafeteros.org/
[7] https://www.cenicafe.org/

According to CENICAFE data, fresh mucilage has an average a water content of 89.1%. This indicates that it is a very wet fermentation substrate compared to other fermentation feedstock such as coffee pulp and sugarcane, which usually show a water content of 74.8-76.7% and 73 - 76%, respectively. After water, the main component of coffee mucilage is carbohydrate (average content of 8.55%). Neu et al. (2016) show in their study the characterization of two batches of Colombian coffee mucilage where the high content of sugars (Table 2) as well as the high water content (between 85-91%) are highlighted (Neu et al., 2016). Other sources stated a more detailed composition (w/w) of 84.2% water, 8.9% protein, 2.5% reducing sugars, 1.6% non-reducing sugars and 1.0% pectin (Clifford, 2012). Considering the above, it can be concluded that coffee mucilage is a residue rich in carbohydrates that can been used as organic substrate for biogas production, by fermentation and/or anaerobic digestion processes.

Table 2 Characterization of dry matter (DM), organic fraction of dry matter (oDM) and Kjeldahl-nitrogen (Kjeldahl-N), glucose, galactose/fructose/xylose (gal/fru/xyl), sucrose, lactic acid, phosphate (PO_4^{3-}), ammonium (NH_4^+) and sulphate (SO_4^{2-}) concentrations of mucilage substrates A and B (Neu et al., 2016).

Substrate	DM [%, w/w]	oDM [%, w/w]	Kjeldahl-N [g L^{-1}]	Glucose [g L^{-1}]	Gal/fru/xyl [g L^{-1}]	Sucrose [g L^{-1}]	Lactic acid [g L^{-1}]	PO_4^{3-} [g L^{-1}]	NH_4^+ [g L^{-1}]	SO_4^{2-} [g L^{-1}]
A	**7.5**	**94.1**	**0.8**	**21.5**	**27.8**	**10.8**	**N.D**	**0.06**	**0.05**	**0.99**
B	**6.2**	**96.4**	**0.9**	**21.7**	**28.2**	**3.1**	**2.9**	**0.06**	**0.02**	**0.14**

The coffee beans have to undergo several processing steps in order to remove the outer parts of the seed, i.e. skin (exopart), pulp (mesocarp), the mucilage layer and the endocarpal parchment (Figure 4). Coffee wastes are usually converted into pellets, which have a high Lower Heat Value (LHV = 18 $MJ \cdot Kg^{-1}TS$) and consequentially represent a very interesting source of renewable energy. The most important characteristics of coffee pellets are their Total Solid (TS) amount of about 90% w/w and high content of organic matter (Battista et al., 2016).

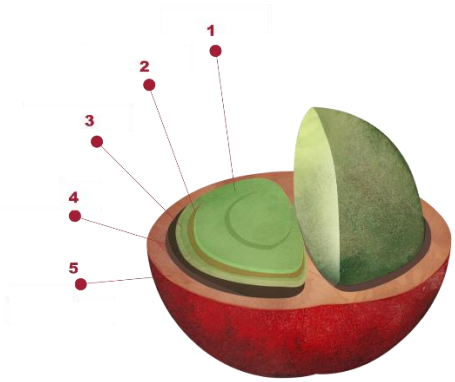

Figure 4 Anatomy of a coffee bean. 1- Bean (endosperm); 2-Silver skin (spermoderm); 3-Parchment (hull/endocarp); 4-Mucilage Pulp (mesocarp); 5-Outer skin (pericarp/exocarp) ("Federación Nacional de cafeteros," 2020)

Coffee crops typically have a main harvest period and a secondary harvest period with lower production. For this reason, it is important to highlight that although the total available residual biomass is known throughout the year, its availability varies over time. In the literature, most of the studies that have investigated coffee residue valorization by anaerobic digestion have worked with pulp or wastewater from the washing process of the fermentation stage, all have been directed towards the production of methane. Dinsdale et al. (1996) found that the mesophilic (30 – 40 °C) condition achieved a lipid removal of 87%, while the highest hemicellulose removal was achieved for the thermophilic (50 – 60 °C) condition (64%). Both temperature ranges reported a volatile solids removal of 58%. However, the composition of methane in the biogas was 65 - 70% under mesophilic and 64% under thermophilic conditions. The percentage of methane is due to the fact that in the bioprocess, CO_2 and H_2 are also produced, where H_2 corresponds to the remaining percentage in the biogas produced by the fermentation and/or homoacetogenesis reactions (Dinsdale et al., 1996). According to Chanakya and De Alwis (2004), methane production from coffee waste may vary from 0.25 to 0.5 $m^3 \cdot kg^{-1}$COD or substrate (Chanakya and De Alwis, 2004). Moreover, recent studies have found hydrogen potential production (77.6 mL $H_2 \cdot g^{-1}$COD) comparable with other substrates of interest such as vinasse and residues of the palm oil process (Hernández et al., 2014).

1.1.2 Cocoa

The fruit of the cocoa tree grows in Central and South America and in West Africa (Torres-Moreno et al., 2015). In Colombia the National Cacao Federation (FEDECACAO[8]) estimates that it will have reached a total area planted of approximately 155,000 hectares, with a production growth close to 26% being foreseen. Moreover, in 2017 in Colombia, 60535 tons of cocoa were produced reaching 6.6% more compared to the previous year. This indicates that it is urgent to propose concrete solutions to the management and recovery of waste coming from this sector, once it constitutes the main source of income for some 52,000 peasant families that derive their sustenance from it[9]. Cocoa residues have been fundamentally valued through the integration in the food chain of animal farms, nevertheless, information about evaluations of this raw material in the bioenergy industry are scarce (Aregheore, 2002; Donkoh et al., 1991; López, 2013).

The cocoa bean constitutes one third (33%) of the fruit weight, leaving in the back of 67% of the fruit as cocoa pod husk (CPH) as a waste by-product (Figure 5). In different words, ten lots of moist CPH are generated for every ton of dry cocoa beans, thereby representing a critical disposal hassle and an underexploited resource. The pod has been defined as an herbal laminated cloth such as 3 highly extraordinary layers: epicarp, mesocarp and endocarp (outer, center, and internal pericarp, respectively).

[8] https://www.fedecacao.com.co/
[9] https://www.finagro.com.co/

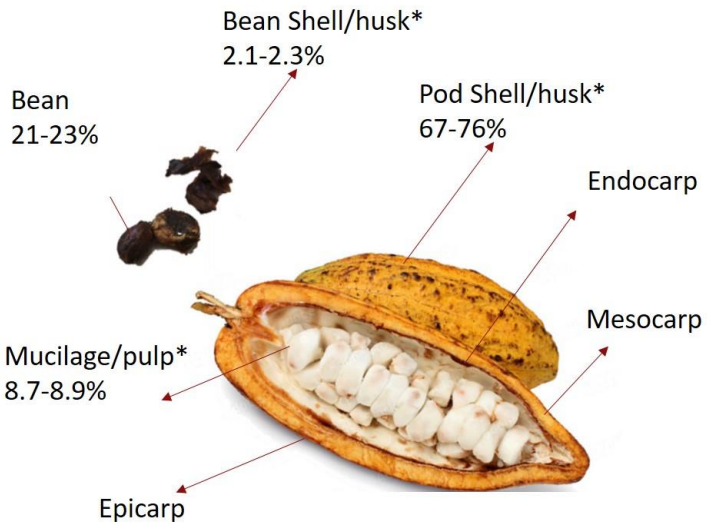

Figure 5 The cocoa fruit structures and wastes* (Campos-Vega et al., 2018).

The endocarp and mesocarp are degraded during the dehydration process of the cocoa bean, they are currently used as fertilizer. However, the mucilage can be recovered through the valorization of its components. The epicarp, mesocarp and endocarp had been analyzed for the chemical composition and compared to the entire cocoa pod husk and it is composed by a high share of ash (47% CPH), hemicellulose (50%), and minerals (K, Ca and P) (41–66%) predominated withinside the epicarp; fiber (44-48%) and cellulose (53%) withinside the mesocarp; protein (50%), crude fat (50%) and pectin (59%) withinside the endocarp. The epicarp changed into the maximum restricting part of CPH withinside the feeding trial, possibly because of the adversarial inhibitory impact of lignin and pectin on CPH usage in broiler diets (Campos-Vega et al., 2018).

Nigam and Singh (2014) show in their study that cocoa pulp is composed of a higher percentage of water and that the second representative compound is mono- and disaccharides (Table 3).

Table 3 Composition of fresh pulp from cocoa (Nigam and Singh, 2014)

Component	Fresh weight of pulp (%)
Water	82 – 86
Mono- and disaccharides	11 – 13
Plant cell-wall polymers	1.5 – 2.8
Proteins, peptides, and amino acids	0.64 – 0.74
Fat	0.35 – 0.75
Citrate	0.29 – 1.3
Trace metals, vitamins, ethanol, etc	Trace

Martínez et al. (2012) show a rigorous characterization of cocoa mucilage from two different locations in Ecuador (Table 4). The study again highlights the content of carbohydrates, which is higher than 67 g/100 g of dry matter) (Martínez et al., 2012). The high content in carbohydrates indicates that, in general, cocoa and cocoa residues are good substrate candidates for ethanol and/or biogas production by fermentation processes (Cinar et al., 2021; Nigam and Singh, 2014).

Table 4 Chemical composition of the different cocoa co-products (cocoa pod husks, cocoa bean shell, cocoa mucilage) (Mean ± SD) (Martínez et al., 2012).

Cocoa mucilage	Cone - Ecuador	Taura - Ecuador
Protein[a]	5.47 ± 0.12	5.56 ± 0.10
Ash[a]	7.51 ± 0.14	7.68 ± 0.18
Fat[a]	1.92 ± 0.06	1.91 ± 0.04
Carbohydrates[a]	68.35 ± 0.16	67.99 ± 0.14
Moisture[b]	9.64 ± 0.13	9.27 ± 0.17

a: g/100 g dry matter; b: g/100 g

1.1.3 Pig farming

The livestock sector in Colombia represents 76% of total agricultural activities, where 40% is the production of cattle, 40% of poultry, 10% of pigs and 10% of other activities. The large amount of residual biomass and the deficiency in its treatment can affect water bodies, soil and air in different ways. The country has a swine population of 5'327,460 animals, distributed in 234,883 farms (DANE, 2020). These animals are located mainly in the departments of Antioquia (32.5%), Cundinamarca (9.2%), Córdoba (6.9%), Valle del Cauca (5.8%), Meta (4.2%), Sucre and Magdalena (4%), where 66.7% of the national population is concentrated.

The pork production technification has allowed progress in the search for controls to improve the environmental aspect. As a result, the farms have different alternatives for the disposal, treatment and use of waste from pig farms. Some of them are irrigation systems of plots for the recovery of soils, composting and vermicomposting processes to produce organic fertilizer, and the reuse of the organic fraction for cattle and fish feed. The implementation of treatment processes to treat and valorize pig farm effluents includes also the use of lagoons (aerobicand/or anaerobic) to remove pathogens, and anaerobic digestion processes to recover biogas.

Animal manure has several environmental implications due to its disposal. These implications have prompted Government to search for techniques that may lead to "sustainable animal farming". Towards this transition, solutions that might help to convert manure into value-added marketable merchandise sound green and caring. As a biodegradable product, manure must now no longer be disposed of in landfills because it includes full-size degrees of nutrients and pathogens. Any unsuitable control of this precious waste can contaminate soil, air and water and additionally motive dangerous microbial build-up within side the environment. Among the best manure management practices which also contribute to sustainability is anaerobic digestion through which, simultaneous waste treatment and bio-energy production could be achieved (Neshat et al., 2017).

Some authors show the advantages and techniques for the treatment of the swine manure focused on biogas production (Astals et al., 2015, 2011; Neshat et al., 2017; Wang et al., 2018; Ye et al., 2013). Swine manure has a methane generation potential per volatile solid (VS) of 0.3 - 0.33 $L \cdot g^{-1}$ VS. Part of this production can focus on obtaining biohydrogen (H_2) during the first stages of degradation, taking advantage of the higher energy content of this vector per unit mass. The hydrogen volume fraction in the biogas produced during the degradation path is 0.26 – 0.33, which is equivalent to a theoretical output of 0.086 $L \cdot g^{-1}$ SV. However, at the end of the process the fraction of hydrogen is less, between 0.01 to 0.1, while the fraction of methane increases between 0.54 to 0.7 [10]. The previous results found by Hernández and Rodríguez (2013) during the evaluation of the operating parameters such as pH and retention time, were around 61.2 and 141.7 mL H_2 / g SV respectively (Hernández and Rodríguez, 2013). This production was comparable with other investigations that have

[10] https://www.porkcolombia.co/wp-content/uploads/2018/07/GUIA-AMBIENTAL-PORCICOLA-opt.pdf

investigated H_2 production potentials of complex organic wastes such as organic fraction of municipal solid waste and/or sewage sludge (Kim et al., 2004a, p.; Lay et al., 1999; Shin et al., 2004; Valdez-Vazquez et al., 2005).

Swine manure is composed of 45% urine and 55% feces, and this mixture usually increases the water content above 80%. This aspect, added to the presence of microorganisms and nutrients, causes spontaneous fermentation processes when the sample is not preserved (refrigeration). This residue has a high heterogeneity in the different physicochemical parameters: chemical oxygen demand (COD), total Kjeldahl nitrogen (NTK) and sulfides (Hansen et al., 1999). In contrast to mucilage's, swine manure has been studied and its characterization has been published in different studies and databases (Phyllis2, 2020; Shen et al., 2020; Wu et al., 2020; Zhang et al., 2021). Table 5 shows the summary (average, maximum, and minimum values) of the swine manure characterization reported in the literature and in the database. Swine manure has a high water content (greater than 90%). In addition, from the CHONS analysis, more than 0.5 wt% in dry material is from sulphur, an important inhibitor element for digestion and fermentation process. Furthermore, the values of calorific value are reported and can be compared with those calculated in models or simulations. Although the characterizations are published for the same country (Netherlands) they show great variety, most likely due to the feeding conditions, soil and age of the animals whose manure was analyzed. One of the elementary characterizations is highlighted (Sample #1084) which reports the percentage (wt% dry) of cellulose 16.6, lignin 1.6, protein 15.1 and total ash + biochemical 33.3. Also Wu et al. (2020) show values of 19.6 wt% hemicellulose, 12.1 wt% cellulose, 8.2 wt% lignin, 2.3 wt% crude lipids and 14.4 wt% crude protein (Wu et al., 2020).

Table 5 Swine manure characterization summary. Proximate analysis, ultimate analysis (macromolecules) and heating value (Phyllis2, 2020; Shen et al., 2020; Wu et al., 2020; Zhang et al., 2021).

		Average	Standar Desviation	Max	Min
Moisture content[a]	wt%	47.06	34.43	92.1	10.9
Ash content[a]	wt%	11.15	5.34	22.3	2.8
Volatile matter[a]	wt%	35.26	21.31	58.4	4.05
Fixed carbon[a]	wt%	8.71	8.23	19.12	1.05
Carbon[b]	wt%	39.31	4.81	45.7	31.04
Hydrogen[b]	wt%	4.77	1.06	6.45	1.72
Oxygen[b]	wt%	25.69	15.81	50.63	3.45
Nitrogen[b]	wt%	2.19	0.19	2.79	0.44
Sulphur[b]	wt%	0.54	0.30	0.94	0.36
Net calorific value (LHV) [b]	MJ/kg	15.87	2.68	17.86	12.83
Gross calorific value (HHV) [b]	MJ/kg	15.82	2.86	17.84	13.79
HHVMilne[b]	MJ/kg	15.86	1.36	17.19	14.47

[a] As received, the material in its original form (included ash and moisture); [b] The dry material (including ash)

1.2 Residual biomass availability

The following sections present an overview on coffee, cocoa and pig production in Colombia. Among the 26 Colombian departments considered in this study, 17 report coffee production more than twice higher than cocoa production (DANE, 2020). Only 7 departments (Bolívar, Córdoba, La Guajira, Meta, Arauca, Putumayo, and Vichada) show higher cocoa production than coffee production, and their total coffee production amounts are relatively low (< 210 tons of coffee/year) compared to the other departments (> 2000 tons of coffee/year). According to DANE data (2017), the departments of Huila, Cauca, Tolima, Caldas, and Antioquia generates 73% of the Colombian coffee production and they are therefore considered as the main Colombian coffee region. Additionally, their coffee production is more than 15 times higher than their cocoa production, thus indicating a much lower availability of cocoa mucilage rather than coffee mucilage (Figure 6).

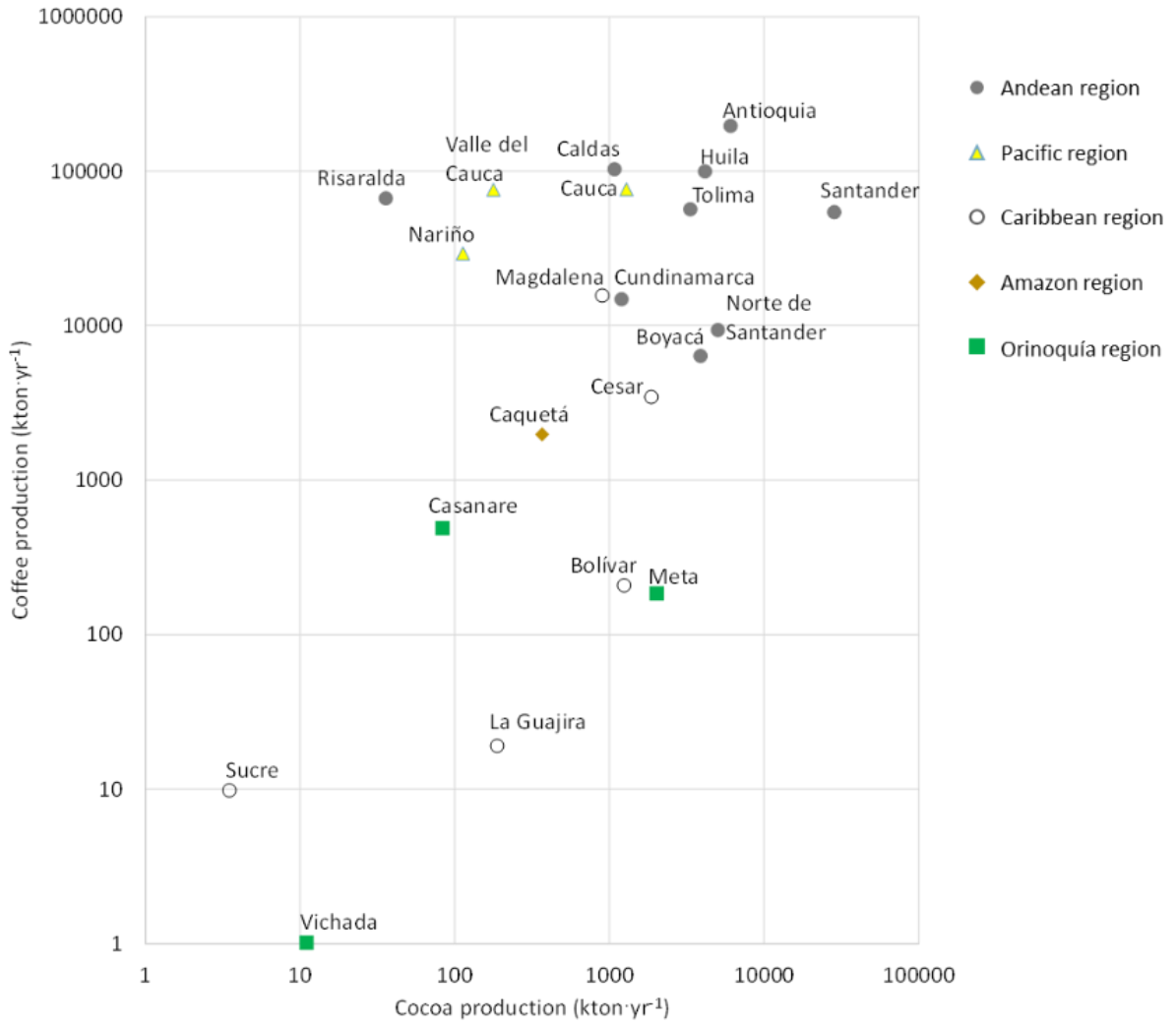

Figure 6 Coffee and cocoa production in 2017 (dried grains for sale)

Table 6 summarizes the coffee mucilage (CFM), cocoa mucilage (CCM), and swine manure (SM) availability data for 26 Colombian departments in 2017. Overall, the data indicates that CFM production dominates over CCM production in the center and south of the Andean region (Antioquia, Huila, Tolima, Caldas, Risaralda, Quindío), in the Pacific region (Chocó, Valle del Cauca, Nariño, Cauca), and more generally in the south-west of Colombia, whereas CCM production dominates over CFM production in the Orinoquía region (Arauca, Casanare, Meta, Vichada), in the Caribbean region (Atlántico, Bolívar, Córdoba, Sucre, La Guajira Cesar, Magdalena), in the north of the Andean region (Boyacá, Norte de Santander, Cundinamarca, Santander), and more generally in the north-east of Colombia. The Amazon

region does not show significant productions of CFM and CCM, with the only exception of the department of Caquetá.

Table 6 Total available amounts of CFM, CCM, and SM (wet mass) in 2017.

Department	CFM (ton)	CCM (ton)	SM (ton)	Ratio SM/total[b]
Antioquia	12790	959.5	1084000	0.987
Arauca	N.A.[a]	1443	37770	0.963
Atlántico	N.A.[a]	N.A.	97990	1.000
Bolívar	13.58	197.1	68790	0.997
Boyacá	414.8	614.4	112600	0.991
Caldas	6718	170.5	87670	0.927
Caquetá	128.9	58.10	39190	0.995
Casanare	31.90	13.19	39180	0.999
Cauca	4988	203.5	62340	0.923
Cesar	225.3	295.0	38920	0.987
Córdoba	N.A.[a]	0.980	229900	1.000
Cundinamarca	968.2	189.7	303300	0.996
Huila	6499	657.3	87790	0.925
La Guajira	1.240	29.74	22600	0.999
Magdalena	1023	142.2	132700	0.991
Meta	12.07	320.2	139600	0.998
Nariño	1913	17.90	88790	0.979
Norte de Santander	611.7	796.1	50170	0.973
Putumayo	N.A.[a]	70.57	19370	0.996
Quindío	1451	N.A.	42890	0.967
Risaralda	4351	5.680	82260	0.950
Santander	3545	4499	57910	0.878
Sucre	0.640	0.550	133300	1.000
Tolima	3693	526.6	48730	0.920
Valle del Cauca	4946	28.18	194100	0.975
Vichada	0.070	1.750	3347	0.999

[a] N.A. = not available data and/or no production reported.

[b] Mass ratio of available SM over the sum of available CFM, CCM, and SM.

SM availability per department in 2017 varies from 3347 ton (Vichada) to 1084000 ton (Antioquia). The mass ratio of available SM over the sum of available CFM, CCM, and SM

(SM/total) varies from 0.878 (Santander) to 1.000 (Atlántico), thus indicating a very larger availability of SM compared to CFM and CCM for all the departments (Figure 7).

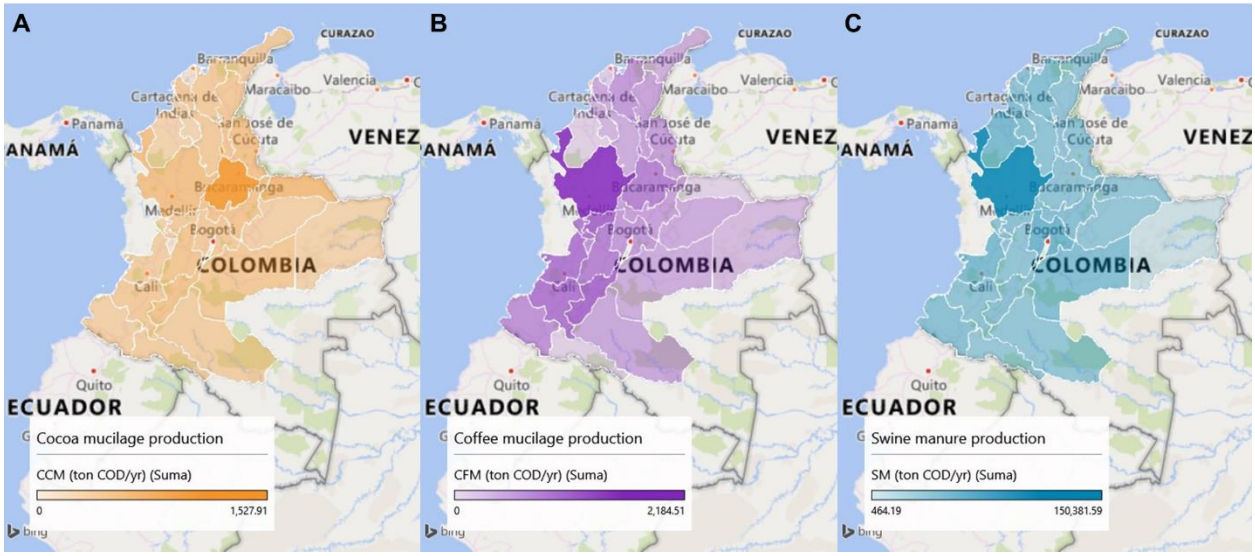

Figure 7 Colombia's available biomass distribution in 2017(A) Cocoa mucilage availability. (B) Coffee mucilage availability. (C) Swine manure availability (DANE, 2020).

1.3 Barriers to the development of biomass valorization processes

The use of residual biomass to produce second-generation biofuels has the advantage of the amount of feedstock available and, compared to first-generation biofuels, does not compete with food commodities. However, currently the biomass valorization processes have technical barriers to overcome. Indeed, the environmental cost-benefit analysis of the valorization processes is still weak due to the variability of the feedstock material, even with a high value of oil, the second-generation biofuels are still not cost competitive in the market, the development of biofuels still require further research and development of the processes. In conclusion, the valorization of residual biomass has technical, economic, capacity, safety, and governmental policy development barriers.

Recent studies show the importance of biochemical processes such as composting, vermicomposting, anaerobic digestion, and landfilling. Varjani et al. (2021) show that bioprocesses such as anaerobic digestion present less operational issues, less maintenance and low cost compared to the others biochemical conversion processes (composting, vermicomposting, and landfilling). However, the disadvantages are the high energy

requirement, the generation of unused by-products and the narrow range of temperature control (Varjani et al., 2021). Residual biomasses such as those from agriculture rich in carbohydrates have been exploited in bioprocesses, specifically in fermentation and digestion. While the application of agricultural biomass rich in lignin ranges from the generation of biofuels by processes such as gasification or pyrolysis to the production of chemicals, pulp, paper, and pharmaceuticals. Although there are studies in the literature on process optimization and improvement, recent studies pay attention on the integration of hydrothermal, thermochemical, physicochemical and bioprocesses to take the advantages of each treatment and increase the efficiency of biomass valorization.

There is no clear candidate for the best valorization route between biochemical and thermochemical processes, one of the reasons why recent studies focus on the development of their integration in biorefinery processes (Demirbas, 2010). Facilities that integrate biomass conversion processes and equipment to processed into plastics, chemical, fuel, heat, and power, as well as high-value components, for example essential oil drugs, or fibers, can be recovered as a preprocessing step with the remaining materials processed downstream.

2.BIOREFINERY STATE OF THE ART

Biorefineries are defined as a process (plant, concept, industrial processes) that is sustainable, as they seek to maximize economic costs, minimize environmental impact, reduce social aspects, replace fossil fuels, and close biomass processing cycles, thus by transformation, fractionation, biological and/or thermochemical conversion, separation and recovery of energy and non-energy resources that can be viable in the market, considering volume and price (IEA, 2021)[11].

The industrial revolution was brought to maturity by the development of combustion engines and the subsequent development of the fossil fuel and chemical industries. There is no turning back to the primitive way of life in the past. However, fossil energy and chemical sources are not unlimited. There is a critical need to return to current industry and human civilization in a sustainable path, and to continue to provide for human needs and requirements even with decreasing fossil reserves (S. Liu et al., 2012). Thus, the key is to develop biorefinery systems that efficiently convert biomass into a variety of products by means of flexible, efficient and zero-waste processes (Santamaría-Fernández et al., 2017). According to this, renewable energy sources are expected to play an important role in the supply of the future energy demand. In the quest for sustainable alternatives, the industry is experiencing a steady growth in the production of bio-based fuels and chemicals that are developing the emerging concept of biorefining (Geraili and Romagnoli, 2015).

The Brundtland report (NGO Committee on Education, 1987)[12] sparked the interest in sustainability by stating that "*sustainable development is development that meets the needs of the present without compromising the ability of future generations to meet their own needs*" (Arifin and Chien, 2008). The interpretation of sustainability remains a debatable subject even if definitions as the one presented above are widely accepted. This is largely related to:

[11] https://task42.ieabioenergy.com/
[12] https://sustainabledevelopment.un.org/content/documents/5987our-common-future.pdf

(1) The fact that environmental and economic aspects are quantitative, while social sustainability is often measured in qualitative terms.

(2) The flexibility of the sustainability concept, which is often reduced to subjective interpretations derived from the norms and values of individuals who seek to implement it (Palmeros Parada et al., 2017).

The biorefinery concept for biomass has been proposed in the literature as a fuel generation alternative, replacing fossil fuel sources through the biological or chemical conversion of different types of biomasses (organic residues, crops, etc.) into a broad plethora of bio-based products, such as fuels, chemicals, power and heat, among other (Banerjee et al., 2013; Gargalo et al., 2017).

A biorefinery should produce a spectrum of marketable products in order to maximize its economic sustainability and to aim for “zero waste”. A variety of different biorefinery configurations are being develop (Gargalo et al., 2017; Katakojwala and Mohan, 2021; Rajesh Banu et al., 2020a, 2020b). Biorefinery may be configured around a large volume product to maximize economies scales and to allow the successful utilization of all inputs with the integration of process operation. The processes that are linked in a biorefinery are the production of liquid or gaseous biofuels (bioprocesses or thermochemical processes), separation processes, purification or synthesis of new compounds. In all cases, biorefineries seek to adjust to the local context, waste minimization and energy integration to increase the production and energy efficiency of the biorefinery. The following sections (2.1 to 2.4) define the processes reported in the literature that are possible to integrate in the design of a biorefinery. In addition, results of Goffé and Ferrasse (2019) indicate that biomass conversion may achieve values between 70 and 80% of energy efficiency through the production of ethanol, syngas, methanol, and methane (Goffé and Ferrasse, 2019).

1.4 Bioprocesses

Bioprocesses have recently revolutionized the industry, as they are shown as an alternative chemical production process that presents energy efficiency, pollutant emissions decrease and the use of waste adding value to the already installed processes. However, many bioprocesses have the disadvantage of high production costs, challenging that the research towards the

optimization and development of bioprocesses is promoting. Figure 8 shows the block diagram of the bioprocesses (fermentation and anaerobic digestion) and the parameters of importance in the operation.

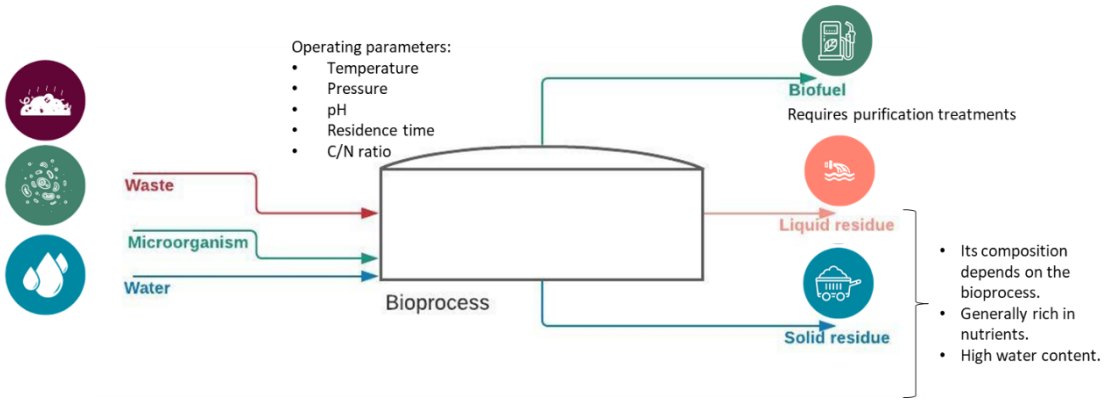

Figure 8 Bioprocesses general diagram (Garritano et al., 2018; Karki et al., 2021)

As shown in the Figure 8, the input to the process (waste, water, and microorganisms) is low cost, this is the first advantage of bioprocesses. The second advantage is that the process has few operational drawbacks. Finally, it does not require constant maintenance.

However, the disadvantages, which are of great weight, require further study of the bioprocesses. Among the disadvantages, the high energy requirements, because the bioprocesses are often carried out between 35 and 55 °C, and additionally the residence times required to achieve the expected yields of bioconversion are usually long (15 - 35 days). Moreover, non-useful by-products are produced, and furthermore the range of temperature and pH control often is very narrow (Varjani et al., 2021). In bioprocesses, different types of gaseous (methane, hydrogen) and liquid (ethanol) biofuels can be obtained, which require separation and purification treatments for their use. As by-products it is possible to recover essential components (amino acids, volatile fatty acids, and nutrients) from the liquid and solid phases, but this also require separation and purification treatments.

1.4.1 Anaerobic digestion

Anaerobic digestion is characterized by reaction wherein biogas is produced from biodegradable materials under anaerobic condition. Composition of the produced biogas depends on the utilized substrate and digestion conditions. Biogas is mostly comprised of

methane (CH_4) and carbon dioxide (CO_2), with minor amounts of other gases including nitrogen (N_2), hydrogen (H_2), hydrogen sulfide (H_2S), ammonia (NH_3) and water vapor (H_2O). The production of biogas occurs through the activity of various microorganisms in four bioconversion steps: hydrolysis, acidogenesis, acetogenesis (also called fermentation) and methanogenesis (Inc et al., 2002; Neshat et al., 2017; Taherzadeh and Karimi, 2008). The process is dependent on the interaction between the diverse microorganisms that can carry out the four bioconversion steps. Figure 9 depicts a simplified go with the drift of the 4 digestion steps defined below.

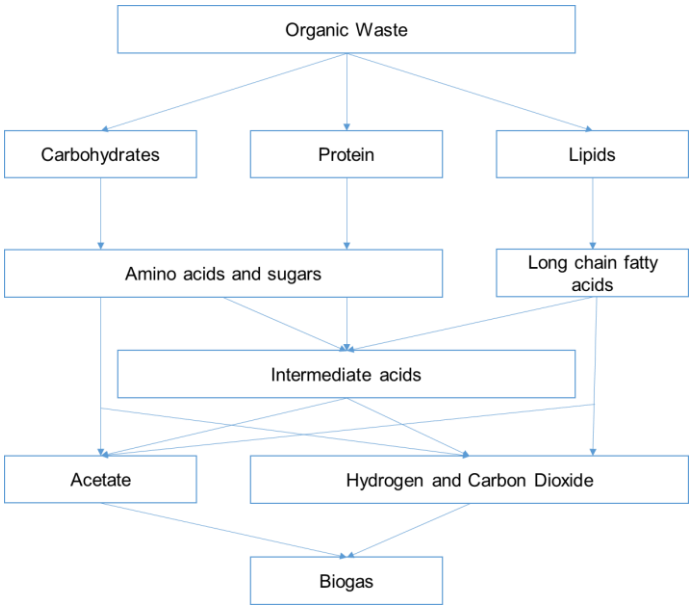

Figure 9 The simplified scheme of pathways in anaerobic digestion (Meegoda et al., 2018).

Anaerobic digestion can serve as an alternative to manure disposal in the pig farming, however, the low carbon to nitrogen (C/N) ratio in animal manures cannot fully satisfy the anaerobic digestion requirements. The environmental parameters to be controlled refer to conditions that must be maintained or ensured for the development of the process. Astals et al. (2018) reported that pH, total ammonia nitrogen (TAN) concentration, and temperature, can affect each other unintentionally. That is, pH can be affected by the other two factors. In addition, the factors can impact the concentration of volatile fatty acids (VFA), which may affect the process yield and methane production. So far, no rigorous study has been found on the relationship between these parameters and how they can affect digestion performance through their effect on the balance between NH_3 and NH_4^+ (Astals et al., 2018). Below, the list of the main parameters affecting anaerobic digestion performances (Meegoda et al., 2018).

- pH: it may affect the conversion pathways of organic substrates during anaerobic processes. Several authors have indicated highest biogas production performances when pH is maintained close to neutrality. Recent authors demonstrate the increase in ethanol, VFA, and methane production when a pH of 7 is maintained in the process (Logan et al., 2021; Zhou et al., 2021).

- Alkalinity: it ensures buffer capacity. An alkalinity higher than 1.5 g/l $CaCO_3$ is recommended to avoid acidification.

- Redox potential: with recommended values below -350 mV, which usually indicates anoxic reducing media

- Nutrients and micronutrients: appropriate concentrations of nutrients (phosphorus, nitrogen, potassium, calcium, etc.) and micronutrients (iron, zinc, nickel, manganese, etc.) are required in the medium to ensure the growth of microorganisms and the synthesis of the enzymes.

- Toxicants and inhibitors: they can kill microorganisms and/or inhibit enzyme and microorganism activities. They concentration must be the minimum possible (O'Callaghan, 2016).

- Temperature: anaerobic digester can be operated in the psychrophilic (room temperature, 10 – 30 °C), mesophilic (30 - 40 °C) or thermophilic (50 - 60 °C) ranges. Growth and reaction rates increase as the temperature range increases, but so does sensitivity to some inhibitors, such as ammonia. In the thermophilic range, higher rates of pathogen destruction are ensured.

- Agitation: depending on the type of reactor, the necessary energy level must be transferred to the system to favor the transfer of substrate to each population or aggregate of bacteria, as well as homogenizing to maintain low average concentrations of inhibitors.

- Retention time. This is the quotient between the volume and the treatment flow rate, i.e., the average residence time of the influent in the reactor, subjected to the action of microorganisms. One of the variables to be maximized in the optimization of anaerobic digestion is the methane production yield. The results of the Zhang et al., 2007 and Babaee

et al., 2011 studies show that 80% of the methane is produced in the first 10 days of the process, showing production yields between 128 and 140 ($mL \cdot VS^{-1}$) at 50 °C. Dhar et al., 2016 shows that there is a constant minimum methane production after 27 days of digestion at 50 °C. Awasthi et al., 2018, on the other hand, reports an optimum retention time of 30 days (Awasthi et al., 2018; Bab&aelig et al., 2011; Dhar et al., 2016; Zhang et al., 2007). Qu et al., 2021 shows in his study that the methane production yield follows a model fitted to the Gompertz function that tends to be constant after day 25 when performed at 36 °C (Qu et al., 2021).

- Organic loading rate (OLR). It is the amount of organic matter introduced per unit of volume and time. Low values imply low concentration in the influent and/or high retention time. An increase in OLR implies a reduction in gas production per unit of organic matter introduced. An optimal technical/economic value for each facility and waste to be treated. Dhar et al., 2016 shows the influence of OLR on methane production, using values between 5.1 and 15.2 g $CODs \cdot L^{-1}$ obtaining the best performance with the highest organic load. On the contrary, Babaee et al., 2011 in its study of anaerobic digestion from vegetables shows that the methane production yield decreases with increasing OLR, obtaining the highest yields at 1.4 kg $VS \cdot m^{-3}d^{-1}$ (Bab&aelig et al., 2011; Dhar et al., 2016).

1.4.2 Anaerobic Co-digestion

Anaerobic co-digestion is the simultaneous anaerobic digestion of two or more substrates, characterized by being a technology in which a mixture of biodegradable organic day substrates or various types of raw materials, of different origin and composition is applied to increase the production of biogas, allowing greater efficiencies of the process, a more cost effective way to balance alkalinity and nutrients (C/N ratio and macro-and micronutrients), and to reduced inhibitors/toxic compounds accumulation so that increase biogas production (Abouelenien et al., 2010; Alatriste-Mondragón et al., 2006; Lar et al., 2010).

Although there is few research on co-digestion of ternary agricultural wastes, there are several research that report biogas production when co-digestion is employed for animal manure and food waste, some of which are listed in the table below (Table 7).

Table 7 Studies where it is demonstrated the increasing of the biogas production in Co-digestion process

Author	Substrate	Remarks
(Zhu et al., 2008)	Municipal food waste and sewage sludge	Higher Bio-hydrogen production 250 mL $H_2 \cdot g^{-1}$ VS
(Sharma et al., 2013)	Poultry litter and thin stillage	Higher Biogas and methane production/Percentage methane in biogas 63.5% Co-digestion of poultry litter and thin stillage may improve the energy economy of both ethanol production and thermophilic digestion.
(X. Liu et al., 2012)	Municipal biomass waste and dewatered sewage sludge	Higher Biogas production A maximum methane production rate of 2.94 $m^3 \cdot (m^3 \cdot d)^{-1}$
(Astals et al., 2011)	Swine manure and glycerin	Higher Methane production 215 mL $CH_4 \cdot g^{-1}$ COD
(Rivero et al., 2014)	mixed sewage sludge and crude glycerol from biodiesel industry	Higher Hydrogen and methane production The maximun production rate was 0.03 $LH_2 \cdot g^{-1}$ CODr or 0.2 $LH_2 \cdot g^{-1}$ VSr and 0.29 $LCH_4 \cdot g^{-1}$ CODr or 1.48 $LCH_4 \cdot g^{-1}$ VSr
(Álvarez et al., 2010; Fonoll et al., 2015; Ye et al., 2013)	Kitchen waste, swine manure, and rice straw	Higher Biogas production 321 L $CH_4 \cdot kg^{-1}$ COD Increments of the methane production between 110% and 180%, depending on the co-substrates biodegradability. Volatile fatty acids concentration raised from 0.07 to 1.70 $g \cdot L^{-1}$
(Ebner et al., 2016)	Food waste: Dairy manure	Dilution of inhibitory compounds such as VFA Bio-methane potentials (BMP) ranged from 165 to 496 mL $CH_4 \cdot g^{-1}$ VS (13–414 m^3 CH4$\cdot t^{-1}$)
(Mendieta et al., 2020)	Crop residues: Sugarcane scum	Higher Specific methane yield, Volatile fatty acids degradation, and VS removal Methane yield was increased by 30.2% and 5.9% compared to substrates in mono-digestion. The maximum methane yield of 0.276 Nm^3 CH4$\cdot kg^{-1}$ VSadded.

Overall, it is shown that co-digestion shows higher methane and hydrogen production yields than mono-digestion or digestion. In addition, it can be generally concluded that it is feasible to integrate organic waste treatment solutions for several companies at the same time. In all cases the yield is greater than 100 $mL \cdot g^{-1}$ VS hydrogen or methane, which exceeds the digestion yields. Hence to conduct an effective anaerobic digestion, there should be another carbon-rich substrate to be co-digested with manure to compensate its carbon deficiency and improve its characteristics for anaerobic digestion (Neshat et al., 2017)

Anaerobic co-digestion is a promising method for waste valorization and aid recovery, even as selling financial and environmental sustainability. However, similar studies ought to cognizance on growing new techniques to analyze the effect of mixing complicated feedstocks and quantify special hydrolysis rates. By improving mathematical models it is

expected to predict the multitude of interactions, analyze the dynamics of the microbial community and the related pathways in substrate degradation (Karki et al., 2021).

1.4.3 Dark fermentation

Dark fermentation is carried out by fermentative hydrogen-producing microorganisms, such as facultative anaerobes and obligate anaerobes (Barca et al., 2016). The possibility of using several types of renewable biomass (including organic waste), the wide range of operational temperature and pressure conditions, and the high biohydrogen production rates, make dark fermentation an attractive option for biohydrogen production. For dark fermentation processes, the choice of substrate plays an important role, as well as, process parameters and environmental factors including metabolic pathways, pH, temperature, organic loading rates, microbial competition, by-products, availability of macronutrients and micronutrients, either in terms of maximizing the biohydrogen yield or in the economy of the process. Moreover, the biohydrogen potential (BHP) mainly depends on the substrate composition in terms of lipids, proteins and most essentially on the carbohydrate content present in soluble form (Elbeshbishy et al., 2017; Ghimire et al., 2015b).

Figure 10 shows the process carried out by the microorganisms, where it can be seen that hydrogen is the main fermentation product that can be used for bioenergy generation. However, dark fermentation is a process that generates residue rich in by-products such as volatile fatty acids (VFAs), ethanol, and nutrients that can be used as raw material in other processes. The fermentation process can be defined with the first three processes of anaerobic digestion (hydrolysis, acetogenesis, and acidogenesis), during these processes, the objective is to eliminate methanogenic bacteria to avoid hydrogen consumption. This is possible by the pretreatment of the microorganism inoculum or by establishing a hostile environment for methanogens in the reactor. There are several types of pretreatments that can be adopted to select hydrogen producing bacteria rather than hydrogen consuming archaea, such as thermal or acidic shock treatments of the inoculum that favor the survive of sporulation hydrogen production bacteria. Sulfate-reducing bacteria (SRB) are capable of capturing the hydrogen produced in dark fermentation (Chen et al., 2021). The literature identifies that inorganic compounds such as heavy metal ions, light metal ions, ammonia, sulfate, and hydrogen gas even are inhibitors of the dark fermentation process. Many of these components are present in

the waste biomass to be treated and are often difficult to remove by traditional pretreatment processes. For this reason, the evaluation of the initial composition of the biomass is another fundamental parameter for bioprocessing optimization (Chen et al., 2021).

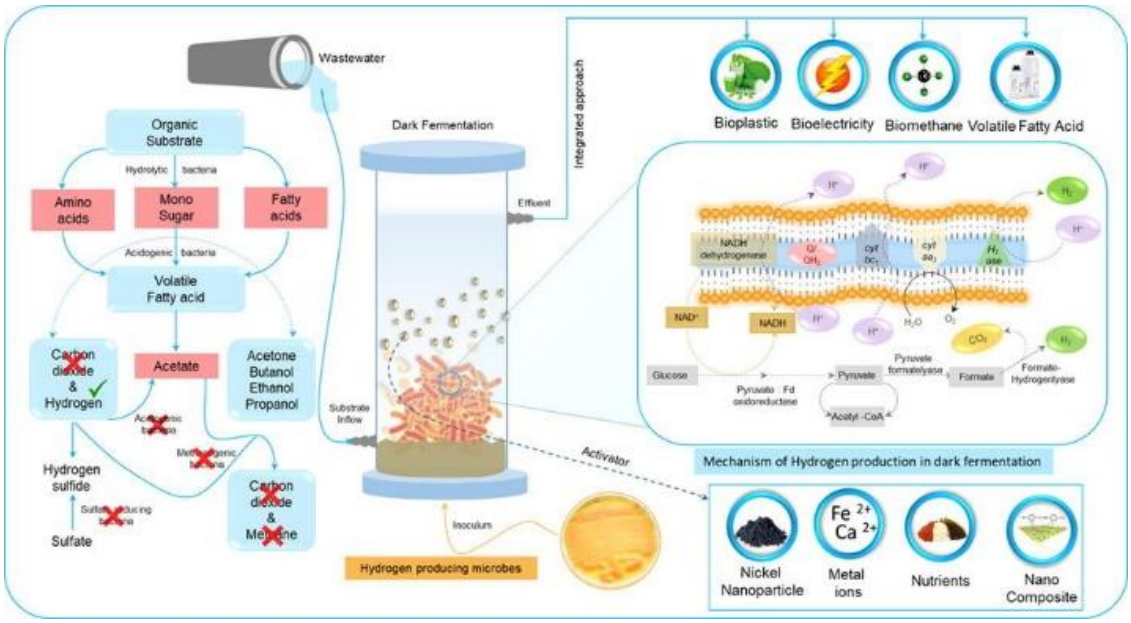

Figure 10 Dark fermentation process (Rajesh Banu et al., 2020a)

Soares et al. (2020) shows the results of 38 studies of hydrogen production from lignocellulosic biomass. Yields vary significantly depending on the biomass used. When straw rice is used, the results show hydrogen production yields between 1.89-4.38 mL $H_2 \cdot g^{-1}$ biomass and around 28 mL $H_2 \cdot g^{-1}$ VS, while for rice husk and rice bran the yields range between 266.4-476 mL $H_2 \cdot g^{-1}$ biomass. The process is mainly dependent on the carbohydrate content of biomass, bioavailability, and biodegradation rate (Soares et al., 2020). Recent authors show that the process can be carried out at a pH between 5.0 and 7.9 and between 30 and 55 °C, this using anaerobic mixed inoculums from pretreated sludge. Moreover, these conditions seek to preferably produce AFVs as the main source for biorefineries. Indeed, regarding experimental and simulation studies the dark fermentation process has yet low yields compared to the theoretical ones (50% yield due to the accumulation of H_2-scavenging reactions which consume the desired H_2) (Sekoai et al., 2021).

Likewise, Łukajtis et al. (2018) have investigated the effect of various operative conditions on hydrogen production yields from compounds such as glucose and sucrose. Their hydrogen production yields range between 1.42 - 4 mol $H_2 \cdot mol^{-1}$ glucose and 1.8-6 mol $H_2 \cdot mol^{-1}$ sucrose. The operational conditions were between 5.5-7.2 pH and 26 - 60 °C. The

conclusion of the study shows that the process presents energetic advantages due to its independence to light which reduces the energetic requirement. However, it is necessary to continue optimizing the process by maximizing hydrogen production and reducing the production of other by-products when the main interest is hydrogen. It should also be noticed that other added value by-products can be recovered from the effluents of dark fermentation, such as organic acids, 1,3-propanediol and ethanol. In addition, hydrogen production liquid waste (HPLW) could be applied as feedstock for the production of methane, lipids, bioplastics and electricity. HPLW could also be used in a photofermentation system, generating more H_2 in a hybrid process (Łukajtis et al., 2018; Sekoai et al., 2021; Soares et al., 2020).

The intense agro-industrial activities provide a wide range of organic by-products and waste biomass such as manure, fruits and vegetables waste, slaughterhouse waste, olive mill waste. These complex wastes rich in carbohydrates, proteins or lignocellulosic biomass could be valuable feedstock sources for bio-energy production. Dark fermentation processes can be set up in order to valorize these wastes by recovering biohydrogen. However, literature data on BHP of these agro-industrial complex waste are scarce and reported only in a few studies (Ghimire et al., 2015b; Gonçalves et al., 2014; Guo et al., 2014).

1.4.4 Bioprocess simulation models

The study and development of kinetic models in bioprocesses are important to understand the dynamic behaviors and to optimize the operational conditions. Several models have been proposed in the literature for digestion, co-digestion and fermentation processes (Bai et al., 2015; D. Li et al., 2021; H. Li et al., 2020; Penumathsa et al., 2008, p. 1; Sun et al., 2021). The models classification can be divided into two types: dynamic or non-dynamic models and white-box, grey-box, or black-box models. The dynamic and non-dynamic models are described by ordinary differential equation (ODE) models and describe behaviors over time. The dynamic ones show continuous predictions in time and are simulated by the discrimination of the difference equations, while the non-dynamic ones only predict time-independent variables. The difference between white, grey, and black-box models is based on the amount of a priori information included. While white-box models are deductive and use a priori information to describe the biochemical reactions that occur during digestion, black-

box, or data-driven models, link directly to the output without including any prior knowledge of the physical and chemical reactions that occur. Grey-box or mechanistic-inspired models are those in which the parameters have a physical interpretation but are adjustable, e.g., by a parameter estimation procedure. This is usually the result of an approximation or simplification of the described process. Because bioprocesses are of high complexity, most dynamic models are of this type. Mathematical models of bioprocesses involve a large number of variables and dynamic equations for the components included. This is due to the wide variety of carbohydrates, proteins and amino acids, fats, long chain fatty acids (LCFA), volatile fatty acids (VFA), alcohols, esters, and aldehydes that are typically involved in the bioconversion processes. In addition, in many cases, parameters that influence the behavior of the bioprocess must be added (e.g. pH, temperature and others). For this reason, the best and most developed models are grey-box models.

Andrews and Pearson developed the first model focused on the anaerobic digestion process in 1965, where the digestion substrate was assumed to consist of dissolved organic substances, and the model contemplates the reactions of the acidogenesis and acetoclastic methanogenesis stages. However, the complexity of compounds found in biomasses has led to the development of new generally applicable models that consider effects on reactions, e.g. NH_3, NH_4^+, NO_2^-, NO_3^- inhibition highly contained in animal manure, pH modulation, long-chain fatty acids (LCFA) inhibition, H_2 inhibition/regulation. In order to consolidate the developed models and obtain the best convergence, in 2002 the 'IWA Task Group on Mathematical Modelling of Anaerobic Digestion Processes' developed the Anaerobic Digestion Model No. 1 (ADM1) which provided the necessary basis for the development of new validated models (Batstone et al., 2002; Donoso-Bravo et al., 2011).

ADM Model and updates

The International Water Association's Anaerobic Digestion Model No. 1 (ADM1) is a widely used model, which describes the equations assuming perfect mixtures and the components are expressed as a function of the chemical oxygen demand (COD) (kg COD·m^{-3}). The model includes biochemical and physicochemical processes and is divided into five stages as shown in Figure 11. The first stage describes the disintegration of extracellular compounds into carbohydrates, lipids, proteins, and inters. The second stage describes the

enzymatic process of hydrolysis where simple molecules such as monosaccharides and long chain fatty acids (LCFA) are obtained. The third stage describes the process of acidogenesis or fermentation, where compounds react to form hydrogen, acetate and volatile fatty acids (VFA). In stage four, acetogenesis is carried out, which involves the reaction of VFA to acetate. Finally, stage five models the acetoclastic and hydrogenotrophic methanogenesis. The model considers first-order kinetics of biochemical processes and biomass death. In addition, it adds inhibition with respect to pH, hydrogen production in acetogenesis, free amino in stage five, as well as inhibition due to the presence of CO_2, HCO_3^-, NH_3, NH_4^+. The ADM1 model has been validated in bioprocesses for the bioprocess simulation of organic wastes such as animal manure (Astals et al., 2011; H. Li et al., 2020; Page et al., 2008), agricultural wastes (Antonopoulou et al., 2012; Galí et al., 2009), municipal wastes, and sludge, by modifying the composition and kinetics equations. The process modeling results have allowed to improve the operations and thus the yields of the process regarding biogas production.

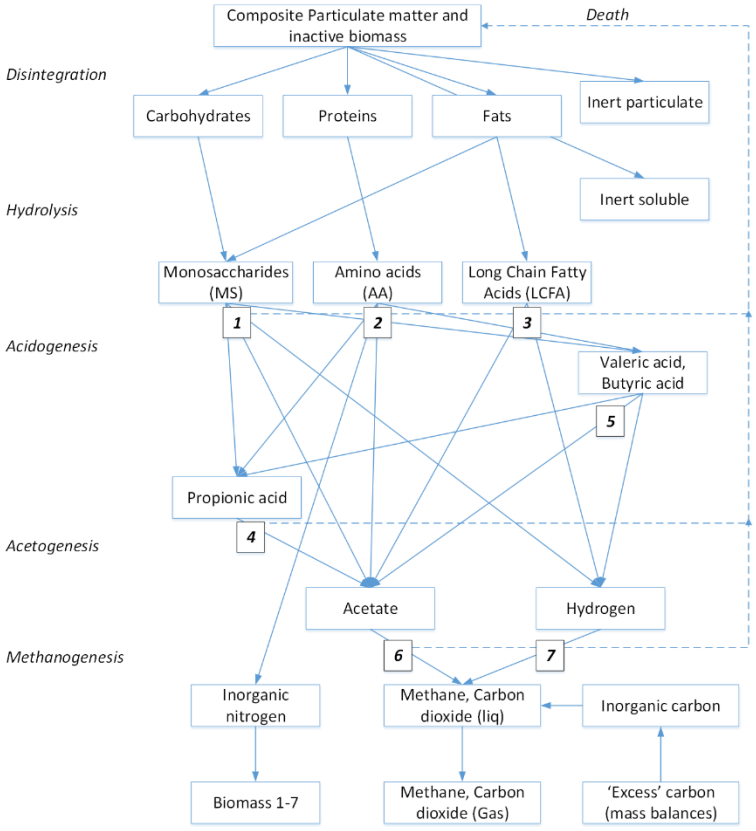

Figure 11 The reaction paths described in ADM1, with the following, microbial groups: 1 – Sugar degrades, 2- Aminoacid degraders, 3 – LCFA degraders, 4 – Propionic acid degraders, 5 – Butyric and valeric acid degraders, 6 – Acetoclastic methanogens , and 7 – Hydrogenotrophic methanogens

Among the applications of the ADM1 model, the simulation of hydrogen fermentation and process optimization are also reported (Peiris et al., 2006; Penumathsa et al., 2008; Zaher et al., 2009). The widely use and application of the ADM1 model in methane and hydrogen production simulation validates the model selection for the startup of the biorefinery to be simulated. The minimal errors observed between the model and the experimental data allow validating its use in the current research works. However, it is important to highlight that authors such as Abbassi-Guendouz et al. (2012) have shown that the model in processes such as digestion are sensitive to the amount of total solids (TS) in the initial blend and therefore the model cannot be applied directly to blends with TS<10% (Abbassi-Guendouz et al., 2012). On the contrary, Pastor-Poquet et al. (2018) shows a new ADM1-based model developed to simulate the solids and reactor mass/volume dynamics of homogenized high-solids anaerobic digestion (HS-AD) reactor. This model was validated with experimental data, highlighting that the model suggested a 5 - 15% difference between the simulated and experimental TS and VS contents. due to the initial drying process at 105 °C which results in errors during experimental measurements due to the loss of volatile compounds such as NH_3, VFA and CO_2 (Pastor-Poquet et al., 2018).

The main objective in the model adaptations has been to simplify the model for a specific substrate application or for its application in simulation and prediction. Table 8 shows some of the modifications and improvements that have been published on the ADM1 model.

Table 8 Extensions, modifications, and adaptations of ADM1 model

Authors	ADM1 Extension/adaptation	Application
(Batstone et al., 2002)	$CaCO_3$. precipitation	Various.
(Batstone et al., 2003)	Acetogenesis of isovalerate.	Protein rich substrate.
(Fedorovich et al., 2003)	Sulphate to H2S reduction by oxidising propionate, acetate, butyrate/valerate and hydrogen oxidising biomass.	Sulphate rich substrate.
(Parker and Wu, 2006)	Methoxylated aromatic compounds, methyl mercaptan, dimethylsulphide conversion into hydrogen sulphide (microbial). Metal sulphide precipitation.	Sulphur rich substrate.
(Tugtas et al., 2006)	Oxidation of nitrate to nitrite, nitric oxide, nitrous oxide and nitrogen by propionate and butyrate/valerate degraders. Non-competitive inhibition by nitrogen oxides.	Various.
(Rodríguez et al., 2006)	pH and hydrogen dependence of carbohydrate fermentation stoichiometry.	Various.
(Peiris et al., 2006)	Lactate and ethanol as intermediates.	Bio-hydrogen production
(Fountoulakis et al., 2006)	Degradation of di-ethylhexyl phtalate (sorptionedesorption based kinetics).	Sludge.

(Kleerebezem and van Loosdrecht, 2006)	Powered expression for hydrogen inhibition of acetogenesis and hydrogen consumption in methanogenesis.	Various.
(de Gracia et al., 2009; Wett et al., 2006, p. 1)	Distinction between particulate and dead biomass. Inclusion of inert decay products.	Various.
(Shimada et al., 2007)	Storage of reserve polymers by microorganisms.	Digestion with rapid changing conditions.
(Myint et al., 2007)	Particulate and soluble cellulose and hemicellulose. Hydrolysis kinetics considering surface colonization and biodegradation.	Particulate containing cellulose and hemicellulose.
(Yasui et al., 2008)	Substrate classification on degradation properties.	Sludge.
(Penumathsa et al., 2008)	Variable stoichiometry according to Rodríguez et al. Lactate degradation (microbial).	Bio-hydrogen production.
(Fezzani and Cheikh, 2008)	Inhibition of acetogenic methanogenesis by total VFA.	Various.
(Zaher et al., 2009)	Cyanide hydrolysis and uptake. Cyanide inhibition of acetogenes. Classification into cyanide resistant and non-resistant methanogenes.	Cyanide containing wastes. Can be generalised to other toxics.
(Ramirez et al., 2009)	Contois kinetics for disintegration and hydrolysis, Hill function for ammonia inhibition	Sludge.
(Fezzani and Cheikh, 2009)	Particulate and soluble phenols. Degradation by hydrolysis (1st) and acidogenesis (Haldane).	Phenol rich substrate.
(Palatsi et al., 2010)	LCFA uptake (Haldane). LCFA inhibition of acetogenes and hydrogenotrophic methanogens (non competitive) or via adsorption-based inhibition.	Lipid rich substrate.
(Bollon et al., 2011)	Lumping of disintegration, hydrolysis and acidogenesis.	Dry digestion.
(Mairet et al., 2011)	Contois kinetics for hydrolysis.	Particulate waste.
(Esposito et al., 2011)	Surface-based kinetics for hydrolysis.	Particulate waste.
(Hierholtzer and Akunna, 2012)	Sodium as an extra variable. Non-competitive inhibition of sodium on acetoclastic methanogens.	Sodium rich substrate.
(Zhang et al., 2015)	Effects of calcium and magnesium ions Effects of inorganic components	Various
(Flores-Alsina et al., 2016)	Extended with P, S and Fe biological and physico-chemical reactions.	Various
(Frunzo et al., 2019)	Consideration of biochemical, physicochemical, sorption, complexation and precipitation equations.	Various
(Sun et al., 2021)	Extension of syngasbiomethanation Gas-liquid mass tranfer, inhibition equations of CO and H_2	Various

Since the beginning of the AMD1 model modifications with the study of Batstone and Keller in 2002, great interest has been shown in the recovery and precipitation of additional compounds that complement the use of bioprocesses. Recent works such as Möller and Müller (2012) shown that approximately 65.5 million cubic meters of digestate are obtained from bioprocesses in Germany, show the interest of the same (wet or dry) in its specific use

as fertilizer for its composition and nutrients such as: N, S and P in their organic/inorganic and soluble/insoluble forms (Möller and Müller, 2012).

Overall, the variations between 2002 and 2013 have been focused on the generations of inhibition extensions. While in recent years, extensions have been developed from the three processes involved:

- Biochemical processes: release of metal ions, sulfur (S), and phosphorus (P) during hydrolysis of complex organic matter, and their uptake during biological conversion processes; inhibition and stimulation effects of trace elements on methanogenesis reactions.

- Chemical processes: precipitation processes of metal ions taking into account the association/dissociation processes of carbonate, phosphate and sulfide species; complexation reactions of metal and soluble components; metal sorption on particulate components, e.g. inert and microbial biomasses.

- Physical processes: liquid-gas transfer of hydrogen sulfide.

Advantages and disadvantages

Although the model attempts to be adapted and eventually simplified for specific applications, its original format is often used where detailed characterization of the biomass is required, which make difficult industrial replicability. (Weinrich and Nelles, 2021) show a simplified model of 4 processes, 10 components and 11 parameters compared with the original ADM model (19 biochemical and 9 chemical processes, 24 components and 52 parameters). These simplifications have made it possible to apply the model in simulation processes for some wastes (corn, swine manure, algae). Therefore, it is possible to work in the future on the sizing and optimization of the design and operation.

The second disadvantage is related to the microbial communities; their complexity makes the models highly sensitive, modifying the yields according to the dominant communities, thus in particular in the hydrolysis stage where approximately 12 *genera* are active. It is believed that future developments will be focused on the mathematical relationship and behavior of microbial communities (diversity and activities), reducing the error between

model and experimental results. One of the advantages is that the description of the bioprocesses by stages allows to study the production yield of the different compounds, specifically optimizing the production of the compound of greatest interest.

1.5 Thermochemical processes

Thermochemical conversion approach is one of the green modes to transform biomass into biofuel. This method is more effective in comparison to biochemical path because of its flexibility in dealing with diverse kinds of biomass and it's also one of the direct, fast, and easy routes of conversion methods. In this procedure, thermal decomposition of natural matters happens at very high temperature in which biomass decomposes, among other, in bio-oils and biogases. Thermochemical conversion are subdivided into 5 different processes which include direct combustion, torrefaction, pyrolysis, gasification, and hydrothermal treatment, as referred to in Figure 12 (Alhazmi and Loy, 2021; Das et al., 2021).

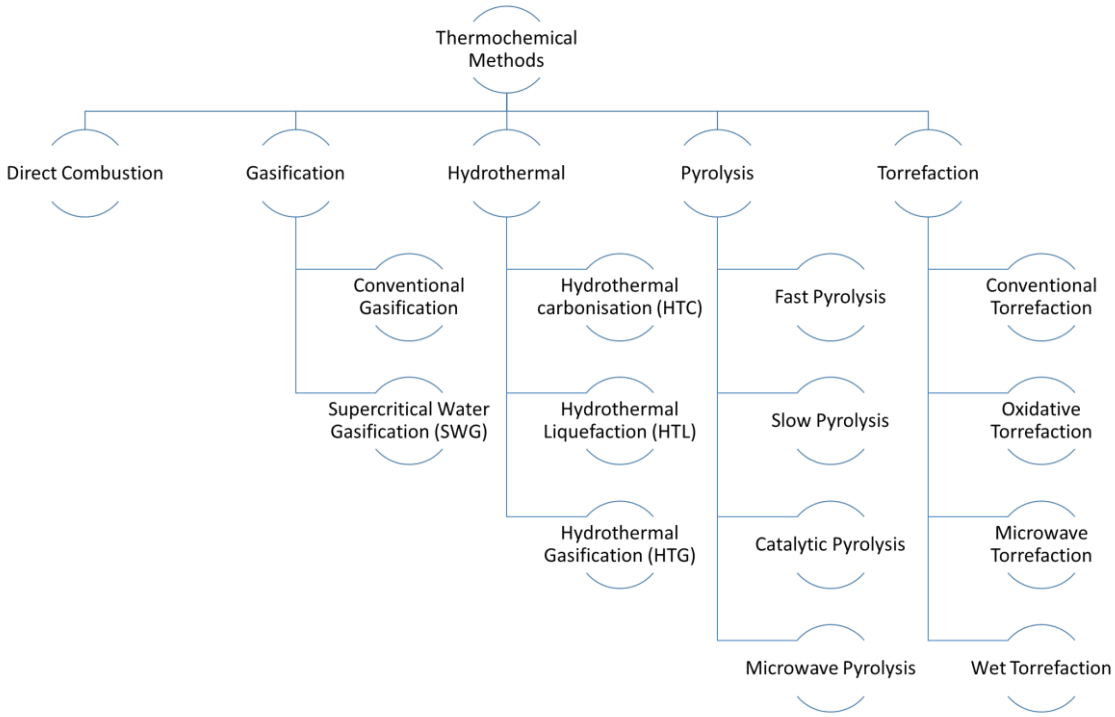

Figure 12 Schematic layout of thermochemical process and its classifications

Thermochemical processes consider classical pathways such as incineration or combustion. They mainly produce heat, water, and unused gases such as CO_2 and other gases

(nitrogen oxides, acetaldehyde, carbon monoxide, etc.) depending on the reactant and combustion quality. These processes can be used to generate steam for industry or electricity via turbines and cogeneration technologies. However, these processes are non-material recovery routes. Pyrolysis and gasification of solid fuels are considered the most attractive thermochemical processes for energy recovery from various wastes. This is because these technologies offer high yields for renewable energy production and conversely low carbon production as well as improved waste management techniques (Faraji and Saidi, 2021; Goffé and Ferrasse, 2019).

Although thermochemical processes are options for the production of biofuels from waste biomass, some authors have studied the disadvantages of biomass when used in these processes. One of the main factors they mention as a disadvantage is the high-water content as, among other, it reduces the heating value and requires energy intensive drying steps. Table 9 shows the disadvantages and main challenges to be met when using biomass in thermochemical processes.

Table 9 Disadvantages of biomass feedstock used for thermochemical conversion (Dai et al., 2019).

Biomass characteristics	Main challenges
High water content	Reduce the heating value
	Require energy intensive drying step
	Reduce the efficiency of the conversion process
	Increase storage and transportation costs
	Increase risks of biological degradation
	Increase corrosion because of condensation of water in flue gas
Low bulk and energy density	Increase storage and transportation costs
	Require high feeding capacity
Poor grindability	Increase grinding energy
Hygroscopic nature	Up-take moisture during storage
	Increase risks of biological degradation
High oxygen content	Reduce the number of C-H bonds
	Reduce the heating value and energy density
	Reduce the thermal stability
High alkali metal content	Cause ash-related problems
Heterogeneity	Wide variation in properties

1.5.1 Direct combustion

About 90% of the total energy from biomass is obtained by direct combustion of different types of biomass at high temperatures (800-1000 °C). The essential requirement for this process is that the moisture content of the biomass should be less than 50%. These combustion plants can produce between 20 and 50 MWe with an efficiency of 25-30%. During combustion, biomass is converted into carbon dioxide, water, steam, and heat. Generally, the combustion process is carried out in combustion chambers and the thermal energy produced is about 20 MJ/kg on average. The advancements in fluidized bed systems and gas cleaning have increased the power generation capacity of these plants to 50-80 MWe with electrical efficiency of 30-40% (Alhazmi and Loy, 2021).

1.5.2 Gasification

In the last decade, a renaissance of gasification technology has begun. Gasification is one of the established thermochemical conversion methods that converts biomass into gaseous fuels. The carbonaceous material in the biomass is converted into synthesis gases (syngas). H_2, CO, CO_2 and CH_4 are the primary gases produced during the gasification process with other combustible gases such as C_2H_4, C_2H_6, C_3H_8, etc. (Das et al., 2021). Figure 13 shows a schematic layout of the different gasification processes.

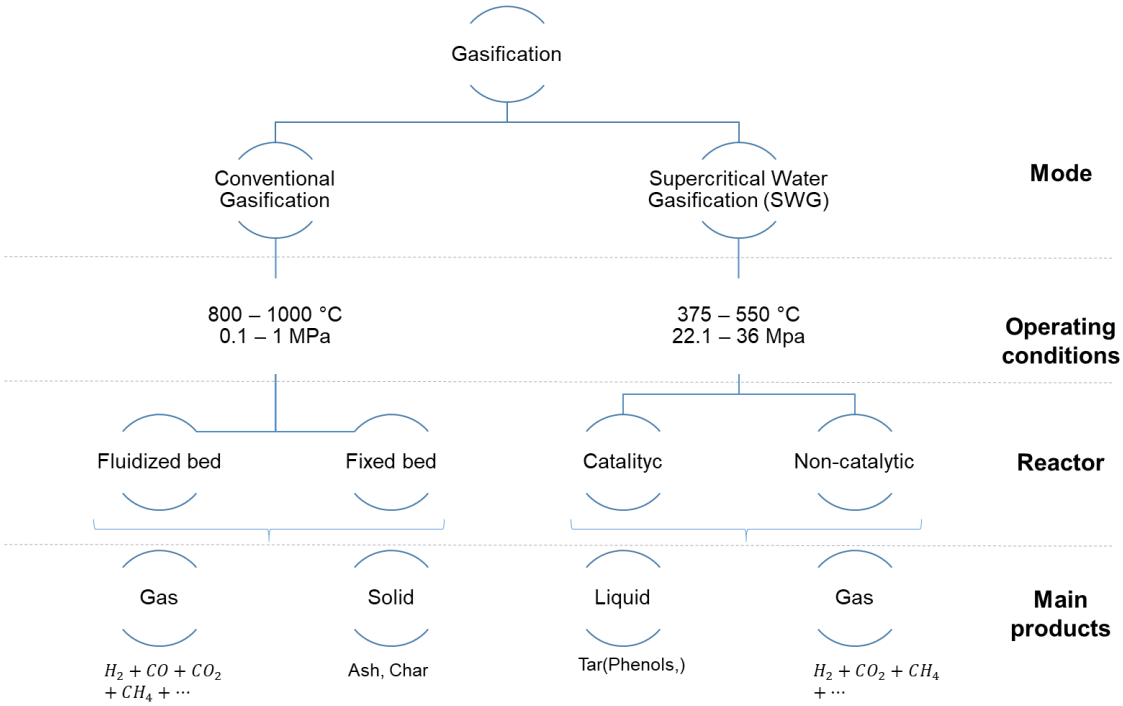

Figure 13 Schematic layout of gasification processes.

Recent studies have investigated the gasification efficiency when solid digestate is used in gasification processes. In particular, Guo et al. (2021) presents an energy efficiency between 49 to 66.9% of an anaerobic digestion followed by gasification of the solid phase. However, the efficiency equation only considers the input and output mass, assuming that the entire energy consumption of the process comes only from the process. It also takes into account the calorific value of the biogas (H_2, CO, CH_4) and also of by-products such as C_2H_4, C_2H_6, C_3H_8 and C_6H_6 (Guo et al., 2021). However, the study shows that the integration of bioprocesses followed by gasification can solve the problem of digestate valorization and transfer the high cost of raw materials currently involved in biomass gasification. It is shown that efficiency is closely linked to the digestate drying process, which can also be related to seasonal and regional factors.

1.5.3 Pyrolysis

Pyrolysis involves the decomposition of biomass in the temperature range of 350 to 550 °C, which can be extended up to 700 °C in the absence of air. The high temperature of this process allows the volatile components of the biomass to vaporize. These vapors are then

condensed at high pressure to form liquid fuel. The liquid fuel/bio-oil, essentially a dark brown liquid with high viscosity and low calorific value, produced in this process can be used directly for static heating or electricity generation. Its chemical composition is quite broad and mainly includes acids, alcohols, aldehydes, phenols, and oligomers.

The main advantage of this bio-oil is that it can be stored and transported directly without the need for further purification. In addition to the bio-oil, the process also produces biochar, biogas, and other useful chemicals (Alhazmi and Loy, 2021). Figure 14 shows the detail of the types of pyrolysis that can be performed, which change depending on the temperature range, type of reactor used and, consequently, the difference in the concentration and efficiency of the products and by-products.

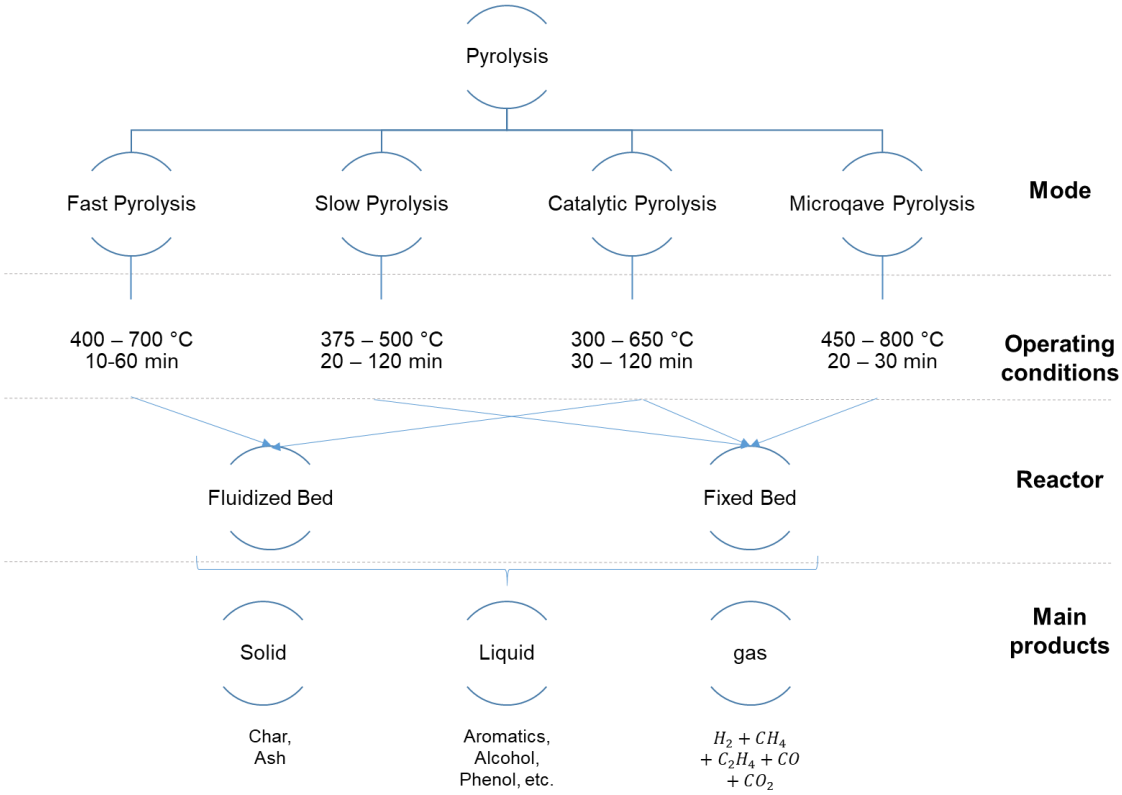

Figure 14 Schematic layout of pyrolysis processes (Das et al., 2021).

The high content of phenolic compounds in bio-oil can be directly used for phenolic resin synthesis. Therefore, selective production of desired products in bio-oil has been extensively studied because of its remarkable potential as an alternative to petrochemical resources. However, complications arise because the complex compounds, high water content and high acidity type of biomass feedstock significantly affect product quality. In addition, biomass

feedstock has disadvantages, including strong hydrophilicity, low energy density, geographical ubiquity, and low bulk density, which may cause high cost during biomass conversion and may limit the development of biomass conversion (Dai et al., 2019).

1.5.1 Subcritical hydrothermal treatment

Subcritical hydrothermal processes remove, deconstruct, and transform organic solid wastes into valuable resources. Four types of hydrothermal processes are found in the literature, of which three are non-oxidative (HTH = hydrothermal hydrolysis, HTC = hydrothermal carbonization, and HTL = hydrothermal liquefaction), and one is oxidative (WO = wet oxidation).

The HTH process is mainly run at 120 to 200 °C and 20-150 bar in nitrogen presence. One of the products of interest in HTH are natural fertilizers and products such as acetic acid, butyric acid, methanol, nitrogen, and phosphorus. Additionally, it shows 70-80% reductions in total suspended solids.

The HTC process is carried out at 150 - 300 °C and 13 - 70 bar and it converts biomass into hydrochar, process water, and gaseous products. The HTL process has been studied for the production of bio-oil and hydrochar from biomass, thus obtaining products and by-products with HHV calorific value of 36.7 and 4.58 $MJ \cdot kg^{-1}$ respectively. HTL operates between 150-350 °C and 50-250 bar and its main products are crude oil, sugars, amino acids and fatty acids (Munir et al., 2018). Wet oxidation (WO) operates at 150 - 300 °C and 20-150 bar. Its products of interest are high carbon content polymer, organic acids, nitrogen, and phosphorus. The process is carried out in the presence of oxygen.

Hydrothermal processes have recently been used for mineral recovery. Zhang et al. (2020) shows recovery of phosphorus (P) with efficiencies up to 88.85% when the process is carried out at temperatures between 60-180 °C and residence time between 15 - 45 min (Zhang et al., 2020). Hydrothermal treatments may require a large energy input and the addition of catalysts or solvents. Recent studies have focused their efforts on operational optimization, demonstrating the relationship and importance of temperature and residence time in hydrothermal processes and the kinetics of their reactions modifying the products and yields according to the product of interest (Ruiz et al., 2021).

1.5.2 Advantages and disadvantages of thermochemical processes

The advantages of thermochemical processes have been demonstrated when they are part of the pretreatment of biomass before bioprocessing or as the main process in biorefineries. Thermochemical process facilities allow easy configuration, and easy heat transfer depending on the reactor design (e.g. PyRoss reactor, plasma reactor and microwave reactor for pyrolysis). Yields are between 35 to 70 wt% for bio-oil and 13 to 22.5 wt% for gas when the inlet are lignocellulose biomass. Gasification, on the other hand, has the advantage of high mass conversion yield and energy efficiency, thus producing biogas compositions with CO_2 percentages between 5 and 30 %v/v (Elgarahy et al., 2021; Seo et al., 2022). Thermochemical processes have a great development of studies, only in 2020 there are twice as many articles on thermochemical processes (combustion, gasification, pyrolysis) compared to bioprocesses (anaerobic digestion and fermentation). Studies show how to improve their efficiency or optimize the operation according to the product of interest (Elgarahy et al., 2021). For example, Tan et al. (2017) concluded that the bio-oil produced by fast pyrolysis at lower temperature (250 °C) produces more alcohols, while the bio-oil produced at higher temperature (650 °C) contains more aromatics and carbonyls (Tan et al., 2017).

Despite this, there are not many studies that present thermochemical processes (pyrolysis, gasification, and combustion) as processes for the valorization of biomass after bioprocessing (e.g. digestate). Currently, conventional management strategies for the solid phase include thermochemical processes and although they show increases of up to 25% in biogas production, their energy efficiency in some cases is equal or lower, due to the fact that these processes require a process of phase separation and dehydration of the solid, generating additional energy consumption in the process (Cesaro, 2021). On in contrast, hydrothermal processes have been the recent focus of research in the integration with bioprocesses and digestate valorization. Wang and Lee, 2021 present a review on 18 studies between 2017-2020 where nutrients are recovered from digestate by hydrothermal treatments. They indicate high recovery potential for nitrogen (up to 66.6%) and phosphorus (up to 87.6%) recovery, mainly by hydrothermal conversion of nitrogen and phosphorus contained in the biomass,

and followed by nutrient precipitation as struvite and/or calcium phosphate (Wang and Lee, 2021).

1.6 Gas separation and recovery

Gas separation and recovery processes are necessary to avoid deterioration of equipment and piping, environmental contamination, and process cost overruns. Considering that the gases of interest are methane (CH_4) and hydrogen (H_2), the separation processes are focused on the removal of H_2S, CO_2, CO, NH_3 and H_2O. The separation of CH_4 and H_2 is realized depending on the use of these gases, since sometimes it is convenient to leave the mixture of the two gases, which is used as hythane.

There are many conventional physicochemical methods (e.g., direct oxidation, ozone oxidation, liquid redox, and adsorption processes) for removing pollutants. However, these methods have many problems such as:

- High initial investment cost.
- High energy requirement.
- The formation of secondary pollutants.

To overcome the problems associated with physical-chemical methods, continuous research is being conducted on biological methods (e.g., bioreactors). Even if in most cases, they are not suitable for commercial use due to low conversion or elimination capacities and inhibitory effects at high removal gases concentrations, the use of biofilters has been accepted as a suitable alternative to conventional methods for treating gases emissions.

1.6.1 Bio-filters

The high concentration of H_2S (about 1000-2000 ppmv) in raw biogas forms extremely corrosive acids that attack the biogas-fueled equipment and the metallic accessories of biogas technology. The efficient operation of a biofilter depends on the selection of a suitable packing material that has high porosity, good water retention capacity, and the ability to retain the microbial community on the selected support medium. Recent studies have shown

some advantages (e.g., low cost, ease of manufacture, waste management) of adding biochar as a medium to biofilters. Biochar refers to the solid material obtained by thermal conversion of organic wastes in the absence of oxygen, e.g., pyrolysis. It is used as a sorbent to remove a variety of pollutants due to its properties such as high pore size distribution, large surface area and good ion exchange capacity. The properties of biochar depend on the type of feedstock, the process residence time (10 min to several hours) and the pyrolysis temperature, the heating rate (generally a few degrees min^{-1}).

Recent authors have reported the efficiency of biofilters on the biogas generated from anaerobic digestion. They have obtained results of H_2S removal between 19 to 33 $g/m^3 \cdot h$ (greater than 99%) and methane gas concentration greater than 97%. The experiments have been carried out in periods between 80 s and 94 days with operating conditions of 54 °C and a pH of 8 (Das et al., 2019; Porté et al., 2019).

1.6.2 Water scrubber

The process works by flowing the gas through a water sprinkler. The gases to be removed are absorbed in the water (Figure 15). Recent authors report the effectiveness of the process obtaining methane gas with a concentration between 95 and 99% and losses between 2 to 5% of CH_4. Also, studies have been carried out on its operational (from 14 for 100 m^3/h biomethane to 9.1 for 500 m^3/h biomethane) and investment costs (From 10100 euros for 100 m^3/h of biomethane to 3500 euros for 500 m^3/h of biomethane). In addition, energy consumptions between 0.26 and 0.97 kWh/Nm^3 have been reported (Benizri et al., 2019; Chen et al., 2015; Noorain et al., 2019; Ullah Khan et al., 2017).

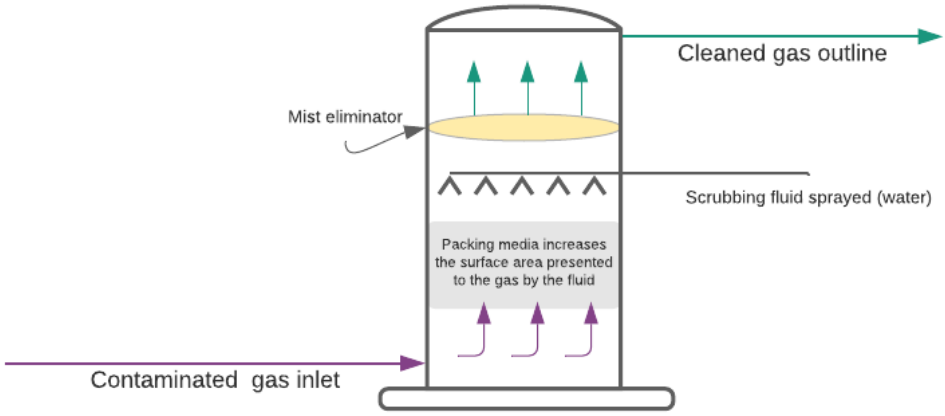

Figure 15 Water scrubber, also called gas scrubbing or wet scrubber process diagram.

High pressure water scrubbing is the most commercially feasible technology for biogas purification due to its simplicity and performance reliability. However, the disadvantage of this technology is the electricity cost. Therefore, water scrubbing at near atmospheric pressure are proposed, which requires lower specific electricity consumption. Water scrubbing at atmospheric pressure is limited to very small plants and is usually not offered by commercial suppliers because a higher liquid-to-biogas flow ratio is required. In addition, high purification efficiency is difficult to achieve.

Overall, water scrubber use benefits are:

- Prevent a variety of pollutants from entering the air through the exhaust (from sulfur to acid gases that contribute to acid rain.
- The units are quite robust and can tolerate a wide range of temperatures, making them ideal for operation in almost any environment.

On the other hand, its disadvantages are related to the maintenance that must be frequent, the equipment being susceptible to corrosion.

1.6.3 Pressure swing adsorption

The pressure swing adsorption (PSA) process is currently used in the industry for different applications, among which are:

- Gas drying.

- Solvent vapor recovery.
- Fractionation of air.
- Production of hydrogen from steam methane reformers (SMRs) and petroleum refinery offgases.
- Separation of carbon dioxide and methane from landfill gas.
- Carbon monoxide-hydrogen separation.
- Normal isoparaffin separation.
- Alcohol dehydration.

The main objective of the PSA downstream of bioprocesses is the separation of biogas (H_2 and/or CH_4) from CO_2. Due to its different applications, its design has been studied and optimized. Recent studies show recovery efficiencies greater than 98% and final gas concentration flow rates from 95 to 99% (Chen et al., 2015; Klein et al., 2018; Ullah Khan et al., 2017). It is important to highlight that different studies specify the need for previous desulfurization processes. The operational conditions of the process studied are temperature between 3 °C to 38 °C and pressure between 101325 to 3040000 Pa. Authors such as (Ullah Khan et al., 2017) report losses of the main biogas (CH_4) up to 4% and consumptions between 0.24 - 0.6 kWh/Nm^3.

1.6.4 Reforming to H_2

Hydrogen production is a process that becomes interesting in the study of biorefineries not only because of the hydrogen heating value (its value is higher than that of other gases, such as methane), but also because from a sustainability point of view it is a process that contributes to the consumption of carbon dioxide, reducing emissions to the atmosphere. However, one of the current problems with the process is the carbon monoxide (CO) production as a gaseous by-product, which must be integrated into the biorefinery process. In addition, the feed inlet conditions must be clean of H_2S (Ullah Khan et al., 2017).

Different authors discuss the two best known reforming processes, steam methane reforming (SMR) and dry methane reforming (DMR). SMR is the process where endothermic oxidation-reduction reactions of methane are made in presence of water for the hydrogen and carbon monoxide production. Generally, the tendency for carbon formation will increase with decreasing H_2O/CH_4 and CO_2/CH_4 ratios of the feed gas and increasing temperature. On the other hand, DMR is only performed in the presence of carbon dioxide. Although the two are related, in their production they are differentiated by the difference in the H/C ratio. High conversions require high temperatures, due to the endothermic nature of the DMR reaction. Methane conversion is additionally increased slightly by operating with excess CO_2. This will also influence the H_2/CO ratio of the product, which drops with excess CO_2 due to a larger amount of CO (Mortensen and Dybkjær, 2015; Rezaei and Dzuryk, 2019).

The SMR process can be operated at temperatures between 600 °C and 1500 °C and pressures between 2 to 40 MPa, operational conditions that are related to methane conversion efficiency, energy efficiency and H_2/CO ratio in the output stream. Despite the high temperatures and pressures, different authors report energy efficiencies between 60 to 90% and methane conversions up to 95%.

1.6.5 Methanol synthesis

Methanol has a variety of industrial applications. Its most frequent use is as a feedstock for the production of methyl t-butyl ether (MTBE), which is a gasoline additive. It is also used in the production of formaldehyde, acetic acid, chloromethanes, methyl methacrylate, methylamines, dimethyl terephthalate and as a solvent or antifreeze in aerosol paints and coatings.

Methanol is a potential substitute for petroleum. It can be used directly as a fuel replacing gasoline in gasoline-diesel blends. Methanol has greater potential for use compared to other conventional fuels because it produces less ozone, lower emissions of pollutants, particularly benzene and polycyclic aromatic hydrocarbons and sulfur compounds, and has low vapor emissions. It can also be used in the production of biodiesel. Furthermore, methanol is used in Colombia as a raw material for the manufacture of biodiesel, made from natural and biodegradable elements such as vegetable oils (palm oil), a fuel that has tripled its demand in the last three years. Reports presented by the Colombian Ministry of Mines and Energy show

that the installed plants require 108.65 kg of methanol for each ton of biodiesel produced, most of which is currently imported (fedebiocombustibles - COL, 2021; MinMinas - COL, 2021).

Currently, all methanol produced worldwide is synthesized by a catalytic process from carbon monoxide and hydrogen. In addition to CO_2 capture, methanol synthesis eliminates the need to compress or liquefy CH_4 for transport impacting economic evaluations. This reaction uses high temperatures and pressures and pressures, which requires large and complex industrial reactors. The most widely used industrial processes are those developed by Lurgi Corp. and Imperial Chemical Industries Ltd. (ICI), using any of the three feedstocks (natural gas, liquid hydrocarbon mixture or coal). Based on the ICI, reaction between gas phase CO_2 and H_2, as raw materials, occurs over a $Cu/ZnO/Al_2O_3$ catalyst under the adiabatic process (Lee et al., 2020; Lundgren et al., 2013; Puig-Gamero et al., 2018).

The two factors outlined above show methanol synthesis as a promising technology that provides for the production of a necessary feedstock and the reduction of greenhouse gas (CO_2) emissions. Figure 16 shows a general diagram of the methanol synthesis unit, in which conversions of up to 25% CO_2 have been reported and methanol as the main product can be obtained with 99% purity with lower stage numbers in a distillation tower.

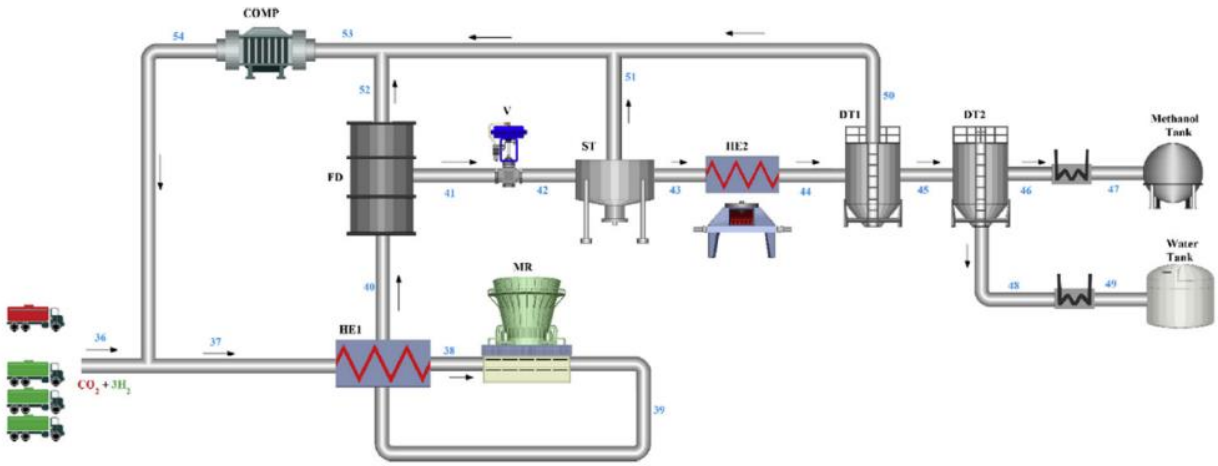

Figure 16 Schematic diagram of the methanol synthesis unit (Nami et al., 2019).

As shown in Figure 16, the process has H_2 and CO_2 as input and methanol and water as output, the process shows CO_2 capture by direct synthesis which according to the study by Nami et al. (2019) shows greater efficiency and economic benefits compared to the indirect

method which generates additional CO as the resulting gas in addition to water. Recirculation in the system ensures that CO_2 emissions to the environment are minimized. In addition, the process does not have high energy demands. In other words, the objective of the process, in addition to generating methanol as a product of interest, is to minimize the environmental impact of greenhouse gas (CO_2) emissions. The methanol synthesis studies show the variation of conversion, process efficiency and costs as a function of factors such as temperature, H_2/CO_2 ratio, and pressure. The study of Le et al. (2020) presents the sensitivity analysis of the process from the simulation performed in Aspen Hysys, thus showing that the process is highly affected by pressure and H_2/CO_2 ratio rather than temperature. Figure 17 shows the efficiency and cost results reported in the study. Figure 17A-B shows the yields obtained by Lee et al, 2020 as a function of pressure, temperature, and H_2/CO_2 ratio where the methanol production yield varies between 10 and 35%. Figure 17-C-D shows the results of the techno-economic study as a function of plant capacity and methanol generation ratio as a new product. These properties are important for the optimization of the model as they have been validated experimentally. Furthermore, it is evident that the higher methanol conversion represents the higher CO_2 conversion.

Generally, the study shows the technical, economic, and environmental feasibility of CO_2 hydrogenation for methanol synthesis in the indirect method. By means of the sensitivity analysis, the optimum yield points of the process are shown.

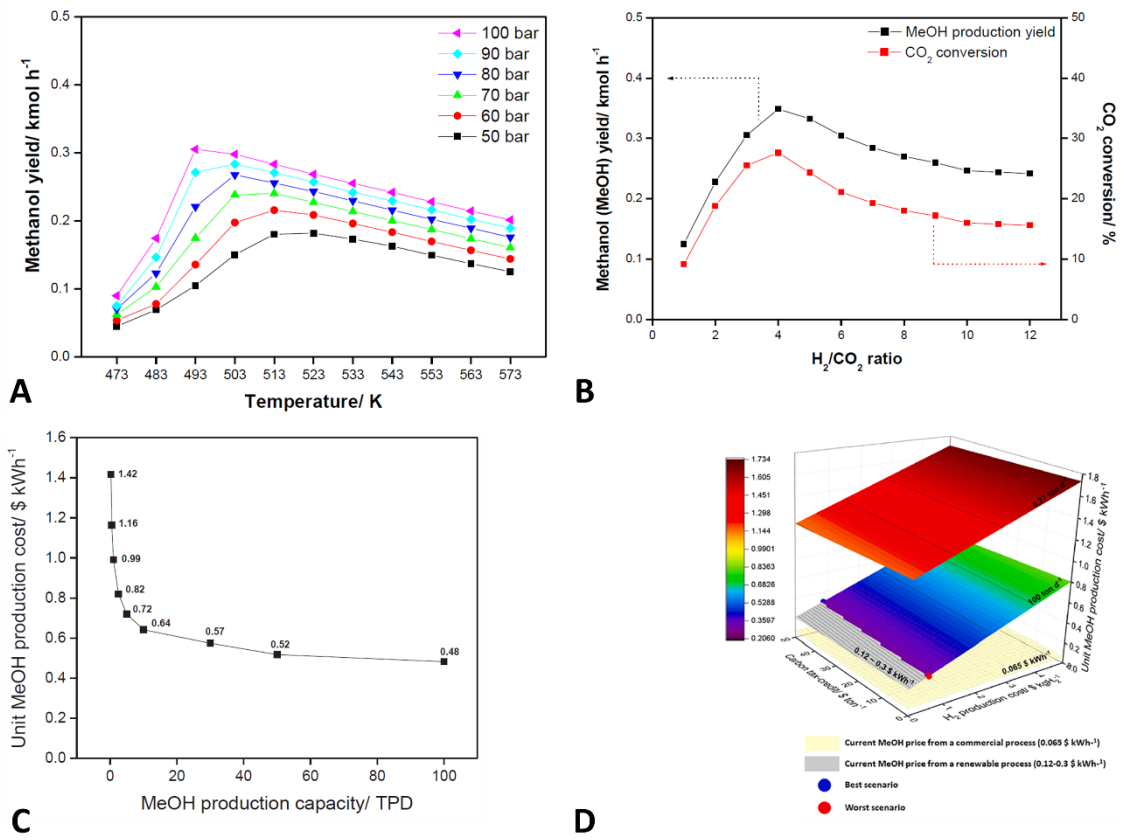

Figure 17 Renewable methanol synthesis from renewable H_2 and captured CO_2. Techno-economic analysis was performed for renewable methanol synthesis (A) Effect of the operating pressure on the methanol (MeOH) yield in the temperature range of 473–573 K at a fixed H_2/CO_2 ratio of 3 for a recycled MeOH synthesis process. (B) Effect of the H_2/CO_2 ratio on the methanol (MeOH) yield (left side) and CO_2 conversion (right side) for the recycled process at 493 K and 100 bar. (C) Unit MeOH production costs according to the MeOH production capacity. (D) Effect of the H_2 production cost and CO_2 tax-credit on the unit MeOH production cost at different MeOH production capacities of 0.27 and 100 TPD. (Lee et al., 2020)

1.7 Separation and recovery of liquids and solids

In bioprocesses, the degradation of matter is generally presented, depending on the process and operational conditions, the main biofuel is obtained, as well as by-products of interest. Different studies have shown that the liquid and solid phase can have an additional valorization process. Initially, thermochemical processes such as those explained in section 1.5 are proposed. In addition to thermochemical processes and searching the optimal conditions of the biomass, it is necessary to take into account processes such as precipitation, decantation, dehydration centrifuges, liquid-liquid extractions and even the use of by-

products through the production of new products such as the production of polyhydroxyalkanoates (PHA) and polyhydroxybutyric acid (PHB).

1.7.1 Precipitation

Precipitation is the most common unit operation in downstream processing. Although it is difficult to give a definitive statistic, it is estimated that more than 80% of downstream processes have at least one precipitation stage. Because of its different objectives, precipitation is carried out in different ways.

Amorphous precipitation is usually carried out without specific control of super saturation (i.e., the difference between the actual concentration and the equilibrium concentration of the biomolecule), and thus without control of the nucleation rate (i.e., the rate of formation of new crystal particles). The solid phase formed by precipitation results from the formation of nuclei that grow into small primary crystals (0.1-10 mm) that agglomerate (not always in large sizes) and thus may contain impurities trapped in the final particles. The first attempt to systematize a theory of protein solubility (and of the effect of salts on it) was presented by Hofmeister in a series of papers between the 1880s and 1890s. Since then, a comprehensive theory of precipitation has been sought, with relative success: although many aspects of precipitation have been elucidated, the need to take into account the peculiarities of biomolecules and precipitating agents has become a matter of interest. No single general theory has been developed and it is doubtful that one will ever be developed. Even colloidal-type theories, which have been quite successful, are currently in question, since they cannot explain many experimentally observed phenomena (de Alcântara Pessôa Filho et al., 2019).

Physicochemical methods include chemical precipitation, Larraagoiti Kuri et al. (2017) show that he effectiveness of all the method, however, relies on to a total solid level of 0.5–3.0% (Larragoiti-Kuri et al., 2017). Several studies reported the technical and economic feasibility of recovering nutrients via struvite ($NH_4MgPO_4 \cdot 6H_2O$) precipitation from wastewater treatment plants. Effluents from the AD plants treating nutrient-rich waste streams such as swine and poultry manure could be an ideal substrate for recovering nutrients via struvite precipitation (Hernandez et al., 2018; Sawatdeenarunat et al., 2016). The precipitation stage is important in the effluent or digestate of bioprocesses for better utilization of the solid and liquid phases. It has been shown that in precipitation up to 90% of

the phosphorus present is found in the sludge, which makes it an important by-product due to its abundance. Finally, the precipitation of by-products such as struvite has been shown to decrease pathogenic populations (Ma et al., 2018).

Struvite is a macronutrient compound produced by chemical precipitation at an alkaline pH with an optimum amount of ammonium, phosphorus, and magnesium. This process transfers nutrients from the liquid phase to the solid phase, producing struvite, which can be used as a slow-release fertilizer struvite recovery can be successfully integrated into the composting process to improve the agronomic value of composting. In addition, struvite precipitation would reduce the amount of sludge that needs to be removed from wastewater treatment plants. Several matrices were studied to investigate struvite formation, such as urban wastewater, swine wastewater, chicken wastewater, cattle wastewater, human urine, and digested sludge. As a result, these effluents could be used for struvite recovery, achieving high struvite crystallization and precipitation efficiency (Ochoa et al., 2021). Processes such as integrated hydrothermal carbonization (HTC), acid leaching and activation process to recover up to 94.3% phosphorus from digestate use hydrothermal process and struvite precipitation by hydrothermal process at 60 ~ 180 ◦C for 15 ~ 45 min coupled with H_2O_2 and HCl leaching to achieve 88.2% phosphorus recovery (Wang and Lee, 2021).

1.7.2 Liquid-liquid extraction

Liquid-liquid extraction is a purification technique used in workup to separate compounds based on their relative solubilities in two immiscible solvents. The extraction technique can be used to purify compounds or to separate mixtures of compounds, such as when isolating a product from a reaction mixture (known as extractive workup). It also finds application in the isolation of natural products, as in the extraction of caffeine from tea leaves.

The principles of liquid-liquid extraction in flow-through are based on immiscibility of the organic and aqueous phases and liquid pressure. This is both the total system pressure and the cross-membrane pressure applied in the separator part of the apparatus.

Figure 18 shows the process diagram of the liquid-liquid extraction. The process can be carried out at standard temperature and pressure, with and without agitation, factors that affect the separation performance. The liquid-liquid extraction process has been proposed in

the construction of biorefineries and biomass treatment for the recovery of volatile fatty acids. Volatile fatty acids are a subgroup of fatty acids with carbon chains of less than six carbons.

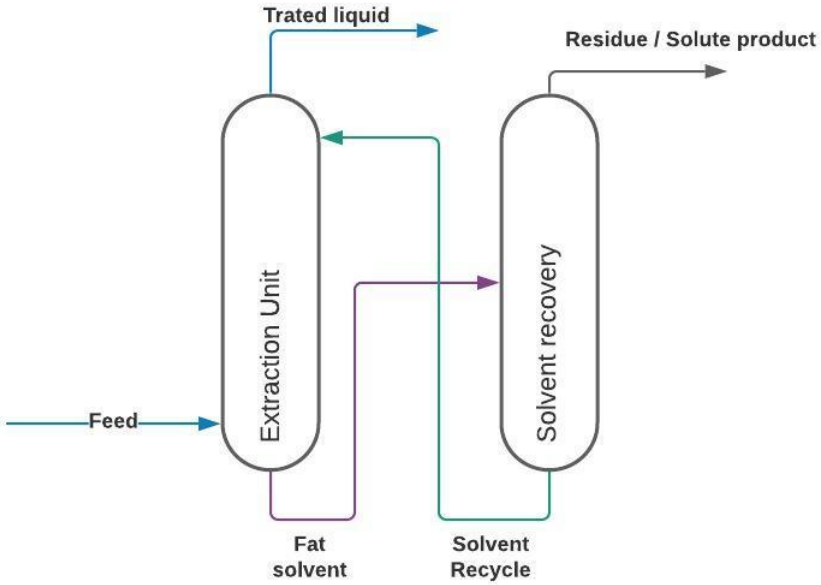

Figure 18 Liquid-liquid extraction and solvent recovery flow diagram.

Their volatility is due to their short carbon chain, in contrast to long-chain fatty acids, which are solid at room temperature. The short-chain fatty acids are:

- Formic acid
- Acetic acid
- Propionic acid
- Butyric acid
- Isobutyric acid
- Valeric acid
- 2-Methylbutanoic acid

In hydrolysis, complex organic polymers in organic waste are broken down into simpler organic monomers by enzymes excreted from microorganisms. Subsequently, in the

acidogenic stage, these monomers are fermented by the acidogens conventionally, VFAs are produced chemically from petroleum-derived compounds. petroleum-derived compounds. These chemical processes are energy intensive and have a negative impact on the environment, so their biological production is gaining immense interest (Singhania et al., 2013). In particular, it has been shown that in processes such as dark fermentation, the digestate in the liquid and solid phase has a composition of interested VFAs, so its extraction is often studied. VFAs are also used as raw material for the production of polyhydroxyalkanoates (PHAs) and polyhydroxybutyrate (PHB).

1.7.3 PHA/PHB fermentation

Polyhydroxyalkanoates (PHAs) are natural polymers produced by bacteria and used as a nutrient reservoir. PHAs have attracted the attention of the scientific community due to their strong tendency to be biodegradable, their physical and mechanical properties, comparable to those of petroleum-derived plastics (these polymers have properties ranging from rigid and brittle to rubber-like plastics) and for being produced from renewable resources. PHAs are a family of optically active biological polyesters with (R)-3HA monomer units. The 3-hydroxyalkanoate acids are all in the R configuration due to the stereospecificity of the polymeric enzyme, PHA synthetase.

There is a wide range of applicability for PHAs, and they can be classified into two main groups:

- Biodegradable disposable packaging
- Pharmaceutical area

Each area takes advantage of mechanical properties and low production costs. There is also an area of research in bioprocesses where research work is carried out with PHA and mixtures with natural materials such as natural rubber or latex.

Polyhydroxybutyrate (PHB) is the first known member of this family, it has mechanical properties like polypropylene with the added advantage of biodegradability. However, it is not currently a material that can displace polypropylene, as its price difference is very large. From the biotechnological point of view, PHB is interesting because it has properties similar

to those of propylene and polyethylene, so this compound can be used as a raw material in the industry, replacing materials with a long degradation time (Dinesh et al., 2020).

The first processes developed for the production of PHA with microorganisms were carried out through fermentation processes using the bacterium Ralstonia eutropha, which is capable of producing PHB from glucose, or Polyhydroxybutyrate-Valerate (PHBV) from glucose and propionate, substrates whose high cost affected the final price of the polymer obtained (Yoneyama et al., 2015).

Bacteria of the genus *Azotobacter* come from the azotobacteraceae family, these are Gram-negative bacteria that live in soils and fresh water, in fact they can also grow in low oxygen concentrations and reproduce by binary fission and use sugars, alcohols and organic salts to grow. *Azotobacter Vinelandii* is a bacterium that thanks to its metabolic and genetic capabilities (several copies of its chromosome) has been of great study. It produces two polymers of industrial use in the absence of nitrogen sources, both are alginate and PHB. PHB can be produced by combining various substrates under different growth conditions including aerobic/anaerobic, temperature, pH and submerged/solid state fermentation (Figure 19). Many researchers presented relevant substrate to produce PHB such as renewable resources (eg. starch, cellulose, sucrose) (Elbeshbishy et al., 2017).

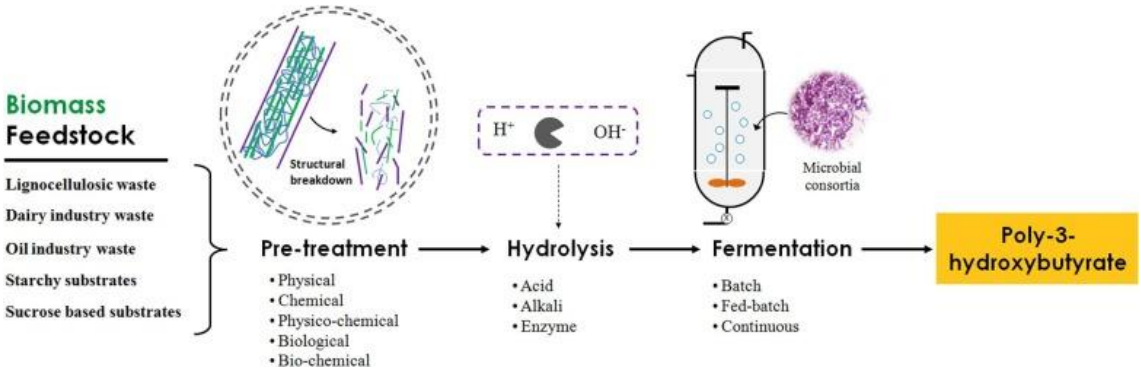

Figure 19 Conversion of biomass to polyhydroxybutyrate (Elbeshbishy et al., 2017)

1.8 Biorefinery design

In recent years, there has been increasing research into bioprocesses and thermochemical processes to replace petrochemicals as an option for biofuel production. However, the costs and the mass and energy efficiencies are still lower than those of petroleum-based refineries (Amoah et al., 2019). For this reason, the concept of biorefinery has been developed in recent

years. According to the International Energy Agency (IEA) Bioenergy Task 42, a biorefinery is defined as "*A sustainable processing of biomass into a spectrum of marketable products and energy*" (IEA, 2021). A biorefinery is a facility that comprises a series of processes that incorporate technological conversions and bioprocesses to produce biofuels. Its main objective is the integration of processes and the maximization of the utilization of residual biomass. The input to a biorefinery is somewhat heterogeneous, i.e., it can range from material with complex molecules such as lipids and proteins to simple sugars, volatile fatty acids, and others. This leads to a wide variety of biorefinery models. Maximizing biomass recovery is not the only challenge of biorefineries. In recent years' models have been developed that add objective functions such as maximizing energy yield and reducing atmospheric emissions, introducing the sustainable biorefinery concept, integrating the process in circular economy studies (also: Bioeconomy and circular bioeconomy) (Klein et al., 2018; Moncada et al., 2013; Sy et al., 2018).

There are different models of biorefinery design proposed in the literature (Bao et al., 2011; Kelloway and Daoutidis, 2014; Moncada et al., 2013; Posada et al., 2013; Santibañez-Aguilar et al., 2016). However, Moncada B. et al. (2016) design can be classified according to three design points:

- Superstructures and conceptual design.
- Optimization.
- Combination of the two previous ones.

The biorefinery design process continues to be a challenge for research and development since there are a large number of alternatives that vary according to: the type of biomass available, technologies, products of interest, policies, laws and other elements (Moncada B. et al., 2016). For this reason, the biorefineries reported by different authors present a specific case study applied to a country, a certain type of biomass and with the interest of a specific product. For example, in the case of South American countries such as Colombia and Brazil, or in Indonesia, there may be ten times more possibilities than in Europe when dealing with lignocellulosic material, so the problem centers on what type of technology to opt for, what

product is of interest and how to combine lignocellulosic biomass with other types of waste biomasses (Bioenergy IEA, Task 40, 2006, p. 40; Fallot et al., 2009).

1.8.1 Conceptual design

In process engineering, several authors have applied this strategy to the design of various chemical plants, but rarely to biorefineries. In general, feedstocks and products are selected based on availability, market needs, and hierarchy and sequence, among other factors. In other words, by applying basic process design rules. However, there are some limitations depending on applications and uses. For example, higher value-added products have the highest priority over bulk products such as energy. These include functional foods, metabolites, etc.

However, it is very important to satisfy each of the sectors and to induce more sophisticated technological schemes to use the best feedstocks and their composition and to make the necessary integrations between the different generations of biorefineries. The concept involves three types of analysis, technical, economic, and ecological, and two types of integration, mass, and energy.

Generally, biorefinery design is based on single experimental processes that are described in the literature and have shown the best performance. This methodology is usually based on process synthesis using process simulation software. Additional optimization steps are needed before the detailed design is developed (Moncada B. et al., 2016).

Figure 20 shows a biorefinery superstructure focused on the maximum utilization of the raw material (spent coffee grounds) presented by Rajesh Banu et al. (2020b). In the conceptual design the bioprocesses and thermal processes are individually integrated with separation processes and extraction of by-products. Overall, the valorization of biomass in different processes is studied. As an advantage, it is evident that coffee residues have potential for biological and thermochemical processes. However, the integration of processes and the valorization of the digestate after the bioprocesses is not shown. Moreover, in anaerobic digestion only biogas is shown as a product of interest, while in the other processes there is bio-oil, biodiesel, bioethanol, biogas, and the use of residues such as fermentation residues that are used for anaerobic digestion or the production of fuel pellets.

Two points of this study are highlighted. The first is the feasibility of using coffee residues in bioprocesses or thermochemical processes. Anaerobic digestion in a direct way for the biogas production. The second is the combination of bio-products through the sequence of hydrolysis, fermentation and anaerobic digestion approached to the production of bioethanol, fuel pellets and biogas where the biomass valorization can be increased.

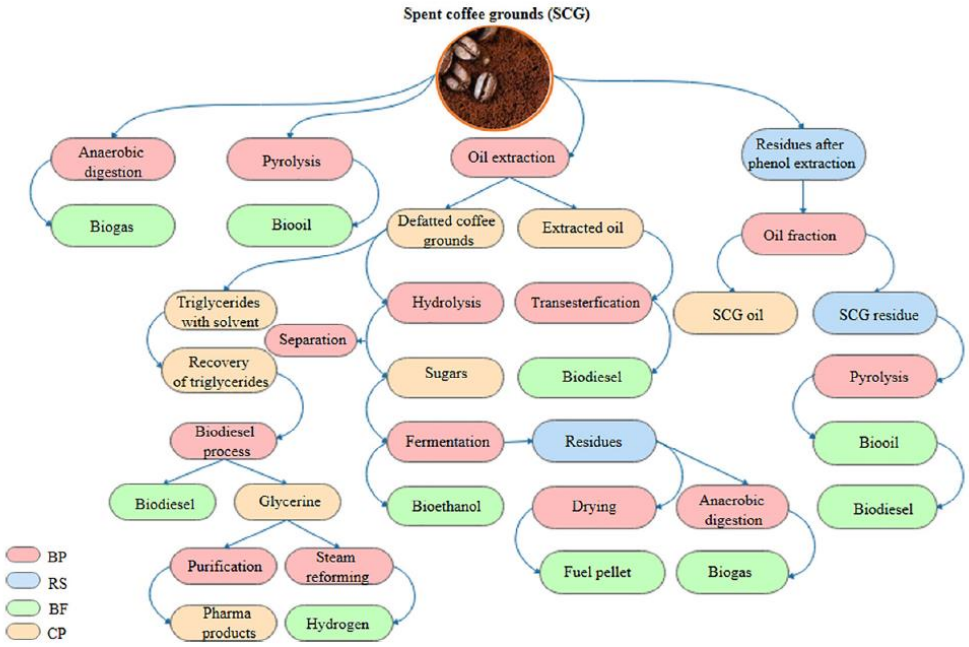

Figure 20 The various integrated biorefinery routes of biofuel production (BP- Biorefinery process; RS – Residues; BF- Biofuel; CP- Co products)(Rajesh Banu et al., 2020b)

As a result, Figure 21 presents the different routes optimized for the case study biorefinery that optimizes the production of biopolymers, caffeine, bio-sorbents, biochar, carbon material, and antioxidants. In the process it is shown that the first stage of the bioprocess is of great interest for obtaining by-products such as PHA and carotenoid, however this must be accompanied by dehydration processes of the solids and time control in the bioprocess to ensure only reach the hydrolysis phase. On the other hand, the solid phase (biochar) is shown as a product of interest as activated carbon. The routes shown, although they perform an integration of processes, do not show the interest towards the optimization of energy efficiency.

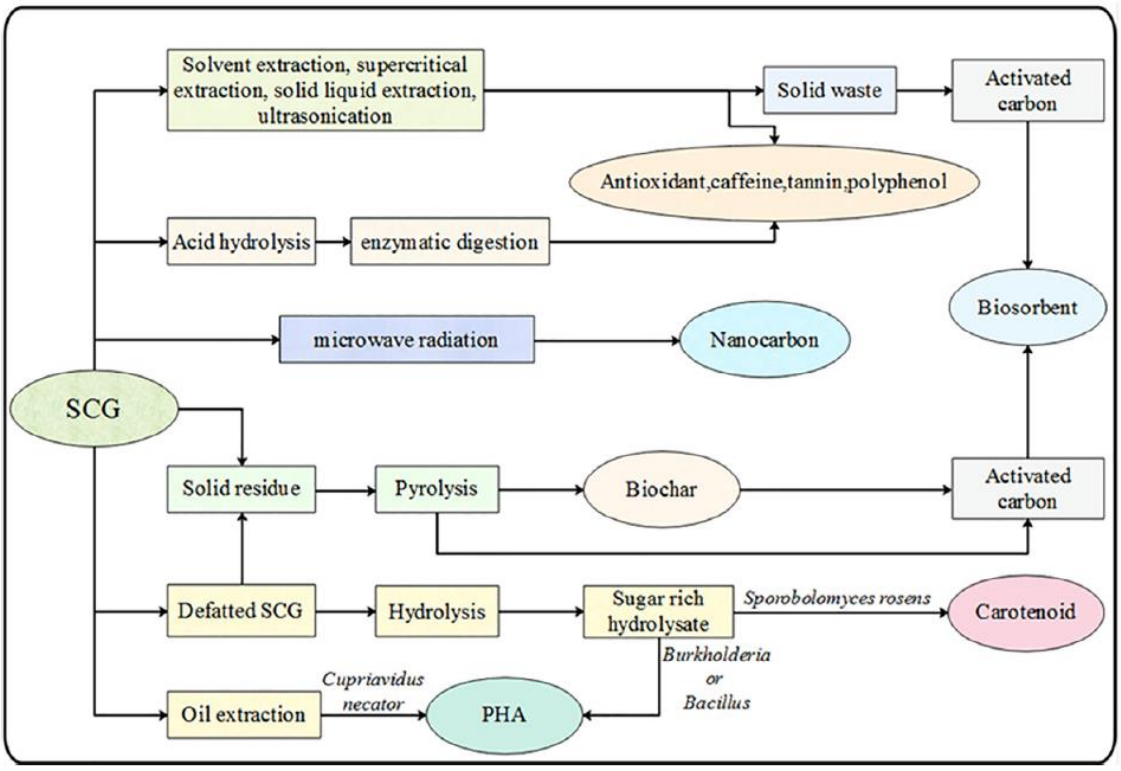

Figure 21 The various integrated biorefinery routes of value added products recovery (Rajesh Banu et al., 2020b)

On the other hand, Surendra et al. (2015) presents in its review a superstructure based on anaerobic digestion as the main bioprocess (Figure 22), the study shows the different routes that can have the biogas, the digestate (liquid and solid phase), integrating processes such as algae production, thermochemical processes, separation, extraction, and synthesis of new products. The review concludes by showing the complexity of the technical-economic and environmental analysis to guarantee the viability of the biorefineries.

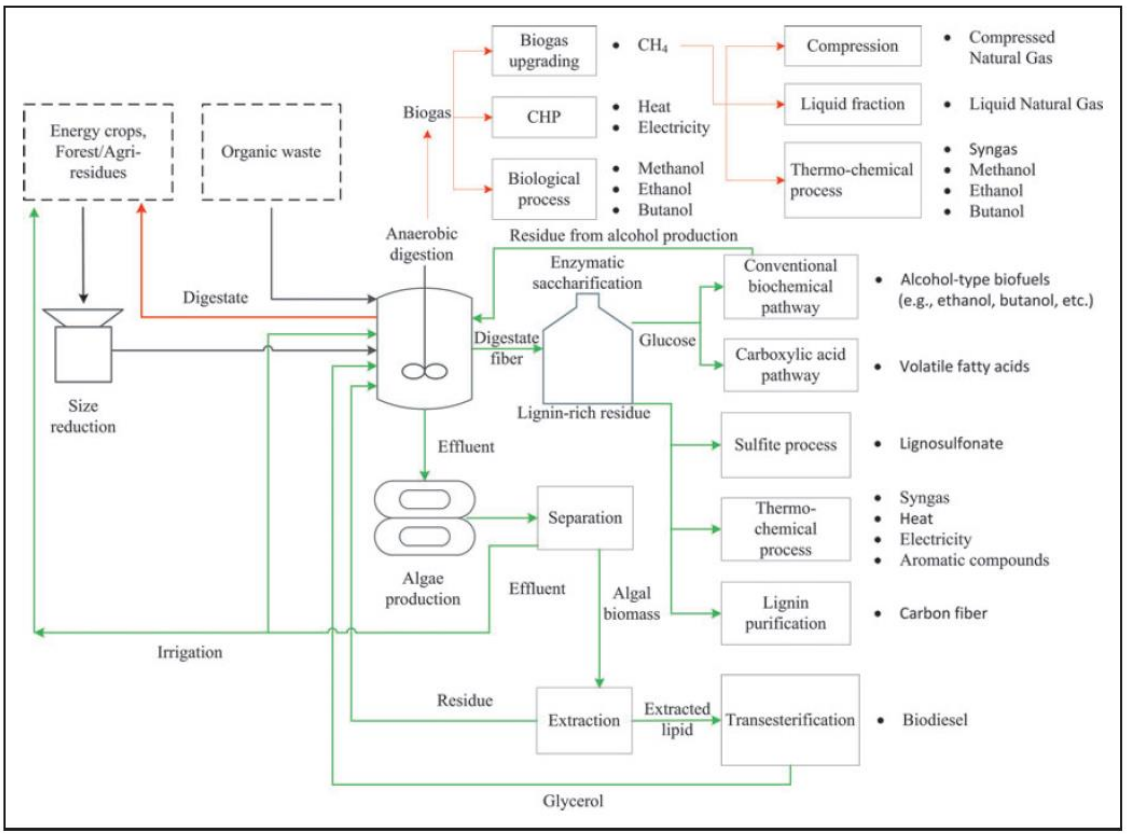

Figure 22 Schematic of an AD-based biorefinery for producing biofuels and biobased products (Surendra et al., 2015).

Similarly, Bastidas-Oyanedel et al. (2015) presented a review of biorefineries applied to dark fermentation and the different possible routes of products and by-products (Figure 23). The study concludes by showing that the dark fermentation biorefinery presents a high flexibility in the different downstream processing options, considering the composition of its residues. Furthermore, the products of dark fermentation can be purified and/or use as platform chemicals in subsequent (bio)process to produce fuels, fine chemicals, and bio-syngas. These features make dark fermentation a core bioprocess in the biorefinery concept. The studies in Figures 22 and 23 show the possible routes to be followed theoretically after anaerobic digestion and fermentation. As an advantage it is shown that the products and residues can be utilized in multiple ways. However, the theoretical studies do not show technical-economic and environmental analyses that show the viability of the routes for the by-products.

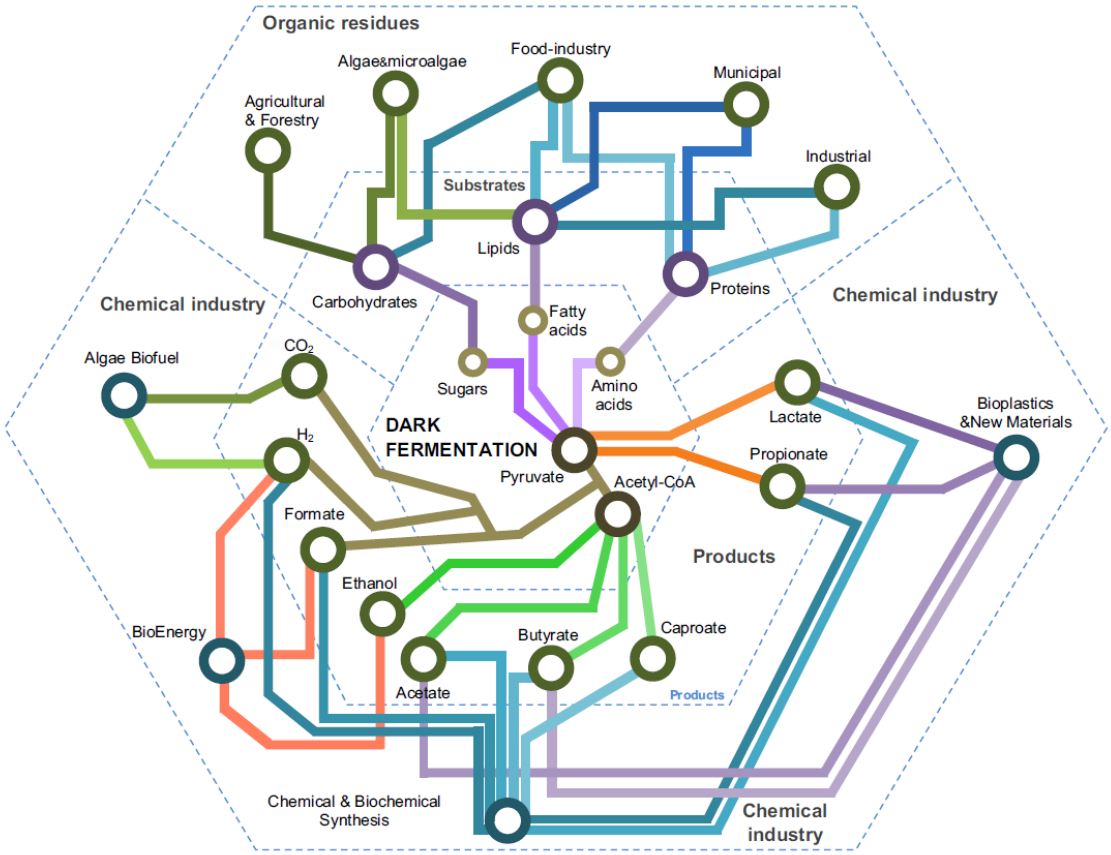

Figure 23 Dark fermentation as a core bioprocess in the bio-society (Bastidas-Oyanedel et al., 2015)

1.8.2 Optimization

The methodological approach to biorefinery design based on the concept of optimization considers a follow-up of the chemical species, connecting the different streams with the available processing technologies, and using potential configurations of interest. Optimization is developed through the formulation of mathematical models (e.g., linear, and non-linear mixed integer programming models MIP - MINLP) and their objective is to maximize the yield or economic potential depending on constraints such as process models, species distribution and flows with respect to conversion technologies and techno-economic data. This methodology takes a set of feedstocks and products that achieve multi-objectives when synthesized (e.g., minimum production cost, maximum yield) using several processing technologies (conversion routes). The optimization-focused conceptual design procedure attempts to make a quick sweep of numerous alternatives to generate a conceptual design of

the main biorefinery components, integrate technologies, and lay the foundation for a detailed techno-economic analysis (Moncada B. et al., 2016).

Bao et al. (2011) presents three case studies in which this methodology is applied. The first case considers obtaining a maximum yield for bio-gasoline production from cellulosic biomass by choosing a technology pathway that maximizes gasoline yield based on the idealistic case of assuming the maximum theoretical yield for each technology block. In the second case, the level of complexity is increased by taking two biomass feedstocks and including conversion and yield data. The third and last case studies the minimum recovery period of the process in economic terms as an optimization objective (Bao et al., 2011).

The solution of these cases demonstrates the effectiveness and applicability of the developed approach and illustrates its ability to generate a wide range of pathways that achieve the same objective but vary significantly in their components and interconnections. However, this approach may provide solutions with difficulties of application at the industrial level (considering mature and only scientifically preliminary technologies). For example, Gong and You (2015) consider an example of an integrated superstructure capable of producing biodiesel, hydrogen, propylene glycol, glycerol-tert-butyl ether, and poly-3-hydroxybutyrate from microalgae (Gong and You, 2015). The superstructure considers alternative technologies and equipment, such as gasification technologies, refrigeration options, hydrogen production sources and Fischer-Tropsch synthesis catalysts (Gong and You, 2014a, 2014b). The economic objective is measured by net present value (NPV), and the environmental concern is measured using global warming potential (GWP).

1.8.3 Biorefinery development

Based on the processes studied during the literature review and the biorefinery conceptual construction method, a biorefinery superstructure is proposed for the treatment of the biomass under study (cocoa mucilage, coffee mucilage, and swine manure). Figure 24 divides the super structure into 9 steps (feeding, bioprocesses, separation of solids and liquids, thermochemical processes, separation and improvement of biogas, physicochemical processes, generation of new products, potential products and finally their uses). In the case of the superstructure presented, the pretreatment processes are not exposed, which are exposed by authors such as Clauser et al. (2021) indicating the initial phase of the

bioprocesses (hydrolysis and acidogenesis) as pretreatment of the substrate. However, when comparing the said superstructure, all the proposed phases are identified from the feeding to the uses for a fermentation process, which the authors identify as purification, conversion, and concentration and which are shown by means of recovery, purification, and concentration processes to obtain xylitol, formic acid, levulinic acid, furfural, and others. In this case, thermochemical processes for fermentation residues are not contemplated and in its results an analysis is made considering technical factors, economic analysis, and economic strategies to improve the production costs, finding results of viability of the schemes. On the other hand, the scheme presented is in agreement with those presented by Clauser et al. (2021) showing the frequency with which recent biorefinery schemes start with the dark fermentation process in substrates rich in carbohydrates and starch. The short time of the dark fermentation process implies small reactors generating ease of operation in the other equipment, as well as giving priority to the generation of hydrogen, a gas with higher calorific value. Authors such as Alibardi et al. (2020) and Moncada B. et al. (2016) show that after simple processes such as dark fermentation, the recovery of VFAs to produce PHA/PHB and PLA is feasible. As well, when digestion processes are operated after fermentation, it is more viable to recover nutrients and generate compost for agriculture.

In this context, the superstructure presented in Figure 24 generates viable connections following main studies and recommendation (Alibardi et al., 2020; Clauser et al., 2021; Moncada B. et al., 2016).

The superstructure gives a general idea of the different possible routes. Therefore, the first biorefinery scheme focuses on the results obtained in the evaluation of energetic potential for the dark fermentation followed by anaerobic digestion process (ADF). Processes P, Q and R of the Figure 24 show the treatment and separation of biogas that allow to bring it to the quality (purity) of use for energy production or its sale as fuel. Regarding the digestate (solids and liquid), the current simulation considers all the compounds in liquid phase and the percentage of water exceeds 90% in all cases. Considering that most of the authors perform nutrient recovery and compost generation processes, these processes (Processes E and H, Figure 24) were selected in the biorefinery for the environmental assessment. On the simulation of the schemes, the treatment of gases was prioritized as the main product, since they are a direct source of energy for the agroindustry, which currently consumes 1% of the

country's final electricity consumption per year (IEA, 2020). The following two schemes are based on the possible combinations that the superstructure shows for biogas (Production of by-products, W, X and Z, Figure 24).

The conceptually proposed superstructure for the biorefinery is consistent with the processes proposed by Rajesh Banu et al. (2020b) who proposes bioprocessing (AD and DF) as well as thermochemical processes for the core design for coffee grounds waste. However, in the scheme there are no flow relationships between the processes. Unlike the process of the same author, which is based on the routes for the generation of added value that has as its main objective the production of other products such as PHA, carotenoid, activated carbon, among others. One of the most similar superstructure schemes is the one presented by Surendra et al., 2015 where it presents AD followed by bioprocesses such as: enzymatic, algae and the integration of thermochemical processes. Comparing the schemes shows that the superstructure of Surendra et al. (2015) broadens the working range of thermochemical allowing to obtain products such as butanol, lignosulfonate. The rest of the by-products are considered. It is evident that in the literature the exclusive recovery of methane in digestion processes is found more frequently, omitting the percentage of hydrogen generated. Furthermore, there are no proposals for processes such as ADF in biorefinery superstructure schemes.

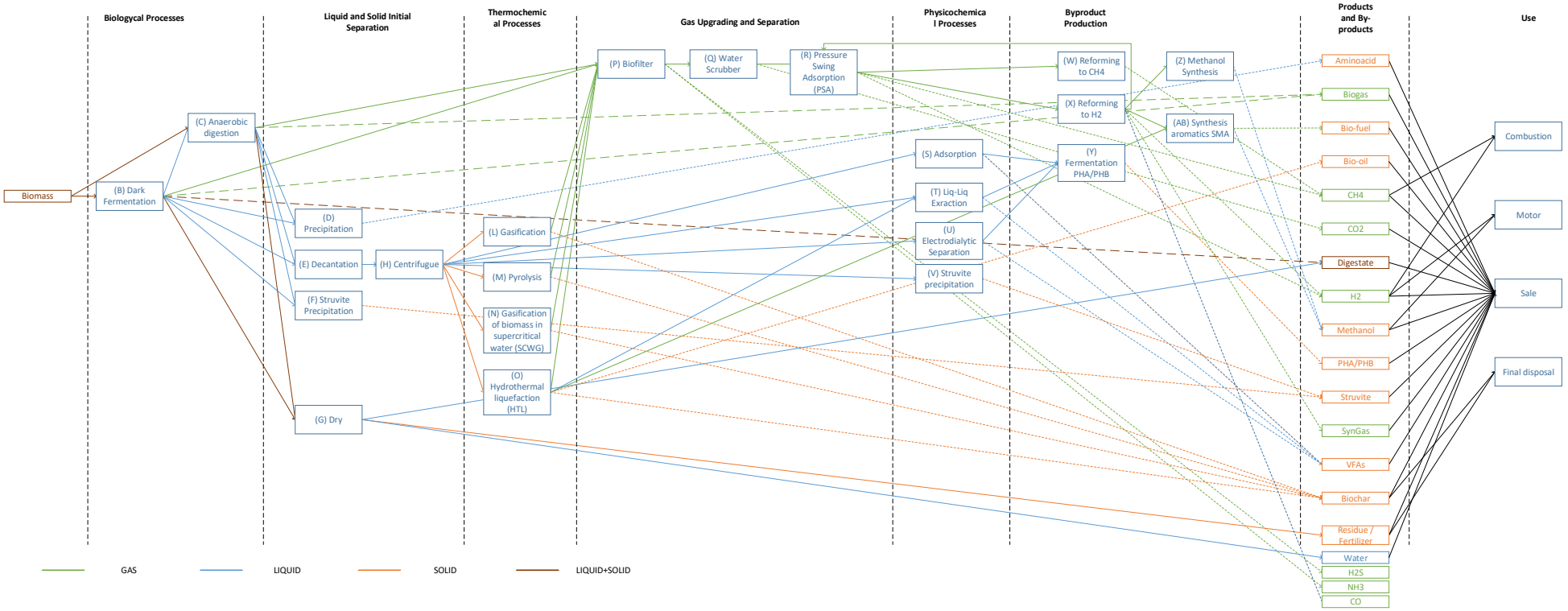

Figure 24 Theoretical superstructure for biorefinery scheme construction based on AD and DF bioprocesses.

1.9 Techno-economical evaluation

The sustainable evaluation is complemented by the techno-economic evaluation of the processes whose main objective is to demonstrate the economic viability of the proposed schemes. For the realization of the technical-economic evaluation it is necessary to calculate the capital cost and the operational cost.

The capital cost is the value of initial investment, part of the sizing of the equipment to calculate their prices including transportation factors, nationalization taxes, installation, and others. Depending on the stage of engineering, the equipment is considered in the capital cost and thus its percentage error with respect to the real value. The equipment presented in recent studies include tanks, transport equipment (pumps), compressors, instrumentation, installation, piping, insulation, electrical installation and civil adequacy.

The operational cost is the related price per unit of working time of the plant (e.g., $/day) and it relates all the constant costs and, according to the plant design stage, the margin of error. The operational costs presented are raw materials, service or utility requirements (water, steam, electricity, fuels, refrigerants, chemical consumption), human resources, waste disposal, and transportation (Seider et al., 2008).

Depending on the stage (analysis or engineering), certain costs are assumed in the evaluation, and their values are calculated with databases (e.g., SuperPro, Aspen Plus), national and international cost reports, heuristic equations, cost equations (with tax factors, annual increment, etc.), articles or past processes in the industry. Recent studies show the economic viability of biorefineries by calculating the Net Present Value (NPV), Internal Rate of Return (IRR) and Payback Period (PBP). Those indexes are calculated by means of a sensitivity analysis or the study of production over time between 5 and 10 years (Arora et al., 2018; Demichelis et al., 2018; Sy et al., 2018).

1.9.1 Environmental assessment

Environmental analysis can be developed following Life Cycle Assessment (LCA) methodology, where potential environmental impacts are quantified and identified from the beginning to the end of a process. The system boundaries can be considered from any segment of the product chain [Gate-to-Gate, Cradle-to- Gate, Cradle-to-Grave, Cradle-to-

Cradle] to include various stages like biomass cultivation, transport, processing of biomass and products manufacture in biorefinery, transport of products to the consumers, customer use of the products, and product disposal to the environment.

The LCA is carried out in four phases: identification of the objective and scope, which establishes the reason for the study, its application and who it is aimed at. It should be noted that the LCA can have different scopes depending on the stages of the life cycle to be analyzed, as summarized by the following points.

- The door-to-door LCA, which includes only the stages of the production process followed to obtain the final product.
- The cradle-to-grave LCA, which considers, in addition to the stages of the production process, the extraction and preparation of raw materials.
- The door-to-grave LCA, which includes the production process of the product, the extraction and preparation of raw materials.
- The cradle-to-grave LCA, which covers the production process of the product and its subsequent final disposal.
- The cradle-to-grave LCA, which studies the extraction and transport of raw materials, the production, distribution and use of the product and its final disposal.
- The cradle-to-cradle LCA, which, in addition to the stages mentioned above, takes into consideration the reintroduction of the product in the same production cycle or in another.

The next stage is the inventory analysis, in which the input and output streams of the production process are identified and quantified. Subsequently, in the impact assessment, the results of the inventory analysis are used to determine the contribution of the production process to each impact category. Finally, the interpretation of results is carried out in which conclusions and recommendations are made according to the objectives and scope of the study to enable decision making. Although studies of energy production from waste biomass have been developed under the LCA approach, there is very little information associated with the potential environmental impacts of biohydrogen synthesis following the FO route.

The development of the LCA depends on the method selected for the assessment, as it allows the results to be compared between schemes, with other studies or with processes already in place. For example, the selection of site-specific methods was beneficial for assessment from the perspective of regional characteristics, while the choice of generic site-specific methods was conducive to assessment in relation to the full range of negative impacts. In some assessment methods, environmental or social mechanisms are used to relate so-called intermediate impact categories to final impacts or damages. For example, CO_2 emissions can be used directly as a stand-alone indicator of environmental performance, but they can also be counted together with other emissions as greenhouse impacts through their global warming potential (midpoint level). In addition, global warming impacts can be assessed as human health damages (endpoint level) through mechanisms related to, for example, changes in disease incidence and population displacement. In addition, some impacts cannot be quantified or are best described by qualitative characteristics, particularly when impacts on society are involved. In these cases, indicators of a qualitative nature can be used to relate the project to impact categories through a semi-qualitative analysis, for example using scales from 1 to 10 (Katakojwala and Mohan, 2021). One of the methods that has been used in the evaluation of biorefineries in recent years is described below.

1.9.2 Life cycle impact assessment

ReCiPe is an impact assessment (LCIA) method in an LCA. In Life Cycle Impact Assessment (LCIA), emissions and resource removals are translated into a limited number of environmental impact scores using so-called characterization factors.

There are two common methods for deriving characterization factors, namely at midpoint level and at endpoint level. ReCiPe calculates:

- 18 midpoint indicators
- 3 endpoint indicators

Midpoint indicators focus on individual environmental problems, for example climate change or acidification. Endpoint indicators show environmental impacts at three higher levels of aggregation, namely 1) effect on human health, 2) biodiversity and 3) resource scarcity. Converting midpoints to endpoints simplifies the interpretation of the LCIA results. However, with each aggregation step, uncertainty in the results increases.

The Figure 25 shows an overview of the structure of ReCiPe where the relationship between LCI parameters (left), midpoint indicator (middle) and endpoint indicator (right) in ReCiPe 2016 is explained (National Institute for Public Health and the Environment, 2021).

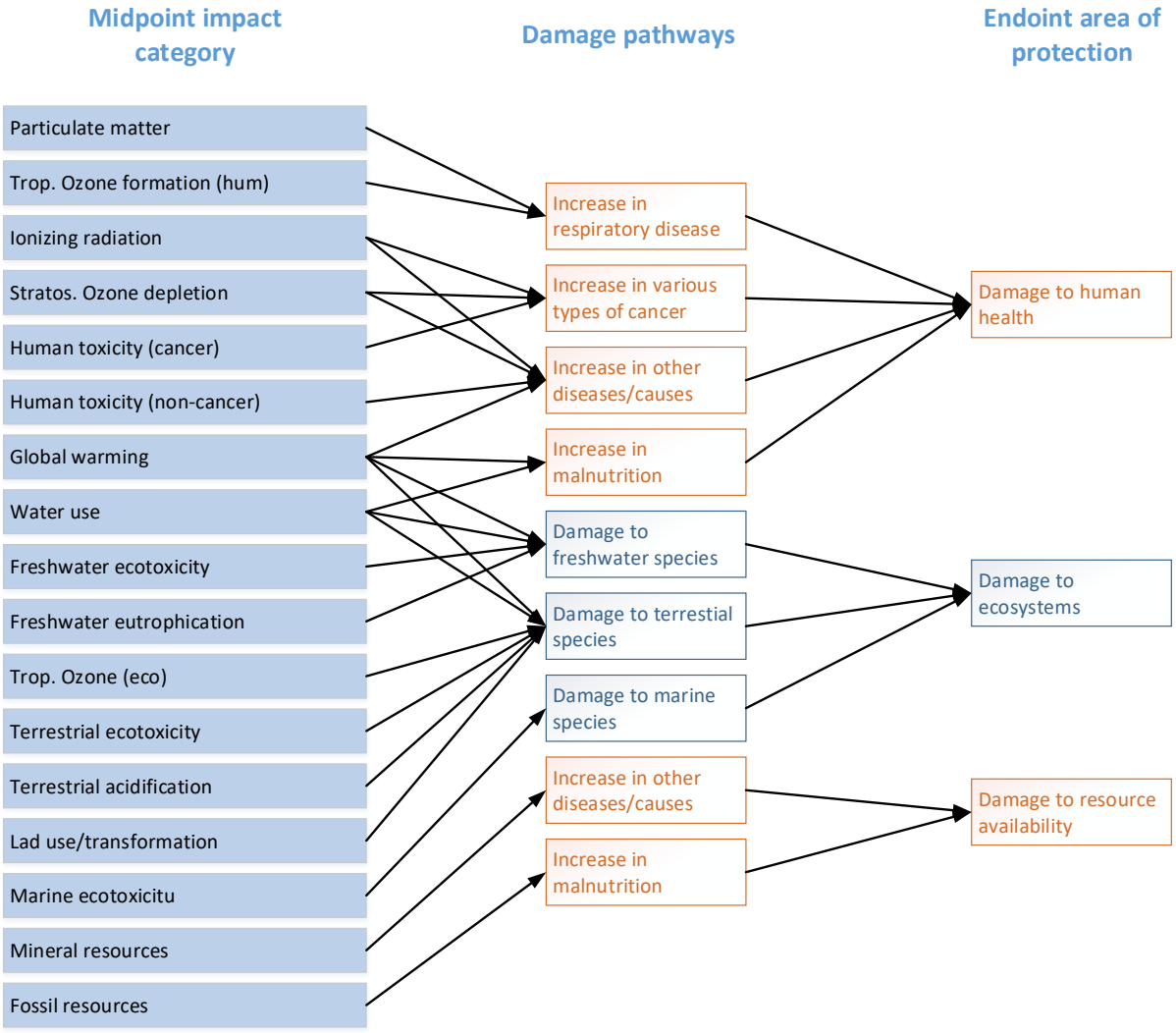

Figure 25 Overview of structure ReCiPe (National Institute for Public Health and the Environment, 2021).

3.CONCLUSIONS

Within the context of a continuous increase in energy demand worldwide, the economic and environmental problems generated using of fossil fuels are more and more important. Therefore, biomass is shown as a viable and sustainable alternative for energy generation. In addition to the generation of biofuels, biomass processes can provide raw materials for new processes and the production of by-products that will add value to the design of biorefineries. As an example, the production of methanol, volatile fatty acids, biopolymer among others could be mentioned. The study of biomass treatment is still a subject of debate due to the energy and production yields finally obtained, generating new challenges in the optimization of bioprocesses and thermochemical processes. At least, waste treatment support for the growth of agro-industry.

In the Colombian context, coffee, cocoa, and swine manure are part of the growing agro-industrial activities. Currently, almost all the residual biomass from the above-mentioned wastes is used for composting or incineration processes. However, the literature shows the interest in the use of coffee and cocoa due to their high carbohydrate content (> 60% w/w dry) and pig manure, due to the amount available for biogas production in bioprocess and thermochemical process. The bioprocess, anaerobic digestion and dark fermentation, studies have focused on improving methane and hydrogen production yields by experimentally adjusting operating time, initial organic load, temperature, and inoculum. The best results are obtained at neutral pH, between 10 and 20 days of dark fermentation processes and between 20 and 30 days of anaerobic digestion. Recent authors have presented a relationship between pH and C/N ratio with respect to biogas production yield, showing that at lower C/N (9 to 12) production yields are close for all pHs while at C/N ratios between 15 and 17 better yields are obtained at pH = 11 or 12. Above all, in all studies a high relationship is found with biomass composition, especially with carbohydrate content. The development of mathematical models of bioprocesses has been based on the ADM1 model and its recent modifications that have allowed to adjust the biogas production estimations in anaerobic digestion and dark fermentation validating the results with the yield value of biogas, CH_4 or H_2 production and their respective experimentally measured values. By contrast, thermochemical processes, by their nature, are simpler to simulate since their modeling depends on the reactions, kinetics

involved and operational conditions. It reports not only production yields but also energy yields and energy integration showing energy efficiencies greater than 60% are one of the most viable processes for biomass. In particular, hydrothermal processes that allow high water content are the current focus of study for the optimization, such as pretreatment of biomass or treatment of digestate resulting from bioprocesses.

Although bioprocesses and thermochemical processes are well developed in the literature, they are still a source of development. Nowadays, studies are looking for the bioprocess and thermochemical processes integration to maximize biogas and energy production yields. Literature reviews present the possibility of generating biorefineries as optimal valorization processes of residual biomass. However, there is no rigorous study that studies the yields and production and energy efficiencies of such integrations. Moreover, there is no complete study in the literature of the three biomasses available for Colombia and their possible mixtures. Therefore, a list of 23 bioprocesses, thermochemical, separation and production processes that valorize biomass is presented. Furthermore, it is shown that the use of the digestate for its valorization is related to the quality (water concentration); high water concentrations have generated deficiencies in the digestate valorization processes related to the dehydration process. Considering that of the three biomasses, swine manure is the one that is present in the majority, it is concluded that the final digestate will have a high-water content, which makes it not very viable for thermochemical processes. Thus, this work is focused on energy optimization by obtaining biogas (CH_4, H_2 and CO) via biological processes (anaerobic digestion, AD, and dark fermentation, DF) and reducing CO_2 emissions (Processes B, C, E, H, P, Q, R, X, Z from Figure 24). Based on the mentioned above and looking for viable alternatives to the treatment of biomass, aims are to use the technological tools for the study of biorefinery designs that integrate the bioprocesses with the separation, reforming, and synthesis technologies for new by-products.

The study requires the experimental study and the development of simulation models of the bioprocesses (AD and DF), simulations that are validated with the experimental results and calculations of theoretical maximums. Based on the simulation results and the availability of residual biomass, it is necessary to calculate the energy potential of the biomasses studied in the whole Colombian territory and the energy efficiencies of the bioprocesses designed in series, in order to present the best treatment proposal. Following the previous results and in a conceptual way, three biorefinery schemes are presented that seek

the maximum use of biomass, however, to guarantee the optimal design of the processes, 4 different scenarios are presented for each scheme that integrate plant design and energy integration heuristics. For the evaluation of the biorefineries, an energy analysis is performed, based on the results of the process simulation. The sustainability of the biorefineries is evaluated using the life cycle analysis method. From the study, a methodology for the design and evaluation of biorefineries as sustainable alternatives for the treatment of biomass and generation of biofuels is shown. Methodology and simulation designs that can be applied in the biorefinery field to different case studies.

CHAPTER II MATERIALS AND METHODS

1.INTRODUCTION

Recent studies and biorefinery approaches for biomass valorization have focused on reported yields for the different bioprocesses and thermochemical processes. However, rigorous studies of production and energy efficiencies to justify the biorefinery design models are not found in the literature. Therefore, experimental processes and/or simulation models must be developed in biorefinery schemes to evaluate them technically and environmentally.

The validation of the mathematical models from the experimental perspective is particularly necessary for bioprocesses, since process yields depend on the characterization of the residual biomass. Therefore, this chapter presents materials, and methods for the experimental development of anaerobic digestion and dark fermentation for the treatment of blends of the three biomasses under study (coffee mucilage, cocoa mucilage, and swine manure), followed by the implementation of the ADM1 mathematical model in simulation, the validation of the model, and the study of Colombia's energy potential from the bioprocesses.

Following the development and optimization of the bioprocesses, the materials, and methods for the development of the simulation of the separation, reforming, and synthesis processes that allow the valorization of the biogas obtained from the bioprocesses and the formulation of biorefinery schemes are presented. The process integration approach focuses on the biorefinery optimization, increasing the biogas production and minimizing the impact produced by the greenhouse gas emissions. For the evaluation, the steps of mass yield analysis, life cycle assessment, pinch analysis and energy yield are detailed at the end of this Chapter.

2.EXPERIMENTAL SET-UP OF THE BIO-PROCESS

This first section of Chapter II describes the experimental design for the hydrogen and methane production from the dark fermentation (DF) and anaerobic digestion (AD) processes. The experiments were carried out at Colombian Universities (Universidad EAN, Universidad Cooperativa de Colombia and Universidad Santo Tomas). Swine manure was collected directly from the pig sheds of the Marengo agricultural center of the National University of Colombia. Pig farms usually wash the sheds, obtaining a liquid residual biomass, so the manure was worked in dilution for the study. The coffee mucilage was collected after the process of coffee grinding and before preserving it in the freezer, it was sieved to remove large particles, leaving only the soluble phase. The cocoa mucilage, on the other hand, was extracted directly from the fruit through a manual operation and then preserved frozen. These last two residues, due to their high sugar content, required a strictly low temperature to be maintained throughout the collection and treatment process.

1.10 Experimental design

The design was proposed considering the volume of H_2 as dependent variable for dark fermentation, and the volume of CH_4 as dependent variable for anaerobic digestion. The independent variables proposed for the two biological processes were the coffee mucilage to cocoa mucilage ratio (CFM:CCM), the carbon to nitrogen ratio (C/N), and the substrate concentration (gCOD/L) of each blend, all evaluated at three levels, low (denoted as -1), midpoint or medium (denoted as 0) and high (denoted as +1). In the ratio of substrates, coffee and cocoa mucilage prevailed as carbon sources, while swine manure was the nitrogen source. The chemical oxygen demand concentration was used to study the response to low, medium, and high concentration blends. Finally, the C/N ratio sought to associate the response to the stability of the process, the most typical values reported are between 20-30 C/N (Carotenuto et al., 2020), given that high carbon and/or nitrogen contents can affect the dynamics of the microorganisms. The experiments were carried out in triplicate and in cases where operational problems or uncertainty in the results were encountered, the experiments were repeated.

A Box-Behnken design (*Table 10*), based on the three independent parameters already mentioned above, was used to determine the number of blends for the comparative experiments: (i) the dried mass ratio between CFM and CCM (CFM:CCM ratio), (ii) the mass ratio of C to N (C/N ratio), and (iii) the total organic load. For each parameter, three levels were considered: the CFM:CCM ratios were 3:1, 1:1, and 1:3; the C/N ratios were 25, 35, and 45; and the organic loads, based on chemical oxygen demand (COD), were 2, 5, and 8 $gCOD \cdot l^{-1}$. SM was used as N rich substrate to set the C/N ratio of each blend. Then, distilled water was added to set the COD concentrations of each blend.

Table 10 Total organic loads, CFM:CCM dried mass ratios, and C/N mass ratios of the different blends used for laboratory experiments of AD and DF.

Blend	Organic load $gCOD \cdot l^{-1}$	Substrates ratio CFM:CCM	C/N ratio
1	2	3:1	35
2	2	1:3	35
3	8	3:1	35
4	8	1:3	35
5	5	3:1	25
6	5	1:3	25
7	5	3:1	45
8	5	1:3	45
9	2	1:1	25
10	8	1:1	25
11	2	1:1	45
12	8	1:1	45
13	5	1:1	35

The experiments were carried out in a thermostatized bath with a temperature control system and a volume displacement system for the measurement of biogas (methane and/or hydrogen) from each mixture, using a NaOH solution (pH > 10) as a CO_2 trap. The experiments were carried out in 250 mL bottles with a total working volume of 200 mL (Figure 26).

The inoculum originally used was from a mixed culture of the anaerobic wastewater treatment plant of the Alpina company, in this type of culture there are both hydrogen-consuming and hydrogen-producing microorganisms. For this reason, the inoculum was heat pretreated (90°C at 30 min, followed by cooling with ice) to eliminate hydrogen consuming microorganisms such as methanogenic archaea, which are unable to sporulate at high temperature conditions. The inoculum used for each bottle was 20.62 ml and distilled water was used to complete the total working volume. However, as the inoculum came from a bioreactor. Two reactors, hereafter referred to as "blanks", containing a dilution of the inoculum were set up and the production of methane and hydrogen was monitored. The biogas produced from each blank reactor was subtracted from each of the experimental reactors. Assuming that it corresponded to methane or hydrogen production according to the process (AD or DF respectively).

The bottles were placed on a thermostable plate under mesophilic conditions (35°C) and a buffer solution (10 ml) was added to maintain the pH condition of 5.5 for dark fermentation. All bottles were sealed with rubber and silicone stoppers.

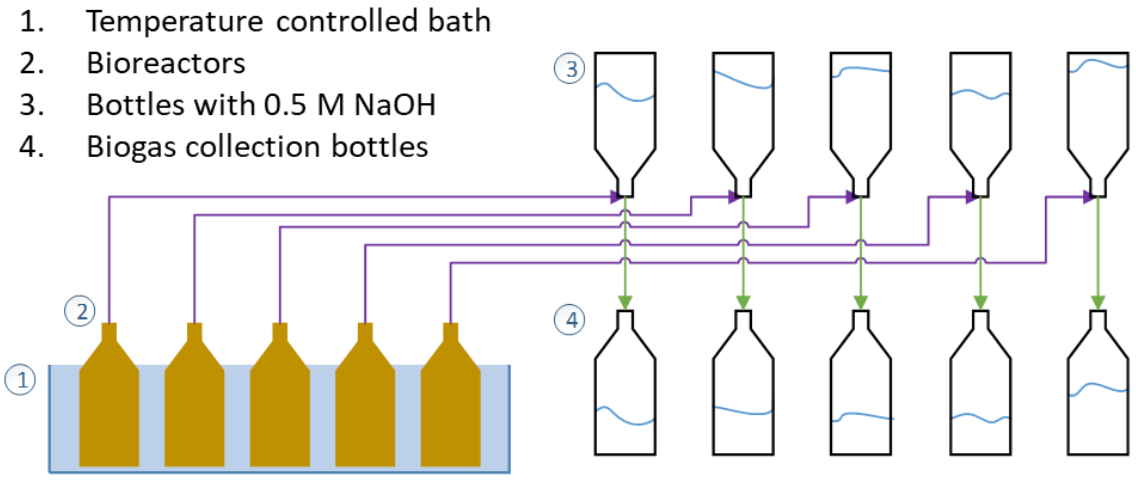

Figure 26 Experimental set-up of AD and DF bioprocesses for methane and hydrogen production with volume displacement and biogas collection (Ochoa et al., 2021; Rangel et al., 2021).

The duration of the tests was between 10 and 20 days for AD, and between 5 and 12 days for DF experiments following the optimum production yield value reported in the literature. (Gao et al., 2021; Qi et al., 2021; Qu et al., 2021). The experimental biogas yields (mL CH_4·g COD^{-1} and mL H_2·g COD^{-1} for AD and DF, respectively) were calculated based on the cumulated volume of biogas produced from each experiment. All the tests were performed in triplicate and average biogas yields were determined for each experimental condition.

The residual biomasses selected for this study were coffee mucilage (CFM), cocoa mucilage (CCM) and swine manure (SM), which are related to the most relevant agro-industrial activities in Colombia. Methanogenic granulated sludge was obtained from the Alpina S.A. sewage plant in Sopo, Cundinamarca (Colombia) and used as inoculum. Cocoa mucilage was collected from a medium-scale farm during the processing of the fruit into cocoa beans. Swine manure was obtained from the Centro de Investigación Agrícola Marengo (C.A.M.) of the Universidad Nacional de Colombia located in Mosquera - Cundinamarca and coffee mucilage was collected during the mechanical demucilagination process in a farm located in Cundinamarca. These residues were studied as a substrate. The biogas was collected continuously in the collection system (Tedlar® bags). The system allowed to maintain pH and temperature conditions before its analysis.

1.11 Analytical methods

1.11.1 Biomass characterization

The biomass characterization was carried out partially in the research group's laboratory, while another part of the biomass was sent to a private laboratory to obtain the results of its characterization. It is important to note that characterization was not carried out for all the tests performed. In order to use the simulation, it was necessary to perform an initial characterization of the biomass at the beginning of each experiment.

Total volatile solids (TVS) and total organic load (COD) of the samples were determined by standard methods (APHA 2005). Total carbohydrate (glucose and xylose), cellulose, hemicellulose, lignin, and protein were determined by high performance liquid chromatography (HPLC), by using a chromatographer Agilent Model 1200 (Agilent Technology, USA). Total organic carbon (C) was determined by the Walkley Black titration method according to the Colombian technical norm NTC 5167 (2003). Total organic nitrogen (N) and total organic sulfur (S) were determined after acid digestion according to the Kjeldahl method and to the barium sulfate precipitation method, respectively. Then, oxygen (O) and hydrogen (H) contents were estimated stoichiometrically.

1.11.2 Gas analysis

As the experiments were set up with a biogas collection system (Tedlar® bags). One litter from a NaOH solution 1M (pH > 10) was used as carbon dioxide gas (CO_2) trap and, therefore, it is assumed that the displaced gas only corresponds to CH_4 in AD process and H_2 in DF process.

1.12 Experimental Biogas production yields

The daily biogas volume measurement allowed to obtain the total volume of biogas produced at the end of the experiment. In the two processes, for the thirteen proposed blends, the volume of biogas was measured with respect to the initial organic load.

For the anaerobic digestion process, the total methane production was measured, following the equation (Eq. 1), where ml CH_4 is the volume of methane produced per unit of volume (ml) and the chemical oxygen demand (COD) the total organic content of the blend per unit of volume (g COD).

$$Yield_{AD} = \frac{ml\ CH_4}{g\ COD_i} \quad \text{Eq. 1}$$

For the dark fermentation process, the total hydrogen production was measured, following the equation (Eq. 2), where ml H_2 is the volume of hydrogen produced per unit of volume (ml) and COD the total organic content of the blend per unit of volume (g COD).

$$Yield_{DF} = \frac{ml\ H_2}{g\ COD_i} \quad \text{Eq. 2}$$

3.SIMULATION MODEL DEVELOPMENT AND EVALUATION

1.13 Bioprocess

1.13.1 Components and properties specifications

The simulation includes 63 components (Table 11) of which 60 are declared as conventional components and only 3 as pseudocomponents (proteins, insoluble proteins, and inert components). The physicochemical properties among the compounds were calculated with the Soave-Redlich-Kwong method (SRK-based method). Additionally, properties were calculated with the NRTL and IDEAL methods. The process simulation to evaluate the mass and energy balance was carried out in the simulation software Aspen Plus V11. In all cases the simulation compounds were only considered in liquid and gas phases.

Table 11 Selected components specifications

	Component ID	Component name	Alias		Component ID	Component name	Alias
1	WATER	WATER	H2O	**32**	**PROLINE**	PROLINE	C5H9NO2-N8
2	GLYCEROL	GLYCEROL	C3H8O3	**33**	**HYDROGEN**	HYDROGEN	H2
3	OLEIC-AC	OLEIC-ACID	C18H34O2	**34**	**METHANE**	METHANE	CH4
4	DEXTROSE	DEXTROSE	C6H12O6	**35**	**INDOLE**	INDOLE	C8H7N
5	ACETI-AC	ACETIC-ACID	C2H4O2-1	**36**	**FROMAMID**	FORMAMIDE	CH3NO
6	PROPI-01	PROPIONIC-ACID	C3H6O2-1	**37**	**H2S**	HYDROGEN-SULFIDE	H2S
7	ISOBU-01	ISOBUTYRIC-ACID	C4H8O2-4	**38**	**CH4S**	METHYL-MERCAPTAN	CH4S
8	ISOVA-01	ISOVALERIC-ACID	C5H10O2-D3	**39**	**BENZENE**	BENZENE	C6H6
9	H+	H+	H+	**40**	**PHENOL**	PHENOL	C6H6O
10	OH-	OH-	OH-	**41**	**H2CO3**	CARBONIC-ACID	H2CO3
11	NH3	AMMONIA	H3N	**42**	**HCO3-**	HCO3-	HCO3-
12	NH4+	NH4+	NH4+	**43**	**CO3-2**	CO3--	CO3-2
13	CO2	CARBON-DIOXIDE	CO2	**44**	**HS-**	HS-	HS-
14	C5H7NO2	ETHYL-CYANOACETATE	C5H7NO2	**45**	**CELLULOS**	CELLULOSE	CELLULOSE
15	ARGININE	ARGININE	C6H14N4O2-	**46**	**HEMECE**	GLUTARIC-ACID	C5H8O4

			N2		**LL**		
16	HISTIDIN	HISTIDINE-E-2	C6H8N3O2-E	**47**	**GLUCOSE**	DEXTROSE	C6H12O6
					TRIOLEI		
17	LYSINE	LYSINE	C6H14N2O2	**48**	**N**	TRIOLEIN	C57H104O6
18	TYROSINE	TYROSINE	C9H11NO3	**49**	**TRIPALM**	TRIPALMITIN	C51H98O6
19	TRYPTOPH	TRYPTOPHAN	C11H12N2O2	**50**	**PALM**	1-HEXADECANOL	C16H34O
						SN-1-PALMITO-2-	
20	PHENYLAL	L-PHENYLALANINE	C9H11NO2	**51**	**SN-1--01**	OLEIN	C37H70O5-1
						SN-1-PALMITO-2-	
21	CYSTEINE	CYSTEINE-E-2	C3H6NO2S-E	**52**	**SN-1--02**	LINOLEIN	C37H68O5-1
22	METHIONI	METHIONINE	C5H11NO2S	**53**	**XYLOSE**	D-XYLOSE	C5H10O5
					FURFURA		
23	THREONIN	THREONINE	C4H9NO3	**54**	**L**	FURFURAL	C5H4O2
					LINOLEI		
24	SERINE	SERINE	C3H7NO3	**55**	**C**	LINOLEIC-ACID	C18H32O2
25	LEUCINE	LEUCINE	C6H13NO2	**56**	**STARCH**	CELLULOSE	CELLULOSE
					ETHANO		
26	ISOLEUCI	ISOLEUCINE	C6H13NO2-I	**57**	**L**	ETHANOL	C2H6O-2
					PROTEIN		C13H25O7N3
27	VALINE	VALINE	C5H11NO2	**58**	*****		S
					INS-		C4.39H8NO2.
28	GLUTAMIC	L-GLUTAMIC-ACID	C5H9NO4	**59**	**PROT***		1
29	ASPARTIC	ASPARTIC-ACID	C4H7NO4	**60**	**ACETATE**	CH3COO-	CH3COO-
30	GLYCINE	GLYCINE	C2H5NO2-D1	**61**	**INERT***		INERT
					CARBO-	CARBON-	
31	ALANINE	ALANINE	C3H7NO2	**62**	**01**	MONOXIDE	CO
					METHA-		
				63	**01**	METHANOL	CH4O

* Pseudocomponent

The pseudo components were calculated with the ASPEN property's method with the following properties (Table 12):

Table 12 Pseudocomponents properties included in Aspen Plus

Component	Average NBP (K)	Gravity Density (kg/cum)	Molecular weight
PROTEIN	343.15	1430	367.42
INS-PROT	343.15	1430	116.3949
INERT	1000	3000	100

1.13.2 Anaerobic digestion and dark fermentation

A maximum of three units were used in Aspen Plus to simulate all stages of the biological processes (Figure 27). The first unit is a stoichiometric reactor (RStoic) that simulates the hydrolysis stage for both the AD and DF processes. It calculates the mass flows for carbohydrates, proteins, and fats based on the hydrolysis reactions and fractional conversions (Table 13) (Rajendran et al., 2014).

Table 13 Hydrolysis reaction included in AD and DF simulations

No.	Compound	Hydrolysis reaction	Fractional conversion of reactants
1	Cellulose	$(C_6H_{10}O_5)_n + H_2O \rightarrow n\ C_6H_{12}O_6$	0.4 ± 0.2
2	Cellulose	$C_6H_{10}O_5 + H_2O \rightarrow 2C_2H_6O + 2CO_2$	0.5 ± 0.1
3	Hemicellulose	$C_5H_8O_4 + H_2O \rightarrow 2.5C_2H_4O_2$	0.5 ± 0.2
4	Hemicellulose	$C_5H_8O_4 + H_2O \rightarrow C_5H_{10}O_5$	0.5 ± 0.1
5	Protein	$C_{13}H_{25}O_7N_3S + 6H_2O \rightarrow 6.5CO_2 + 6.5CH_4 + 3H_3N + H_2S$	0.6 ± 0.3
6	Triolein	$C_{57}H_{104}O_6 + 3H_2O \rightarrow C_3H_8O_3 + 3C_{18}H_{34}O_2$	0.6 ± 0.3
7	Tripalmate	$C_{51}H_{98}O_6 + 8.436H_2O \rightarrow 4C_3H_8O_3 + 2.43C_{16}H_{34}O$	0.6 ± 0.3

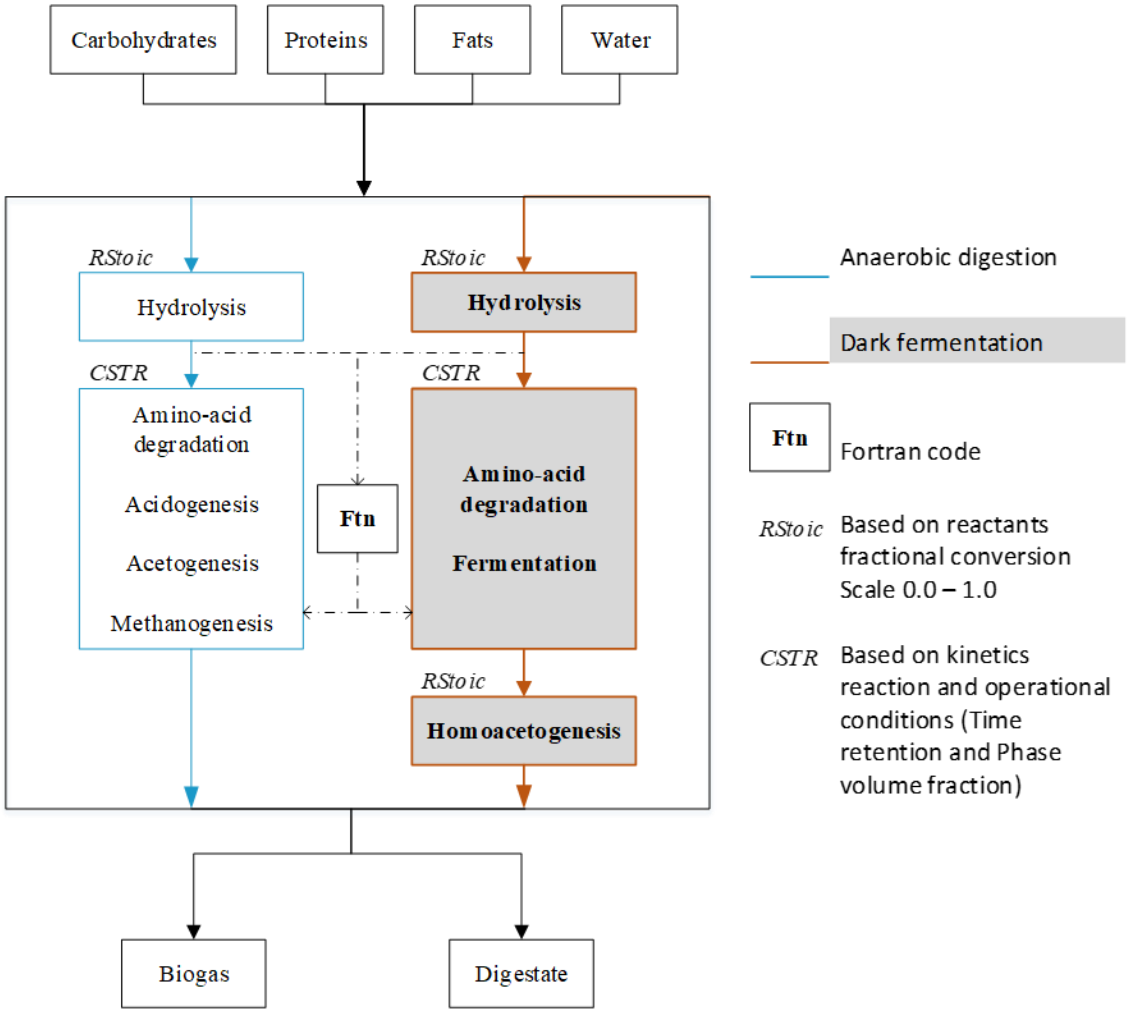

Figure 27 Block diagram of simulated processes in Aspen Plus

The second unit is a continuous stirred tank reactor (CSTR) for both the AD and DF processes. The CSTR was selected following the most common operating mode of AD and DF reactors in the literature (Adarme et al., 2017; Barca et al., 2015; Neshat et al., 2017; Rajesh Banu et al., 2020b). The CSTR simulates the processes of amino acid degradation, acidogenesis, acetogenesis and methanogenesis for AD, and amino acid degradation and

fermentation for DF (Figure 27 Block diagram of simulated processes in Aspen Plus). A set of 42 reactions was used to describe the main metabolic pathways associated with the bioconversions for the AD and DF processes (Rajendran et al., 2014). The compounds for the amino acid degradation, acidogenic, acetogenic, methanogenic, and fermentation reactions included in the simulation models for AD and DF processes come from the feed substrates and/or from the hydrolysis stage. Table 14 shows the kinetic reactions supposed to follow first-order kinetics (Angelidaki et al., 1999). Simulations were performed according to the process simulation model (PSM) proposed by (Rajendran et al., 2014).

Table 14 Amino acid degradation, acidogenic, acetogenic, methanogenic, and fermentation reactions included in the simulation models for AD and DF processes (The enumeration of the reactions continues from the hydrolysis reactions, Table 13).

Rxn No.	Compound	Stoichiometry	Pre-exponential factor [=] s^{-1}	AD	DF
Amino acid degradation reactions					
8	Glycine	$C_2H_5NO_2 + H_2 \rightarrow C_2H_4O_2 + NH_3$	$1.28 * 10^{-02}$	X	X
9	Threonine	$C_4H_9NO_3 + H2 \rightarrow C_2H_4O_2 + 0.5\ C_4H_8O_2 + NH_3$	$1.28 * 10^{-02}$	X	X
10	Histidine	$C_6H_8N_3O_2 + 4\ H_2O + 0.5\ H2 \rightarrow CH_3NO + C_2H_4O_2 + 0.5\ C_4H_8O_2 + 2\ NH_3 + CO_2$	$1.28 * 10^{-02}$	X	X
11	Arginine	$C_6H_{14}N_4O + 3\ H_2O + H2 \rightarrow 0.5\ C_2H_4O_2 + 0.5\ C_3H_6O_2 + 0.5\ C_5H_{10}O_2 + 4\ H_3N + CO_2$	$1.28 * 10^{-02}$	X	X
12	Proline	$C_5H_9NO_2 + H_2O + H_2 \rightarrow 0.5\ C_2H_4O + 0.5\ C_3H_6O_2 + 0.5\ C_5H_{10}O_2 + H_3N$	$1.28 * 10^{-02}$	X	X
13	Methionine	$C_5H_{11}NO_2S + 2\ H_2O \rightarrow C_3H_6O_2 + CO_2 + H_3N + H_2 + CH_4S$	$1.28 * 10^{-02}$	X	X
14	Serine	$C_3H_7NO_3 + H_2O \rightarrow C_2H_4O_2 + H_3N + CO_2 + H_2$	$1.28 * 10^{-02}$	X	X
15	Threonine	$C_4H_9NO_3 + H_2O \rightarrow C_3H_6O_2 + H_3N + H_2 + CO_2$	$1.28 * 10^{-02}$	X	X
16	Aspartic acid	$C_4H_7NO_4 + 2\ H_2O \rightarrow C_2H_4O_2 + H_3N + 2\ CO_2 + 2\ H_2$	$1.28 * 10^{-02}$	X	X
17	Glutamic acid	$C_5H_9NO_4 + H_2O \rightarrow C_2H_4O_2 + 0.5\ C_4H_8O_2 + H_3N + CO_2$	$1.28 * 10^{-02}$	X	X
18	Glutamic acid	$C_5H_9NO_4 + 2\ H_2O \rightarrow 2\ C_2H_4O_2 + H_3N + CO_2 + H_2$	$1.28 * 10^{-02}$	X	X
19	Histidine	$C_6H_8N_3O_2 + 5\ H_2O \rightarrow CH_3NO + 2\ C_2H_4O_2 + 2\ H_3N + CO_2 + 0.5\ H_2$	$1.28 * 10^{-02}$	X	X
20	Arginine	$C_6H_{14}N_4O_2 + 6\ H_2O \rightarrow 2\ C_2H_4O_2 + 4\ H_3N + 2\ CO_2 + 3\ H_2$	$1.28 * 10^{-02}$	X	X
21	Lysine	$C_6H_{14}N_2O_2 + 2\ H_2O \rightarrow C_2H_4O_2 + C_4H_8O_2 + 2\ H_3N$	$1.28 * 10^{-02}$	X	X
22	Leucine	$C_6H_{13}NO_2 + 2\ H_2O \rightarrow C_5H_{10}O_2 + H_3N + CO_2 + 2\ H_2$	$1.28 * 10^{-02}$	X	X
23	Isoleucine	$C_6H_{13}NO_2 + 2\ H_2O \rightarrow C_5H_{10}O_2 + H_3N + CO_2 + 2\ H_2$	$1.28 * 10^{-02}$	X	X
24	Valine	$C_5H_{11}NO_2 + 2\ H_2O \rightarrow C_4H_8O_2 + H_3 + CO_2 + 2\ H_2$	$1.28 * 10^{-02}$	X	X
25	Phenyalanine	$C_9H_{11}NO_2 + 2\ H_2O \rightarrow C_6H_6 + C_2H_4O_2 + H_3N + CO_2 + H_2$	$1.28 * 10^{-02}$	X	X
26	Tyrosine	$C_9H_{11}NO_3 + 2\ H_2O \rightarrow C_6H_6O + C_2H_4O_2 + H_3N + CO_2 + H_2$	$1.28 * 10^{-02}$	X	X
27	Typtophan	$C_{11}H_{12}N_2O_2 + 2\ H_2O \rightarrow C_8H_7N + C_2H_4O_2 + H_3N + CO_2 + H_2$	$1.28 * 10^{-02}$	X	X
28	Glycine	$C_2H_5NO_2 + 0{,}5\ H_2O \rightarrow 0.75\ C_2H_4O_2 + H_3N + 0.5\ CO_2$	$1.28 * 10^{-02}$	X	X
29	Alanine	$C_3H_7NO_2 + 2\ H_2O \rightarrow C_2H_4O_2 + H_3N + CO_2 + 2\ H_2$	$1.28 * 10^{-02}$	X	X
30	Cysteine	$C_3H_6NO_2S + 2\ H_2O \rightarrow C_2H_4O_2 + H_3N + CO_2 + 0.5\ H_2 + H_2S$	$1.28 * 10^{-02}$	X	X
Acidogenic reactions					
31	Dextrose	$C_6H_{12}O_6 + 0.1115\ H_3N \rightarrow 0.1115\ C_5H_7NO_2 + 0.744\ C_2H_4O_2 + 0.5\ C_3H_6O_2 + 0.4409\ C_4H_8O_2 + 0.6909\ CO_2 + 1.0254\ H_2O$	$9.54 * 10^{-03}$	X	
32	Glycerol	$C_3H_8O_3 + 0.4071\ H_3N + 0.0291\ CO_2 + 0.0005\ H_2 \rightarrow 0.04071\ C_5H_7NO_2 + 0.94185\ C_3H_6O_2 + 1.09308\ H_2O$	$1.01 * 10^{-02}$	X	
Acetogenic reactions					
33	Propionic acid	$C_3H_6O_2 + 0.06198\ H_3 + 0.314336\ H_2O \rightarrow 0.06198\ C_5H_7NO_2 + 0.9345\ C_2H_4O_2 + 0.660412\ CH_4 + 0.160688\ CO_2 + 0.00055\ H_2$	$1.95 * 10^{-07}$	X	
34	Isobutyric acid	$4H_8O_2 + 0.0653\ H_3 + 0.8038\ H_2O + 0.0006\ H_2 + 0.5543\ CO_2 \rightarrow 0.0653\ C_5H_7NO_2 + 1.8909\ C_2H_4O_2 + 0.446\ CH_4$	$5.88 * 10^{-06}$	X	
35	Isovaleric acid	$C_5H_{10}O_2 + 0.0653\ H_3N + 0.5543\ CO_2 + 0.8044\ H_2O \rightarrow 0.0653\ C_5H_7NO_2 + 0.8912\ C_2H_4O_2 + C_3H_6O_2 + 0.4454\ CH_4 + 0.0006\ H_2$	$3.01 * 10^{-08}$	X	
36	Linoleic acid	$C_{18}H_{32}O_2 + 15.356\ H_2O + 0.482\ CO_2 + 0.1701\ H_3N \rightarrow 0.1701\ C_5H_7NO_2 + 9.02\ C_2H_4O_2 + 10.0723\ H_2$	$3.64 * 10^{-12}$	X	
Methanogenic reactions					
37	Acetic acid	$C_2H_4O_2 + 0.022\ H_3N \rightarrow 0.022\ C_5H_7NO_2 + 0.945\ CH_4 + 0.066\ H_2O + 0.945\ CO_2$	$2.39 * 10^{-03}$	X	
38	Hydrogen	$14.4976\ H_2 + 3.8334\ CO_2 + 0.0836\ H_3N \rightarrow 0.0836\ C_5H_7NO_2 + 3.4154\ CH_4 + 7.4996\ H_2O$	$2.39 * 10^{-03}$	X	

Fermentation reactions				
39	Dextrose	$C_6H_{12}O_6 + 2H_2\ O \rightarrow 2CH_3\ COOH + 4H_2 + 2CO_2$	$2 * 10^{-02}$	X
40	Dextrose	$C_6H_{12}O_6 \rightarrow CH_3CH_2CH_2COOH + 2H_2 + 2CO_2$	$2 * 10^{-02}$	X
41	Dextrose	$C_6H_{12}O_6 \rightarrow 2CH_3CH_2OH + 2CO_2$	$2 * 10^{-02}$	X

PSM model is based on the ADM1, and it includes ammonia inhibition on the calculations of the kinetic constants for the conversion reactions, thus according to the anaerobic model of Angelidaki et al. (1993 and 1999). The model also takes into account variables such as pH and temperature to the calculations of the kinetic constants by correlation functions, as presented by previous studies (Serrano, 2010; Siegrist et al., 1993; Vavilin et al., 1994). All these correlation functions were developed through calculator blocks available in Aspen Plus. Each calculator block had a FORTRAN code to determine the kinetic constants of the conversion reactions. In addition, for DF process a calculator block was integrated in the model to establish the restriction of hydrogen gas production yield from carbohydrates within the values 1 to 4 mol H_2·mol hexose^{-1}, where 4 is the maximum stoichiometric yield (Alexandropoulou et al., 2018).

Table 15 Kinetics rate equations from Angelidaki's model are mixed with the extra kinetic equations from AMD1 in order to find the most complete kinetic expression.

Conversion	Ec. #	Kinetic equation	Reaction No.
Acidogenic glucose degrading step:	**Ec. 1**	$\mu = \mu_{max}(T)\left(\frac{1}{1+\frac{K_S}{[(C_6H_{10}O_5)_S]}}\right)\left(\frac{1}{1+\frac{K_{S,NH_3}}{[T-NH_3]}}\right)\left(\frac{1}{1+\frac{[LCFA]}{K_{I,LCFA}}}\right)F(pH)$	31
Lypolytic step:	**Ec. 2**	$\mu = \mu_{max}(T)\left(\frac{1}{1+\frac{K_S}{[GTO]}}\right)\left(\frac{1}{1+\frac{K_{S,NH_3}}{[T-NH_3]}}\right)\left(\frac{1}{1+\frac{[LCFA]}{K_{I,LCFA}}}\right)F(pH)$	32
Amino-acid degrading step:	**Ec. 3**	$\mu = \mu_{max}(T)\left(\frac{1}{1+\frac{K_S}{[A]}}\right)F(pH)$	8-30
LCFA acetogenic step:	**Ec. 4**	$\mu = \mu_{max}(T)\left(\frac{1}{1+\frac{[LCFA]}{K_{I,LCFA}}+\frac{K_{I,LCFA}}{[LCFA]}}\right)\left(\frac{1}{1+\frac{K_{S,NH_3}}{[T-NH_3]}}\right)F(pH)$	33, 36
VFA (propionate, butyrate acetogenic step:	**Ec. 5**	$\mu = \mu_{max}(T)\left(\frac{1}{1+\frac{K_S(T)}{[A]}}\right)\left(\frac{1}{1+\frac{K_{S,NH_3}}{[T-NH_3]}}\right)\left(\frac{1}{1+\frac{[HAc]}{K_{I,HAc}}}\right)\left(\frac{1}{1+\frac{[LCFA]}{K_{I,LCFA}}}\right)\left(\frac{1}{1+\frac{[H_2]}{K_{I,H2}(T)}}\right)F(pH)$	34, 35
Aceticlastic methanogenic step:	**Ec. 6**	$\mu = \mu_{max}(T)\left(\frac{1}{1+\frac{K_S(T)}{[HAc]}}\right)\left(\frac{1}{1+\frac{K_{S,NH_3}}{[T-NH_3]}}\right)\left(\frac{1}{1+\frac{[NH_3]}{K_{I,NH_3}}}\right)\left(\frac{1}{1+\frac{[LCFA]}{K_{I,LCFA}}}\right)F(pH)$	37
Hydrogen utilizing step:	**Ec. 7**	$\mu = \mu_{max}(T)\left(\frac{1}{1+\frac{K_S(T)}{[H_2]}}\right)$	
pH effect:	**Ec. 8**	$F(pH) = \frac{1+2*10^{0.5(pK_I-pK_h)}}{1+10^{(pH-pK_h)}+10^{(pK_I-pH)}}$	Lower and upper inhibition [ADM1]
	Ec. 9	$F(pH) = \begin{cases} pH < pH_{UL} \mid e^{\left(-3\left(\frac{pH-pH_{UL}}{pH_{UL}-pH_{LL}}\right)^2\right)} \\ pH > pH_{UL} \mid I = 1 \end{cases}$	Lower inhibition [ADM1]

Types of inhibition:	Free ammonia and hydrogen inhibition Non competitive inhibition; Secondary substrate inhibition (5-12):

"Where: S is the substrate for insoluble carbohydrates or for the insoluble proteins; k is the reaction rate; Rs is the substrate utilization rate; μmax(T) is the temperature-dependent maxim specific growth rate; Ki is the half-saturation constant; Ks, NH_3 is the half saturation constant for total ammonia; [T-NH_3] is the total ammonia concentration; Ki denotes inhibition constants. F(pH) is the pH growth-modulating function." Kinetic rate calculation [green Angelidaki's model and blue ADM1]

41Table 16 Kinetic data from Angelidaki's model and ADM1

Group	μmax (d^{-})	EA (J/mol)	K_s (g/L)	m*[2]	$K_{s,NH3}$[e] (g/L)	K_i (g/L)	m*2	$K_{i,LCFA}$ (g/L)	$K_{i,H2}$ (g/L)	m*[2]	pH_{LL}	pH_{UL}
Glucose acidogens	5,1 70	-35616	0,5 (glc)	0,025	0,05	--		5,0[c]	--		5,5*[1]	4*[1]
Lipolytic	0,53	--	0,01 (GTO)	--	0,05	--		5,0[c]	--		5,5*[1]	4*[1]
LCFA-degraders	0,55 10	-21472	0,02 (ol.)	0	0,05	--		5,0[d]	5,0E-06	-2,5E-7	5,5*[1]	4*[1]
Amino-acid degraders	6,38 70	-14143	0,3 (aa.)	0	--	--		--	--		5,5*[1]	4*[1]
Propionate degraders	0,49 20	-18108	0,259 (HPr)	0,01	0,05	0,96 (Hac)		5,0[c]	1,0E-05	3,25E-7	5,5*[1]	4*[1]
Butyrate degraders	0,67 30	-17043	0,176 (HBt)	0,01	0,05	0,72 (Hac)		5,0[c]	3,0E-05	1E-6	5,5*[1]	4*[1]
Valerate degraders	0,69 30	-17043	0,175 (Val)	0,01	0,05	0,40 (Hac)		5,0[c]	3,0E-05	1E-6	5,5*[1]	4*[1]
Methanogen	0,60 16	-29136	0,120 (Hac)	7,5E-3	0,05	0,26 (NH3)	7,82E-3	5,0[c]	--		6	7
Hydrogen utilizing step	35	0	5,0E-05 (H_2)	215E-6	--	--		--	--		5	6

**[1] Are only low-pH inhibition.*

**[2] "m" is the temperature dependence constant of [KT=m*(T-35) +KT=35ºC], its calculations are found in appendices as Activation energy calculations.*

[c] Noncompetitive inhibition

[d] Haldane-type inhibition

[e] Estimated from data published by Hashimoto et al., 1981; Hashimoto, 1983; Angelidaki and Ahring, 1993; Angelidaki and Ahring, 1994.

The third unit was developed and applied for the DF process to simulate the homoacetogenic stage, which involves the consumption of hydrogen (H_2) and carbon dioxide (CO_2) gas (Eq. 3) (Saady, 2013).

$$4H_2 + 2CO_2 \rightarrow CH_3COOH + 2H_2O \qquad \Delta G° = -104.0 \text{ kJ/mol} \qquad \text{Eq. 3}$$

H_2 consumption by homoacetogenesis usually increases by increasing the mass transfer limitation of H_2 from the liquid to the gas phase (Saady, 2013). In this study, the minimum conversion rates reported in the literature (Saady, 2013) were considered to simulate low mass transfer limitation conditions in the DF reactors. According to this, homoacetogenesis is carried out in an Rstoic block with a conversion factor of 0.1 ± 0.1, as a function of the H_2 and CO_2 composition of the biogas produced during the fermentation step. The methanogenic stage controls the H_2 concentration as H_2 is consumed by hydrogentrophic methanogenesis (pathway n° 38, Table 14). Therefore, the homoacetogenic stage is discarded for the AD process.

1.13.3 Process simulation

Simulation of the biological processes of AD and DF was performed in Aspen Plus V9 software, the Soave-Redlich-Kwong (SRK) method was chosen as it correlates and calculates the mole fractions and activity coefficients. In addition, the SRK model is suitable for vapor-liquid equilibrium (VLE) (Madeira et al., 2017b). The biogas production performances of each substrates blend (*Table 10*) were further simulated at three different process schemes: anaerobic digestion (AD), dark fermentation (DF) and dark fermentation followed by anaerobic digestion (ADF). The main objective was to identify the most suitable blends and process schemes, to produce biogas or a specific gas (CH_4, H_2, CO_2), using a comparative simulation approach, thus taking into account relevant factors such as the C/N ratio and the organic load of the feed. Indeed, previous studies have already shown that these factors may significantly affect biogas production performance (Kovalovszki et al., 2017; Mosquera et al., 2020; Xie et al., 2016; Zhang et al., 2014). All the simulations were performed at 35 °C and 0.1 Mpa, and according to hydraulic retention times of 20 and 10 days for AD and DF, respectively.

For each simulation in Aspen Plus, the carbohydrates, proteins, fats, and water mass fractions of the feed substrate were included in the reactor inlet stream. The volumetric biogas production rates were calculated based on the mass amount of methane (CH_4), hydrogen (H_2), and carbon dioxide (CO_2), and on the density of each compound at standard conditions (0.716 kg $CH_4 \cdot m^{-3}$; and 0.09 kg $H_2 \cdot m^{-3}$, at 25 °C and 0.1 Mpa). Then, the biogas yields (mL biogas·g COD^{-1}) were calculated to assess the biogas production performance.

Finally, the validation of the AD and DF models was carried out by a graphic correlation of CH_4 production yields for AD and H_2 production yields for DF (mL·g COD^{-1}) simulated and those resulted from batch laboratory tests that aimed at evaluating the biogas production potential of different blends of CFM, CCM, and SM.

$$Val_{dif} = \frac{Y_{sim}}{Y_{exp}} \quad \text{Eq. 4}$$

1.13.4 Assessment of energy recovery potential in Colombia

The energy recovery potential in Colombia was based on residual biomass production data of 26 departments (out of the 32 Colombian departments) according to the agricultural production reports of the National Department of Statistics, the Colombian Institute of Agriculture, and the National Pork Producers Association (DANE, 2020). A factor of 0.75 was used to estimate the CFM and CCM effectively available (Şenol, 2019), thus assuming 25% of losses in their collection. In addition, the SM availability was calculated as the 75% of the total SM from technical farms (ICA, 2018). Once the availability of CFM, CCM and SM was established, the annual total was divided as daily flow and the ADF process was simulated for each department. The inlet organic load of 26 $gCOD \cdot l^{-1}$ was used as input value for all the departments simulations based on the COD concentration of the substrates (*Table 24*, section 1.17) and their total available amounts for each department (*Table 6*). Temperatures and heat duties, from the results of ADF simulations, were analyzed and gathered to perform the heat integration procedure, according to the pinch method, thus considering the minimum approach temperature Δtmin of 3 °C. Heat transfer from the effluents was integrated in the calculations by considering their cooling down to a temperature of 25 °C (Abdou Alio et al., 2021).

For each department, the total daily masses of inlet substrate $M_{substrate}$ (CCM, CFM, SM) ($kg \cdot day^{-1}$), outlet biogas M_{biogas} (NH_3, CO_2, H_2, CH_4, H_2S) ($kg \cdot day^{-1}$), and outlet digestate $M_{digestate}$ (propionate, butyrate, ethanol, benzene, acetate, furfural, residual carbohydrates, and proteins) ($kg \cdot day^{-1}$), were calculated based on the results from simulations. Then, total input power P_{input} ($MJ \cdot day^{-1}$), substrate power $P_{substrate}$ ($MJ \cdot day^{-1}$), biogas power P_{biogas} ($MJ \cdot day^{-1}$), and digestate power $P_{digestate}$ ($MJ \cdot day^{-1}$) were determined by equations (5-8), respectively, where LHV is the related lower heating value (MJ/kg) and $P_{process}$ ($MJ \cdot day^{-1}$) represents the energy flow required to heat the feedstock, since the ADM1 model does not show association with the heat of reaction calculation and the ADF reactor energy data does not show consistency with the bioprocesses (it does not take into account cell growth and other factors that maintain the reactor temperature without additional energy requirements).

$$P_{input} = P_{substrate} + P_{process} \qquad \text{Eq. 5}$$

$$P_{substrate} = M_{substrate} \cdot LHV_{substrate}$$ Eq. 6

$$P_{biogas} = M_{biogas} \cdot LHV_{biogas}$$ Eq. 7

$$P_{digestate} = M_{digestate} \cdot LHV_{digestate}$$ Eq. 8

The energy recovery potentials E (toe) from biogas and digestate by ADF process were calculated using equations (9) and (10), respectively, where d represents the days of the year (365) and f_E represent the conversion factor ton of oil equivalent per Joule ($2.388 \cdot 10^{-5}$ toe/MJ).

$$E_{biogas} = P_{biogas} \cdot d \cdot f_E$$ Eq. 9

$$E_{digestate} = P_{digestate} \cdot d \cdot f_E$$ Eq. 10

The energy recovery yields for biogas (CH_4 and H_2) η_{biogas} (%), digestate $\eta_{digestate}$ (%), and total energy recovery η_{total} (%) were calculated by equation (11-13), respectively.

$$\eta_{biogas} = \frac{P_{biogas}}{P_{input}}$$ Eq. 11

$$\eta_{digestate} = \frac{P_{digestate}}{P_{input}}$$ Eq. 12

$$\eta_{total} = \frac{P_{biogas} + P_{digestate}}{P_{input}}$$ Eq. 13

Finally, a sensitivity analysis of the ADF model was made to assess the effect of nine different organic loads (from 2 to 26 $gCOD \cdot l^{-1}$) on the total energy recovery yields η_{total} (%) for the five departments with the highest production of coffee, cocoa, and pork (Antioquia, Boyacá, Cundinamarca, Meta, and Santander).

1.14 Conceptual biorefinery design

As it was presented the conclusion from the theoretical study, shows a superstructure with different possible routes for products and by-products, and from which it is possible to optimize production for different biorefinery schemes. The purpose of the conceptual study of the processes is to identify the treatment and evaluation trend for biogas and digestate produced after the bioprocesses and the definition of the processes to be carried out in the

biorefinery schemes to be proposed as an alternative in the agroindustry applied to the department of Santander. Indeed, the department of Santander presents two important characteristics in the study. The first is that the current availability is close to one of the blends proposed for laboratory validation, showing a balanced relationship between swine manure and coffee and cocoa mucilage's. The second is that it is the department with the highest cocoa production and the highest coffee production growth.

Based on the two bioprocesses studied, the liquid and solid separation, thermochemical, gas separation and purification, physicochemical, and synthesis or by-product production processes were evaluated conceptually. For the theoretical construction the following parameters were taken into account: operational conditions (temperature, pressure, time retention, kinetics), feed composition and moisture conditions for each process (Maximum water concentration requirement or substrate C/N ratio for bioprocesses, H_2O/CH_4 in the reforming), required pretreatments (Preheating, dehydration, compression), yields and previous studies.

1.15 Biorefinery models

Three biorefinery processes were simulated, considering the production of biogas (CH_4 and H_2) as the main product, the synthesis of a new product, and the use of the digestate after the bioprocesses, this with the purpose of comparing the energy and environmental efficiency as a new proposal for waste treatment in a region. As a first process, the use of anaerobic digestion and dark fermentation bioprocesses followed by refining is always contemplated. Thus, the processes are aimed at the maximum production of the same product from the same starting biomass.

The proposed schemes were designed to satisfy the following aspects:

- Objectives of the initial project funded by Colciencias (FP44842-38-2017 - – contract 038-2017): development of models based on energy, by-products, and materials recovery.

- Needs of the sector: exported products, energy requirements and waste treatment.

- Theoretical energy and economic efficiency reported for the by-products (digestate).

As it will be calculated after, a digestate with a water percentage higher than 98% is obtained. This value prevents its direct treatment in thermochemical processes that require percentages lower than 30% (Achinas et al., 2017).

1.15.1 Simulation model by processes

Following the hierarchy presented by Moncada et al. (2016), the two bioprocesses that develop the main reactions of the process are initially presented, followed by separation and purification processes. In order to improve the process, the following recycling are taken into account. Additionally, reforming and synthesis processes are included to culminate with energetic integration processes and evaluation of the utilities and schemes as shown in Figure 28.

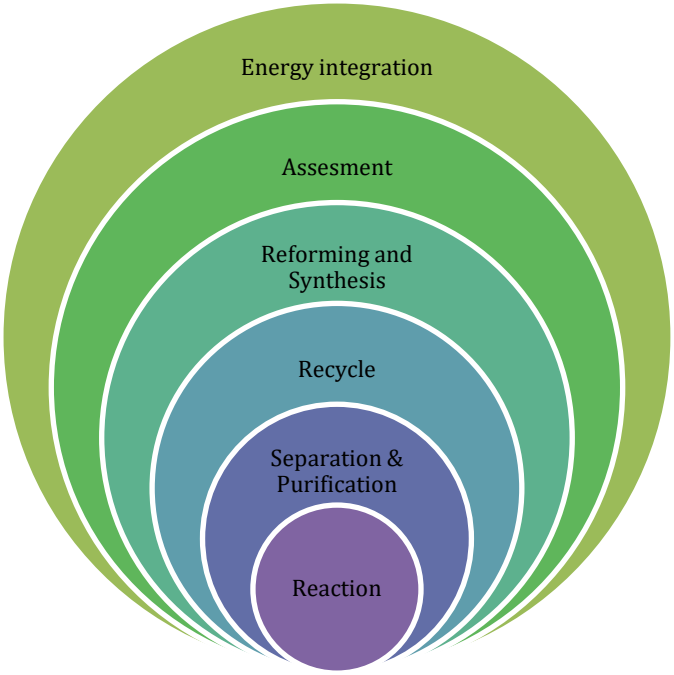

Figure 28 Technique hierarchies for process design

Biorefinery schemes include physicochemical and thermochemical refining processes. The information used for each of the processes used for the simulation of the three schemes is presented below.

Biofilter

As shown in the first chapter, biofilters have obtained viable efficiencies for the separation of undesirable gases (H_2S, NH_3 and CO_2). The simulation of the biofilters was based on the reported efficiencies, without taking into account the interaction of the molecules, in other

words, only the separation efficiency and loss of the gas of interest was considered. The biofilter was simulated with the Sep block which combines one inlet stream and separates it into two or more outlet streams (Das et al., 2019; Porté et al., 2019). The operating conditions are:

- Temperature: 327.15 K
- Pressure: 101325 Pa
- Split fraction: NH_3 = 0.98; H_2S = 0.98

Considering that biogas leaves the bioreactors at 308.15 K, a preheating up to 54 °C was carried out before entering the biofilter. Separation by Sep block only requires the percentage of separation, established by the suppliers or the literature, in the model it is not possible to integrate the interactions between molecules or sizing factors for future economic calculations. However, the advantage is that the literature reports the gas separation efficiency and the percentage of losses of the gas of interest of the currently used technologies, properties adequate to simulate the process.

Pressure swing adsorption

As shown in the literature, pressure swing adsorption (PSA) is a process that complements biofilters by removing the CO_2 and NH_3. Moreover, PSA is highly efficient in the separation of H_2 gas. The PSA process works at high pressures and approximately 308.15 K. Accordingly, a compressor must be installed prior to the separation process. The Mcompr unit was used as a two-stage isentropic compressor. The pressure of the last stage was set to 30 atm and the same pressure rate in each step. For the calculation of the heat capacity the rigorous method was chosen according to the literature (Puig-Gamero et al., 2018).

Subsequently, three separation units were simulated with the Sep model in the Aspen flowsheet. The operating conditions of each of them are presented as follows:

Separator 1: its function is to remove the hydrogen present in the current flow (Klein et al., 2018; Manish and Banerjee, 2008).

- Temperature: 308.15 K

- Pressure: 3039750 Pa
- Split fraction: H_2 = 0.95

Separator 2: its function is the methane purification, additional gases (CO_2, NH_3, H_2) are removed (Chen et al., 2015; Puig-Gamero et al., 2018; Ullah Khan et al., 2017).

- Temperature: 308.15 K
- Pressure: 3039750 Pa
- Split fraction: NH_3 = 0.9; CO_2 = 0.9; H_2 = 0.05; CH_4 (loses)=0.09

Separator 3: the last separator has the function of obtaining pure methane as the main product. This separator assumes perfect separation of the available methane.

- Temperature: 308.15 K
- Pressure: 3039750 Pa
- Split fraction: CH_4 = 1

Reforming to H_2

The reforming process was carried out in an Rgibbs reactor using as reference the equations (11-13), presented in chapter 15 from (Smith et al., 2007) and in Khoshnoodi and Lim (1997).

$$CH_4 + H_2O \rightarrow CO + 3H_2 \qquad \Delta H_{298} = 206.2\ kJ/mol \qquad \text{Eq. 14}$$

$$CH_4 + CO_2 \rightarrow 2CO + 2H_2 \qquad \Delta H_{298} = 247.9\ kJ/mol \qquad \text{Eq. 15}$$

$$CO + H_2O \rightarrow CO_2 + H_2 \qquad \Delta H_{298} = -41\ kJ/mol \qquad \text{Eq. 16}$$

The operational conditions were:

- Temperature: 1073.15 K

- Pressure: 3000000 Pa
- Maximum number of fluid phases: 2 (including vapor phase)
- Calculation option: restrict chemical equilibrium- specify temperature approach or reaction extents
- Process products: H_2, CO, CO_2, CH_4 and H_2

Methanol synthesis

The methanol synthesis process is carried out at high temperatures and pressures and based on the process presented by Puig-Gamero et al. (2018). For this reason, prior to the reactor it is necessary to include a heat exchanger that increases the system temperature and stream pressure, then a compressor and finally the reactor.

The heat exchanger was simulated with the following operational conditions:

- Temperature: 250 °C (523.15 K)
- Pressure: 5066250 Pa

The compressor was simulated with an isentropic compressor model compressor that generates a discharge pressure of 6079500 Pa and increases the temperature up to 284.44 °C (557.59 K).

Finally, a REquil at 220 °C (493.15 K) and 5.066×10^6 Pa was used for the synthesis reactions. The reactions were linked in a stoichiometric way, as well as the heat of reaction as shown following the Eq. 17 to Eq. 19 (Lee et al., 2020).

$$CO_2 + 3H_2 \rightarrow CH_3OH + H_2O \qquad \Delta H_{298} = 49.5\ kJ/mol \qquad \text{Eq. 17}$$

$$CO_2 + H_2 \rightarrow CO + H_2O \qquad \Delta H_{298} = 41.2\ kJ/mol \qquad \text{Eq. 18}$$

$$CO + 2H_2 \rightarrow CH_3OH \qquad \Delta H_{298} = -90.5\ kJ/mol \qquad \text{Eq. 19}$$

1.15.2 Sensitivity analysis

During the literature review process, it was identified that the H_2 reforming and methanol synthesis reactors are sensitive to operating conditions (pressure and temperature). Moreover, depending on the conditions, the hydrogen and methanol production, CO_2 consumption and energy consumption for each of the equipment is calculated. Additionally, design heuristic No. 7 states: for competing series or parallel reactions, adjust temperature, pressure, and catalyst to obtain high yields of the desired products. For the initial chemical distribution, assume that these conditions can be satisfied: obtain kinetic data and test this assumption before developing a base case design. Then, in the simulation of the two processes it is necessary to perform a sensitivity analysis to define the optimal conditions under which the process will be carried out. Table 17 shows the input and output variables in the sensitivity analysis of the H_2 reforming process and Table 18 shows the input and output variables in the sensitivity analysis of the methanol synthesis process. The advantage of the sensitivity analysis is that it allows to evaluate the optimal operational conditions for maximum hydrogen and methanol production and minimum energy consumption therefore improving the final technical evaluation of the proposed biorefinery schemes.

Table 17 Model analysis tool; Sensitivity, Reforming reactor variables

Input Variable	Property	Process	Unit	Start point	End point	No. of points
1	Temperature	Reforming reactor	°C	800	1000	21
2	Pressure		atm	2	30	21
Output Variable	Property		Process		Unit	
H_2 OUT	Flow		Reforming reactor		l/day	
CO OUT	Flow		outline		l/day	
R103ENER	Net duty		Reforming reactor		MW	

Table 18 Model analysis tool; Sensitivity, Methanol synthesis reactor variables

Input Variable	Property	Process	Unit	Start point	End point	No. of points
1	Temperature	Methanol syntesis reactor	°C	220	300	9
2	Pressure		atm	50	100	11

Output Variable	Property	Process	Unit
CO OUTRX	Mole-Flow	Methanol syntesis reactor outline	kmol/day
CO_2 OUTRX	Mole-Flow		kmol/hr
H_2 IN	H_2 Mole-Flow	Methanol syntesis reactor inline	kmol/hr
CO_2 IN	CO_2 Mole-Flow		kmol/hr
CO IN	CO Mole-Flow		kmol/hr
METOL OUT	METHANOL Mole-Flow	All schema (Total production)	kmol/hr
CO OUT	CO Mole-Flow		kmol/hr
CO_2 OUT	CO_2 Mole-Flow		kmol/hr
H_2 PROD	H_2 Mole-Flow		kmol/hr
QE107	Net duty	Methanol syntesis reactor	MW

The values of the sensitivity analysis allow to obtain the performance of carbon dioxide consumption and carbon monoxide generation. These results allow to treat the data and to compare with previous studies. The following equations (20 and 21) were used to calculate the yields of CO_2 and CO conversion, respectively.

$$Y_{CO_2} = \frac{(CO_2\ IN - CO_2\ OUTRX)*100}{CO_2\ IN} \quad \text{Eq. 20}$$

$$Y_{CO} = \frac{(CO\ IN - CO\ OUTRX)*100}{COIN} \quad \text{Eq. 21}$$

1.15.3 Biorefinery schemes

In this section the three simulated schemes and the stream ratios in them are shown. The operational properties of for each unit of process are described in Section 1.15.1. For all the schemes presented below, the models in Aspen Plus are built for the bioprocess and gas treatment section. The digestate treatment process was only considered theoretically for the life cycle analysis. In other words, although digestate treatments are represented in the diagrams, they were not simulated.

Biorefinery scheme No. 1

The first scheme (scheme No. 1) aims at producing methane and hydrogen as products and digestate (liquid phase) as by-product. It is composed of an initial mixer of biomass, inoculum, and water, two main bioprocesses (DF, AD) followed by biogas purification and digestate treatment (Figure 29). Following the design heuristic No. 5 *"Do not purge valuable species or species that are toxic and hazardous, even in small concentrations. Add separators to recover valuable species. Add reactors to eliminate toxic and hazardous"* and the recommendations of the literature that indicate not to purge or treat toxic or hazardous species, even in low concentrations, the separation of pollutant gases was implemented in the scheme No. 1 and it is directed to the production of biogas (H_2 and CH_4) (Seider et al., 2008).

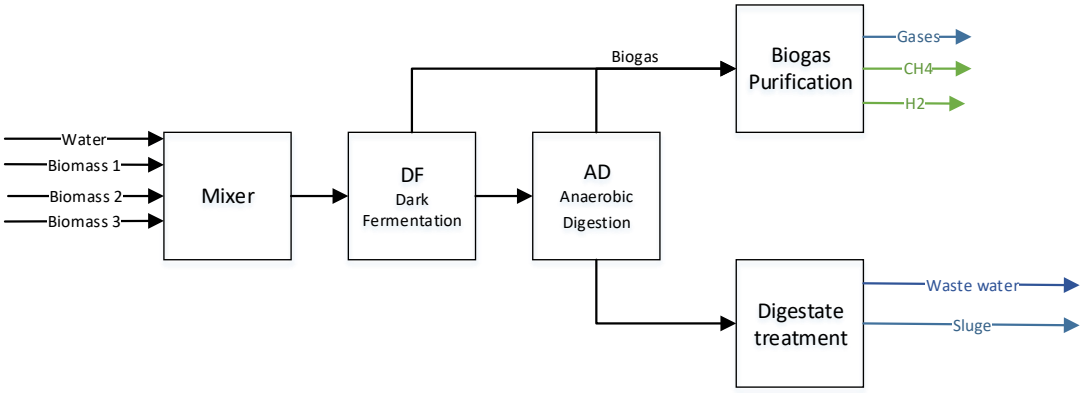

Figure 29 First biorefinery scheme. Bioprocess units, separation of initial products and by-products (Biorefinery No.1).

Figure 30 shows the block diagram of the biorefinery scheme No. 1. To complement the energetic process, exchangers and compressors that lead to the operational conditions of each process are included. The biogas treatment process consists of a biofilter (S101) that removes the corrosive and highly polluting gases (H_2S and NH_3) and then includes three PSA separators that separate and purify H_2 and CH_4. The digestate treatment process consists of a decanter followed by a centrifuge to remove the water from the solids that will be treated as nutrient-rich sludge for fertilizer production.

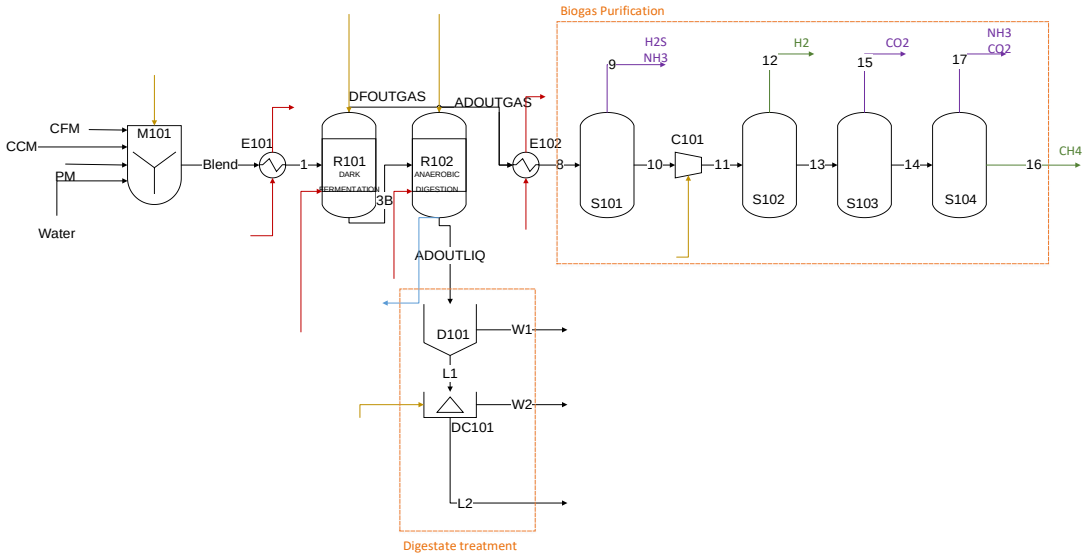

Figure 30 Block diagram of the first biorefinery scheme (Biorefinery No.1).

Biorefinery scheme No. 2

The second global simulation scheme is represented in Figure 31 and aims at the production of hydrogen as the main product and nutrient-rich sludge for fertilizer production as a by-product. The hydrogen is realized from a reforming of the methane obtained after anaerobic digestion. Biorefinery scheme No. 2 applies design heuristic #4 which states: Introduce liquid or vapor purge streams to provide exits for species that:

- Enter the process as impurities in the feed
- Produced by irreversible side-reactions

The actions before are recommended when these species are in trace quantities and/or are difficult to separate from the other chemicals.

Taking into account that prior to reforming there is already a gas separation process that in the literature reports high technology and efficiency, the hydrogen generated is recirculated to the biogas purification process in order to improve the purity of the hydrogen obtained at the end of the biorefinery in scheme No. 2.

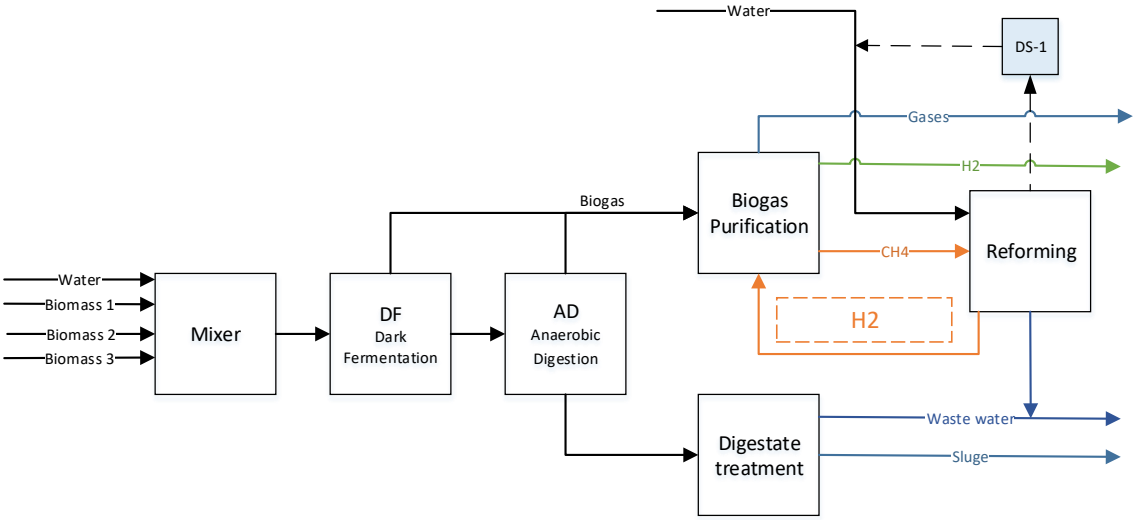

Figure 31 Second biorefinery scheme. Bioprocess units, hydrogen production (Biorefinery No.2).

Dark fermentation, anaerobic digestion, biogas purification and digestate treatment process is simulated in the same way as the biorefinery scheme No. 1. For the reforming process, a reactor with a methane and water mixture is used, as described in the literature (see section 1.15.1 in page 97). Additionally, a separator is included to dehydrate the reactor effluent. The gas obtained is recirculated to the biogas treatment system and the wastewater exits the process. For the reforming process it is required to add water to the reforming reactor. The amount of water used is calculated by a DS-1 design specifier based on the theoretical ratios (Table 19).

Table 19 Design specification DS-1.

Variable		**Definition**	
CH_4		Mole-Flow Stream=21 Substream=MIXED Component=METHANE Units=kmol/hr	
H_2O		Mole-Flow Stream=21 Substream=MIXED Component=WATER Units=kmol/hr	
Specifications		**Manipulated variable**	
Spec:	H_2O/CH_4	Type:	Mole-Flow
Target.	3	Stream:	Water2
Tolerance:	0.5	Substream: Component:	Mixed Water
Manipulated variable limits		Units:	kmol/hr
Lower:	18		

Upper: 55

Figure 32 shows the block diagram including the processes and heat and work streams of scheme No. 2.

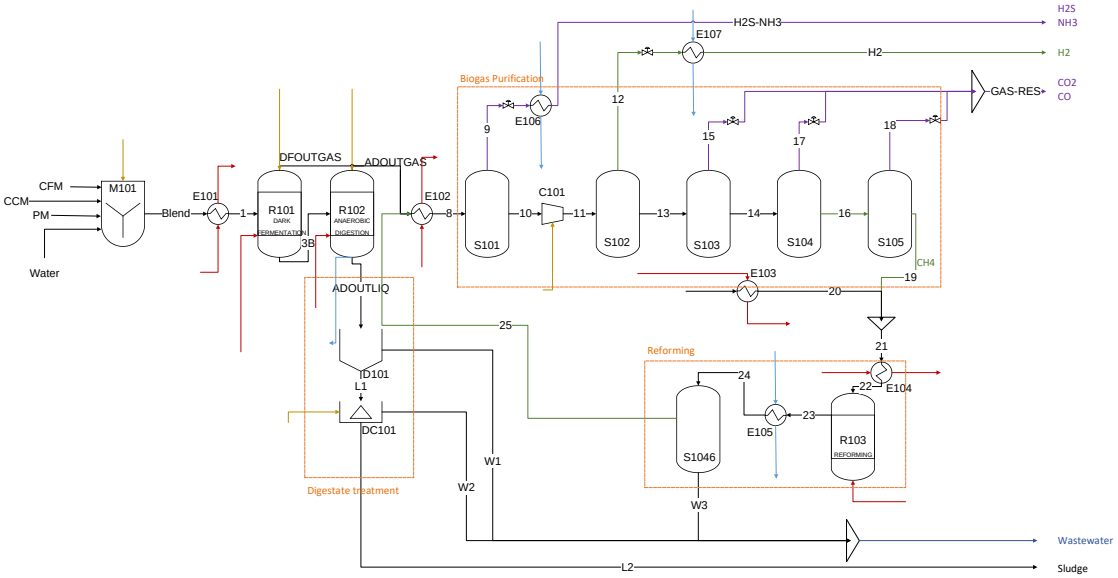

Figure 32 Block diagram of the second biorefinery scheme No. 2.

Biorefinery scheme No. 3

The main objective of scheme No. 3 is to reduce the gas emission in the atmosphere. Recent studies have implemented methanol synthesis as the main by-product using H_2 and CO_2 as production reagents. Although the literature reports low yields in the process, a H_2/CO_2 ratio at the reactor inlet is required to increase the performance of the reactor. According to literature data, in this study the stoichiometric reactant ratio H_2/CO_2 equal to 4 was considered (Lee et al., 2020). Figure 33 shows the overall scheme No. 3 of the biorefinery. In this scheme the separation process presented in scheme No. 2, the reforming process presented in scheme No. 2 and the methanol synthesis process are contemplated. Then, hydrogen and methanol are the products of interest, and the by-product is again the sludge from the digestate, rich in nutrients for fertilizer production.

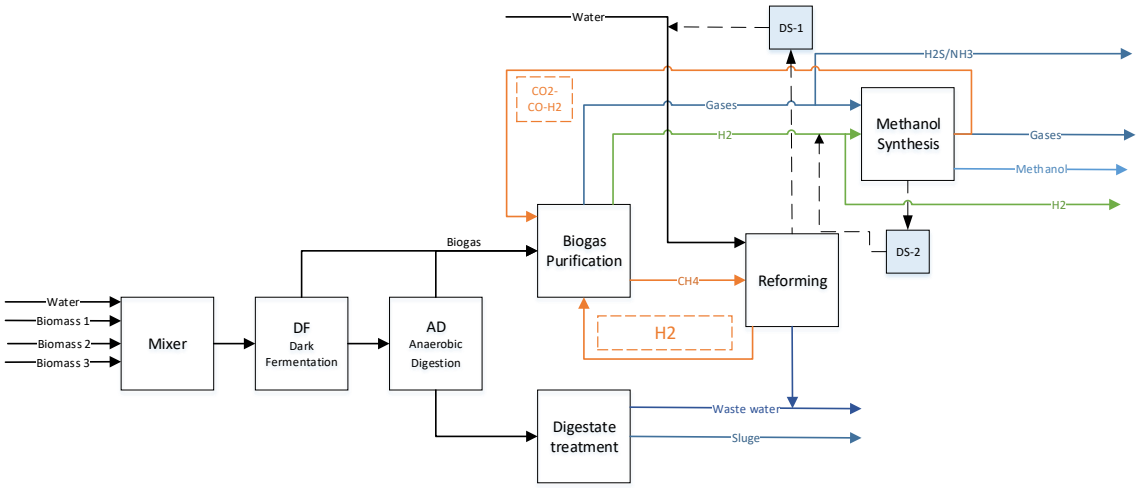

Figure 33 Biorefinery scheme No.. 3. Bioprocess units, hydrogen production.

Scheme No 3 considers the following design heuristics for its simulation:

- Heuristic No. 2: Use an excess of one chemical reactant in a reaction operation to completely consume a second valuable, toxic, or hazardous chemical reactant. In this case, excess hydrogen is used for CO_2 consumption.

- Heuristic No. 4: For the implementation of the recirculation of toxic or unreacted compounds due to low process conversion (CO_2).

- Heuristic No. 5: In the treatment of biogas, the elimination of toxic and hazardous products predominates.

- Heuristic No. 10: Attempt to condense vapor mixtures with cooling water. Then, use: (No. 9) Separate liquid mixtures using distillation and stripping towers, and liquid-liquid extractors, among similar operations.

According to the sensitivity analysis performed by Lee et al. (2020) the highest methanol production and CO_2 conversion is produced at a H_2/CO_2 stoichiometric reactant ratio between 3 to 5 when the process is carried out at 493 K and 100 bar. For this reason, a design specification block (Table 20) is included in the simulation which modifies the hydrogen flow splitting ratio at the flow divider upstream of the methanol synthesis process, ensuring that the amount of incoming hydrogen complies with the ratio.

Table 20 Design specification DS-2.

Variable		**Definition**	
H_2		Mole-Flow Stream=29 Substream=MIXED Component=HYDROGEN Units=kmol/hr	
CO_2		Mole-Flow Stream=29 Substream=MIXED Component=CO2 Units=kmol/hr	
Specifications		**Manipulated variable**	
Spec:	H_2/CO_2	Type:	Block-Var
Target.	4	Block:	M105
Tolerance:	1	Variable:	FLOW/FRAC
		Sentence:	FLOW/FRAC
Manipulated variable limits		ID1:	H_2
Lower:	0.1		
Upper:	0.9		

As shown in Figure 34, the methanol synthesis process consists of a reactor where the conversion of hydrogen to methanol is carried out by means of the reactions described in section 1.15.1. To achieve the operational conditions, a heat exchanger and a compression that guarantee temperature and pressure of the process are simulated prior to the reactor. Subsequently, a separation is performed where part of the gas (CO_2, CO and H_2) that does not react in the process is recirculated. The final stream is a mixture of methanol and water.

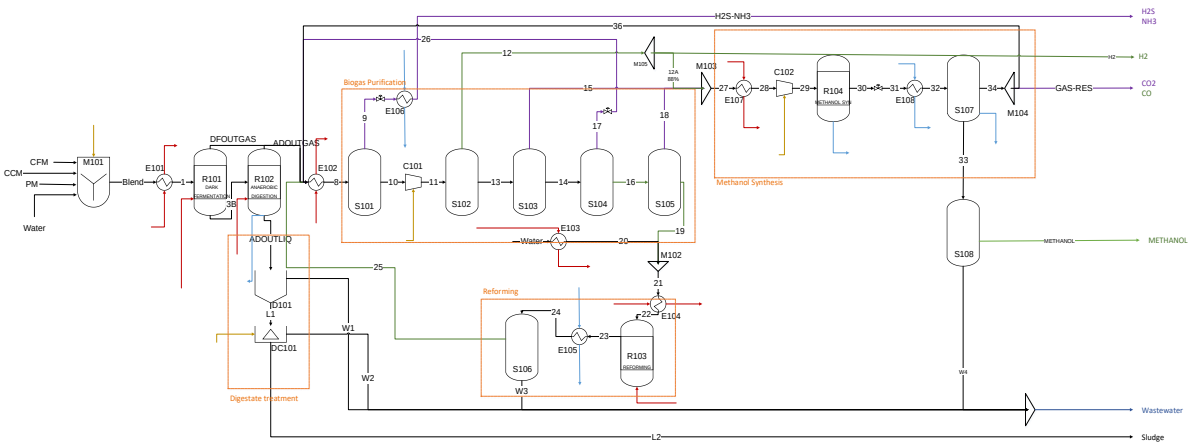

Figure 34 Block diagram of the third biorefinery scheme (Biorefinery No.3).

Aspen Plus simulation flowsheets

Figure 35, 36 and Figure 37 show the flowsheets used for the simulation of the biorefineries schemes No 1, 2 and 3, respectively. The flowsheets of the three biorefinery schemes start with four feed streams: three of the residual biomass substrates characterized with the mass fraction on a dry basis and one water stream. The mixture of the four streams goes to a heat exchanger that increases the temperature from ambient to bioprocess temperature (T=35 °C). The blend then goes to a duplicate block which is intended to give the option to study the bioprocesses in parallel and in series. The biorefinery scheme No. 1 shows the three main stages of the biorefinery scheme No. 1 (DF, AD and biogas purification), and which have the specificities given in this section. The biorefinery scheme No. 2 adds the reforming process and includes the water input required for the process, as the gas of interest in this process is hydrogen (H_2-A stream) is produced in a single stream as a product of the biorefinery, the waste gases (CO, CO_2) are blended into a final stream (GAS-RES). The biorefinery scheme No. 3 uses the residual gases blended with a fraction of the hydrogen in the M103 mixer to perform the methanol synthesis process added in the last scheme. The H_2/CO_2 ratio is given by specification block B6. Block B1 of the figures is intended to select the input stream, in all cases the ADINPUT2 stream was taken which corresponds to the liquid result of the fermentation. The simulations aim to obtain the mass and energy balances to assess in a technical feasible way the performance of the proposed processes.

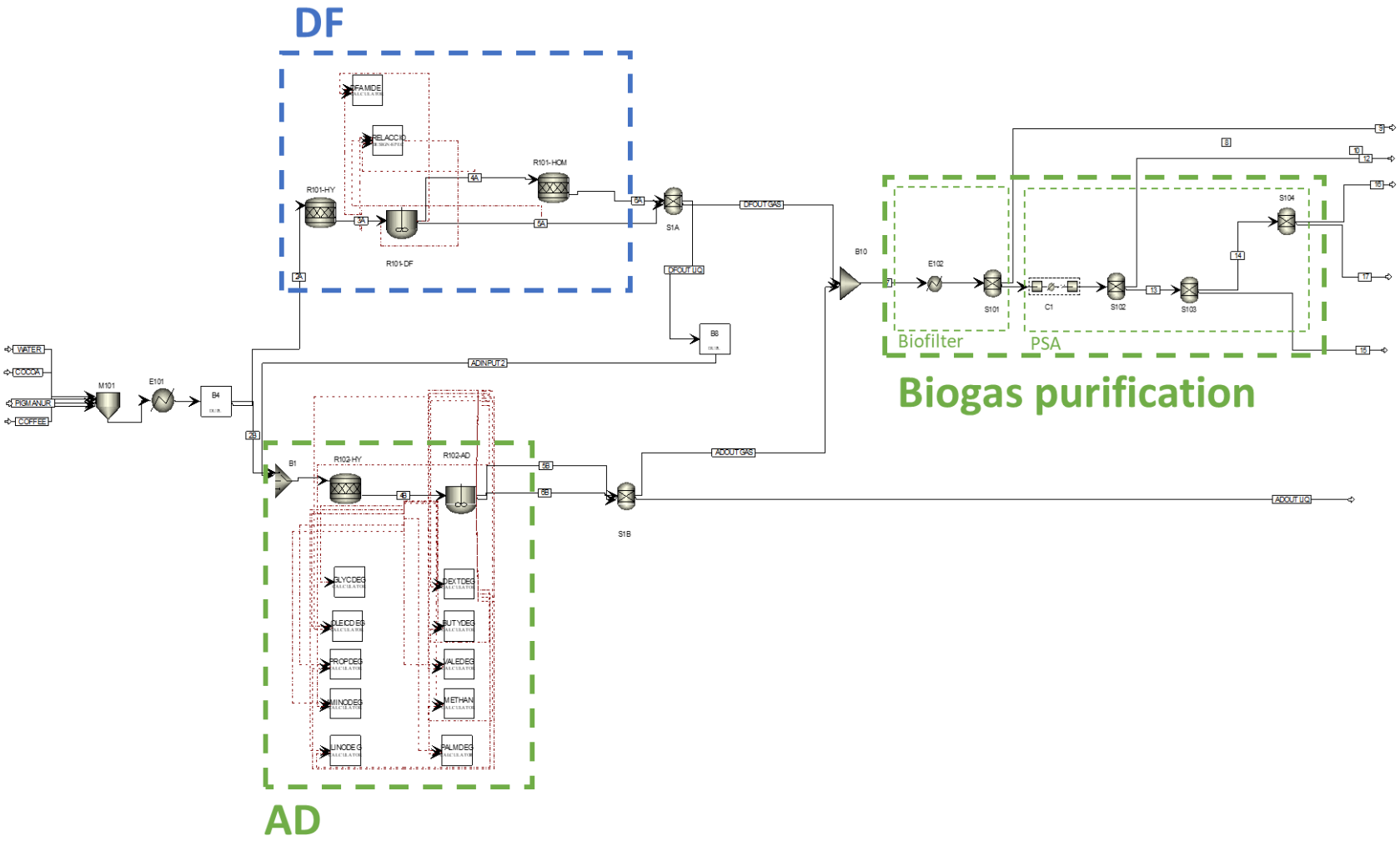

Figure 35 Aspen Plus flowsheet simulation of biorefinery scheme No. 1

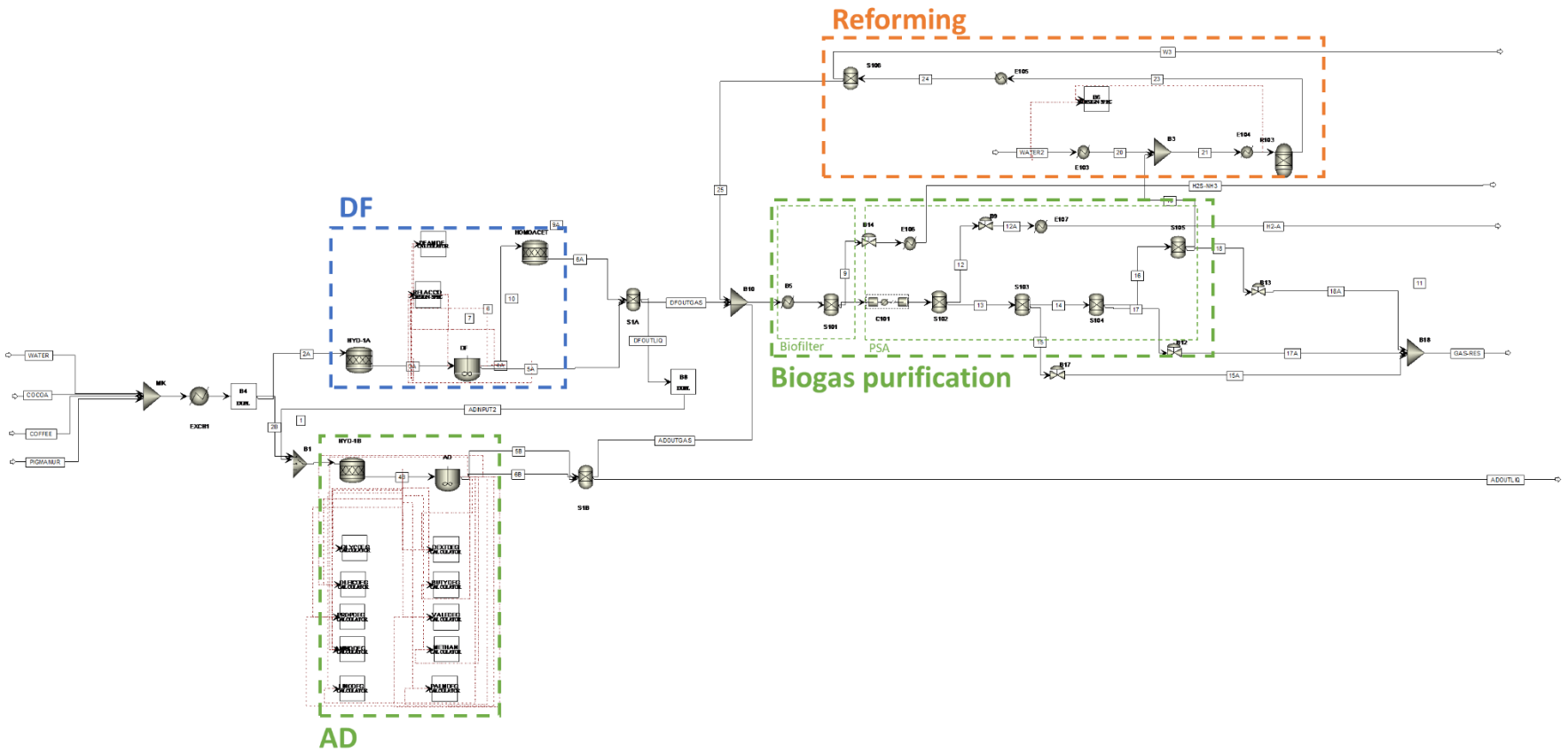

Figure 36 Aspen Plus flowsheet simulation of biorefinery scheme No. 2

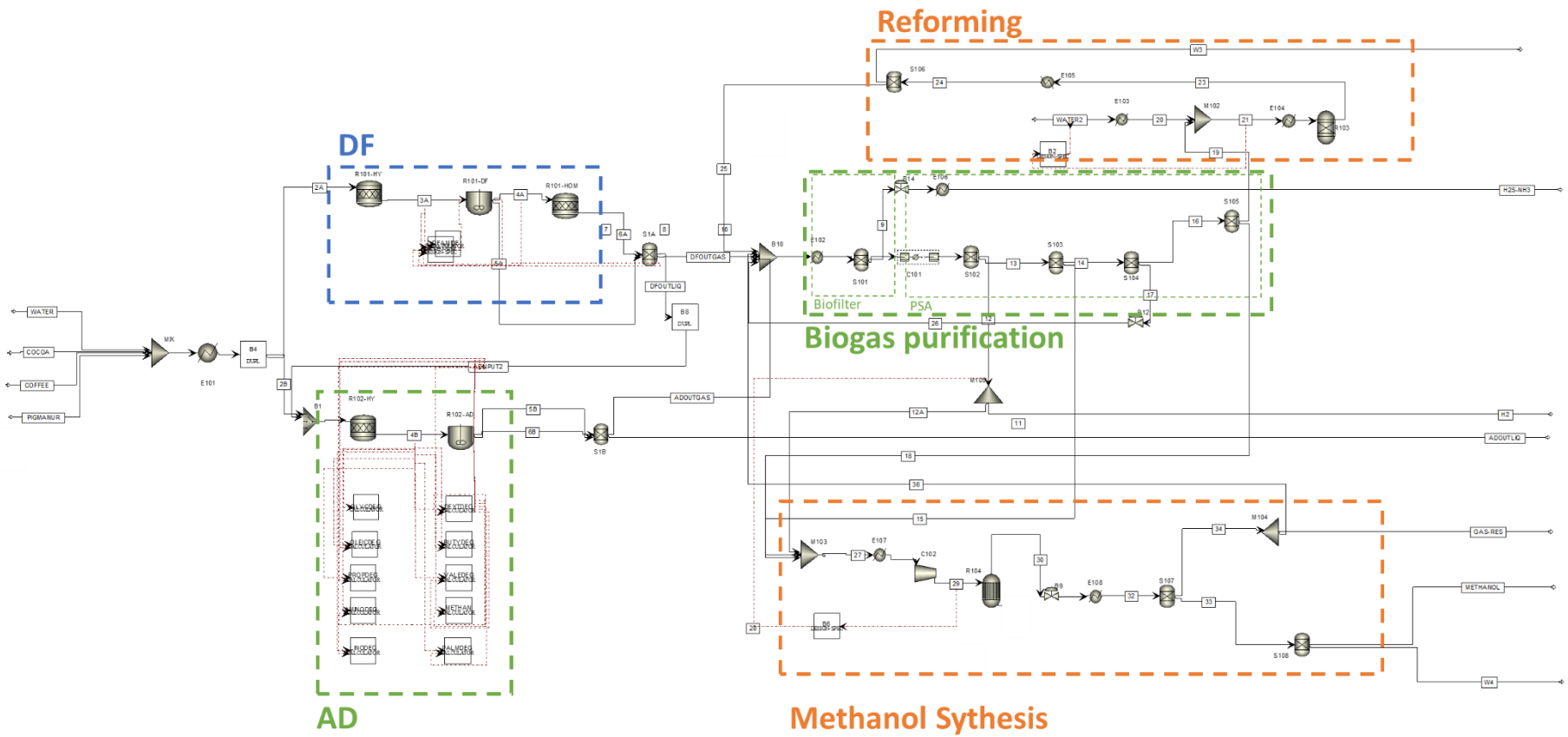

Figure 37 Aspen Plus flowsheet simulation of biorefinery scheme No. 3

1.16 Biorefinery evaluation

The evaluation of the biorefinery schemes seeks to determine the feasibility of their implementation. For this purpose, the results of the simulation performed in Aspen Plus (mass and energy balance) of each scheme were taken and evaluated by means of the three aspects described below. The case study for the evaluation was the department of Santander, taking the total available biomass and an initial organic load ratio of 26 gCOD·l^{-1}.

1.16.1 Biogas mass yield

The simulation was carried out for three processes: anaerobic digestion (AD), dark fermentation (DF) and a serial process starting with dark fermentation followed by anaerobic digestion (ADF), thus to maximize the use of biomass for biogas production. Biogas production is measured with respect to the initial organic load and was calculated according to the equation (Eq. 22). The aspect seeks to determine which of the three schemes allows the highest biogas production.

$$\eta_{mass_i} = \frac{m_i}{m_{COD-inlet}} x100 \qquad \text{Eq. 22}$$

Where Y indicates the conversion yield of compound i as a function of the organic load entering the biorefinery, m_i is the mass produced of compound i and $m_{COD-inlet}$ is the organic load entering the system. The analysis was performed for the main compounds of each scheme as follows:

- Scheme No. 1: H_2, CH_4, CO_2 and digestate.
- Scheme No. 2: H_2, CO_2, CO, and digestate.
- Scheme No. 3: H_2, CO_2, CO, CH_3OH, and digestate.

The study of the yields is carried out with the mass values on a dry basis.

1.16.2 Environmental assessment

The environmental evaluation of the schemes was carried out following the life cycle assessment (LCA) methodology, through SimaPro 9.2 Faculty license software. LCA is a

comprehensive method for assessing the environmental impacts of products and processes. According to the standards of ISO, LCA is divided into four steps:

- Step 1: goal and scope definition, system boundaries and functional unit (FU) of analysis are described.
- Step 2: life cycle inventory (LCI), material and energy inputs and their subsequent outputs are established along the considered process chains.
- Step 3: life cycle impact assessment (LCIA), the potential environmental impacts are evaluated.
- Step 4: the results are summarized, and conclusions are drawn in order to make recommendations for improvements in the final interpretation step.

Step 1: Goal and scope definition, system boundaries and functional unit (FU) of analysis are described.

The goal established in the present study was compares the environmental impact of biogas and byproducts production through bioprocesses, biogas separation and purification, reforming, and ethanol synthesis, following the case study (valorization of biomass available in the department of Santander, Colombia). Therefore, LCIs are collected for biogas (CH_4, H_2) production by bioprocess (ADF), H_2 production by reforming, methanol production by synthesis, production of digestate after bioprocesses and their treatment, as well as the supply of services and biomass.

The system boundaries were defined by sub-processes. Table 21 describes the sub-processes involved in each scheme, inputs, and outputs, considered in an attributional door-to-door LCA. The functional unit (FU) was in all cases one (1) ton of the total biorefinery production. Considering that each biorefinery has more than one product of interest, for the FU (1 ton of product), a contribution was assigned to each product (H2, CH4, methanol and digestate). The assignment was made according to the heat value contribution ratio at the output biorefinery scheme. Considering that the main objective of the study is to compare the biorefineries according to their energy yield.

As shown in Table 21, in the environmental impact assessment inputs, the analysis only considers swine manure. This is due to the fact that massive valorization technologies have not been developed for coffee and cocoa mucilage, and therefore, CCM and CFM are not found in the database as techno-sphere sources.

Table 21 Limit of processes studied in the LCA of each proposed biorefinery.

Scheme NO.	Process (Equipment according to PFD)	Input	Output
1	Bioprocess (ADF) H_2 recovery (S101 – S102) CH_4 recovery (S103 – S104) Digestate treatment (D101 – DC101)		CH_4 H_2 Digestate CO_2
2	Bioprocess (ADF) H_2 recovery (S101 – S102 – S103 – S 104 – S105 – R103 – S106) Digestate treatment (D101 – DC101)	Mass flow (Swine Manure) Water Heating Cooling	H_2 Digestate CO_2
3	Bioprocess (ADF) H_2 recovery (S101 – S102 – S103 – S 104 – S105 – R103 – S106) Methanol synthesis (R104 – S107 – S108) Digestate treatment (D101 – DC101)		H_2 Methanol CO Digestate CO_2

Step 2: life cycle inventory (LCI), material and energy inputs and their subsequent outputs are established along the considered process chains.

The inventory, material and energy balance were based on the results obtained in the Aspen Plus simulation, in order to obtain an analysis related to the availability of energy and the values associated with Colombia. Below is the list of services and biomass related to the software.

- Electrician, low voltage {CO}|Electrician, low voltage {CO}|Electrician, low voltage {ROW}|Electrician, low voltage {CONSEC}|CONSEQ, s.

- Heat, stream, a chemical industry {ROW}|Heat market, stream, no chemical industry.
- Water, fully softened {RER} | Water market, fully softened | Conseq, s.
- Refrigerant R134a {GLO} | Market for refrigerant R134a {GLO} | Market for refrigerant R134a {GLO}.
- Tap water {CO}|Tap water market {GLO} | Conseq, s.
- Swine manure, swine, on the pig farm/RER MASS.

Considering that the heating and cooling services are different from those established by Aspen, the pertinent conversions were made. In the case of electricity, the input is specified in the energy consumption, and it is possible to use the one established in the simulation. In the case of cooling water and refrigerant, the energy consumption and heat capacity of water and R134a refrigerant (due to its frequent use in Colombia) were used to establish the consumption of the services and indicate them in the software.

Step 3: life cycle impact assessment (LCIA), the potential environmental impacts are evaluated.

In order to compare with the literature results, the ReciPe method was selected, which presents the impact factors related to the Table 22.

Table 22 Impact categories reported with the ReciPe method in the LCA methodology

Impact category	Unit
Global warming	kg CO_2 eq
Stratospheric ozone depletion	kg CFC11 eq
Ionizing radiation	kBq Co-60 eq
Ozone formation, Human health	kg NOx eq
Fine particulate matter formation	kg PM2.5 eq
Ozone formation, Terrestrial ecosystems	kg NOx eq
Terrestrial acidification	kg SO_2 eq
Freshwater eutrophication	kg P eq
Marine eutrophication	kg N eq
Terrestrial ecotoxicity	kg 1,4-DCB
Freshwater ecotoxicity	kg 1,4-DCB
Marine ecotoxicity	kg 1,4-DCB
Human carcinogenic toxicity	kg 1,4-DCB
Human non-carcinogenic toxicity	kg 1,4-DCB
Land use	m2a crop eq

Mineral resource scarcity	kg Cu eq
Fossil resource scarcity	kg oil eq
Water consumption	m3

Step 4: the results are summarized and conclusions are drawn to make recommendations for improvements in the final interpretation step.

The evaluation was performed first on individual sections of each scheme and then between biorefineries. Schemes No. 1 and 2 were then divided into four sub-processes and scheme No. 3 into five sub-processes, and the percentage impact of each sub-process on the refinery was compared for each scheme, to visualize the process with the highest environmental demand or impact.

The final objective of the method is to compare the damage to human health, ecosystems, and available resources among the three biorefining schemes. For the analysis, graphs of the impact values in each section of the biorefinery schemes are plotted. The bar diagram allows to evaluate the total result, and to compare where the greatest impacts of each scheme are found, while the radial diagrams allow to compare the results between the schemes and to give an answer about the feasibility of implementation, as well as to show weak points to improve in the processes to reduce the generated impacts.

1.16.3 Pinch analysis

The PINCH method analyzes energy integration through the possible interaction between hot streams or processes (which require heat dissipation) and cold streams (which require heat inputs) with the objective of minimizing the process irreversibility's. The objective is to calculate hot/cold utility consumption, the analysis and target are performed with the minimum temperature approach difference (PINCH point). This method allows to estimate the minimum heat requirement (MER) for the process.

The heat flows data of the process was obtained from the simulation in Aspen Plus for the three biorefinery schemes. The temperature interval diagram is done on the appropriate temperature difference. Data are summarized to plot the cold composite curves for all common cold streams and the hot composite curves for all hot streams. At the pinch point, the temperature difference is fixed (ΔT_{min} = 3 °C). With the results of the PINCH analysis,

the minimum heat requirements that allow to calculate the energy efficiency of the proposed schemes are obtained.

PINCH evaluation scenarios

Three scenarios were analyzed for each biorefinery scheme where all the streams produced were cooled to ambient temperature (25 °C), this to guarantee the total utilization of the stream's enthalpy.

- Scenario 1. The first scenario is the biorefinery scheme obtained at the end of the process model simulation, i.e., without any modification.

- Scenario 2. The second scenario eliminates from the analysis the heat value required for the CSTR reactors of the AD and DF processes. Although the literature reports variable energy consumption of the bioprocesses, the bioconversion models do not consider the dynamics of the process, which allows maintaining the temperature through the equilibrium of the kinetics, the energy exchange with the ambient temperature and the increase of the microorganisms. Especially, heat transfer with the ambient temperature is important since in Colombia the minimum and maximum average multiannual average temperatures are between 20 and 32 °C parameter that allows to work the bioprocess without extra-heating; moreover, current AD in small and medium scale at agroindustry work at ambient temperatures.

- Scenario 3. The third scenario eliminates from the analysis the heat value required for the CSTR reactors of the AD and DF processes (as already considered for scenario 2), and in addition it includes the combustion of a methane fraction produced at the end of the ADF process. Since all three schemes require additional heating power, the combustion of methane gas is aimed at supplying the requirement of the process. Methane was chosen as the easiest gas to produce and the one that is produced in the greatest quantity after the ADF process. Additionally, the optimal percentage of combustion was calculated to balance heating requirement of each biorefinery scheme. Indeed, burning methane decrease process methane conversion and then final heat requirement.

- Scenario 4. The third scenario (Considered only for schemes No. 2 and 3) eliminates from the analysis the heat value required for the CSTR reactors of the AD and DF processes (as already considered for scenario 2), and in addition it includes the complete combustion of the process residual gases (CO and H_2). Since all three schemes require additional heating power, the combustion of residual gas is aimed at supplying the requirement of the process. Residual gases were chosen as the easiest gas to be burned and which does not change the amount of H2 production as the main product in schemes No. 2 and 3.

In scenario 3, methane combustion used an RStoic with methane inlet stream and an air stream. The amount of the air stream was calculated automatically with a design specification that guarantees the required oxygen for the available methane (Table 23). The reaction equation (Eq. 23) was determined with 100% methane conversion efficiency and the combustion operating conditions were 1673.15 K and 101325 Pa.

$$CH_4 + 2O_2 \rightarrow CO_2 + 2H_2O \qquad \text{Eq. 23}$$

Table 23 Design specification: Oxygen estimate required for total methane combustion

Variable		**Definition**	
CH_4		Mole-Flow Stream=CH_4-Burn Substream=MIXED Component=METHANE Units=kmol/hr	
O_2		Mole-Flow Stream=AIR Substream=MIXED Component=O_2 Units=kmol/hr	
Specifications		**Manipulated variable**	
Spec:	O_2/CH_4	Type:	Mole-Flow
Target.	2	Stream:	AIR
Tolerance:	0.5	Substream: Component:	Mixed O_2
Manipulated variable limits		Units:	kmol/hr
Lower:	1		
Upper:	100		

Energy analysis

The global energy efficiency η_G (%) of the biorefineries follows the same methodology as the assessment of potential energy recovery in Colombia for the ADF process proposed in section 1.13.4. That is, efficiency is calculated with the equation below:

$$\eta_G = \frac{P_{output}}{P_{input}} x100 = \frac{F_{CH4}*LHV_{CH4}+F_{H2}*LHV_{H2}+F_{CO}*LHV_{CO}+F_{Methanol}*LHV_{methanol}}{F_{biomass}*LHV_{biomass}+Q_{heating}} x100 \quad \text{Eq. 24}$$

Where the P_{output} refers to output power including the stream power (F_i is the mass flow kg·h^{-1} and LHV_i the lower heating value kJ·kg^{-1}), according to the products of interest for each biorefinery scheme and the cooling target energy (kJ/h) obtained in the PINCH analysis. The P_{input} refers to the power from the biomass and the heating target energy from the PINCH analysis

Recommended designs

The temperature difference analysis function is included directly in the Aspen Energy software, using the network generated with the initial simulation, an analysis of costs, number of heat exchangers, heating, and cooling costs, etc. was performed based on the minimum. The design recommendation option was used with data selection on: flow, utilities, economics data. As a restriction, a maximum of 10 branches per stream, a maximum of 10 alternative designs for each scheme were indicated and a minimum temperature difference (ΔT_{min}) of 3 °C. Subsequently, an economic and energetic evaluation was carried out based on the investment, operational costs and heating and cooling consumption presented for the energy integration alternatives.

4.CONCLUSION

Experimental data collected from the literature allows characterizing the residual biomass and validating the carbohydrate content to optimize methane and hydrogen production in co-digestion. Likewise, the experimental matrix is used to validate the production yield obtained in the simulation models. It should be highlighted that the complexity of the model and the volume of reaction equations in the bioprocesses may probably introduce uncertainties in the results, since the model does not consider the selectivity, and especially the influence of the inoculum used in the experimental model.

The conceptual design of biorefineries theoretically shows a great variety of processes. The proposed processes look for the practical implementation for the application of agroindustry and/or adaptation of the processes that have already been installed (especially AD). For this reason, biogas treatment and greenhouse gas reduction processes are added to improve the performance of the biorefineries, through separation, reforming, and synthesis processes.

Finally, the use of the proposed schemes will be validated through mass yield, energy and environmental analyses that allow to compare the processes with traditional processes for the methane, hydrogen, and methanol production, as well as to evaluate the benefit of the residual biomass treatment and valorization process. The life cycle assessment will allow evaluating the impact of biogas treatment, reforming, and synthesis on human health, ecosystems, and available resources through the presentation of the fourth step corresponding to the potential environmental impact graphs. While the energy yield calculation allows biorefinery schemes to compare energy production with traditional and thermochemical processes to validate their feasibility.

CHAPTER III POTENTIAL ENERGY RECOVERY IN COLOMBIA, BIOPROCESSES EVALUATION

1.INTRODUCTION

The results of the entire work are presented in the following two chapters (e.g. Chapter III and Chapter IV). The objectives of Chapter III, entitled “Potential energy recovery in Colombia, bioprocesses evaluation”, are to validate the simulation of the bioprocesses, the optimization of the bioprocesses by maximizing the biogas production, and the evaluation of the energy potential from the simulation for each department of Colombia. As shown in the literature, the availability of residual biomass in Colombia varies significantly by region. Moreover, it has been shown that depending on the region, biomass characterization may vary, most likely due to soil conditions, solar radiation, and animal feeding. To validate the ADM1 model, experimental data, using different compositions related to the variation of the three substrates studied are necessary.

2.EXPERIMENTAL RESULTS

1.17 Biomass characterization

Table 24 shows the results obtained from the characterization of the three substrates studied. The humidity of the coffee mucilage reports higher values than those found in the literature, however it is close to that reported by previous studies (Puerta-Quintero and Ríos-Arias, 2011; Clifford, 2012). These differences may be due to the location of the sample (department), to the maturity of the fruit and to the water added in the processing of the coffee and in the mechanical de-mucilage. Regarding coffee, the values of carbohydrates (86.21%) and ash (3.78%) are close to those reported by Puerta-Quintero and Ríos-Arias (2011) on a dry basis (81.4% w/w and 4.04% w/w respectively). On the contrary, the protein value of the sample is lower than that reported by Clifford (2012), this may be due to the characteristics of the soil where it is grown. In general, it is highlighted that in the results as in the literature, the major composition of the dried coffee mucilage corresponds to carbohydrates.

Regarding cocoa mucilage, the values of carbohydrates and protein are in the range reported by Nigam and Singh (2014) and Martínez et al. (2012), regarding fats the value is higher than the one reported by Nigam and Singh, 2014, but it is in the range reported by Martínez et al., 2012, a study that relates values from South America and due to the characteristics of the soil generate values close to one. The case of cocoa mucilage is susceptible to the time and method of extraction since in the process fermentation reactions are quickly generated. The ratio of volatile and total solids evidences the high biodegradability of coffee mucilage and cocoa mucilage, since values close to one for this ratio indicate a high content of organic matter susceptible to be transformed. The chemical oxygen demand and total Kjeldahl nitrogen parameters are related to the working dilution. However, the carbon-to-nitrogen ratio suggests hand in hand with the concentration of reducing sugars, the high availability of carbon material available for fermentation towards hydrogen production or the production of volatile fatty acids required for methane forming reactions.

Table 24 Composition of coffee mucilage, cocoa mucilage, and swine manure.

Parameters	Coffee Mucilage (CFM)	Cocoa Mucilage (CCM)	Swine manure (SM)
C (%w/w)[a]	38.88	40.22	37.24
H (%w/w)[a]	6.30	6.35	5.06
O (%w/w)[a]	50.28	49.35	34.89
N (% w/w) [a]	0.72	0.72	4.08
S (%w/w) [a]	0.05	0.05	0.28
C/N	54	55.9	9.1
Protein (%w/w) [a]	4.5	4.5	25.5
Fat (%w/w) [a]	0.23	1.32	6.08
Carbohydrates (%w/w) [a]	86.21	70.26	3.39
Lignin (%w/w) [a]	0.01	2.36	4.12
Hemicellulose (%w/w) [a]	2.63	12.04	35.14
Cellulose (%w/w) [a]	2.88	6.19	7.19
Total volatiles solid ($g \cdot l^{-1}$)	53.7	79.8	19.6
Organic content ($gCOD \cdot l^{-1}$)	27.4	32.8	26.2
NTK ($mg \cdot l^{-1}$)	230.4	387.9	1204
%FDN	8.79	24.51	67.21
%FDA	4.46	10.66	22.12
%FDK	2.91	6.27	7.61
%SiO2	0.032	0.076	0.42
%Ash	3.78	3.32	18.57
%TDN	84.718	80.378	72.356

[a]Based on dried mass

Regarding swine manure, in relation to the databases and articles consulted on elemental analysis, it is evident that carbon, hydrogen and oxygen are close to the average values. However, a lower value of nitrogen and sulfur is evidenced, which can be attributed to the feeding of the pigs and the age of the pigs. Regarding the value of ashes, it is identified that the value is within the range of the literature on the maximum value. Swine manure also has one of the highest sulfur contents, a condition that would favor the activation of sulfate reducing bacteria during the anaerobic processes. This could interfere mainly in dark fermentation and hence in hydrogen production.

In relation to the use of blends, swine manure has a high nitrogen content that could stabilize the anaerobic digestion process, but decreases the opportunity to generate hydrogen

and methane depending on the C/N relation (Carotenuto et al., 2020; Dhar et al., 2016; Li et al., 2015). The elemental value CHONS and the experimental data %FDA allow to calculate the calorific value of the substrates and the digestible energy (energy in substrate that is available to humans or animals through digestion and it is measured as the difference between the gross energy content and the energy lost in feces) by means of the theoretical equations (Eq. 25-27), where LHV is the Low Calorific Value and DE is the Digestible Energy.

$$LHV = 0.001 * (348{,}35C + 938{,}70H - 108{,}00O + 62{,}80N + 104{,}65S)\ (kJ/kg) \quad \text{Eq. 25}$$

$$DE = TDN * 0.04409 * 4.184\ (MJ/kg) \quad \text{Eq. 26}$$

$$\%TDN = 87.84 - (0.7 * FDA) \quad \text{Eq. 27}$$

Table 25 Energy values of residual biomass

Parameters	Coffee Mucilage (CFM)	Cocoa Mucilage (CCM)	Swine manure (SM)
LHV (MJ/kg)	14.078	14.692	14.240
DE (MJ/kg)	15.628	14.828	13.348

The high energy digestibility of coffee and cocoa mucilage may be due to the low level of neutral detergent fiber, hemicellulose and high in non-lignified or soluble carbohydrates that are highly digestible, as well as the high digestibility of proteins, fats, and nitrogen free extract. However, the difference with SM is not significant and its protein, cellulose and nutrient content are various in processes such as dark fermentation and nutrient recovery, processes that integrate the biorefinery design.

1.18 Experimental bio-process results

The important value in the experimental phase is the total biogas produced at the end of the experimental time. Figure 38 shows the setups performed. In the evaluation of the substrate mixtures, a slight difference in response time between anaerobic digestion and dark fermentation can be seen (Table 26).

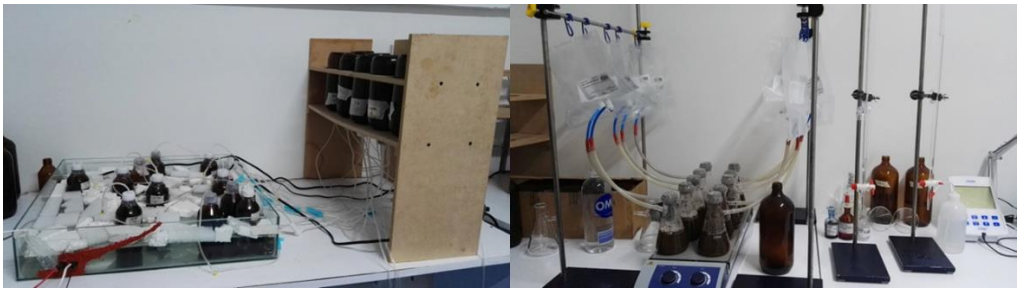

Figure 38 Experimental set-up of AD and DF bioprocesses for methane and hydrogen production with volume displacement and biogas collection.

In both cases the production rates vary over the time of the experiments, which is associated with the complexity of the working substrates - actual substrates. All trials were left for a period corresponding to the variation in biogas production being less than 10% of the cumulative volume. Accordingly, the dark fermentation trials had an average duration of 8 days, while the anaerobic digestion trials took a maximum of 17 days. The production dynamics show that no inhibition is generated in the process by the concentration levels evaluated (The total results (raw material) are shown in Annex I).

Table 26 Experimental biogas average production - results.

Input				AD Biogas output			DF biogas output		
Blend	RS CCM:CFM	Organic content ($gCOD \cdot l^{-1}$)	C/N	Methane Production (ml)	% Deviation	Days (d)	Hydrogen Production (ml)	% Deviation	Days (d)
1	02:02	2	35	253,9	28%	14	108.16	22%	7
2	03:01	2	35	265,3	41%	16	108.52	35%	8
3	01:03	8	35	791,8	6%	17	283.87	15%	10
4	02:02	8	35	627,5	31%	16	180.32	29%	9
5	03:01	5	25	369,0	39%	17	83.38	39%	9
6	01:03	5	25	379,6	39%	15	97.20	44%	8
7	02:02	5	45	407,3	20%	17	100.06	32%	8
8	03:01	5	45	385,0	17%	14	84.20	36%	7
9	01:03	2	25	175,3	22%	14	73.07	12%	9
10	02:02	8	25	696,0	19%	15	226.43	16%	8
11	03:01	2	45	150,1	31%	17	102.55	36%	7
12	01:03	8	45	560,3	36%	16	234.73	28%	8
13	02:02	5	35	252,3	20%	14	149.94	38%	9

Biogas which was produced by the "blank" reactors was subtracted from the total volume of each reactor. Based on the results of the three reactors of each blend, an average and deviation was calculated. For example, the three reactors of blend No. 7 showed a total experimental methane production of 1170, 1136 and 1289 ml CH_4. Methane production of the " blank " reactor measured 791 ml of CH_4. As a result, a total production of 379, 345 and 498 mL of CH_4 was calculated for blend No. 7, resulting in an average of 407.3 mL of CH_4 and a % deviation of 20%. For each of the 13 blends, the calculation process was the same.

Since the results obtained in the "blank" reactors showed a great deal of variability, a second error was introduced to the one given by the deviations of the three reactors of each mixture.

The Table 26 shows that when the initial concentration of the organic load is increased, biogas production increases in both processes. In other words, concentration is a variable in the determination of the experimental design. Mixtures with 8 $gCOD \cdot l^{-1}$ produce up to twice as much biogas. This supports the different sensitivity analyses reported in the literature in relation to the concentration in digestion and fermentation mixtures, reporting concentrations between 20 to 30 $gCOD \cdot l^{-1}$. On the other hand, the C/N ratio does not show a trend in the results, since high methane and hydrogen productions are reported with the three C/N ratio options proposed. In addition, with respect to the deviation of the data, it is shown that the higher concentration cells show less deviation and behaved in a more stable manner during the experimentation.

1.18.1 Experimental process mass yield

Regarding the production yield calculated with Eq. 22, it is generally observed that the mixtures with the lowest concentrations (2 $gCOD \cdot l^{-1}$) generate the highest methane and hydrogen production yield, while the lowest yield is found in the medium concentration mixtures. The bioprocesses, in the experimentation, show that the mass yields increase as the concentration of the organic load decreases (Figure 39A). When the initial organic load is kept constant, it is evident that the hydrogen production yields do not vary significantly, which indicates that the additional variables of the experimental design do not have a significant influence. Figure 39B shows the opposite, when the C/N ratio is kept constant, the methane production yield does not vary significantly (especially for the extreme points 25 and 45), indicating the impact of the other variables such as the initial organic load in the anaerobic digestion process. The results show the influence of the initial C/N ratio on the yield of H2 production in the DF in agreement with recent studies. (Argun et al., 2015).

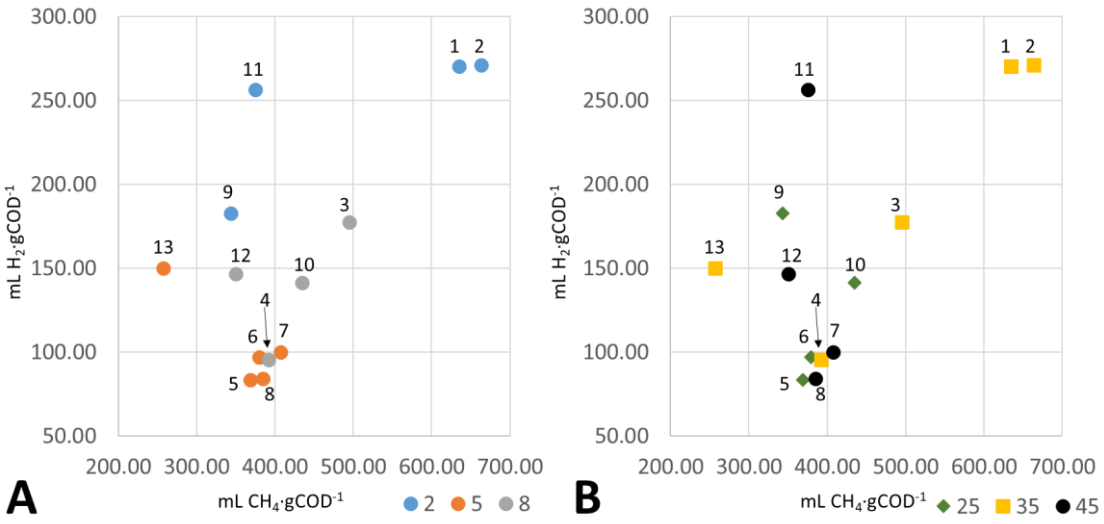

Figure 39 Experimental methane and hydrogen yields from AD and DF bioprocesses: (a) effect of different organic loads of 2, 5 and 8 g.COD.l^{-1}; (b) effect of different C/N ratios of 25, 35 and 45

Above all, the blends that show the best production and yield are those with more than 50% of coffee mucilage plus cocoa mucilage in the total blend. This shows the importance of carbohydrates in the two bioprocesses presented as well as the importance to mix waste. Although CFM and CCM appeared to be a problematic substrate for AD, due to lack of nitrogen (N) and micronutrients, high tannin concentration and inhibition caused by VFA accumulation, co-digestion with SM led to stabilization of the system, mainly because SM provided the remainder (Kampioti et al., 2022).

1.19 Model validation

Figure 40 shows the correlation between simulated and experimental biogas production yields for the different blends tested. Overall, the results show an average ratio between simulated and experimental yields (y_{sim}/y_{exp}) of 0.74 ± 0.20 for AD and 1.17 ± 0.28 for DF (average values ± standard deviations), respectively, thus indicating a good general agreement between the data.

With the only exceptions of blends 1 and 2, the ratio y_{sim}/y_{exp} for AD varied from 0.66 to 1.07 (Figure 40A), thus indicating that the AD model gives a good estimation of CH_4 production yields. The lowest differences were observed for blends 4, 6, 7, 8 and 13 (y_{sim}/y_{exp} ratios of 0.84, 0.82, 0.89, 1.02 and 1.07, respectively), whereas the highest differences were observed for blends 1, 2 and 9 (y_{sim}/y_{exp} ratios of 0.42, 0.45 and 0.53, respectively). The results indicate that the differences between simulated and experimental data for AD increase

by decreasing the organic loads and/or by increasing SM content of the blends. Higher organic loads probably resulted in dominant organic compounds in the blends used for the experiments, thus leading to more stable and more predictable conversion pathways. Moreover, variability on the single substrate composition used for the different experiments, especially for SM, may further explain the differences between simulated and experimental yields.

With the only exceptions of blends 4, 7, and 12, the ratio y_{sim}/y_{exp} for DF varied from 0.77 to 1.28 (Figure 40B), thus confirming the validity of the DF model. The lowest differences were observed for blends 3 and 6 (y_{sim}/y_{exp} ratios of 1.03 and 1.06, respectively), whereas the highest differences were observed for blends 4, 7, and 12 (y_{sim}/y_{exp} ratios of 1.72, 1,94, and 1.43, respectively), thus indicating an overestimation of H_2 production yields compared to the experimental data. The results of DF seem to indicate that the differences between simulated and experimental yields increase by increasing the CCM and/or CFM loads of the blends. Most probably, incomplete hydrolysis of complex carbohydrates (e.g. cellulose, hemicellulose) may account for the lower experimental yields for blends at high loads of CCM and/or CFM (blends 4 and 7, respectively).

The results suggest that variability on single substrate composition between the different experiments and incomplete hydrolysis of carbohydrates may account for the differences between simulated and experimental yields. However, the use of the same AD and DF models for assessing biogas production potential from model substrates may overcome these technical limits of laboratory experiments, thus allowing to compare energy recovery potentials from different blends and different process schemes.

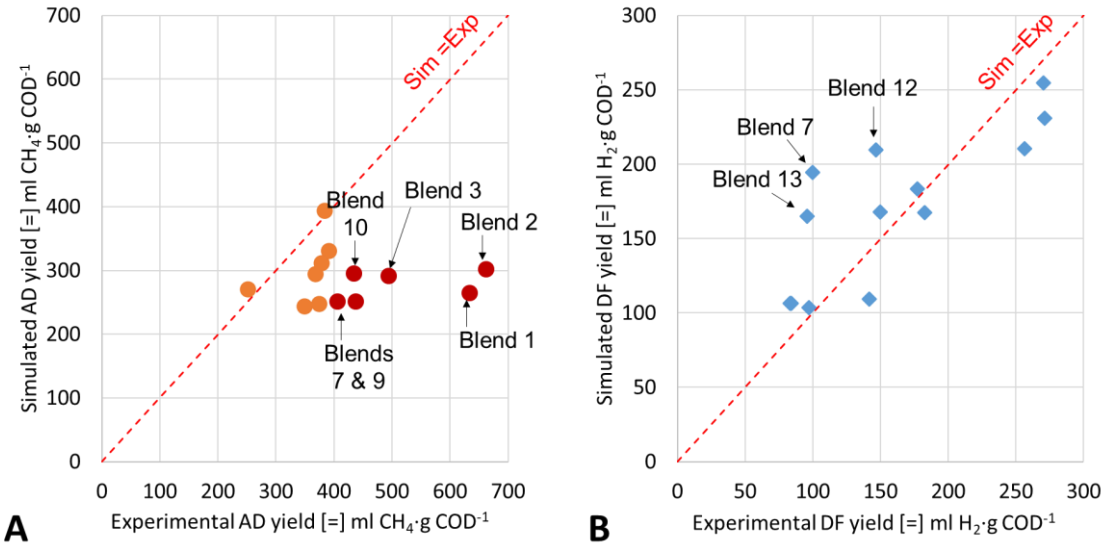

Figure 40 Simulated and experimental biogas production yields: (A) anaerobic digestion (AD); (B) dark fermentation (DF).

1.19.1 Experimental methane production analysis

The significant difference in the production yields for blends 1, 2, 3, 7, 9 and 10 required an evaluation of the production trends for each blend and the comparison of the total production versus the maximum theoretical values. Cumulative methane production values measured in volume were modified to moles using the ideal gas equation (Eq. 28). Where P = 101325 (Pa), R = 8314.463 ($Pa \cdot L \cdot mol^{-1} \cdot K^{-1}$) and T= 308.15 (K)

$$mol\ CH_4 = \frac{PV}{RT} \qquad \text{Eq. 28}$$

Figure 41 shows the methane production ratio as a function of moles of glucose. The moles of glucose were calculated by assuming 94% of the gCOD and the ideal gas law was used to calculate the moles of CH_4. The variation of the experimental data (reactors and replicates) is probably due to the heterogeneity of the substrates, and in particular with the solids content. This heterogeneity was mainly observed in the case of cocoa: the cocoa residues used to prepare the mixtures showed a strong heterogeneity in solids content. Moreover, the characterization of the substrates was done only in the liquid phase, therefore, most probably the blends richer in solids have a higher concentration of total COD than the one shown for the cocoa blend. That may explain the higher than theoretical maximum methane production values (mol CH4·mol glucose^{-1} in the Figure 41).

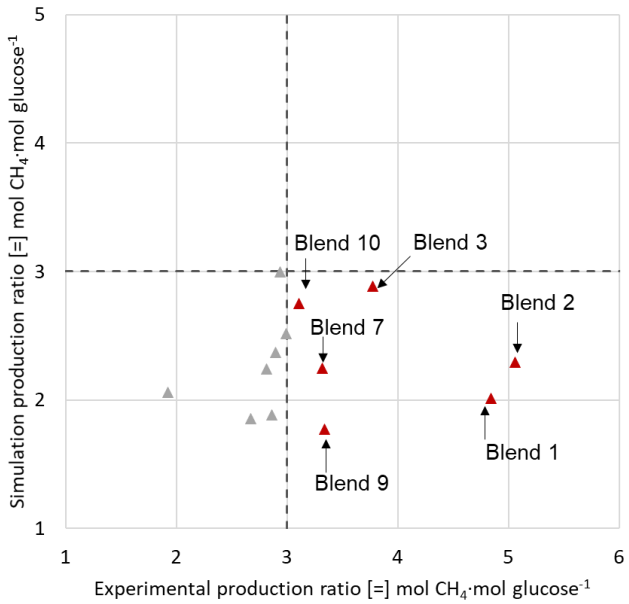

Figure 41 Experimental and simulated methane production compared to theoretical moles of glucose available in the blends.

The cumulative methane production of all blends was analyzed, especially for blends 1, 2, 3, 7, 9 and 10. Above all, it is shown that the two trends are related to the trends of: Type III: Multiple substrates but can be simplified by three categories: easily degradable, slowly degradable and intermediates (Figure 42A). Type IV: Multiple substrates with complex chain of consumption by groups of microorganisms (Figure 42B) (Rakmak et al., 2019). The trend reported by the results has been reported in the literature, however, within the 13 mixtures it shows up to three types of functions in the production, most likely caused by the diversity of the substrates and the times of realization of the tests. The literature shows that first order models are usually used or under the gompertz function. However, as shown by the results on a small scale, the behaviors are remarkably different, making it difficult to unite production to the same function for all mixtures. Five of the six blends shows significant differences in the methane production measurement increasing the standard deviations per blend. (Example: Figure 42, Complete data: Annex I). The difference in trend types difficult the use of a single mathematical function for the methane production, and thus a single production model can be validated. Furthermore, the experimental design was designed between days 0 and 20, while authors such as Bouaita et al. (2022) show that in mesophilic processes the stability of the reactors is shown between the 20th and 30th days.

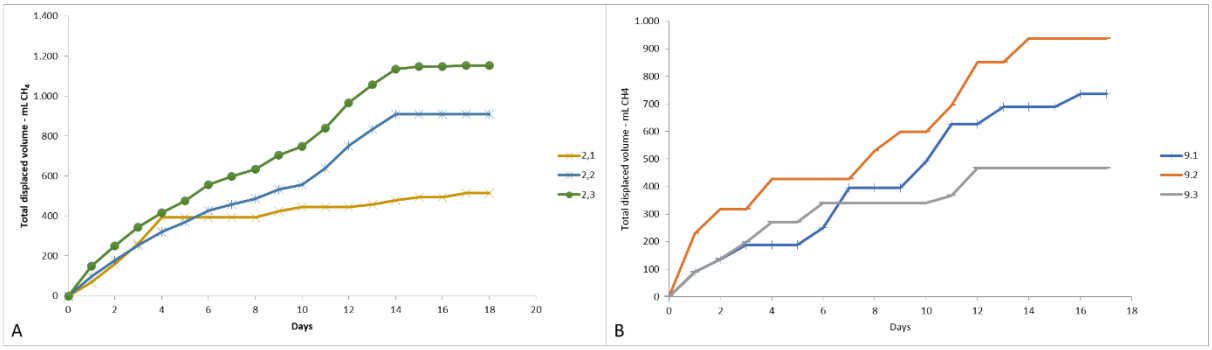

Figure 42 Experimental accumulative methane production per day (A) Blend 2, (B) Blend 9.

Furthermore, as mentioned in the methodology, two reactors were run with the diluted Alpina sludge in each set-up. Figure 43 shows that the cumulative methane production data were completely different between the B1 and B2 reactors for the three experimental batches. As mentioned in the methodology, the " blank " reactors were used to measure the cumulative methane production, using a dilution of the inoculum, with which the same processes were carried out. The difference between the methane production rates increases the complexity with respect to the methane reduction over the value for the experimental designed reactors. Overall, the methane production for the blank experimental reactors shows trends of type III and IV, in agreement with the production trends from the experimental design reactors.

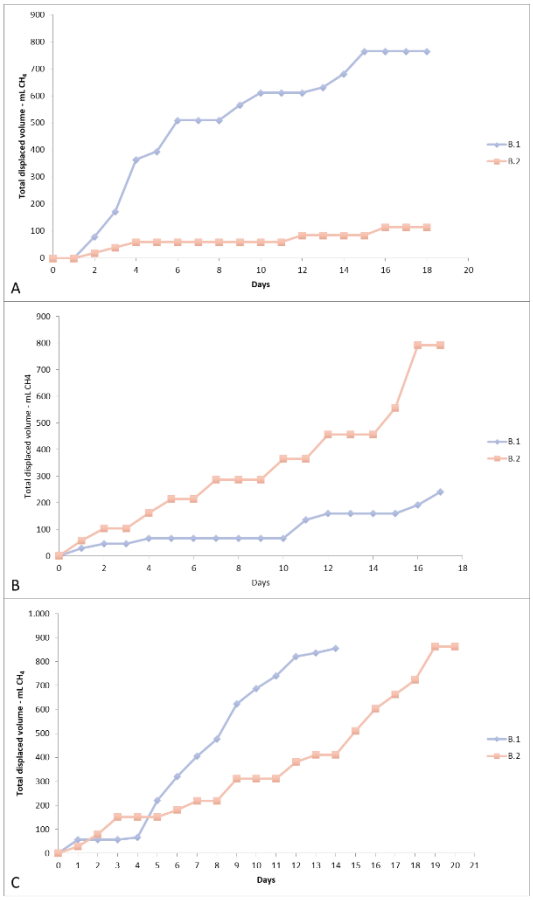

Figure 43 Blank experimental reactor set-ups accumulative methane production (B1 AND B2) per day (A) Blends 1 to 6, (B) Blends 7 to 12, (C) Blends 13 to 15.

A second problem was analyzed during the experiment relates to the CO_2 trap. During the experimental work that the NaOH concentration (1M) and the volume amount (1 L) did not work with 100% separation efficiency. A review of daily observations from the experiments shows no bubbling during CO_2 capture on the NaOH trap, supporting the hypothesis. Based on this hypothesis, the volume displaced represents the biogas produced, mainly composed of CH_4, H_2, and CO_2. Likewise, an attempt was made to improve the separation, but due to the small size of the experiments, it was not possible to get a significant improvement. Also, both numerical and experimental studies indicate that, besides CH_4, H_2 is produced during digestion, with NH_3 and H_2S at lower concentrations. As a result of the lack of a measure of the composition of the gas, errors in the accumulated value of methane production most probably increased. A random test of the samples with the highest variation showed the presence of CO_2 in the collection bags, by using the BIOGAS 5000® Landtec, which measures gas composition and flow with repeatable accuracy, depending on the availability of the material. Furthermore, it shows that the lack of technology for on-line biogas analysis leads to weaknesses in the experimental results obtained. Considering that the anaerobic

digestion process shows productions of 60% CH_4 and 40% CO_2, the volume of blends 1, 2, 3, 7, 9 and 10 were assumed to be biogas and the CH_4 production corresponds to 60% according to what has been reported experimentally for AD (Awasthi et al., 2018; Babaee et al., 2011; Bab&aelig et al., 2011; Dhar et al., 2016; Zhang et al., 2007). Approaching the final values to the theoretical maximum and improving the correlation with respect to the simulation as shown in Figure 44. Despite the fact that the correction is only made at points exceeding the theoretical maximum, this does not guarantee that the mixtures uncorrected for these other gases contain the same proportion of H_2, CO_2 and other gases as the measured CH_4 production. According to the results, the mathematical model meets the theoretical conditions and is agreeable with the published production yield values.

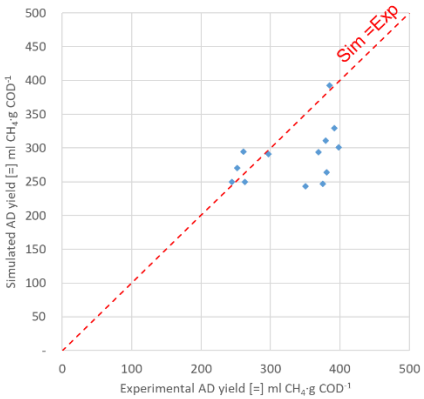

Figure 44 Simulated and experimental CH_4 in AD production yields. The total production of blends 1, 2, 3, 7, 9 and 10 corresponds to 60% of the total reported, referring to methane production.

3.BIOPROCESS SIMULATION

Figure 45 shows the simulated scheme for the initial biological processes. The physicochemical properties among the compounds were calculated with the Soave-Redlich-Kwong method (SRK-based method). Additionally, properties were calculated with the NRTL and IDEAL methods. The process simulation to evaluate the mass and energy balance was carried out in the simulation software Aspen Plus V11. In all cases the simulation compounds were only considered in liquid and gas phases.

Since water is an important parameter in the ratio of the final mixture, the components were always included on a dry basis and the additional water was added by means of the additional current (WATER). The first exchanger (INTERCAM) heats the blend from environment temperature to process temperature (35 °C). The duplicating modules - DUPL (B4, B8, B9 and B2) generate a duplication of the current (composition and operating conditions). Therefore, B4 allows to perform the processes in parallel with the same blend composition and operational conditions (temperature and pressure). The three reactors described in the methodology for the dark fermentation process are simulated in B3-1, DF and HOMOACET, while the two anaerobic digestion reactors correspond to B3 and AD. The B1 equipment fulfills the function of current selection, i.e., when the processes were simulated in parallel, ADINPUT1 was taken as the input current, while when the processes were simulated in series, ADINPUT2 was selected, corresponding to the liquid phase coming out of the dark fermentation.

The simulation of the bioprocesses shows to be sensitive in the selection of the method of calculation of the properties of the compounds. The teams show results in the SRK and NRTL methods. It is important to highlight that although the kinetics and correlations show production results similar to those reported by authors, due to the methods, part of the biogas is deposited in the liquid phase. For this reason, two separators were included as shown in Figure 45 (B12 and B15), separators that work with the ideal gas methods and allow separating the entire biogas production. The analysis of the raw data was performed in two phases. The first phase performs the validation of the model, comparing the mass yields with the experimental yields and then a mass yield analysis of three bioprocess schemes was performed.

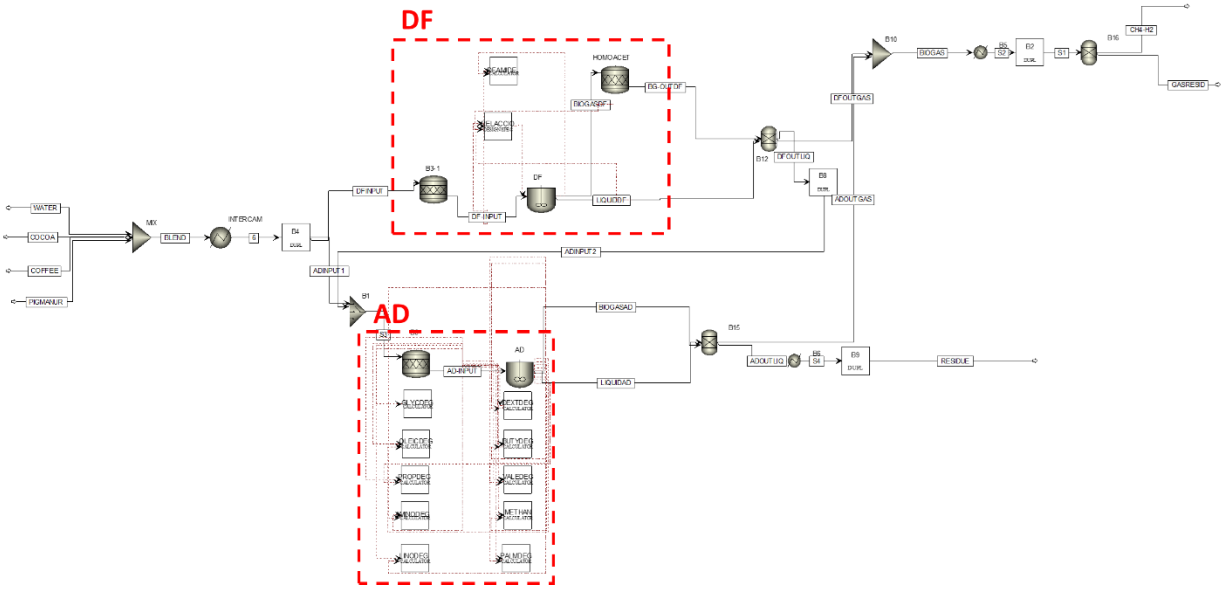

Figure 45 Bioprocess simulation scheme DF = Dark fermentation, AD = Anaerobic digestion.

1.20 Bioprocess optimization

1.20.1 Mass yield evaluation

The total biogas production yields and compositions obtained by the simulations of AD, DF, and DF followed by AD (ADF) processes, for the different substrate blends (Table 10), are summarized in Figure 46.

The biogas production yields for DF varied between 147 and 405 mL biogas·gCOD^{-1}, and the H_2 and CO_2 content of biogas varied between 65-70% and 30-35%, respectively (Figure 46C). These results are in good agreement with the theoretical compositions of biogas from the fermentative pathways used for DF simulation (N° 39 and 40 Table 15 Kinetics rate equations from Angelidaki's model are mixed with the extra kinetic equations from AMD1 in order to find the most complete kinetic expression.) (Gomes et al., 2015). The lowest biogas production yield for DF was observed for blend 9, where the dominant substrate is SM (more than 80% based on total organic load) and COD concentration is 2 gCOD·l^{-1}. Instead, the highest biogas production yield for DF was observed for blend 7, where the dominant substrate is CFM and COD concentration is 5 gCOD·l^{-1}. These differences in biogas production yields are probably primarily related to the different compositions of proteins, fats, and carbohydrates considered for CFM and SM (Table 24). Higher carbohydrate content

of CFM resulted to higher H_2 production yields for blend 7, as carbohydrates represent the most suitable substrate for DF (pathways n° 39 and 4 Table 15), whereas higher protein content of SM resulted to lower C/N ratios that may inhibit DF as described by the ammonia inhibition modules integrated in the model (Madeira et al., 2017; Serrano, 2011). These results are in good agreement with the findings of previous experimental studies (Ghimire et al., 2015a; Zhu et al., 2008), which have indicated that low C/N ratio and high concentration of ammonium ion (NH_4^+) inhibit H_2 production during DF when SM is used as the only substrate, with maximum production yields of 3,65 mL $H_2 \cdot VS^{-1}$. Indeed, higher production yields (from 68 to 652 mL $H_2 \cdot gCOD^{-1}$) were obtained by co-fermentation of substrate blends (e.g. swine manure, sewage sludge, food waste, agro-industrial waste) (Hernández et al., 2014; Kim et al., 2004b; Perera et al., 2012).

The biogas production yields for AD varied between 295 and 459 mL biogas·$gCOD^{-1}$, thus showing a lower variability according to the different blends rather than DF. The CH_4, CO_2 and H_2 biogas components were 57-70%, 29-42%, and 0.3-0.4%, respectively (Figure 46B). Higher yields of biogas production were observed for blends containing higher amounts of CFM and CCM rather than SM. Overall, biogas production yields obtained by simulations are within the ranges reported in the literature (61 - 650 mL $CH_4 \cdot gCOD^{-1}$). This large variability on experimental yields is mainly attributed to the different organic substrates and operating parameters (e.g. retention time, temperature, inoculum) between the different studies (Astals et al., 2015; Garfí et al., 2011; Hernández and Rodríguez, 2013). The blends 12 and 13, with equal CFM and CCM contents, showed the highest biogas yields (433 and 459 mL biogas·$gCOD^{-1}$, respectively) with the highest CH_4 content (70% and 69%, respectively). Therefore, they appear to be the most suitable blends for AD. These results are consistent with the experimental results of Wang et al. (2018), who indicated that biogas production performances of AD are significantly affected by the ratios of swine manure, corn stove and cucumber residues in the co-digested mixture.

The biogas production yields for DF followed by AD (ADF) varied between 602 and 864 mL biogas·$gCOD^{-1}$, and the CH_4, CO_2, and H_2 content of biogas varied between 25-51%, 30-35%, and 17-40%, respectively (Figure 46D). The highest total biogas production yields were observed for blends 7 and 8 (863 and 864 mL biogas·$gCOD^{-1}$, respectively), where the CFM and CCM are above 65% of the total organic load. Additionally, one of the substrates, CFM or CCM, dominates over the others. The lowest yields (< 160 mL biogas·$gCOD^{-1}$) were

obtained for blends 5, 6, 9, and 10, where SM is greater than 80% over the total organic load. However, despite the lowest biogas production yields, these blends also show the highest CH_4 contents in biogas. This appears to confirm that SM is more suitable for CH_4 than for H_2 production, most probably because it has a lower content in carbohydrates compared to the other substrates. While blends with SM loads equal or lower than those of CFM and CCM (blends 7, 8, 11, 12, and 13) generate biogas with CH_4 and H_2 contents comprised between 28 and 40%. ADF showed higher yields of total biogas production compared to AD and DF, this for all the substrate blends studied. As shown in Figure 46A, total biogas production yields for ADF were 1.3 - 2.3 times higher than DF, and 1.5 - 2.4 times higher than AD, thus indicating a greater conversion efficiency of organic substrate to biogas. This is coherent with the assumptions of the ADM1 model that was used for the simulations, as organic products from DF (e.g. volatile fatty acids) represent viable substrates for methanogenesis in the AD process (Hernández et al., 2014), thus increasing the total biogas production yields.

The results from simulations confirm the effectiveness of co-digestion of CFM, CCM, and SM, in a two-step process of DF followed by AD compared to the single process steps. The higher content in proteins, fats, and hemicellulose of SM supports the production of fatty acids, amino acids, and carbohydrates by hydrolysis in the DF step (Table 15). These byproducts are further converted and used as substrates for CH_4 production by acidogenesis, acetogenesis, and methanogenesis in the AD step (Table 15). Instead, the higher content in carbohydrates of CFM and CCM conducted to the production of acetate and H_2 by fermentation in the DF step (Table 15), which are used as substrates for CH_4 production by acetotrophic and hydrogenotrophic methanogenesis in the AD step (pathways 37 and 38, Table 15). Moreover, the simulation results indicate that different organic loads do not seem to have a significant impact on production yields and biogas compositions for the different blends and processes studied. This behavior was related to all blends and processes simulated with the same stoichiometric ratios, considering retention times longer enough to achieve conversion equilibrium, and without considering excess substrate inhibition. However, despite showing the similar production yields, higher organic loads may give higher flow rates of biogas production in real operating conditions, as more organic substrate is available for biogas production per unit of time (Barca et al., 2015).

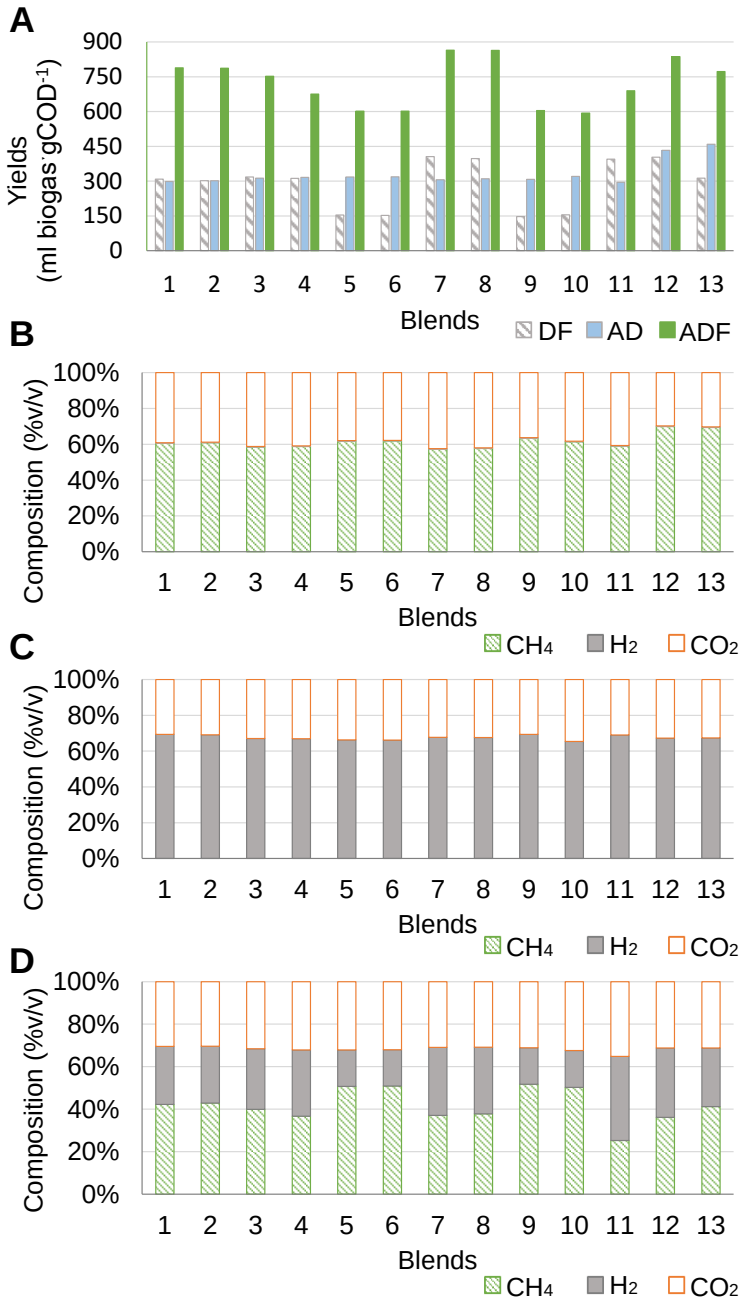

Figure 46 Simulations of AD, DF, and ADF processes for the different substrate blends: (A) Total biogas production yields for AD, DF, and ADF; (B) Biogas composition for AD; (C) Biogas composition for DF; (D) Biogas composition for ADF.

1.20.2 Effect of organic load on energy recovery yield

One of the impact factors on biogas production yields is the input load (Jiang et al., 2020). Figure 47 shows the evolution of total energy recovery yield η_{total} (%) as a function of inlet organic load for the five departments with the highest production of CFM, CCM, and SM (Antioquia, Boyacá, Cundinamarca, Meta, and Santander). The η_{total} (%) values in Figure 47

were obtained by comparative ADF simulations according to the CFM, CCM, and SM production data in 2017. The results indicate that η_{total} (%) increases from 52.1 - 60.6% to 68 - 75.9% by increasing inlet COD from 2 to 26 gCOD·l^{-1} for all the departments. This was primarily related to the lower energy consumption for the initial heating of the feed, since the higher the COD concentration, the lower the feed flow to be heated. However, the rate of η_{total} (%) increase appears to decrease by increasing organic load, thus suggesting an optimal inlet COD concentration to obtain higher η_{total} (%) while maintaining acceptable yields of substrate conversion. Moreover, increasing the inlet COD concentration over the average value of the available raw mixtures (26 gCOD·l^{-1}) would require a further energy consumption (e.g., drying and membrane processes) that may affect the energy recovery efficiency of the full process. Among the departments in Figure 47, the department of Santander shows the highest η_{total} (%) for all the inlet COD concentrations. This was probably because Santander has the highest ratios (CFM+CCM)/SM and C/N, thus resulting in higher biogas production performances compared to the other departments.

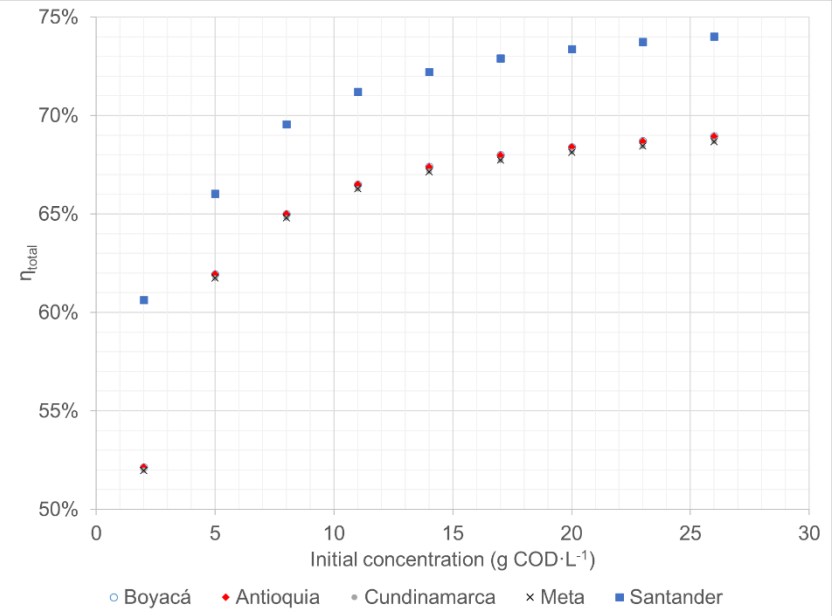

Figure 47 Total energy recovery yield as a function of inlet organic load: comparative ADF simulations according to CFM, CCM, and SM production data in 2017 from Eq. 13

1.21 Evaluation of energy recovery potential in Colombia from ADF bioprocess

Table 27 summarizes the energy recovery potential (toe) from the biogas and digestate obtained for each department based on production data of 2017, as well as the energy recovery yields for biogas η_{biogas} (%), digestate $\eta_{digestate}$ (%), and the total energy recovery yields η_{total} (%) (Eq. 11-13 section 1.13.4). The highest energy recovery potentials from biogas were observed for the departments of Antioquia, Córdoba, and Cundinamarca (48990, 10160, and 13460 toe, respectively), which are the departments with the highest cumulated productions of CFM, CCM, and SM. Instead, the lowest energy recovery potentials from biogas were observed for the departments with the lowest cumulated productions of CFM, CCM, and SM (Putumayo and Vichada, 866 and 148 toe, respectively). According to the energy consumption data in 2017 (IEA, 2020), the total energy recovery potential from the biogas (151.6 ktoe) could supply up to 70% of the energy demand for agriculture/forestry activities in Colombia (215 ktoe for 2017).

Table 27 Energy recovery potential from biogas and digestate, energy recovery yields for biogas and digestate, and total energy recovery yields obtained by ADF simulation according to the total availability of CFM, CCM, and SM in 2017 (inlet organic load 26 gCOD·l^{-1}).

Department	Energy recovery potential from biogas (toe)	Energy recovery potential from digestate (toe)	ηbiogas (%)	ηdigestate (%)	ηtotal (%)
Antioquia	48990	1137	48.9	20.1	69.0
Arauca	1882	41	50.9	19.6	70.5
Atlántico	4325	102	48.3	20.2	68.6
Bolívar	3061	72	48.5	20.1	68.6
Boyacá	5093	118	48.9	20.1	69.0
Caldas	4391	94	51.4	19.5	70.9
Caquetá	1750	41	48.6	20.2	68.8
Casanare	1735	41	48.4	20.2	68.6
Cauca	3152	67	51.7	19.4	71.1
Cesar	1779	41	49.2	20.0	69.2
Córdoba	10160	240	48.4	20.2	68.6
Cundinamarca	13460	317	48.4	20.2	68.6
Huila	4460	94	51.8	19.4	71.2
La Guajira	1003	24	48.5	20.2	68.7
Magdalena	5953	139	48.7	20.1	68.8
Meta	6216	146	48.5	20.2	68.7
Nariño	4060	93	49.2	20.0	69.1

Norte de Santander	2377	53	50.0	22.2	72.2
Putumayo	866	20	48.6	20.2	68.8
Quindío	2003	45	49.7	19.9	69.6
Risaralda	3961	87	50.5	19.8	70.3
Santander	3468	66	55.5	18.7	74.2
Sucre	5895	139	48.4	20.2	68.6
Tolima	2500	52	52.0	19.4	71.4
Valle del Cauca	8950	204	49.4	20.0	69.4
Vichada	148	3	48.4	20.2	68.6

As shown in Table 27, the energy recovery yields for biogas η_{biogas} (%) varied between 48.3 to 55.5%. The highest η_{biogas} (%) were observed for the departments of Cauca, Huila, Santander, and Tolima (51.7, 51.8, 55.5 and 52%, respectively), which are the departments with the highest CCF/SM and/or CCM/SM production ratios. On the contrary, the departments with lower CCF/SM and/or CCM/SM production ratios (Atlántico, Córdoba, Sucre, and Vichada) usually present lower energy recovery yields for biogas η_{biogas} (%) and higher energy recovery yields for digestate $\eta_{digestate}$ (%). This seems to confirm that although SM is less effective than CFM and CCM in biogas production, it is more effective for recovering other by-products from digestate (e.g. propionate, butyrate, ethanol, benzene, acetate, and furfural). As shown in Table 27, the total energy recovery yields η_{total} (%), which include biogas and digestate energy (Eq. 13 section 1.13.4), varied between 48.9% (Atlántico, Sucre, and Vichada) to 55.5% (Santander). The results indicate higher total energy recovery yields η_{total} (%) for the departments with higher CCF/SM and/or CCM/SM production ratios, thus confirming that CFM and CCM are more effective than SM for energy recovery by ADF processes. However, it should be noted that, as this is a theoretical study on energy recovery potential, it does not take into account factors such as seasonal fluctuations in agro-industrial production and variability on substrate composition between the different production sites due to breeding and cultivation methods, and to soil and climatic characteristics.

For each department, the potential recovery of biogas and digestate was evaluated by comparative ADF simulations according to the total available amounts of CFM, CCM, and SM in 2017, and considering for all the simulations an inlet COD concentration of 26 g $COD \cdot l^{-1}$. As shown in Table 28, the total mass of biogas recovered per department varied from 307.6 ton (Vichada) to 102200 ton (Antioquia), whereas the total mass of digestate

recovered per department varied from 146.3 ton (Vichada) to 47580 ton (Antioquia). The main components of biogas were CO_2 and CH_4, with an evaluated production potential ranging between 176.6 - 58960 ton and 105.7 - 34950 ton, respectively, whereas the main components of digestate were ethyl cianoacetate and propionate, with an evaluated production potential ranging between 11.19 - 3693 ton and 10.08 - 3295 ton, respectively.

Table 28 Total mass and main components of biogas and dried mass and main components of digestate obtained by ADF simulation according to the total availability of CFM, CCM, and SM in 2017 (inlet organic load 26 $gCOD \cdot l^{-1}$).

Department	Mass of biogas (ton)	Main components of biogas			Mass of digestate (ton)	Main components of digestate						
		CH_4 (ton)	**H_2 (ton)**	**CO_2 (ton)**		**Ethyl cianoacetate (ton)**	**Propionate (ton)**	**Butyrate (ton)**	**Ethanol (ton)**	**Benzene (ton)**	**Acetate (ton)**	**Furfural (ton)**
Antioquia	102200	34950	1472	58960	47580	3693	3295	1458	927.0	387.6	370.3	2008
Arauca	3964	1334	63.47	2326	1719	140.2	116.8	54.34	35.17	13.73	13.91	72.25
Atlántico	8994	3093	125.2	5162	4280	327.4	296.7	129.6	82.74	34.90	33.15	181.0
Bolívar	6386	2183	91.69	3680	3012	230.9	207.5	91.50	58.49	24.52	24.90	127.3
Boyacá	10640	3627	155.9	6152	4954	383.4	342.4	151.5	96.81	40.27	38.65	209.2
Caldas	9312	3094	156.5	5506	3915	324.3	269.4	127.2	78.91	31.76	32.06	163.4
Caquetá	3650	1247	52.51	2104	1717	132.0	119.1	52.27	33.35	14.00	13.09	72.60
Casanare	3616	1238	51.42	2081	1716	131.0	118.4	51.99	33.19	13.98	14.09	72.51
Cauca	6691	2220	113.5	3962	2792	232.5	192.0	91.10	56.48	22.63	22.96	116.4
Cesar	3723	1266	55.29	2156	1717	133.7	118.8	52.76	33.71	13.95	13.00	72.49
Córdoba	21130	7265	294.2	12130	10060	769.0	695.6	304.4	194.4	81.99	80.30	425.2
Cundinamarca	28070	9598	402.3	16170	13250	1016	915.0	402.7	256.8	108.0	107.7	559.9
Huila	9447	3149	157.7	5583	3945	329.7	271.2	128.6	80.06	31.91	31.84	164.6
La Guajira	2087	717.0	29.23	1199	989.5	75.89	68.55	30.01	19.17	8.063	7.684	41.84
Magdalena	12430	4242	180.6	7177	5815	448.6	402.9	177.6	113.1	47.38	44.98	245.6
Meta	12960	4434	185.6	7467	6124	469.1	422.8	185.9	118.8	49.86	49.38	258.8
Nariño	8505	2886	127.4	4934	3899	304.7	269.8	120.5	76.27	31.76	30.62	164.3
Norte de Santander	5007	1682	79.48	2930	2227	177.4	155.4	69.55	44.52	18.05	11.15	94.06
Putumayo	1803	618.6	25.51	1037	849.8	65.44	58.79	25.84	16.52	6.915	6.617	35.91
Quindío	4198	1424	63.45	2440	1892	150.1	130.8	59.10	37.22	15.40	15.06	79.54
Risaralda	8339	2809	131.2	4879	3655	295.1	250.5	116.0	72.54	29.69	31.94	153.0
Santander	7453	2425	141.9	4514	2768	251.6	182.5	95.36	61.13	21.58	25.98	114.5
Sucre	12260	4215	170.7	7036	5833	446.2	404.4	176.6	112.8	47.56	45.24	246.7
Tolima	5302	1763	89.61	3141	2195	184.4	149.5	71.87	44.76	17.71	19.49	91.41
Valle del Cauca	18730	6373	277.9	10850	8549	672.2	591.2	265.0	167.5	69.60	67.60	359.9
Vichada	307.6	105.7	4.293	176.6	146.3	11.19	10.08	4.429	2.829	1.192	1.217	6.181

4.CONCLUSIONS

The results presented in this Chapter contribute to the development of AD and DF models to assess biogas production performances from residual biomass. The characterization of the residual biomass of the agroindustry allows the use of simulation tools to obtain production potential and future technical-economic evaluations.

Specifically, to produce the bioprocesses in series (ADF), it was observed that the initial DOC concentration and the C/N ratio are properties that contribute to the operational optimization, since they showed a correlation with the hydrogen and methane production yield, respectively.

The results indicate that the local availability of different types of residual biomass represents the most influential parameter in assessing the energy recovery potential in Colombia. For this reason, for the use of the model it is important the characterization of the biomass and continuous mixtures, as well as the adjustment or variation in the conversion fraction of the reactants in the hydrolysis reaction equation.

The optimization of the bioprocesses through the proposed design of bioprocesses in series (ADF) and the minimization of the water content, increase the biogas production to more than double and maximize the energy yield of the process, which helps to calculate the maximum potential of the residual biomass according to its availability. The energy recovery potential in Colombia for 2017 is 155.1 ktoe according to the local production amounts of CFM, CCM, and SM. Overall, energy recovery yields improve by increasing CFM/SM and/or CCM/SM ratios of the feed, and by increasing organic load from 2 to 26 $gCOD \cdot l^{-1}$.

The energy yield of bioprocesses must then be analyzed including the biogas treatment processes. Especially for the need to remove sulfur, ammonia and CO_2, minimum requirement for the use of methane and hydrogen for heat and/or electricity generation. Furthermore, to improve energy efficiency, processes such as reforming should be studied that seek to produce hydrogen because its heating value is higher than that of methane. Finally, in addition to the initial capture of waste gases, it is necessary to use them within the process for the valorization or production of new products. For this reason, the

implementation of new processes and their technical-environmental evaluation are sought to visualize them as possible solutions for the Colombian agroindustry.

CHAPTER IV BIOREFINERY SCHEMES EVALUATION

1.INTRODUCTION

This Chapter IV, entitled “Biorefinery schemes evaluation”, summarizes the main results of the environmental and technical analysis of three biorefinery schemes for the production of CH_4, H_2, CO, methanol, and digestate, as products of interest for the valorization of swine manure, coffee mucilage, and cocoa mucilage available in the department of Santander, Colombia. The department of Santander presents the highest growth in the three agroindustry’s studied, and it is also the largest cocoa producer, supplying a high amount of carbohydrates according to the results shown in the previous chapter.

Having established the maximum biogas yield with the minimum water content and the simulation of the bioprocesses in series (ADF) in the previous Chapter III, the simulation results are shown here when the separation, reforming and synthesis processes are added. The Chapter IV seeks to complement the application of biomass valorization, which is why it begins its study with the available yield for the total available biomass and the sensitivity analysis of the reforming and synthesis processes that can be used in the production of the biomass.

2.CONCEPTUAL DESIGN OF BIOREFINERY

1.22 Simulation of the biorefinery schemes

All three biorefinery schemes show simulation results consistent with the literature. In the following sections, the results are analyzed from the mass and energy point of view. All raw data of the simulated equipment can be found in Annex I.

1.22.1 Products mass yield

Table 29 shows the relevant mass production results for the three biorefinery schemes. For the scheme No. 1, the biogas composition is within the range of those reported in the initial validation of the bioprocesses (45% CH_4, 23% H_2 and 32% CO_2). Also, it is highlighted among the results that the biogas yields (175 mL H_2 gCOD·L^{-1} and 378 mL CH_4 gCOD·L^{-1}) are in agreement with those reported with the blend No. 8 for the ADF process (Figure 42, Chapter III), which shows the importance of co-digestion. The variation with respect to the other mixtures is most probably due to the influence of the C/N mass ratio (Santander case study the C/N = 11), which is coherent with the results shown by Zheng et al. (2021) that show that at C/N ratios below 12 the specific yield of methane is reduced by up to 80%. Similar behaviors are already observed in the literature (Carotenuto et al., 2020; Zheng et al., 2021).

Table 29 Biorefinery schemes mass production results and yields

Biorefinery Scheme	Product (i)	Mass flow - m_i (kg·d^{-1})	Y_i (mL·gCOD^{-1})	η_{mass_i} (Eq 22) (%)
No. 1	**H_2**	369	175	2
	CH_4	5968	378	26
	DIGESTATE	6170	n.a	29
No. 2	**H_2**	2573	1224	11
	CO	9004	337	39
	DIGESTATE	6170	n.a	29
No. 3	**METHANOL**	141	0.01	1
	H_2	1806	859	8
	CO	10561	396	45
	DIGESTATE	6170	n.a	29

The scheme No. 2 is based on the future demand of hydrogen for Colombia. The modal distribution of transportation in Colombia is completely biased to the road mode, which is responsible for the consumption of 88% of the total energy consumption in the transportation activity. This makes it necessary not only to promote electro-mobility, but it is also essential to ensure that other more efficient modes increase their participation in the energy matrix. One of the demands of the Ministry of Science, Technology and Innovation is based on the use of hydrogen as a fuel, thus showing its future demand. The biorefinery scheme No. 2 shows a significant increase in the production of hydrogen as the main compound. It produces six times more in flow with respect to the previous scheme, obtaining yields of 1224 mL $H_2 \cdot gCOD^{-1}$, values that have not been possible to obtain with bioprocesses alone. In relation to the composition of the gases obtained, hydrogen represents more than 60%, which shows higher yields of hydrogen production compared to other processes, such as thermochemical processes (gasification and pyrolysis). This is attributed to the fact that it is the integration of the biological processes and the reforming that generate the utilization of the compounds for its production (Das et al., 2021; Puig-Gamero et al., 2021).

The latest scheme, biorefinery scheme No. 3, aims to reduce emissions into the atmosphere by synthesizing methanol, as well as to fulfill the demand for methanol, a compound that is currently imported into Colombia. The mass balance shows that more than twice the proposed hydrogen is produced compared to the biorefinery scheme No. 1, while the mass yield of methanol is only 1% (mass of methanol recovered per initial mass of COD). The model used the minimum conversion rate presented by Lee et al. (2020). However, the same author relates that the production cost increases significantly when less than 1.64 ton/d is produced, which indicates that there would be an economic cost overrun in scheme No. 3. As shown in Table 29, the conversion efficiency of the process from methane reforming to methanol production is low and agrees with that presented by Surendra et al. (2015).

On the other hand, the CO_2 production yield was evaluated since it is an important factor for the environmental analysis. Table 30 shows the daily mass of CO_2 obtained in the process and the yield with respect to the dry biomass flow. The yield range is between 36 to 62% (mass of CO_2 produced per initial mass of COD). Above all, it shows the high production of CO_2 that the bioprocesses have and that increases the reforming. Authors such as Niu, et al. (2020) report reforming processes using CO_2 as a reaction source to reduce intrinsic impact.

However, the use of metal catalysts such as Ni and Pt is required. While the SMR reforming reactors using water, generate efficiencies with high conversions, energy efficiencies and without the use of catalysts (Niu et al., 2020).

Table 30 Biorefinery schemes, CO_2 mass production and yields

Biorefinery scheme	Mass flow - CO_2 ($kg \cdot d^{-1}$)	Y_{CO2} ($mL \cdot gCOD^{-1}$)	$\eta_{mass_{CO2}}$ (Eq 22) (%)	CO_2e ($kg \cdot d^{-1}$)
No. 1	12356	266	53	176332
No. 2	14413	311	62	30629
No. 3	8424	181	36	8967

According to Table 30, the biorefinery scheme with the lowest CO_2 production efficiency is the No. 3, with a mass production yield of 36% (mass of CO_2 produced per unit of COD) due to the consumption of CO_2 in the methanol synthesis. Also, the last column expresses the mass per day of CO_2 equivalent (CO_2e) of the processes. This is a factor reported by Aspen that considers the energy consumption of the simulated equipment (according to the assigned service). As shown in Table 30, the biorefinery scheme with the lowest reported CO_2e is scheme No. 3. The CO_2e of the biorefinery scheme No. 3 is equivalent to only 5% of the scheme No. 1 and 29% of the scheme No. 2.

Carbon dioxide equivalent generation values are currently compared by mass quantity of biogas or hydrogen generated. For the case of the biorefinery scheme No. 1, a value of 24.82 $kgCO_2e/kg_{Biogas\ (H2 + CH4)}$ is obtained. This value is very close to the values reported in the pollution indicator of the natural gas vapor reforming process (25.05 $kgCO_2e/kgH_2$) and the ethanol reforming process (21 $kgCO_2e/kgH_2$), as described by Lora and Nascimento (2004). Furthermore, according to the literature they are above the upper range of the indicator. On the other hand, biorefinery schemes No. 2 and 3 show values of 11.90 and 11.01 $kgCO_2e/kgH_2$, respectively. These values are within the reported ranges for sustainable reforming and hydrogen generation processes (from 3 to 20 $kgCO_{2e}/kgH_2$) (Madeira et al., 2021, 2017a; Motazedi et al., 2021). It is important to note that the CO_2e values are highly dependent on the utilities or heating services and that these values can be optimized under varying utilities or energy integration designs. Above all, it is demonstrated that in the mass balance of pollutant generation or pollution indicator, biorefinery schemes No. 2 and No. 3 are shown to be the most efficient and sustainable. Its indicators are below those known from

traditional methods, demonstrating the feasibility of the designs (Lora and Nascimento, 2004).

1.22.2 Bioprocess sensitivity analysis

The sensitivity analysis on the bioprocesses obtained in Aspen Plus (Figure 48), shows that the variation of water content in the biomass impacts the production of biogas in DF and AD. In this case, it is shown that H_2 production increases with increasing the water content of the inlet biomass feedstock for the DF and AD processes (Figure 48A and B). On the contrary, CH_4 production decreases with increasing water content (Figure 48B). However, the energy consumption increases significantly in both processes (Figure 48C), so that increasing the amount of water decreases the total energy yield of the bioprocesses, as also demonstrated in section 1.20.2. The sensitivity analysis allows to see the importance of dry bioprocess studies (e.g., dry AD) on the energy consumption impact, which is one of the main weakness of the bioprocesses as reported in the literature. Moreover, the sensitivity analysis highlights the importance of the selection of the product of interest. That is, in schemes that have as a priority the production of hydrogen, the design of water-abundant processes is very likely to be of convenience. Indeed, depending on the water content of the biomass, it could be possible to select the biorefinery scheme leading to one specific product (H_2 or CH_4).

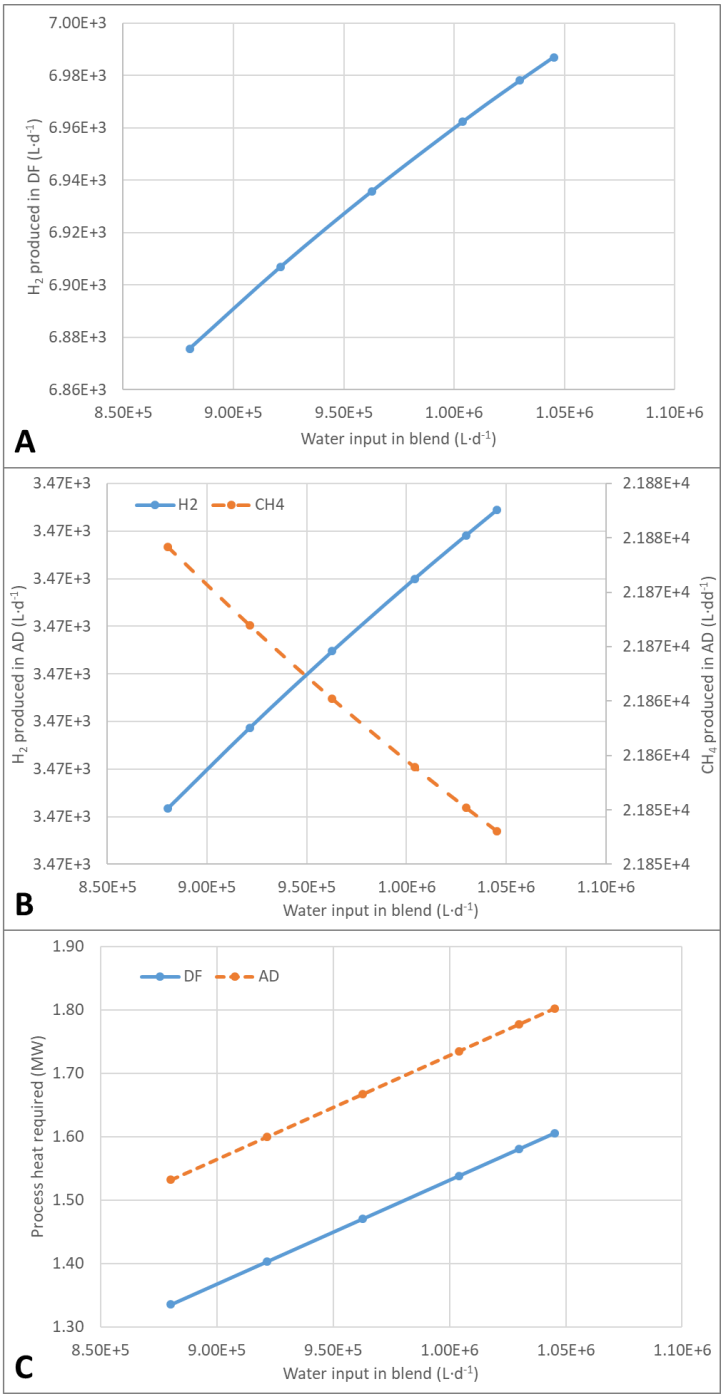

Figure 48 Sensitivity analysis of the bioprocesses, variation of initial water concentration. (A) Hydrogen production in DF; (B) Methane and hydrogen production in AD; (C) Power consumption in DF and AD. Graphs obtained in Aspen Plus.

1.22.3 Reforming sensitivity analysis

Figure 49 shows the results obtained when the pressure and temperature are varied in the reactor that reforms CH_4 to H_2. Overall, the results indicate that the temperature has the

greatest impact of power consumption and biogas production performance. Figure 49A shows how the power consumption of the reforming reactor is directly proportional to temperature, whereas pressure is a property that does not show large changes in the process. Regarding the H_2 production (Figure 49B) at the process output (total production), its highest production is obtained at a temperature of 800 °C, and it increases with pressure. Figure 49C and D, show the yields at the process output, the H_2/CO ratio takes theoretical results (Doassans-Carrère et al., 2014), so it is convenient in the future to simulate processes with catalysis and add restrictions that decrease the ratio, taking into account that at industrial level lower values are replaced. The H_2/CO_2 ratios are within the ranges reported in the literature, which are 0.25 for steam CH_4 reforming and 0.33 for partial oxidation of CH_4 (Armor, 1999). The process also shows that at higher temperatures not only decreases the production of H_2 but also increases the production of CO_2, which indicates a greater environmental impact.

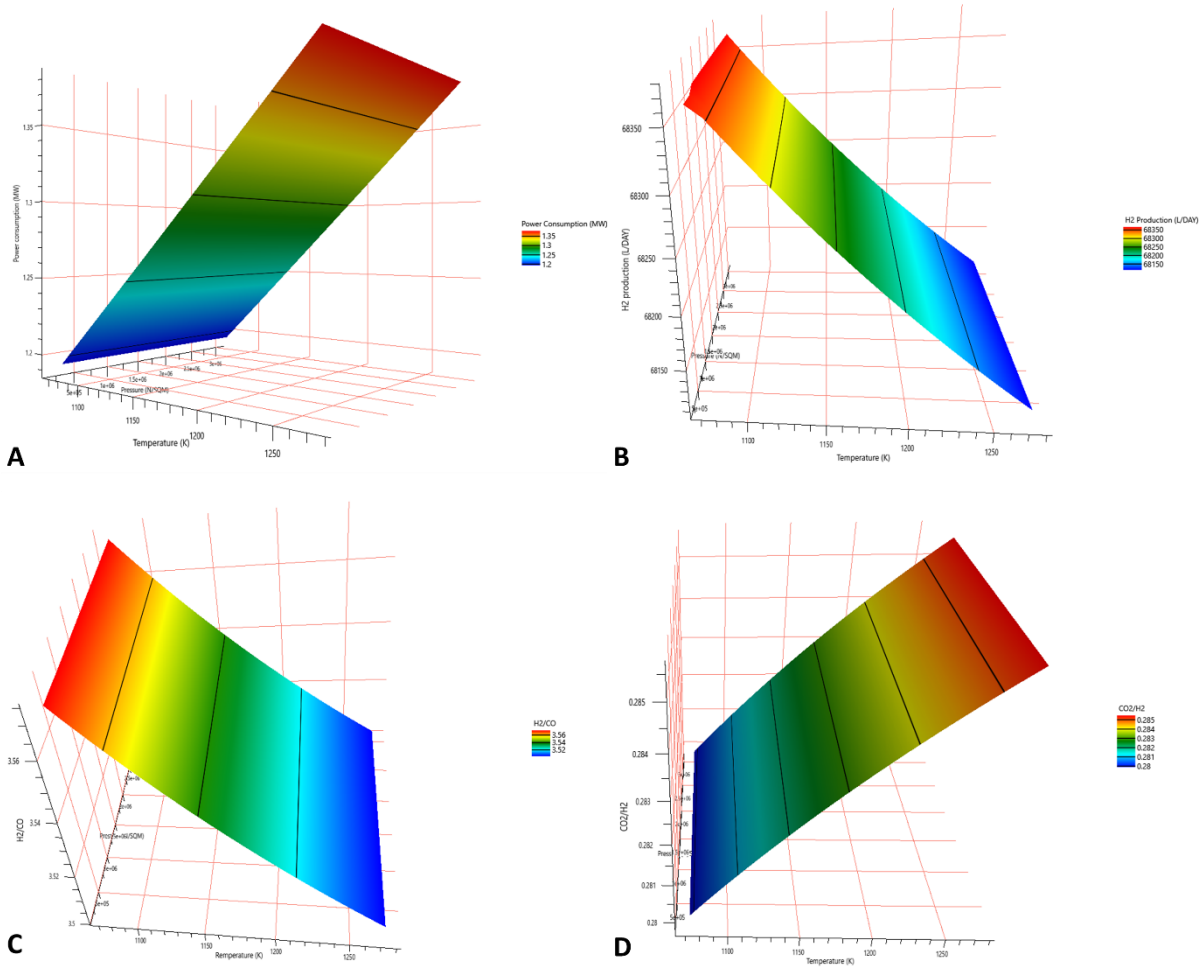

Figure 49 Sensitivity analysis of the CH_4 reforming to H_2 process: effect of temperature and pressure on (A) power consumption; (B) H_2 production; (C) H_2/CO ratio; (D) effect on CO_2/H_2 ratio.

1.22.4 Methanol synthesis sensitivity analysis

Figure 50 shows the results on the equilibrium methanol synthesis reactor when the pressure and temperature are varied. Figure 50A shows that CH_4 production varies significantly as a function of pressure at low temperatures, especially below 520 K, a variation that is also evident in the studies of Lee et al. (2020). Furthermore, the incremental gap in production at high temperatures between the variation of pressures decreases. Above all, it is identified that the highest production values occur near 500 K and at 100 atm.

The conversion of CO_2, on the other hand, increases as a function of temperature. Pressure does not prove to be a property of great impact on CO_2 conversion. The range of increase is within the range reported in the literature. The simulation results by Kiss et al. (2016) and results from Lee et al. (2020) reports a conversion of 17% at temperatures even lower than those studied, but at higher pressures. However, it should be noticed that a study uses catalysts for the optimization of the process (An et al., 2009; Kiss et al., 2016; Lee et al., 2020, p. 2). Lee et al. (2020) shows the analysis at 50 atm and as a function of temperature, these values tend to stabilize from 523 K, also in the same study reports the conversion of CO_2 as a function of gas hourly space velocity (GHS)/h at 50 bar and 523 K reporting conversions between 20 and 28% showing that the values found in the graph Figure 50B are within the reported ranges of CO_2 conversion.

Figure 50C shows the conversion of CO which varies between 8 and 11% lower values than those presented by Puig-Gamero et al. (2018), most likely because the study performed does not consider the reaction that relates the generation of CO (Eq 18), thus increasing the CO output value and hence decreasing the CO conversion. Also, as shown in Puig-Gamero et al. (2018) the use of recirculation of products and by-products increases methanol and CO production, and it decreases CO_2 emissions into the atmosphere.

Finally, Figure 50D shows the variation of reactor energy consumption as a function of pressure and temperature. The highest energy consumption is obtained at the lowest temperatures and pressures that were investigated in the sensitivity analysis. The results show that between 520 and 540 K there is no major change in the energy consumption of the

system when the pressure is varied, determining this as an optimal area of study for the energy saving function.

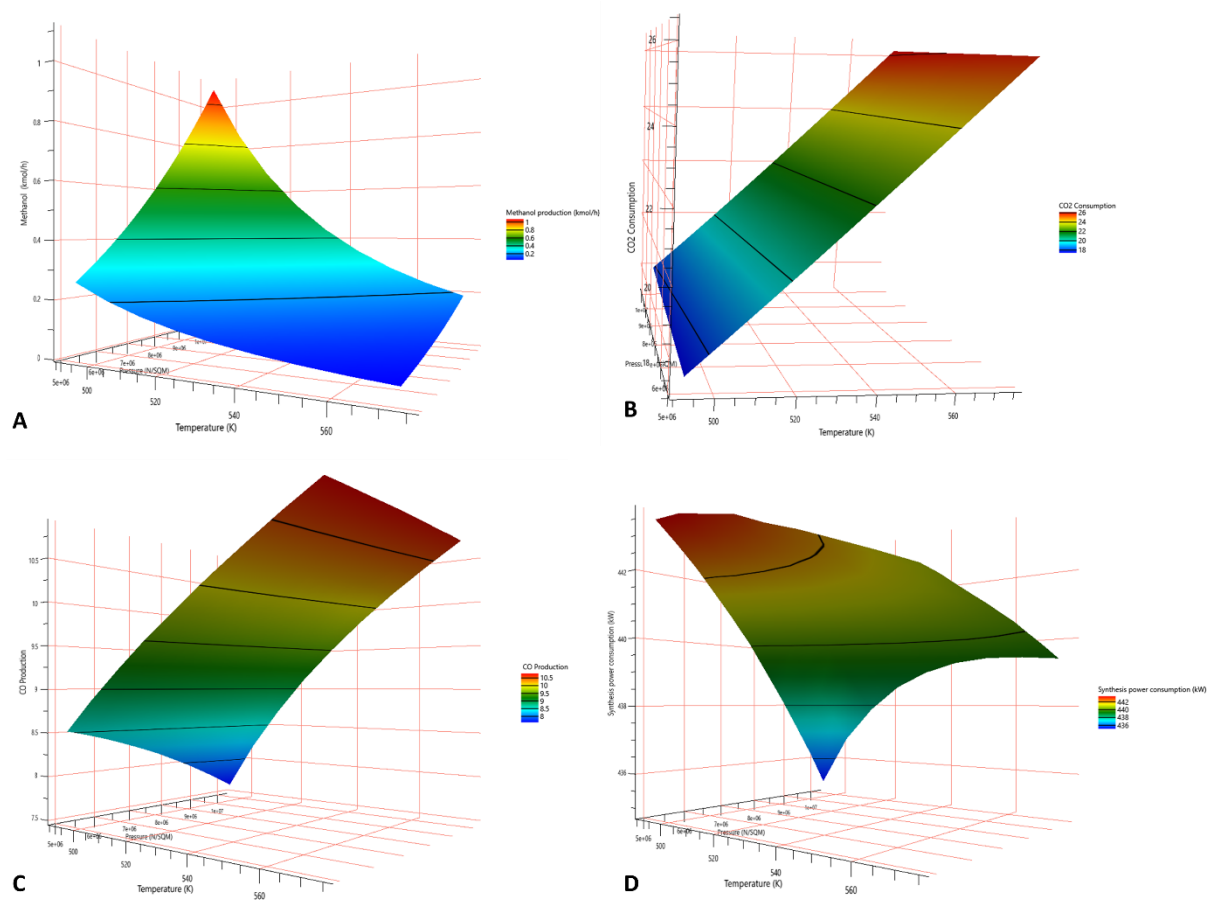

Figure 50 Sensitivity analysis of the methanol synthesis reactor, variation of results as a function of temperature and pressure. (A) Variation in methanol production (kmol/h); (B) Variation in carbon dioxide consumption; (C) Carbon monoxide generation; (D) Reactor power consumption (kW).

1.23 Biorefinery scheme environmental and energy analysis

1.23.1 Life cycle assessment (LCA)

The simulation results were plotted as a process flow diagram (PFD) with mass and energy balances to allow easy reading for inclusion in the life cycle analysis software. Figure 51, Figure 52 and Figure 53, show the schemes used for the LCA analysis of the biorefinery schemes No. 1, No. 2 and No. 3, respectively, obtained from the simulation.

All untreated data obtained in the life cycle analysis are presented in Annex IV for the three biorefinery schemes. The analysis for each of them and their comparison with the processes to produce the main products reported in the literature is presented in the following sections.

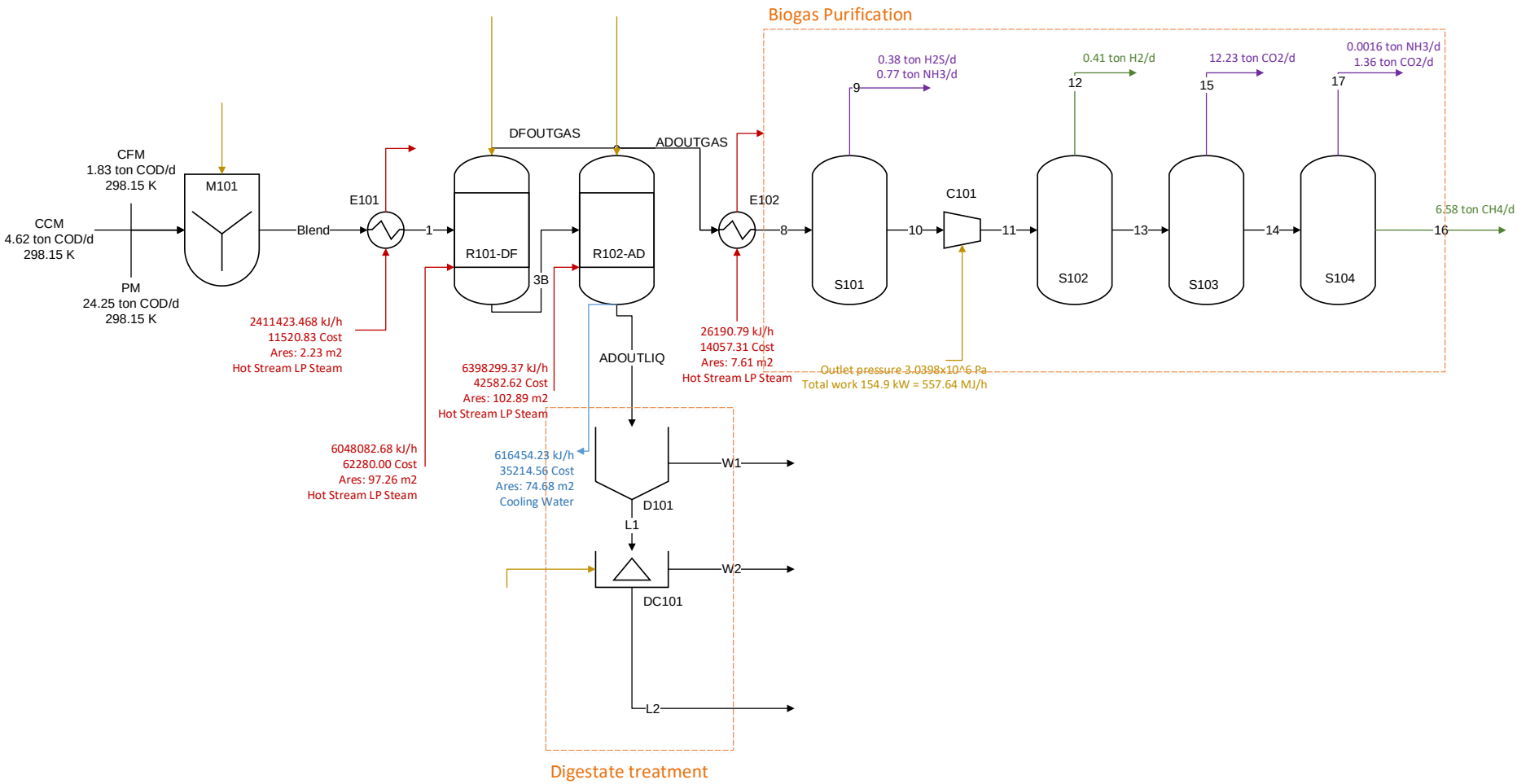

Figure 51 Process flow diagram of inputs and outputs (mass and energy flow) of the biorefinery scheme No. 1 used for the life cycle analysis. The power requirement heating (in red lines) and cooling (in blue lines). Green flow lines show the products of interest (H_2, CH_4 and Methanol), purple and final black flow lines show the process residues.

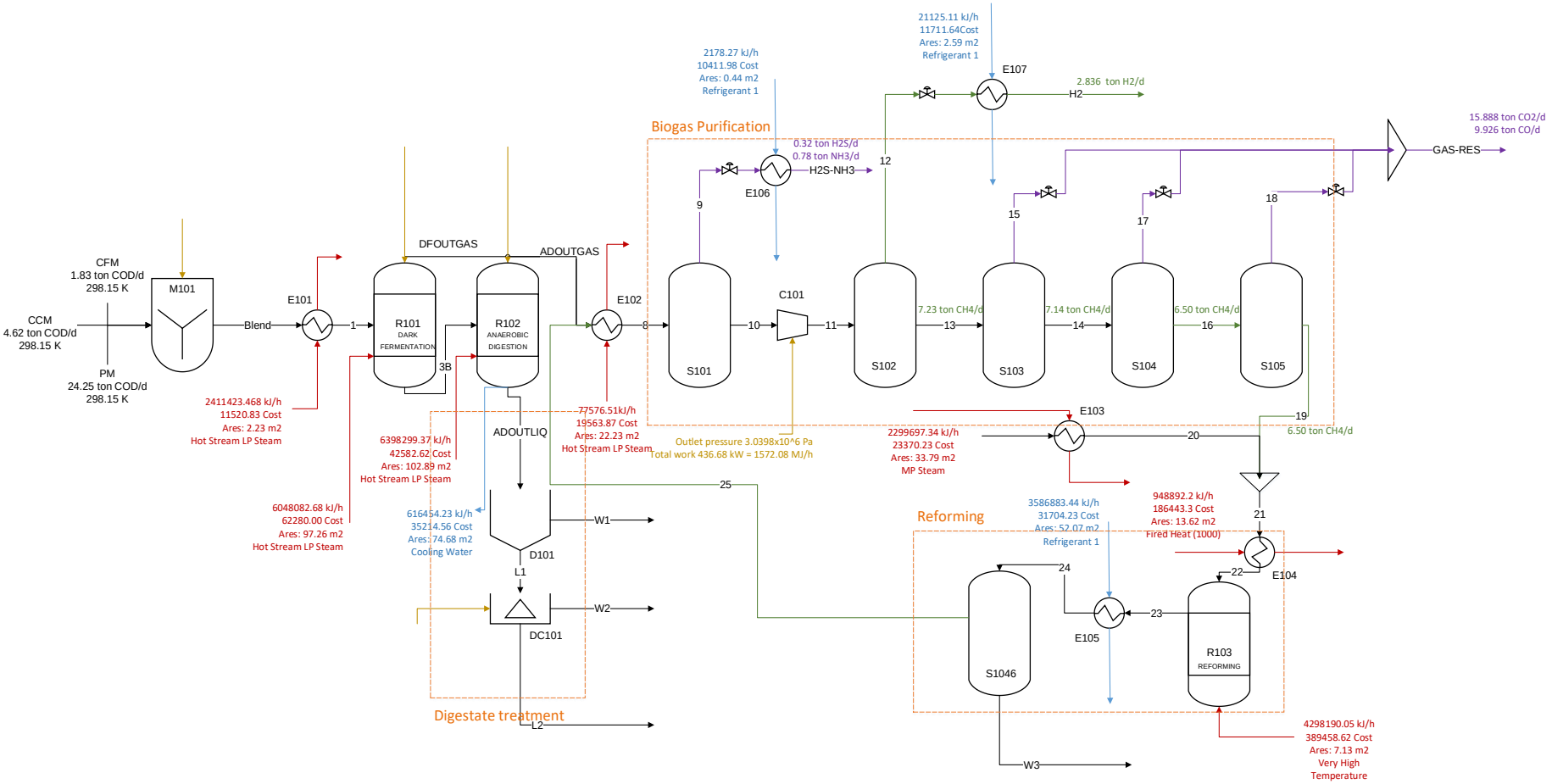

Figure 52 Process flow diagram of inputs and outputs (mass and energy flow) of the biorefinery scheme No. 2 used for the life cycle analysis. The power requirement heating (in red lines) and cooling (in blue lines). Green flow lines show the products of interest (H_2, CH_4 and Methanol), purple and final black flow lines show the process residues.

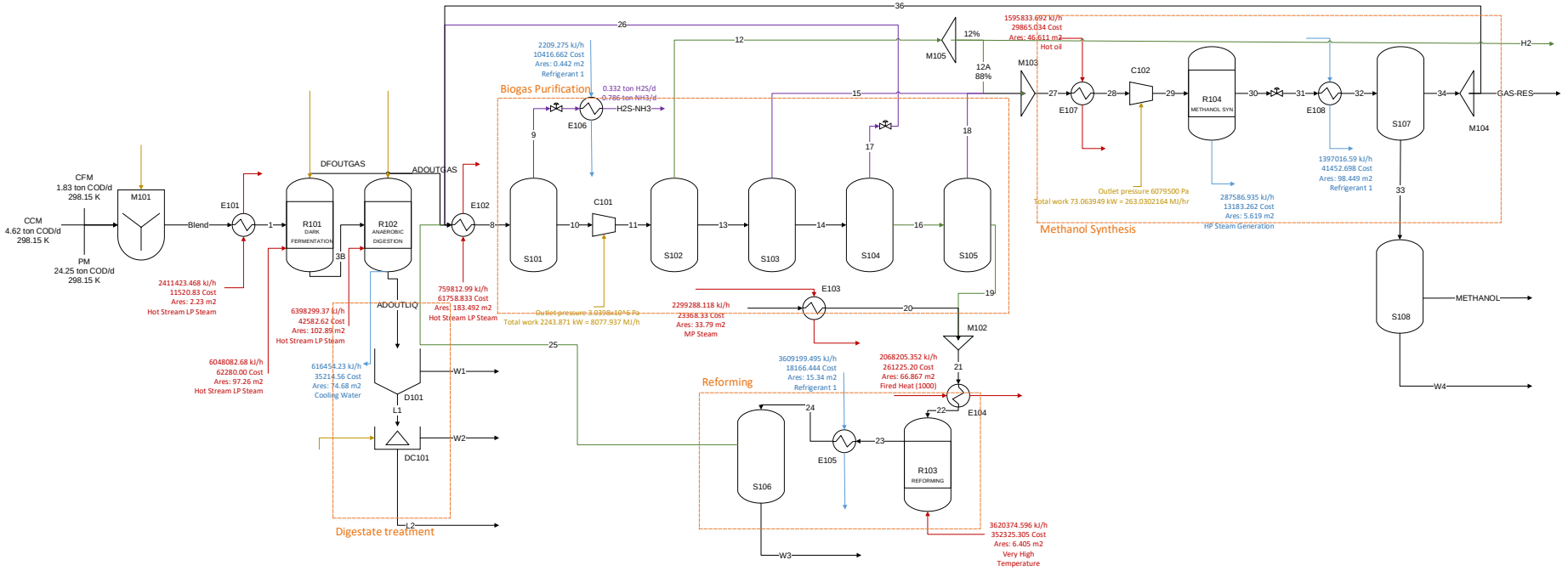

Figure 53 Process flow diagram of inputs and outputs (mass and energy flow) of the biorefinery scheme No. 3 used for the life cycle analysis. The power requirement heating (in red lines) and cooling (in blue lines). Green flow lines show the products of interest (H_2, CH_4 and Methanol), purple and final black flow lines show the process residues.

1.23.2 LCA - Biorefinery scheme No. 1

Figure 54 to shows the results obtained for the biorefinery scheme No. 1 scenario No. 2 when analyzing the LCA according to the ReCiPe midpoint from the bioprocess to the byproducts separation and purification. The results show that:

- 8 Of the 18 impact categories analyzed, 14 show the highest impact on bioprocesses (> 60% of the total), followed by biogas treatment. The impact of bioprocesses corresponds most probably to the use of energy in the heating and mixing of the initial blend. Most of these categories are associated with damage to human health and the ecosystem.

- 8 out of 18 impact categories show minimal impact: Stratospheric ozone depletion ($2.26x10^{-0.3}$ kg CFC11 eq); Ozone formation, Human health ($1.25x10^{01}$ kg NOx eq); Ozone formation, Terrestrial ecosystems($1.28x10^{01}$ kg NOx eq); Freshwater eutrophication (1.53 kg P eq); Marine eutrophication ($1.02x10^{-01}$ kg 1,4-DCB); Land use ($3.80x10^{01}$ m2a crop eq); and Mineral resource scarcity (4.52 kg Cu eq).

- Four of the 18 categories analyzed, greatest impact is shown by: global warming, terrestrial ecotoxicity, human non-carcinogenic toxicity, and fossil resource scarcity, with total values for the biorefinery of $8.91x10^{03}$ kg CO_2 eq., 2.90^{04} kg 1,4-DCB, $2.79x10^{03}$ kg 1,4-DCB and $2.62x10^{03}$ kg oil eq., respectively.

The high value of CH_4 treatment in the terrestrial acidification is due to the ratio of production to heating capacity. In biorefinery scheme No. 1, scenario No 2, the product of greater quantity generated is CH_4 requiring greater consumption in its treatment. However, its heating capacity is lower than that of the second product (H_2), thus generating greater impact in its treatment. Above all, the analysis of the first biorefinery shows that the profile values are equivalent to those presented by Lamnatou et al. (2019) and Surra et al. (2021), which show the impact of bioprocesses, specifically anaerobic digestion in thermophilic processes. With respect to Lamnatou et al. (2019), lower values of global warming and water use were found (Lamnatou et al., 2019; Surra et al., 2021). In addition, in comparison with the analysis of natural gas production, lower values on environmental impact are evidenced, probably because the contributions generated in the extraction work and the use of chemicals for the cleaning of the basin that are used in current fossil extraction processes are omitted. As well as the emission of SO_2 and NO_x and particulate matter emitted in the combustion processes for cogeneration in the service of the compressor stations or in the operation of the natural gas extraction wells (Calderón Carreño and Garay Benítez, 2020; “UPME,” 2020).

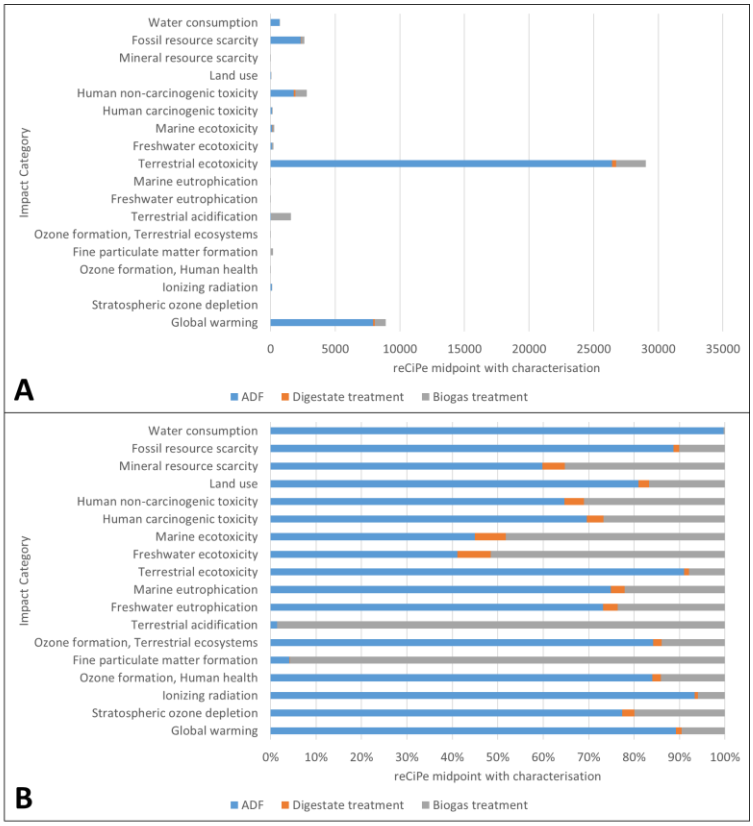

Figure 54 Biorefinery scheme No. 1 scenario 2 results for the whole system in terms of bioprocess, digestate treatment, H_2 and CH_4 separation, and purification, based on ReCiPe midpoint with characterization. The results are presented in different units, depending on the impact category (in Table 22, details about the units can be found). (A) Total impact values, (B) Percentage of participation of the sub-processes in each impact category.

Figure 55 shows the life cycle assessment results for the biorefinery scheme No. 1, scenario No. 3. Methane combustion for biorefinery consumption shows a significant decrease in the biorefinery impacts. The load of impacts corresponds entirely to the treatment and biogas separation, which most likely corresponds to the CO_2 final emissions.

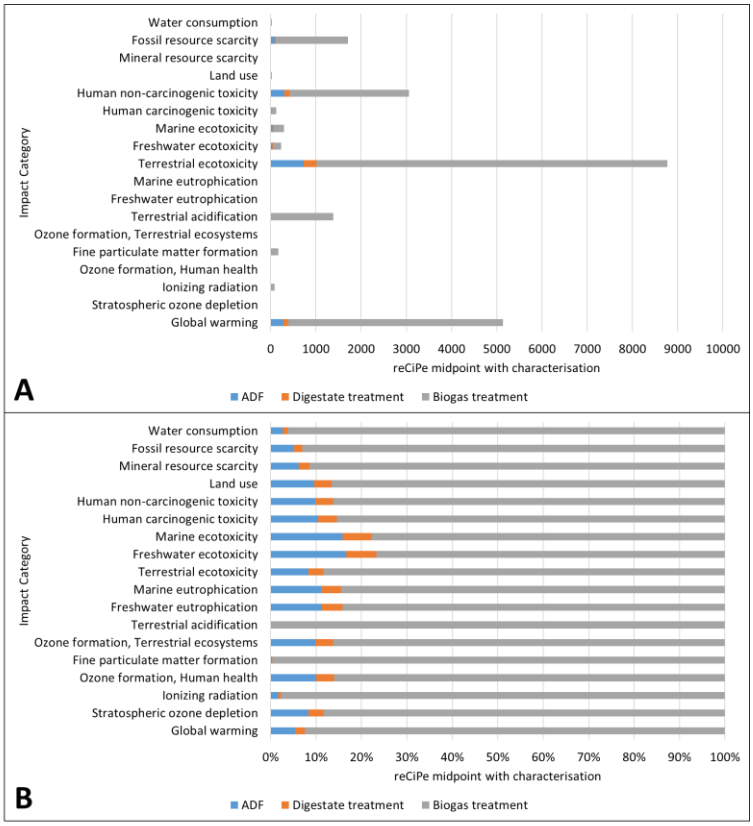

Figure 55 Biorefinery scheme No. 1 scenario 3 results for the whole system in terms of bioprocess, digestate treatment, H_2 and CH_4 separation, and purification, based on ReCiPe midpoint with characterization. The results are presented in different units, depending on the impact category (in Table 22, details about the units can be found). (A) Total impact values, (B) Percentage of participation of the sub-processes in each impact category.

Figure 56 shows the total variation in the impact of biorefinery scheme No. 1 under scenarios 2 and 3. The optimized combustion of methane for process energy generation, according to the PINCH analysis to be presented in the next section. It shows a reduction between 11% and 97% of 13 impact categories. Showing the environmental benefit of energy integration of the processes. Five of the 18 categories increase with methane combustion: Ionizing radiation, Freshwater ecotoxicity, Marine ecotoxicity, Human non-carcinogenic toxicity, and Mineral resource scarcity, increasing by 9%, 10%, 7%, 10%, and 102% respectively obtained in the biorefinery scheme No. 1 scenario 2 most probably due to the generation of flue gases in methane combustion.

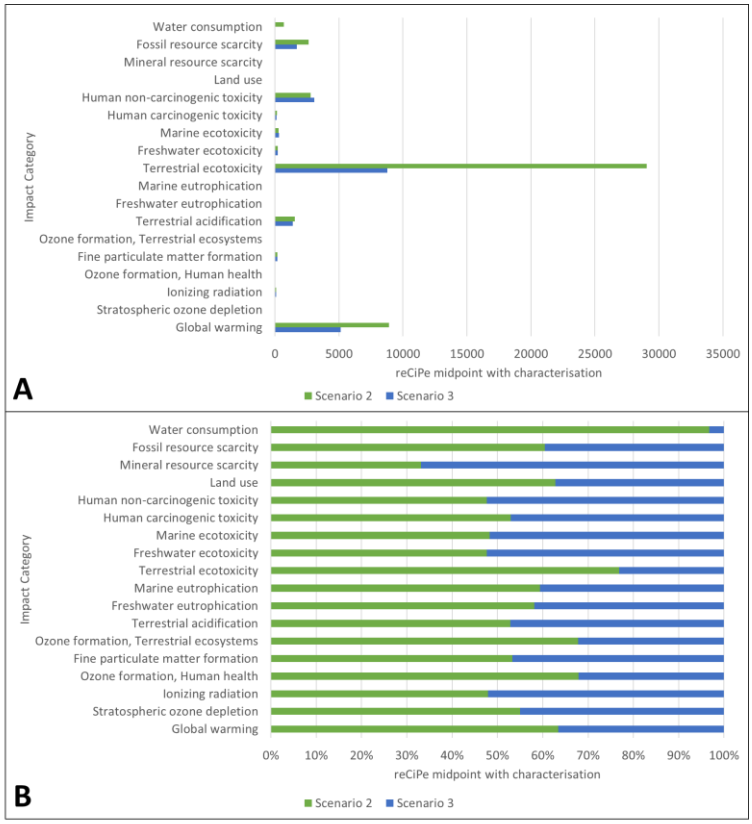

Figure 56 Biorefinery scheme No. 1 scenario 2 and 3 results for the whole system, based on ReCiPe midpoint with characterization. The results are presented in different units, depending on the impact category (in Table 22, details about the units can be found). (A) Total impact values, (B) Impact percentage per scenario.

As shown in Figure 57, the impact decreases in scenarios 2 and 3 are mostly shown per kg of H2, decreasing by more than 50% when energy integration is carried out through methane combustion. In contrast, the evaluation per kg of CH_4 shows that scenario 3 results in the same impact in factors such as global warming and in 5 of the 18 environmental categories the increases. Terrestrial ecotoxicity shows a decrease of less than 50%. Overall, the figure shows that energy integration strongly benefits the biohydrogen production. Scenario 3 values for CH_4 and H_2 production show reduced impact values compared to those presented in the last studies (Postels et al., 2016).

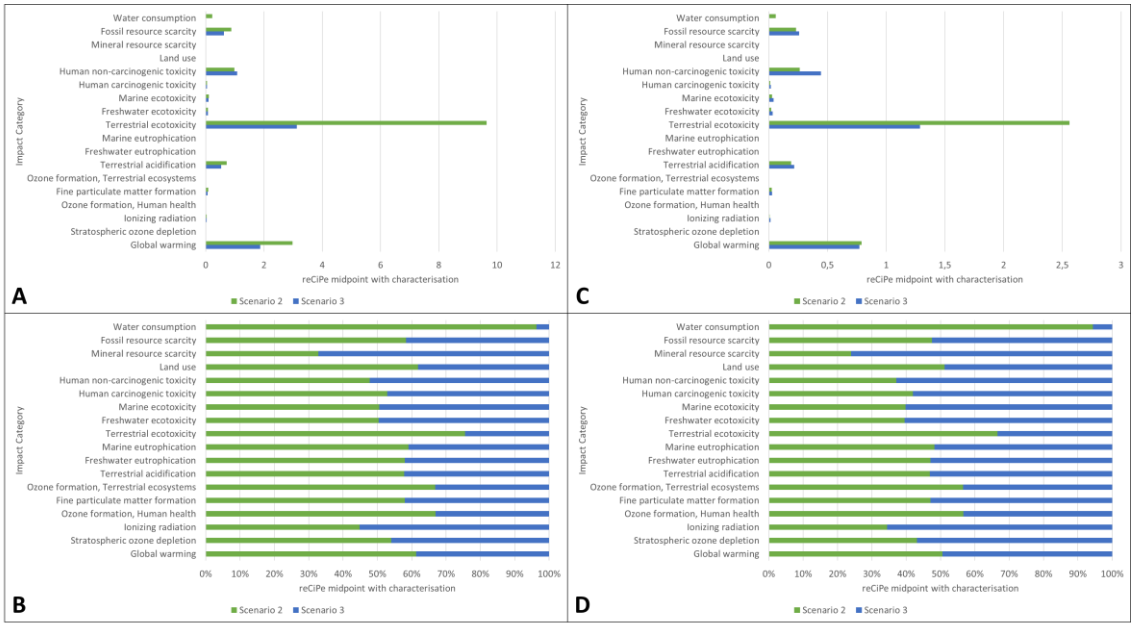

Figure 57 Biorefinery scheme No. 1 results for the whole scenarios. The results are presented in different units, depending on the impact category (in Table 22, details about the units can be found). (A) Total impact values per 1 Kg H_2, (B) Percentage of participation per 1 Kg H_2. (C) Total impact values per 1 Kg CH_4, (D) Percentage of participation per 1 Kg CH_4.

Figure 58 shows that the ADF process and designed separation results in carbon footprint values for methane production are equal to or lower than those reported by the ecoinvent database at the global data, for scenarios 2 and 3 of the biorefinery scheme No. 1. In addition, the water consumption impact factor can be significantly reduced with respect to those reported in the current market. However, factors such as acidification and ecotoxicity are major and need to be addressed on their hot spot to improve the environmental analysis of methane from ADF processes.

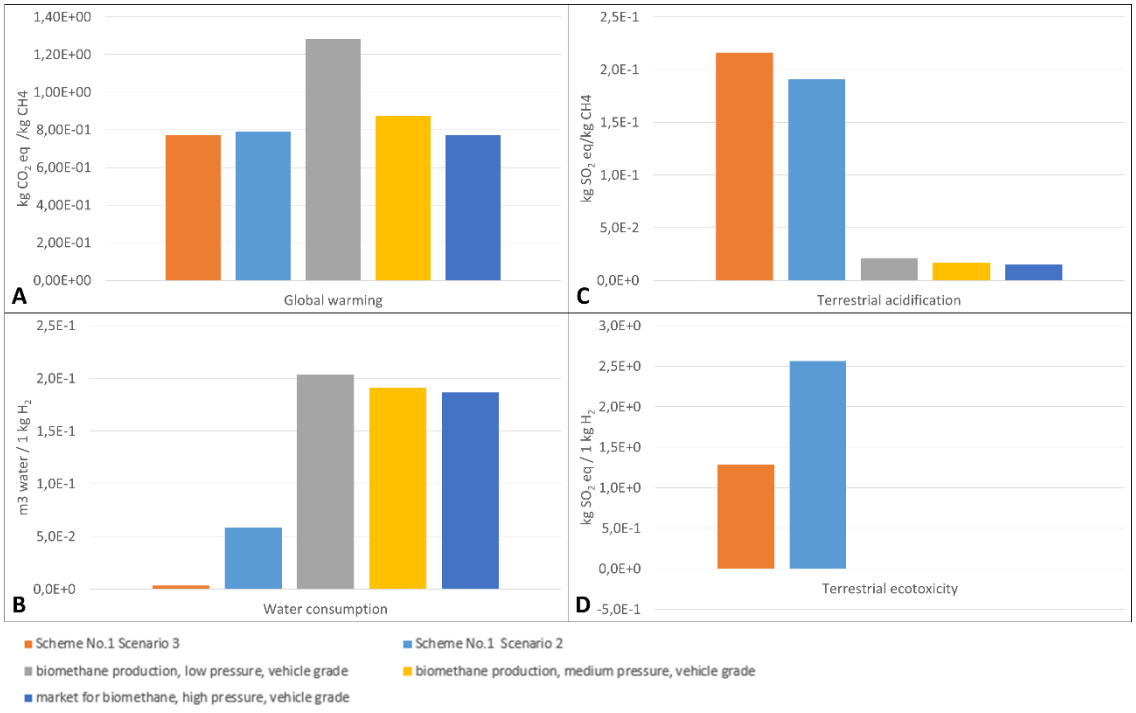

Figure 58 Main categories for the evaluation of biorefinery schemes per kg CH_4 (Commonly generated product). (A) Global Warming (GWP); (B) Terrestrial ecotoxicity; (C) Water consumption; (D) Terrestrial acidification.

1.23.3 LCA - Biorefinery scheme No. 2

Figure 59 – 58 shows the results obtained for the biorefinery scheme No. 2 scenarios 2, 3 and 4 respectively according to the ReCiPe midpoint for the production of H_2 as the main compound and digestate as a by-product. The biorefinery is divided into 3 sub-processes, including bioprocesses, digestate treatment, and H_2 treatment and production. The Figure 56 shows that:

- 17 of the 18 categories analyzed are mostly affected by the reforming process. Most probably because the reforming process impacts with high water use to meet the methane reaction ratio, in addition to the energy consumption for the operational conditions (temperature and pressure).

- The freshwater eutrophication category (due to the discharge of nutrients into soil or into freshwater bodies, and the subsequent rise in phosphorus) shows equivalent values between reforming and bioprocessing. Associated with the consumption of water in the reforming and that is finally discharged.

- 4 of the 18 categories show a significant impact: global warming, terrestrial ecotoxicity, human non-carcinogenic toxicity, and fossil resource scarcity, with total values for the

biorefinery of $4.6x10^{04}$ kg CO_2 eq., $1.27x10^{05}$ kg 1,4-DCB, $1.46x10^{04}$ kg 1,4-DCB and $1.41x10^{04}$ kg oil eq., respectively.

- The reforming process for obtaining H_2 shows an increase in all categories with respect to the previously proposed scheme, which is directly attributed to the high CO_2 generation and water consumption. This difference is in agreement with the one presented by Hajjaji et al. (2016). However, recent studies show that in general, reforming has significantly lower values in the categories of global warming, acidification and levelized cost compared to the traditional processes of H_2 production (Hajjaji et al., 2016; Valente et al., 2021).

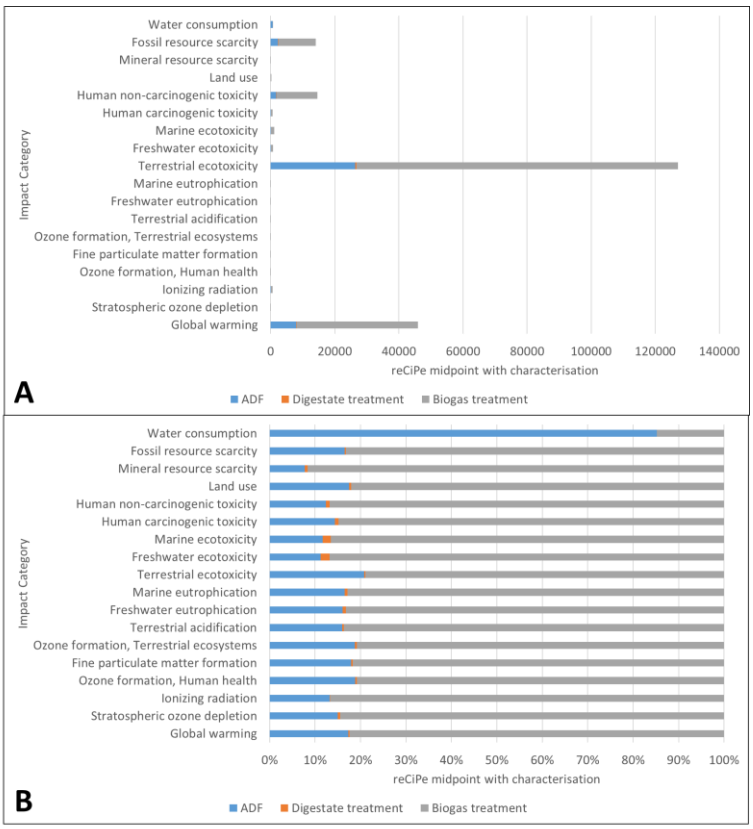

Figure 59 Biorefinery scheme No. 2 scenario 2 results for the whole system in terms of bioprocess, digestate treatment, H_2 reforming, separation, and purification, based on ReCiPe midpoint with characterization. The results are presented in different units, depending on the impact category (in Table 22, details about the units can be found). (A) Total impact values, (B) Percentage of participation of the sub-processes in each impact category.

Figure 60 and 58 shows the results obtained for scenario 3 when an optimal percentage of methane is burned for the energy generation required for the system. The contribution in the sub-processes is notably modified in the bioprocesses and digestate treatment, reducing them to less than 10%, especially in water consumption where the contribution of the bioprocesses is reduced from 90% to less than 1%.

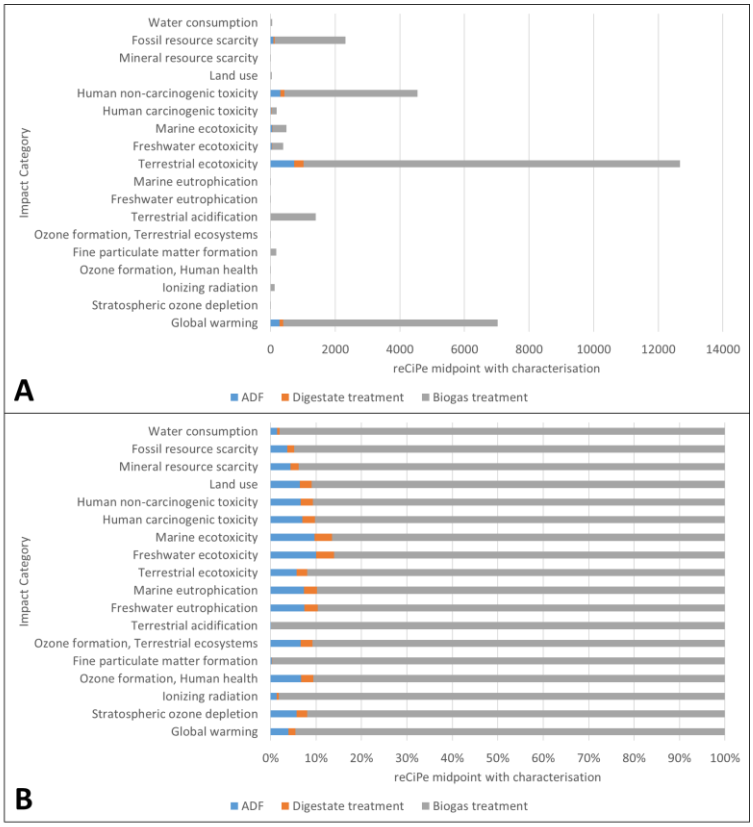

Figure 60 Biorefinery scheme No. 2 scenario 3 results for the whole system in terms of bioprocess, digestate treatment, H_2 reforming, separation, and purification, based on ReCiPe midpoint with characterization. The results are presented in different units, depending on the impact category (in Table 22, details about the units can be found). (A) Total impact values, (B) Percentage of participation of the sub-processes in each impact category.

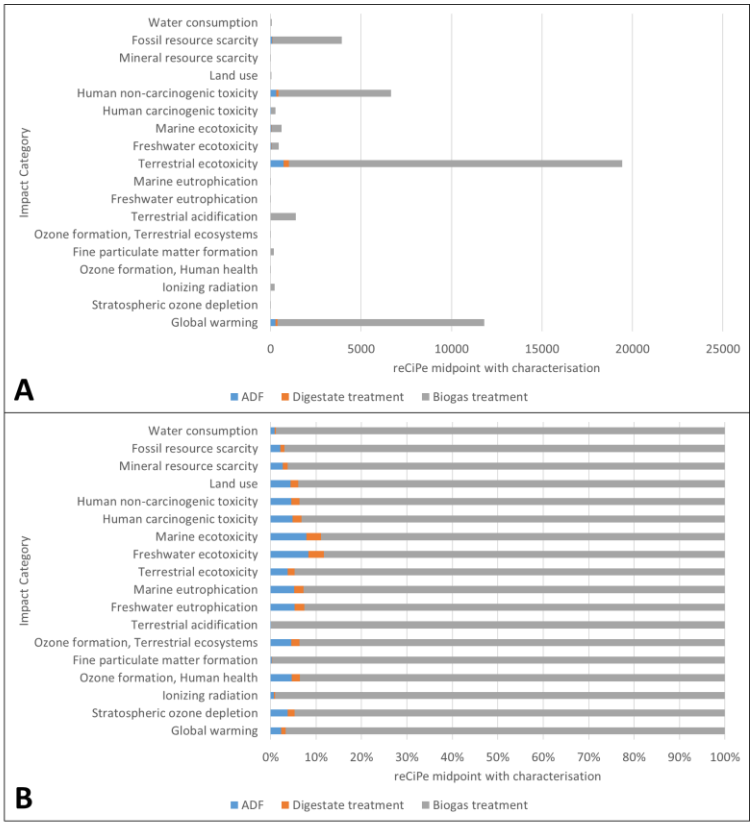

Figure 61 Biorefinery scheme No. 2 scenario 4 results for the whole system in terms of bioprocess, digestate treatment, H_2 reforming, separation, and purification, based on ReCiPe midpoint with characterization. The results are presented in different units, depending on the impact category (in Table 22, details about the units can be found). (A) Total impact values, (B) Percentage of participation of the sub-processes in each impact category.

Figures 59 and 60 show that the impact on the 18 categories is significantly reduced with energy integration for the system and per kg of H_2. It is highlighted that by burning the waste gases of the system (scenario 4) the environmental impacts increase discarding the scheme at the environmental level. Scenarios 3 and 4 show values in the impact factors lower than 10 per kg H2, which are in accordance with those reported by the latest technologies for hydrogen production (Ji and Wang, 2021; G. Li et al., 2020).

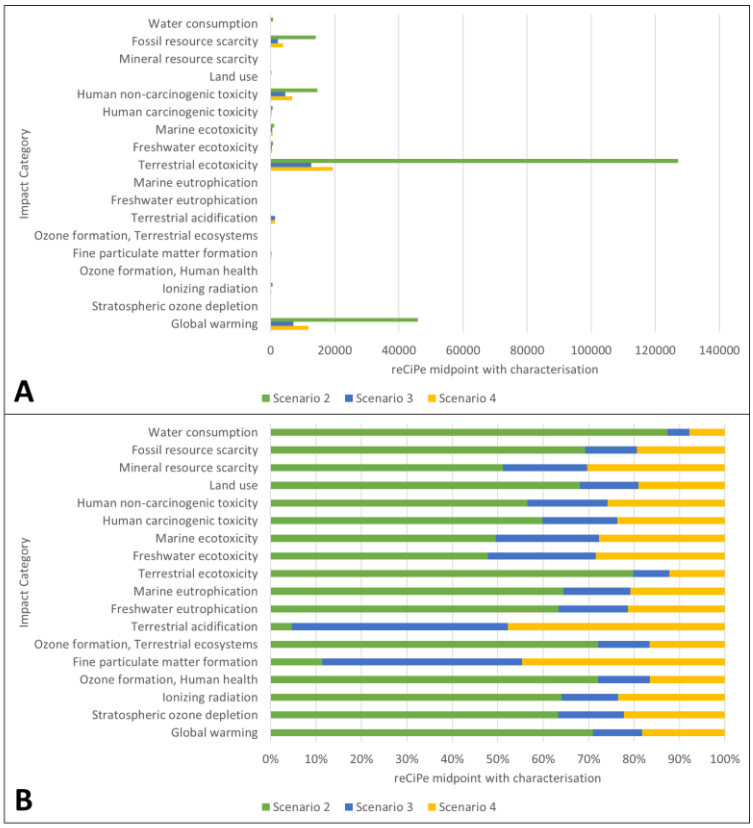

Figure 62 Biorefinery scheme No. 2 scenario 3 results for the whole system in terms of bioprocess, digestate treatment, H_2 reforming, separation, and purification, based on ReCiPe midpoint with characterization. The results are presented in different units, depending on the impact category (in Table 22, details about the units can be found). (A) Total impact values, (B) Percentage of participation of the sub-processes in each impact category.

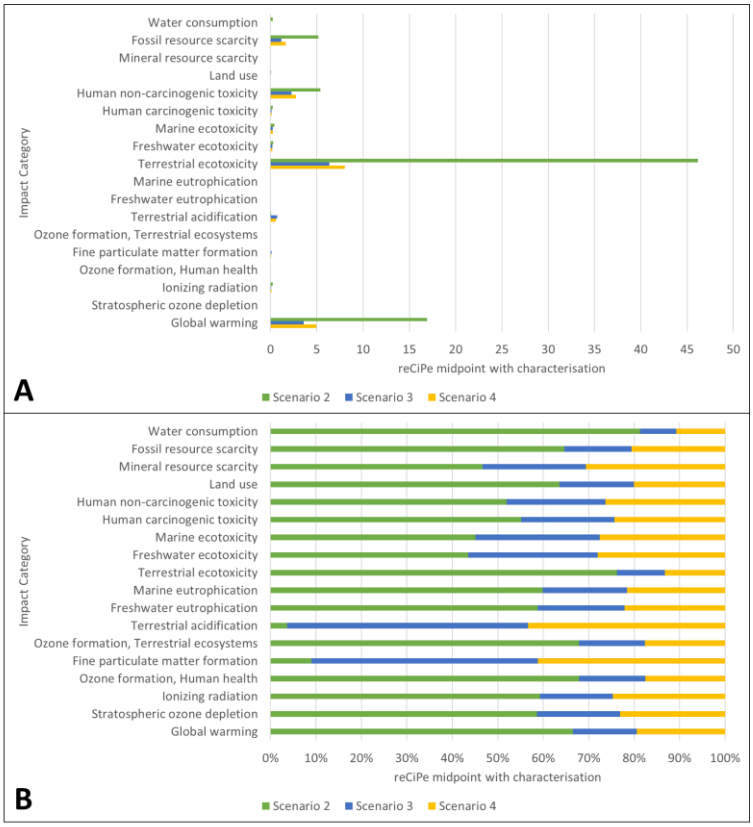

Figure 63 Biorefinery scheme No. 2 results for the whole system, based on ReCiPe midpoint with characterization. The results are presented in different units, depending on the impact category (in Table 22, details about the units can be found). (A) Total impact values per Kg H_2, (B) Percentage of participation of the scenarios in each impact category.

1.23.4 LCA - Biorefinery scheme No. 3

Figure 64-63 shows the results obtained for the biorefinery scheme No. 3 scenario 2, 3 and 4 respectively according to ReCiPe midpoint for the production of hydrogen, methanol, and digestate. The biorefinery is divided into four sub-processes, including bioprocesses, digestate treatment, hydrogen production and separation, and methanol synthesis. The Figure 61 shows that:

- 17 of the 18 categories are highly impacted by the methanol synthesis process with respect to the other 3. Most likely due to the operational conditions of the process. The freshwater eutrophication category again shows equivalent impacts with the bioprocess.

- In the 18 categories, the lowest impact is shown by the digestate treatment. And 9 of the 18 categories show equivalent impact percentages between the bioprocess and the hydrogen production and separation, showing the environmental efficiency of the design compared to the case of biorefinery scheme No. 2.

- 4 of the 18 categories show a significant impact: global warming, terrestrial ecotoxicity, human non-carcinogenic toxicity and fossil resource scarcity with total values for the biorefinery of $6.46x10^{04}$ kg CO_2 eq., $1.71x10^{05}$ kg 1,4-DCB, $2.79x10^{04}$ kg 1,4-DCB and $2.00x10^{04}$ kg oil eq. respectively.

The values obtained are in agreement with those presented by recent authors, where it is shown that the use of the methanol synthesis process increases the impact with respect to reforming by a very low percentage, but additionally that the percentage is allocated to the synthesis, showing significant reduction in the bioprocesses and the reforming process (Lundgren et al., 2013; Renó et al., 2011; Wu et al., 2021). As in the case of Wu et al. (2021), the greatest impact is generated on human health.

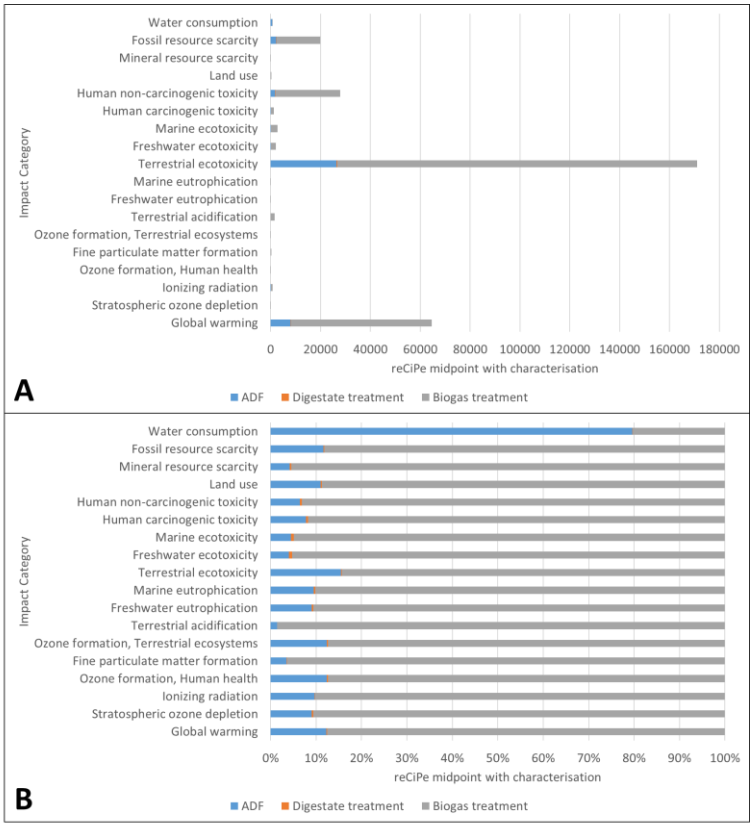

Figure 64 Biorefinery scheme No. 3 scenario 2 results for the whole system in terms of bioprocess, digestate treatment, H_2 reforming, separation, and purification, methanol synthesis based on ReCiPe midpoint with characterization. The results are presented in different units, depending on the impact category (in Table 22, details about the units can be found). (A) Total impact values, (B) Percentage of participation of the sub-processes in each impact category.

Scenarios 3 and 4 show a significant reduction in the 18 impact categories, especially in the ADF and digestion treatment sub-process, where in both cases, the contribution to the total impact generated is reduced by less than 1%. Above all, the greatest impact is attributed to gas treatment, reforming and methanol synthesis as shown in Figures 62 and 63.

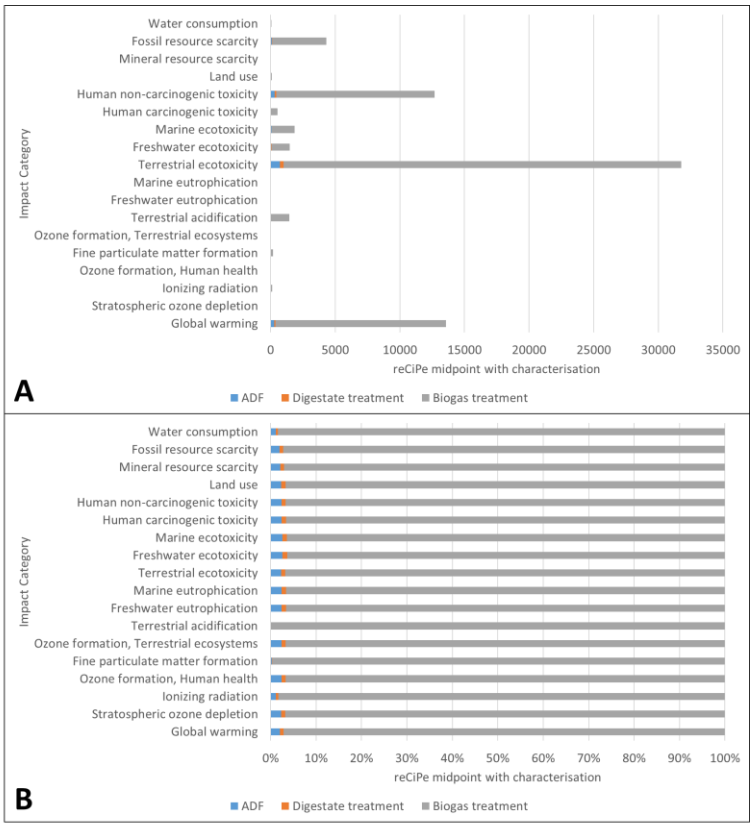

Figure 65 Biorefinery scheme No. 3 scenario 3 results for the whole system in terms of bioprocess, digestate treatment, H_2 reforming, separation, and purification, methanol synthesis based on ReCiPe midpoint with characterization. The results are presented in different units, depending on the impact category (in Table 22, details about the units can be found). (A) Total impact values, (B) Percentage of participation of the sub-processes in each impact category.

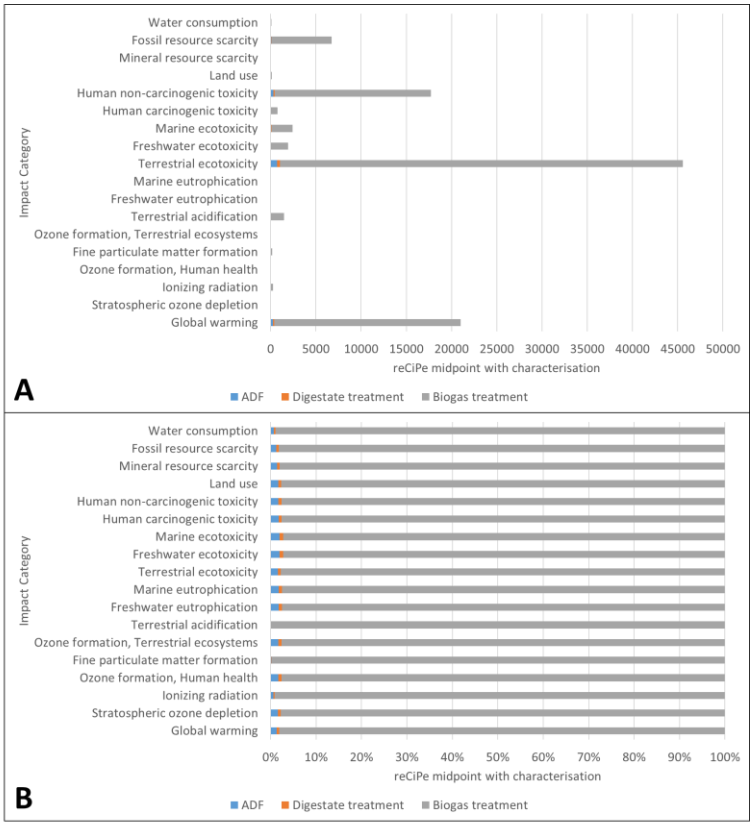

Figure 66 Biorefinery scheme No. 3 scenario 4 results for the whole system in terms of bioprocess, digestate treatment, H_2 reforming, separation, and purification, methanol synthesis based on ReCiPe midpoint with characterization. The results are presented in different units, depending on the impact category (in Table 22, details about the units can be found). (A) Total impact values, (B) Percentage of participation of the sub-processes in each impact category.

Figure 64 shows the comparison in the impact factors for biorefinery scheme No. 3 when energy integration techniques are applied. Above all, it is highlighted that the combustion of a part of the methane, or waste gases, significantly reduces the impact of the process. However, it is evident that the burning of waste gases (scenario 4) brings with it an increase compared to the burning of a portion of methane (scenario 3).

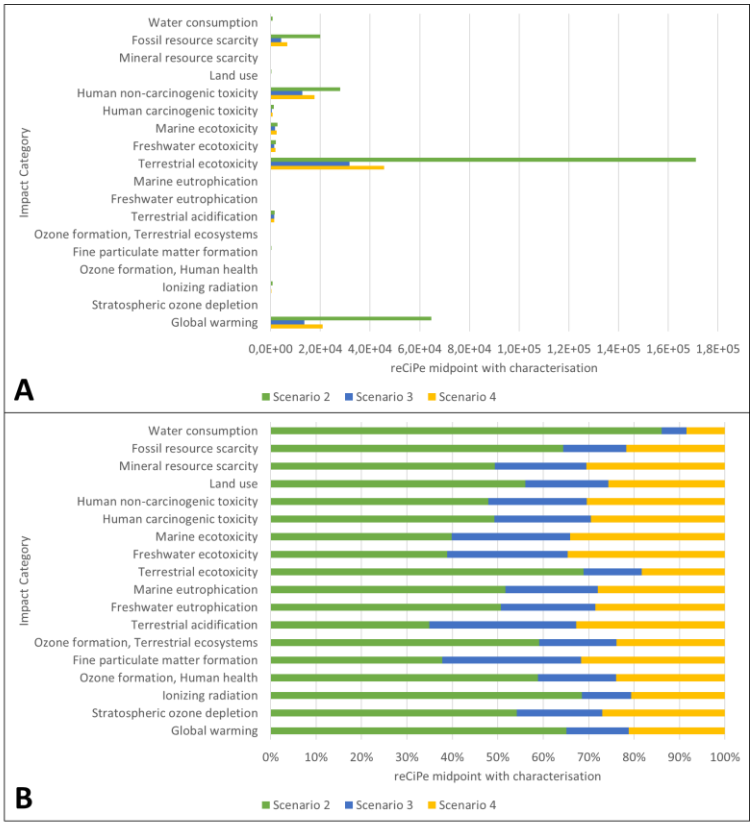

Figure 67 Biorefinery scheme No. 3 scenario 3 results for the whole system in terms of bioprocess, digestate treatment, H_2 reforming, separation, and purification, methanol synthesis based on ReCiPe midpoint with characterization. The results are presented in different units, depending on the impact category (in Table 22, details about the units can be found). (A) Total impact values, (B) Percentage of participation of the sub-processes in each impact category.

For the study of the two main compounds, per kg of methanol and per kg of H2, in all cases scenario 4 shows to be the most favorable for the product, showing a significant reduction in the 18 impact factors and obtaining values equal to or better than the technologies presented in the literature.

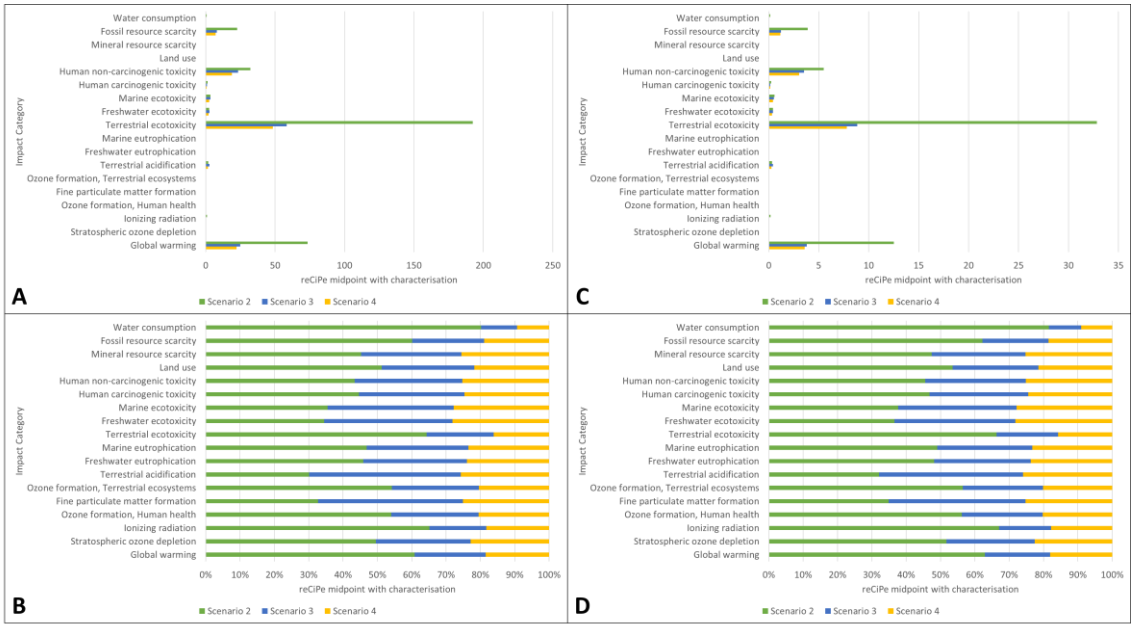

Figure 68 Biorefinery scheme No. 3 scenarios 2, 3 and 4 results for the whole system based on ReCiPe midpoint with characterization. The results are presented in different units, depending on the impact category (in Table 22, details about the units can be found). (A) Total impact values per 1 Kg H_2, (B) Percentage of participation per 1 Kg H_2. (C) Total impact values per 1 Kg Methanol, (D) Percentage of participation per 1 Kg Methanol.

Methanol cannot be compared between refineries, since scheme No. 3 only produces the compound. However, comparisons of the four most representative factors with the LCA ecoinvent database (Global warming, water consumption, Terrestial acidification and Terrestial ecotoxicity) show that the only factor that benefits with respect to that currently reported by the ecoinvent database is water consumption (market for methanol, from biomass 7.82 m3/kg methanol). Nevertheless, factors such as global warming (market for methanol generated from biomass is 0.66 CO2/kg methanol, and market for methanol is 0.3 CO2/kg methanol) increase significantly, which implies improvements in technology selection. In addition, benefits can also be seen in fine particulate matter formation, ozone formation, and terrestrial ecosystems.

1.23.5 Life cycle assessment discussion

Figure 66 shows the comparison of the three biorefinery schemes, taking as a value the scenario with the lowest environmental impact, especially showing that all the factors increase when including processes in the biorefinery, being the biorefinery scheme No. 3 the one with the highest impact, most probably due to the power requirements, water consumption for reforming and the generation of combustion gases (CO_2 emissions) resulting from energy integration. The first difference on the low impact categories is shown in the three categories associated with ecotoxicity (referring to the emission of substances such as heavy metals that can affect the system) that directly influence the quality of ecosystems. The impact is attributed to the energy and service used to maintain the operational conditions of the reforming and methanol synthesis. Additionally, it is shown that biorefinery schemes No. 2 and No. 3 also increase the human toxicity factor with the category of ionizing radiation. Ionizing radiation is an impact category in LCA related to the damage to human health and ecosystems that is linked to the emissions of radionuclides throughout a product or building life cycle. This is most probably due to the use of nuclear power for electricity.

The greatest impact on climate change is shown in the global warming category. Climate change can be defined as the change in global temperature caused by the greenhouse effect that the release of "greenhouse gases" by human activity creates. The increase over the category is most likely due to the additional processes with higher CO_2 generation and electricity use. The three additional categories are associated with ecotoxicity and human toxicity. Overall, it is shown that the impact of biorefinery scheme No. 1 is presented in a homogeneous manner, while biorefineries No. 2 and No. 3 have a greater impact on specific categories that can be optimized to improve the life cycle analysis of the products obtained.

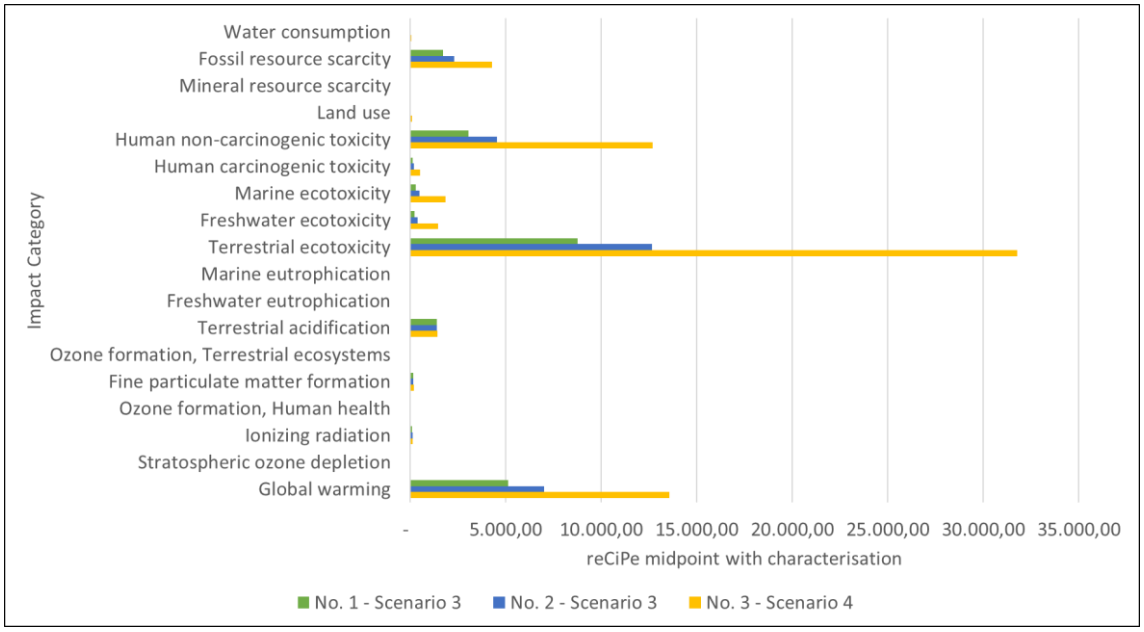

Figure 69 Total impact assessment for biorefinery schemes No. 1, No. 2 and No. 3 based on ReCiPe midpoint with characterization. The results are presented in different units, depending on the impact category (in Table 22, details about the units can be found).

Figure 67 shows the comparison of the three biorefinery schemes after energy integration. Above all, it is shown that in the three cases the greatest impact is found in the damage to ecosystems (figure 67D), followed by the damage to human health. Regarding human health, figure 67A shows that the greatest impact is found in the increase in diseases and malnutrition, most likely due to the generation of particles and post-combustion emissions, as well as the generation of gases such as NH_3 and $H2_]S$. The factors with the greatest impact on the damage to ecosystems correspond to the damage to freshwater species and the damage to terrestial species, most probably due to the requirement of water for the transformation or cooling processes, as well as the occupation of land and emission of material. particulate. Finally, regarding the damage to available resources, once again the impact is generated by the increase in malnutrition, most likely, as mentioned above, due to the use of water as a natural resource.

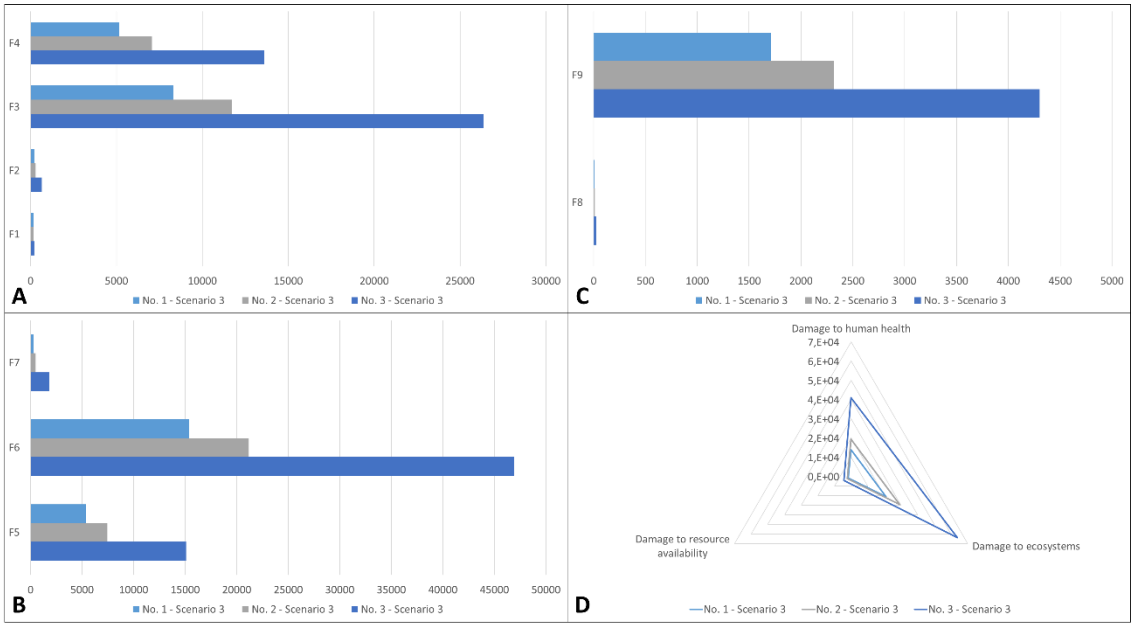

Figure 70 Total impact assessment for biorefinery schemes No. 1, No. 2 and No. 3 based on ReCiPe midpoint with characterization. The results are presented in different units, depending on the impact category (in Table 22, details about the units can be found). F1: Increase in respiratory disease, F2: Increase in various types of cancer, F3: Increase in other diseases/causes, F4: Increase in malnutrition, F5: Damage to freshwater species, F6: Damage to terrestrial species, F7: Damage to marine species, F8: Increase in other diseases/causes, F9: Increase in malnutrition.

Although the overall results show that the No. 1 biorefinery schemes are those that generate overall lower impacts, and that energy integration is shown to be a process that reduces the evaluation categories in LCA, an LCA is comparable when the product and functional unit are the same. Figure 68 compares all schemes and scenarios for the major impact categories. Global warming refers to the anthropogenic addition of greenhouse gases into the atmosphere (e.g. CO_2, CH_4 and N_2O), i.e. it directly characterizes the direct impact on climate change.

Figure 68A shows that energy integration produces a significant reduction in global warming. However, per unit of H_2 production, the change is not significant when part of the product or residual gases are used for the scheme's own energy consumption. And that biorefinery schemes No. 1 and 2 can generate the same global warming impact. A similar behavior is shows in the results of terrestrial ecotoxicity which represents the influences of toxic substances on terrestrial ecosystems (Figure 68B). Although the gases combustion produces a higher amount of CO_2, their use has a lower impact than the use of energy from the Colombian grid, considering that the Colombian grid is mostly based on the use of oil and coal.

In the case of water consumption, Figure 68C shows that the development of energy integration mostly reduces the category in the three cases, and it could be said that the mass integration and high technology selection in the biorefineries construction will exclude this category from the selection, since their result does not show significant changes for the three schemes.

Finally, acidification is caused by pollutants that have the capacity to form H^+ - ions in the ecosystem (air, soil, surface water, ground water). The ReciPe method expresses acidification in kg SO_2-Eq and Figure 68D shows it for the three biorefineries per 1 kg H_2. The figure also shows that the energy integration for schemes No. 2 and 3 increase the category value, most probably due to the emissions produced in the gas combustion, which shows that the use of biogas in the process versus the generation of H_2 increases the acidification process, the category may improve using alternative energies (e.g., solar, wind, etc.). Overall, the global warming per kg H_2 of Scheme No.1 Scenario 3 is close to that reported by the Ecoinvent database for the market for hydrogen, gaseous (Global) (1.57 kg CO_2/kg H_2) and for factors such as water consumption the impact of Scheme No.1 Scenario 3 is 60% of that currently reported for the market for hydrogen, gaseous (Global).

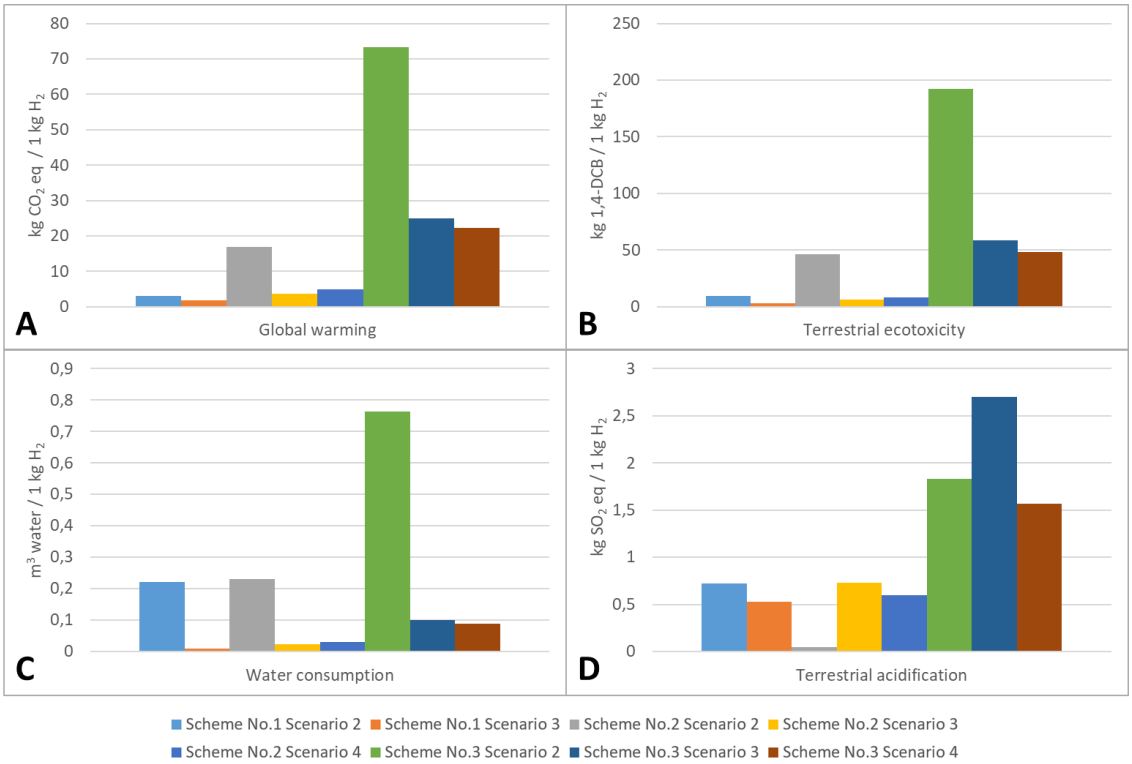

Figure 71 Main categories for the evaluation of biorefinery schemes per kg H_2 (Commonly generated product). (A) Global Warming (GWP); (B) Terrestrial ecotoxicity; (C) Water consumption; (D) Terrestrial acidification.

1.23.6 Pinch analysis

Before analyzing the energy integration for the scenarios proposed in each biorefinery scheme, the minimum temperature range for the three biorefineries was evaluated. Studies of pinch analysis between 3 to 10 °C are found in the literature. Figure 72 shows the analysis of the scheme with different temperature gap (ΔT_{min}) for biorefinery scheme No. 1. In all the targets studied, a significant change is between 5 to 7 °C. Above all, it is shown in Figure 72A that the heat and cold service requirement increases as the temperature gap increases, directly impacting the operational cost of the No. 1 biorefinery scheme.

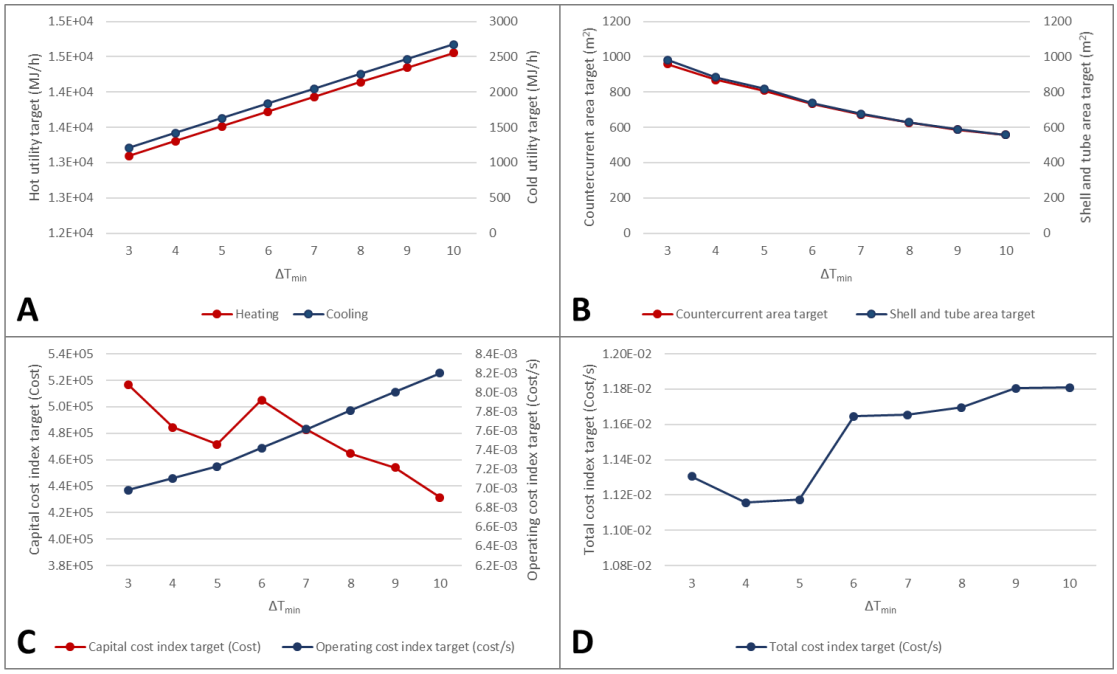

Figure 72 Analysis of consumption and costs as a function of the variation of ΔT_{min}, biorefinery scheme No. 1. (A) Variation of heat transfer, (B) Variation of total heat exchanger area, (C) Variation of capital and operating cost, (D) Change in total cost.

Figure 73 shows the cost and energy consumption analysis for the biorefinery scheme No. 2. As shown in Figure 73A the lowest energy consumption is obtained when the pinch analysis is performed at a ΔT_{min} of 3 °C while the lowest area is obtained when the analysis is performed at a ΔT_{min} of 10 °C (Figure 73B). In particular, the cost trend (Figure 73C and D) changes from a ΔT_{min} of 6 °C onwards. In case an economic optimization is required, it is recommended to use values lower than ΔT_{min} of 9 °C. Between 3 to 9 °C in the biorefinery scheme No. 2, the energy requirement (heat and cold) increases as a function of temperature,

which impacts the operational cost of the process. However, the capital cost is not affected in this temperature gap.

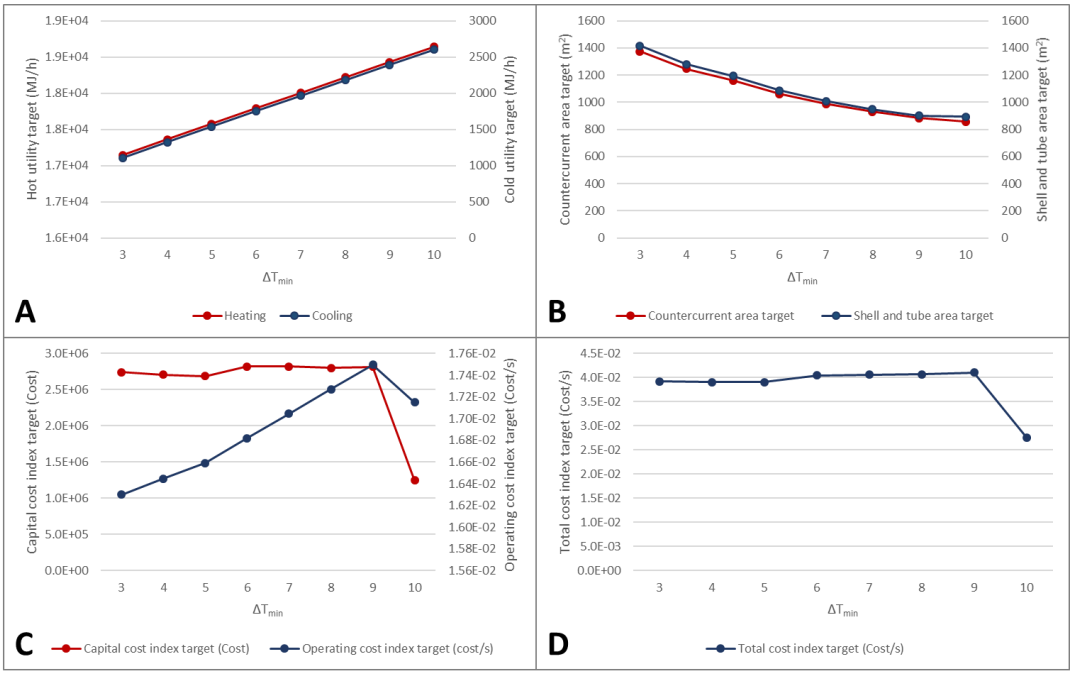

Figure 73 Analysis of consumption and costs as a function of the variation of ΔT_{min}, biorefinery scheme No. 2. (A) Variation of heat transfer, (B) Variation of total heat exchanger area, (C) Variation of capital and operating cost, (D) Change in total cost.

The profit and cost behavior of biorefinery scheme No. 3 is the same as that obtained for scheme No. 2. Figure 74 shows the analysis of the optimization objective when performing heat exchange networks for biorefinery scheme No. 3 showing that the ΔT_{min} optimum is 3°C.

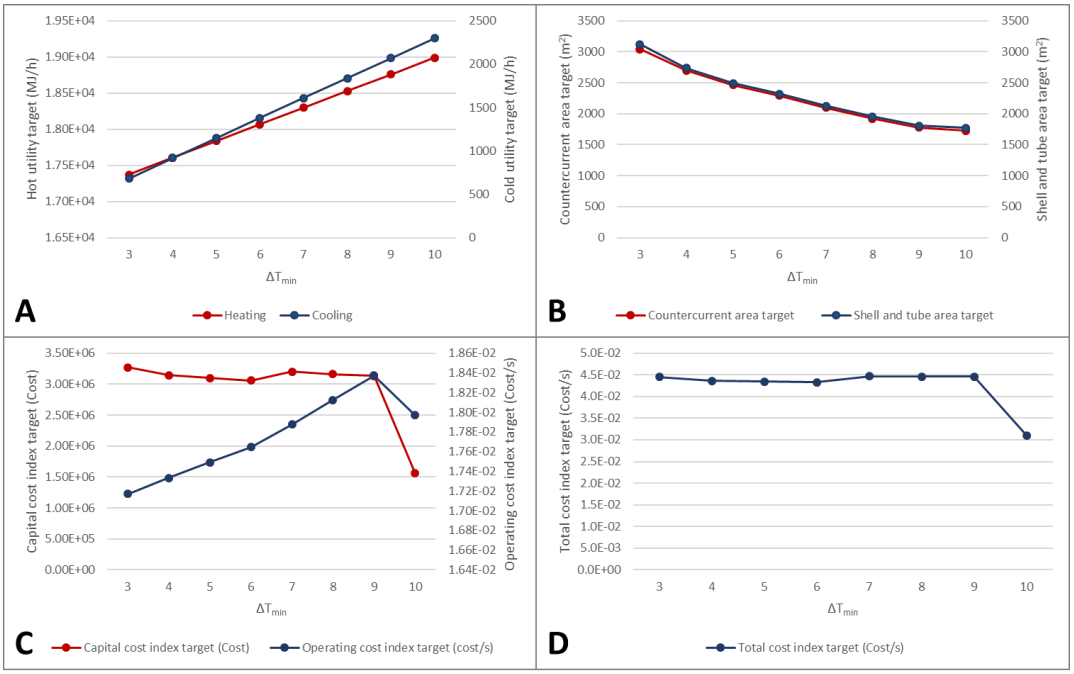

Figure 74 Analysis of consumption and costs as a function of the variation of ΔT_{min}, biorefinery scheme No. 3. (A) Variation of heat transfer, (B) Variation of total heat exchanger area, (C) Variation of capital and operating cost, (D) Change in total cost.

1.23.7 Pinch analysis - Biorefinery Scheme No. 1

Figure 75 shows the pinch analysis for biorefinery scheme No. 1. Fernández-Polanco and Tatsumi, 2016, in his study shows a digestion process of 19 days at 35 °C where the anaerobic digestion process requires constant heating and can consume up to 44% of the energy contained in the biogas produced. The optimization of the study seeks to decrease the use of the energy produced by the thermal hydrolysis pretreatment. Figure 57A shows the energy requirements for the hydrolysis reactors and the anaerobic digestion reactors. However, the energy required for the CSTR reactors only considers the volume and kinetics of the reactions without taking into account sludge recirculation and energy required for micro bacterial growth, which results in values of theoretical consumption that are far from those encounter in the industry (Fernández-Polanco and Tatsumi, 2016). For this reason, CSTR reactors are eliminated for the pinch analysis to energetically evaluate the thermochemical processes.

The minimum required heat (MER) is decreased by 94% when the heat required for the CSTR reactors of the ADF process is removed (MER difference between Figure 75A and B), increasing the efficiency of the process. According to the MER in Figure 75B, methane combustion is required (8.15 x10^5 (kJ·h^{-1})). Figure 75C shows that combustion of 7.5% of methane balances the process. The total energy consumed by the CSTR reactor is equivalent to the theoretical value of the kinetics of the reactions for amino acid degradation, acidogenesis, methanogenesis, and fermentation. Moreover, if the theoretical value were considered, it would be necessary to use 98% of the methane produced, a value that does not represent the one measured in the installed processes (between 20 to 30% for AD alone). As shown in Qi et al. (2021) and Y. Li et al. (2021), the energy yield of the process is a function of the ambient temperature, showing that for the transport, pretreatment (mixing and preheating) and digestion process between 17 to 32% of the methane produced is required, being the transport one of the most demanding of energy consumption. The model proposed in this case optimizes the biomass pretreatment and final biogas treatment requirements (Y. Li et al., 2021; Qi et al., 2021).

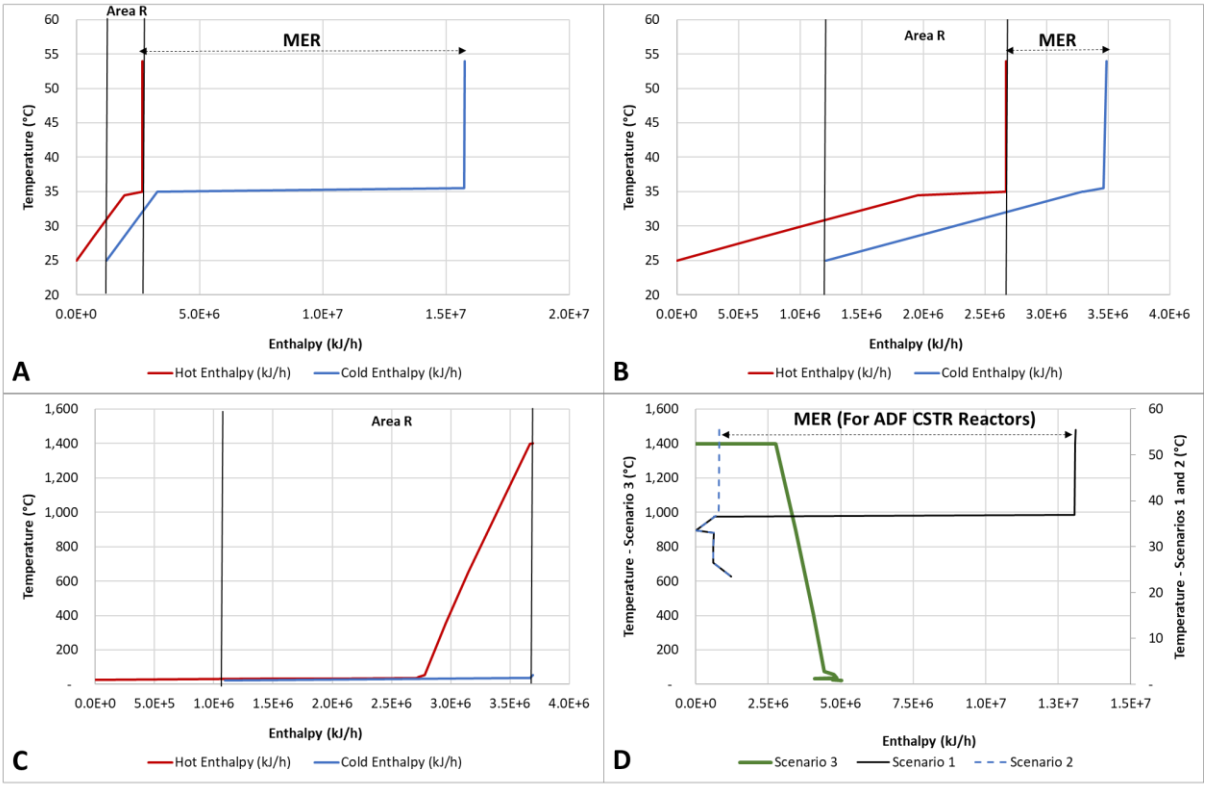

Figure 75 Pinch analysis. The hot (red) and cold (blue) composite curves for the simulation of biorefinery scheme No. 1. The gas temperature is set at 3 °C, the area R indicates the overlap area and MER indicates the minimum

heat requirement. (A) Scenario 1. (B) Scenario 2. (C) Scenario 3. (D) Grand composite curves obtained for the three scenarios.

The report for the task 37 – Energy from Biogas of the IEA, shows that for ADF bioprocesses the percentage of energy consumed (heat and electricity) over energy produced (heat and electricity) is between 4 to 10%, which supports the value finally consumed in the scenario No. 3 for the biorefinery scheme No. 1 and allows obtaining the total energy efficiency of the proposed process of pretreatment, ADF and gas separation (Jerry Murphy et al., 2011).

1.23.8 Pinch analysis - Biorefinery Scheme No. 2

Figure 76 shows the pinch analysis for biorefinery scheme No. 2. The minimum required heat (MER) is decreased by 70% when the heat required for the CSTR reactors of the ADF process is removed (MER difference figure D), increasing the efficiency of the process. According to the MER in Figure 76B, when 30% of the methane produced is burned, the energy required for the entire process of 5.17 $x10^6$ ($kJ \cdot h^{-1}$) is produced. The value does not correspond to a linear function since methane consumption impacts the hydrogen reforming production, water consumption, and the energy consumption of the reforming process, which is the second process with the highest energy consumption in the biorefinery scheme No. 2. The total energy requirement of biorefinery scheme No. 2 is six times higher than that of biorefinery scheme No. 1. Figure 76D shows the grand composite curves of the scenario for biorefinery scheme No. 2, where it is shown that the combustion of 30% of the methane is sufficient to cover the energy consumption of the pretreatment, gas separation and hydrogen reforming. Then the additional 23% of methane required is used for the reforming process. However, as shown by the high energy demand of the reforming process, further studies are required to optimize energy consumption and to prove the benefits of the application of the process and CO_2 capture from the biogas obtained. Cvetković et al. (2021) show that the reforming process followed by AD has a negative LCA balance. However, they report a total energy efficiency of the AD and reforming process of 61%, thus concluding that it is important to take into account the additional environmental factors surrounding the process to support the viability of the process. According to Masoudi Soltani et al. (2021), the efficiency of the production and separation process has high theoretical yields when the CO_2 capture processes are studied in detail (Cvetković et al., 2021; Masoudi Soltani et al., 2021). Faheem et al. (2021) in his study shows that depending on the reforming process from methane, the

energy yield can be negative or positive, obtaining energy yields up to 45% showing the process feasibility even with its energy consumption (Faheem et al., 2021).

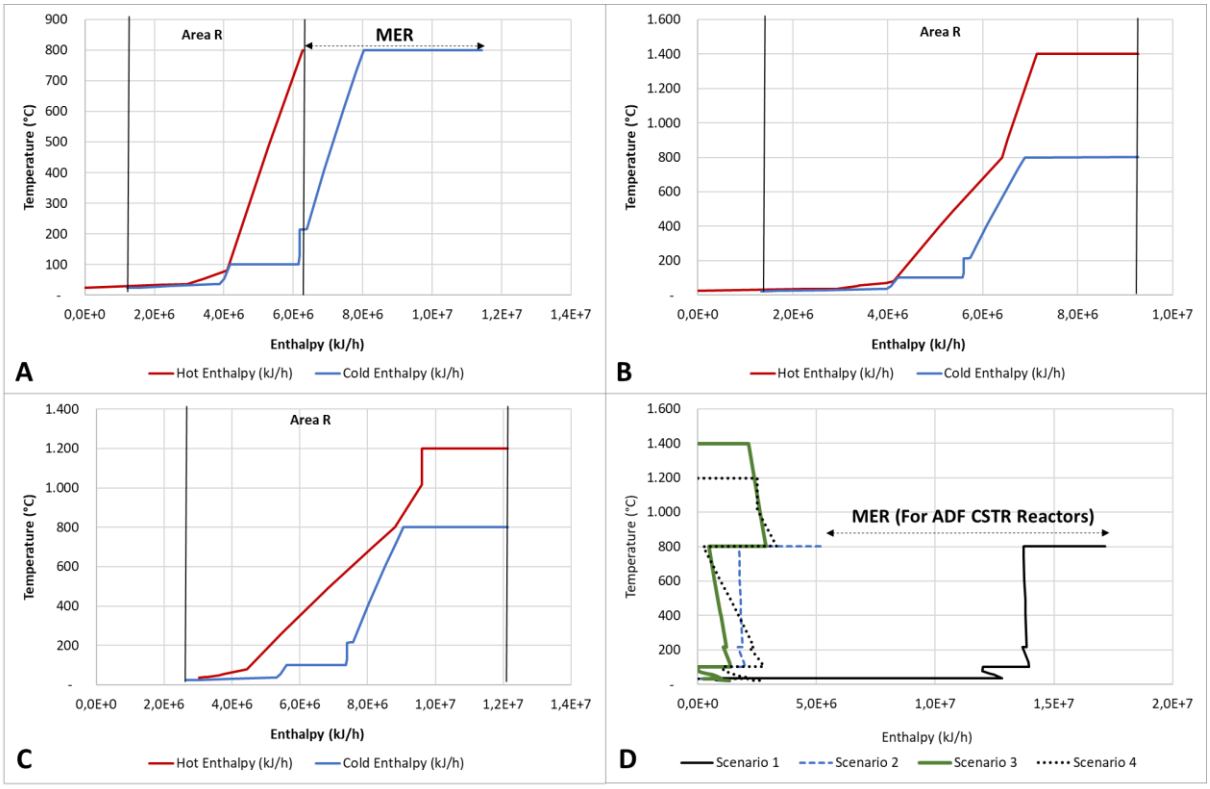

Figure 76 Pinch analysis. The hot (red) and cold (blue) composite curves for the simulation of biorefinery scheme No. 2. The gas temperature is set at 3 °C, the area R indicates the overlap area and MER indicates the minimum heat requirement. (A) Scenario 2. (B) Scenario 3. (C) Scenario 4. (D) Grand composite curves obtained for the four scenarios.

1.23.9 Pinch analysis - Biorefinery Scheme No. 3

Figure 77 shows the pinch analysis for biorefinery scheme No. 3. The minimum required heat (MER) is decreased by 67% when the heat required for the CSTR reactors of the ADF process is removed (MER difference Figure D), increasing the efficiency of the process. Regarding the total energy demand of the biorefinery scheme, it increases 10% with relation to the biorefinery scheme No. 2, which does not mean a significant change as it was shown between the biorefinery schemes No. 1 and No. 2. The total requirement of $5.2x10^6$ ($kJ \cdot h^{-1}$) as shown in Figure 77B is mainly for the reforming process. According to the MER in Figure 77B the 30% combustion of the methane produced in the bioprocesses provides the energy required for the entire biorefinery scheme No. 3. This does not significantly impact the H_2 production as the main product of the biorefinery schemes No. 2 and 3, since it corresponds

to the same value of methane consumed in the biorefinery scheme No. 2. Figure 77D shows the grand composites curves for scenarios 1, 2, 3 and 4 of the biorefinery scheme No. 3, where again the impact of the theoretical CSTR reactors and the low consumption of the methanol synthesis process is shown. Harris et al. (2021) and Nassirpour and Khademi (2020) show that, due to the low energy consumption of methanol synthesis in the process, energy yields between 40 and 60% can be obtained. Furthermore, the environmental benefits are representative due to the CO_2 consumption (Harris et al., 2021; Nassirpour and Khademi, 2020).

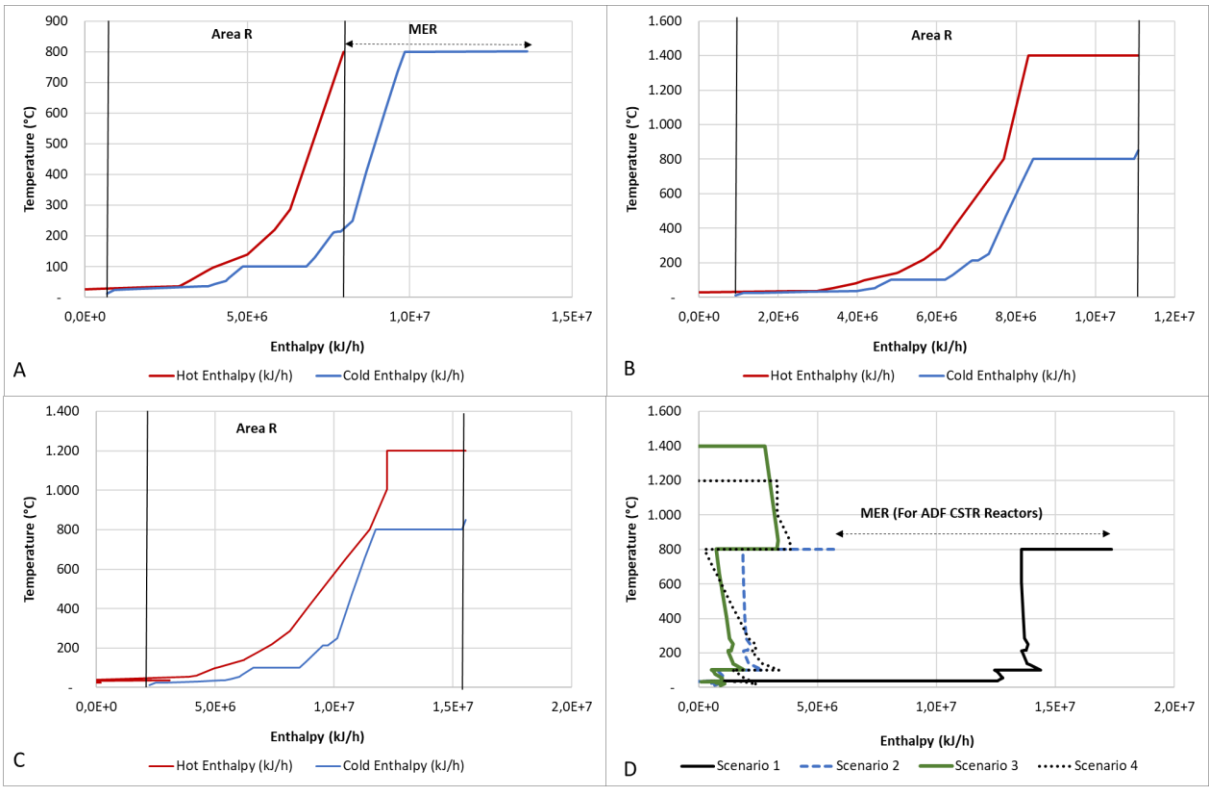

Figure 77 Pinch analysis. The hot (red) and cold (blue) composite curves for the simulation of biorefinery scheme No. 3. The gas temperature is set at 3 °C, the area R indicates the overlap area and MER indicates the minimum heat requirement. (A) Scenario 2. (B) Scenario 3. (C) Scenario 4. (D) Grand composite curves obtained for the four scenarios.

1.23.10 Energy yield

Table 31 shows the energy efficiency results of each proposed biorefinery schemes and for each pinch analysis scenario.

- Scenario 1 - initial biorefinery schemes. Higher energy efficiency for scenario 1 are obtained when biogas is produced, followed by reforming, and obtaining hydrogen as the main product (Biorefinery scheme No. 2 and No. 3). These results are in agreement with previous studies in the literature that have proposed refining as a complement to the biorefinery processes (Jung et al., 2021; Zhao et al., 2020). Manish and Banerjee (2008) show an energy efficiency for hydrogen production by dark fermentation of 9.6%, but energy efficiency increases up to 64% when integrating hydrogen reforming from methane (Manish and Banerjee, 2008). In the same study, energy efficiency is considered when processes are carried out in series (dark fermentation, photofermentation, and anaerobic digestion), reporting efficiency values between 25% and 27%. According to these data, the proposed biorefinery scheme No. 1, 2, and 3 seem to give better efficiency than that reported in the literature.

- Scenario 2 – ADF heating removed. The energy required for the CSTR reactors of the ADF process is removed in the scenario 2. This increased the energy efficiency in the three biorefinery schemes, validating that the digestion and fermentation processes require a fairly high heat demand (Kongjan et al., 2011; Patterson et al., 2011; Willquist et al., 2012). Results show equal energy efficiencies (η_G 52%) for biorefinery schemes No 1 and 2. These energy conversion efficiency values are consistent with those reported by Meng et al. (2017), Li et al. (2018) and Ariunbaatar et al. (2014) of 48%, 53% and 58% respectively. However, they are below the efficiency reported by Yue et al. (2020) of 71% and 78% for ADF processes. It should be noticed that for all of these studies, no process energy consumption was taken into account (Ariunbaatar et al., 2014; Li et al., 2018; Meng et al., 2017; Yue et al., 2020).

- Scenario 3 - ADF heating removed and CH_4 burned. This scenario proposes the energy sustainability of the process through the combustion of CH_4. Table 31

shows that above all the biorefinery schemes decrease their efficiency when CH_4 combustion is considered. The highest decrease is shown in the biorefinery schemes No. 2 and 3, most probably because the amount of available methane is much lower than in scheme No. 1, and much less heat can be recovered by its burning, thus decreasing the global energy efficiency.

- Scenario 4 - ADF heating removed and Residual gases burned. This scenario proposes the energy sustainability of the process through the combustion of residual gases. Table 31 shows that above all the biorefinery schemes decrease their efficiency when residual gases combustion is considered. The highest decrease is shown in the biorefinery schemes No. 2 , most probably because the amount of available hydrogen is much higher than in scheme No. 3, due to the methanol synthesis.

Table 31 Biorefinery schemes energy yields according to the biomass available for Santander in 2017. Production, $Q_{cooling}$ and $Q_{heating}$ are results of the simulation in Aspen Plus, η_G calculated according to equation Eq. 24 section 1.16.3

Scenario	Biorefinery scheme	CH_4 burned (%)	Main products	Production ($kg \cdot d^{-1}$)	η_G (%)	$Q_{Cooling}$ ($MJ \cdot d^{-1}$)	$Q_{Heating}$ ($MJ \cdot d^{-1}$)
1 - Initial biorefinery schemes	No. 1	n.a	CH_4 H_2	5969 369	37	29098	314308
	No. 2	n.a	H_2 CO	2573 9005	38	26580	411527
	No. 3	n.a	H_2* CO Methanol	2513 13730 198	41	16313	416879
2 - ADF heating removed	No. 1	n.a	CH_4 H_2	5969 369	52	29098	19556
	No. 2	n.a	H_2 CO	2573 9005	52	29184	124020
	No. 3	n.a	H_2* CO Methanol	2513 13730 198	55	16313	135921
3 - ADF heating removed and CH_4 burned	No. 1	7.5	CH_4 H_2	3818 369	50	26209	0
	No. 2	30	H_2 CO	1913 6301	47	57564	0
	No. 3	30	H_2* CO Methanol	1806 10562 141	50	21999	0
4 – ADF heating removed, and residual gas burned	No. 2	n.a	H_2	2352	50	63904	0
	No. 3	n.a	H_2* CO Methanol	1673 6965 231,162	47	53556	0

* Includes hydrogen in the residue gas stream.

n.a = not apply

As shown in Table 31, the lowest energy efficiencies were observed for scenario 1 for all the biorefinery schemes. This is coherent by the fact that scenarios 2 and 3 do not consider energy consumption for heating ADF reactors. Overall, in scenarios 2 and 3, the value of heat for cooling are consistent with value needed to maintain ADF reactors at operating temperature for all the biorefinery schemes that were studied.

Also, the results in Table 31 appears to confirm that the integration of the bioprocesses to the reforming processes can lead to an increase in energy yield compared to that reported for the stand-alone ADF processes, as already highlighted by previous studies in the literature that have investigated hydrogen production by steam reforming (Bruni et al., 2019). Moreover, previous studies have also indicated that use of different substrates (alone or in co-digestion) can strongly affect energy efficiencies. Luongo Malave' et al. (2015) show energy efficiency values between 10% and 40% when using the coffee seed skin, and between 35% and 95% when using glucose as a feedstock for the methane and hydrogen production, this without considering the energy process consumption. Their study also shows that the high lignocellulose content is not suitable for the digestion process, as it may decrease the energy yields (Luongo Malave' et al., 2015).

Above all, it is shown that, even with optimization, the bioprocesses still show lower energy efficiencies than the thermochemical ones that present overall yields for hydrogen and methane production higher than 60% (Ondze et al., 2018). Biorefinery scheme No. 2 shows the highest energy efficiency, most probably due to the hydrogen heat value and showing hydrogen production is the most energy efficient, the implementation of hydrogen production in waste treatment shows to be the most efficient way to use biogas (Madeira et al., 2017b).

3.CONCLUSIONS

The results of Chapter IV confirm that biofuel production from alternative renewable sources such as agro-industrial wastes may represent a sustainable way to overcome the shortage of natural deposits of fossil carbon.

In this Chapter IV, three different biorefinery schemes (No. 1, 2, and 3) were simulated, based on experimental data end using modules developed in the previous Chapters II and III, and their results contribute to the environmental study, to the life cycle assessment (LCA), and to the energy analysis of the biorefinery processes applied to the production of biogas and/or methanol from residual biomass. The results indicate the feasibility of biorefinery plant installation for the Colombian department of Santander, thus according to LCA, energy analysis, and environmental data.

Biorefinery scheme No. 1 (which focuses on biogas production by ADF process followed by biogas purification in biofilter) showed the lowest environmental impacts, as well as the lowest energy yields (between 37% and 50%). Whereas the highest energy yields were shown by biorefinery scheme No. 3 (between 41% and 55%), which focuses in the production of hydrogen as the main product and methanol as a by-product. However, biorefinery scheme No. 3 shows the highest impact in the life cycle analysis, most likely associated with the impact on the energy required for reforming. Overall, the environmental impacts observed in this study are primarily related to the consumption of electrical energy and the use of steam.

4.GENERAL CONCLUSIONS AND PERSPECTIVES

This study confirms that biofuel production from residual biomass may represent a sustainable way to overcome the shortage of natural deposits of fossil carbon, and it contributes to develop biorefinery schemes for the energy valorization of Colombian agro-industrial wastes. Three different residual biomasses produced in Colombia were considered in this study, coffee mucilage (CFM), cocoa mucilage (CCM), and swine manure (SM), based on their availability, heating value, and the annual increase production. According to the literature, anaerobic digestion is currently the second most applied bioprocess in Colombia for CFM, CCM, and SW treatment, after composting.

The main objective of this PhD was to evaluate the most suitable biorefinery scheme to recover energy from CFM, CCF and SM by anaerobic digestion (AD) and/or dark fermentation (DF) bioprocesses in Colombia, followed by biological and/or thermochemical processes of biogas purification and/or refining. The ratio of the biogas production yield from bioprocesses with the residual biomass composition and the availability in each Colombian department, makes it a challenge to compare biorefinery schemes with the valorization processes proposed in the literature. Moreover, for the treatment of the bioprocess output streams (biogas and digestate), the literature review showed several possible thermochemical, separation, and reaction processes. These thermochemical processes of biogas separation/purification and digestate valorization are not considered in the design of the current biorefinery in Colombia, because of their complexity and the requirement in proposing simply and applicable solutions. Several previous studies on bioprocesses and biorefinery schemes with residual biomasses from the same agroindustry have been revised. In the literature, it was not found a technical evaluation study of production yields, energy, and environmental impact to determine which is the most suitable process for the blends of CFM, CCM, and SM.

The results of this study also contribute to the development of AD and DF models to assess biogas production performances from residual biomass. First, AD and DF experiments

were performed at laboratory scale in batch reactors, and the experimental methane and hydrogen production yields were determined for 13 different blends of locally available CCF, CFM, and SM in Colombia. Then, AD and DF models were developed from the ADM1 model, and then they were validated by comparing the simulated to the experimental biogas production data. Overall, the results indicated a good agreement between simulated (between 300-490 ml $CH_4 \cdot gCOD^{-1}$ and 100-260 ml $H_2 \cdot gCOD^{-1}$) and experimental yields (between 250-680 ml $CH_4 \cdot gCOD^{-1}$ and 70-280 ml $H_2 \cdot gCOD^{-1}$). The differences between simulated and experimental data were primarily attributed to substrate-composition variability (especially SM) as well as the incomplete hydrolysis processes in real experiments. Indeed, simulation results for AD and DF processes can get over these technical limits of laboratory experiments and compare the energy recovery potentials of different mixtures and different process schemes.

Before to evaluate the energy recovery potential for different Colombian departments, a series of simulations were performed to investigate the biogas production performances of three different process schemes, anaerobic digestion alone (AD), dark fermentation alone (DF), and dark fermentation followed by anaerobic digestion (ADF). The results have shown that the biogas production is more than doubled for ADF rather than AD and DF processes. Moreover, the percentage of carbon dioxide in the biogas from ADF does not increase.

Then, the developed ADF simulation process was employed to evaluate the energy recovery potential in each department of Colombia, according to their local availability of CFM, CCM, and SM. The results indicate a total energy recovery potential in Colombia of 155.1 ktoe according to the local production amounts of CFM, CCM, and SM in 2017. Overall, energy recovery yields improve by increasing CFM/SM and/or CCM/SM ratios of the feed, and by increasing organic load from 2 to 26 $gCOD \cdot l^{-1}$. The results also indicate that the local availability of different types of residual biomass represents the most influential parameter in assessing the energy recovery potential in Colombia. The Andean region has the highest energy production potential, most likely due to its high production of coffee and cocoa, justifying the contribution of carbohydrates, the main compound of mucilage, in co-digestion.

In order to propose feasible, clean, and highly valorized processes, thermodynamic models were used to simulate the processes of gas separation and purification, hydrogen production

from methane reforming and methanol synthesis from hydrogen and carbon dioxide. Biorefinery scheme No. 1 (biogas production by ADF followed by biogas purification by biofilters) showed the lowest environmental impacts, as well as the lowest energy yields (between 37% and 50%). Whereas the highest energy yields were shown by biorefinery scheme No. 3 (between 41% and 55%), which involves refining processes to produce hydrogen as the main product and methanol as a by-product. However, biorefinery scheme No. 3 shows the highest impact in the life cycle analysis, most likely associated with the impact on the energy required for reforming. Even though energy efficiencies are lower than the thermochemical valorization efficiencies of biomass valorization (> 60%), the use of biorefinery schemes are shown to be an option applicable to the Colombian industry. This especially when many of the farms have already implemented anaerobic digestion and can be optimized with the proposed processes for the treatment of biogas and digestate.

The biorefinery schemes were also evaluated with a PINCH analysis where it was shown that the mathematical models used to simulate biological processes still have weaknesses in the energy estimation, since they do not consider recirculation of sludge, biomass growth, heat transfer from the atmosphere and other reactions that decrease the energy requirement. It is therefore proposed for future research to work on the adjustment of the biological models according to the full energy demand. However, for the PINCH analysis when the noise of the bioprocesses is eliminated, it is shown that the biorefinery schemes require between 7.5% and 30% of the methane produced to produce the heat required in the separation, purification, reforming, and methanol synthesis processes. These values are in agreement with those reported in the literature (between 4% and 35%), and they are in accord to the proposition of way energy self-sustainable biorefinery schemes.

The study of biorefineries has increased significantly in recent years at both the experimental and technological levels. Especially, the development of mathematical models has allowed its technical and environmental assessment. The presented study allowed to have a first approach to the development of the Colombian agroindustry and the use of the wastes for the same utilization of the industry. The current models show that it is possible to recover from residual biomass more energy than that required for the agricultural industry. The great contribution of this work is centered in the development of the three biorefinery schemes that can be replicated in the 32 departments of Colombia, and even more using different types of

residual biomass. On the other hand, the proposed models generate less environmental impact in relation to the current energy matrix of Colombia, which is currently linked to the high consumption of fossil fuels. Also, the study initiating energy integration shows the development progress that is possible in the biorefineries, since one of the impact factors on the processes is reflected in the energy consumption related to their operating conditions, especially temperatures and working volumes.

It should be also noticed that, during the last 5 years, pork breeding, coffee, and cocoa production activities have largely increased in Colombia (DANE, 2020). This suggests an interesting potential market of SM, CFM, and CCM valorization as organic substrates for biogas production. However, the fluctuation in production of these residual biomasses may represent a weakness for perspective evaluations, and therefore a regular updating of inlet data for the models is recommended to better follow future production dynamics. Moreover, most of the coffee, cocoa, and pork production activities are located in rural areas, and, currently, more than 20% of transport roads in Colombia are without pavement (DANE, 2020). This may significantly hinder the collection of co-substrates from different production areas, and it may also generate supplementary transport costs. The bioprocess simulation approach developed in this study may be followed to evaluate energy recovery potential from other types of locally available substrates (IEA, 2020), thus showing a flexibility of adaptation to local contexts. Furthermore, the integration of thermochemical (e.g. gasification, pyrolysis, hydrothermal liquefaction) and separation (e.g. membrane, extraction, distillation) processes may allow the recovery of further by-products (e.g. nutrients, biochar, amino acids, organic acids) from the effluents of AD and DF processes (Arora et al., 2018; Cebreiros et al., 2017; Rajesh Banu et al., 2020b; Uddin et al., 2021). Therefore, an accurate life cycle analysis (LCA), integrating energy balances and operating costs for each unit of the process, would be required to identify the best design, location, and size of the biorefinery plants in Colombia.

Several perspectives are identified for the development of biorefineries in Colombia. Currently, a more accurate economical evaluation of the proposed schemes is under progress, this to evaluate the applicability of the biorefinery schemes according to the availability of residual biomasses in the different Colombian departments. In addition, current research projects in Colombia are related to the implementation of pilot scale experiments, this to

evaluate the applicability of the biorefinery schemes at the full agro-industrial scale. The results of this study have generated great interest in the Colombian industry, which led to the application and generation of new research projects that aim at investigating the energy recovery potential from different organic wastes of the department of Santander.

REFERENCES

Abbassi-Guendouz, A., Brockmann, D., Trably, E., Dumas, C., Delgenès, J.-P., Steyer, J.-P., Escudié, R., 2012. Total solids content drives high solid anaerobic digestion via mass transfer limitation. Bioresour. Technol. 111, 55–61. https://doi.org/10.1016/j.biortech.2012.01.174

Abdou Alio, M., Marcati, A., Pons, A., Vial, C., 2021. Modeling and simulation of a sawdust mixture-based integrated biorefinery plant producing bioethanol. Bioresour. Technol. 325, 124650. https://doi.org/10.1016/j.biortech.2020.124650

Abouelenien, F., Fujiwara, W., Namba, Y., Kosseva, M., Nishio, N., Nakashimada, Y., 2010. Improved methane fermentation of chicken manure via ammonia removal by biogas recycle. Bioresour. Technol. 101, 6368–6373. https://doi.org/10.1016/j.biortech.2010.03.071

Achinas, S., Achinas, V., Euverink, G.J.W., 2017. A Technological Overview of Biogas Production from Biowaste. Engineering 3, 299–307. https://doi.org/10.1016/J.ENG.2017.03.002

Adarme, O.F.H., Baêta, B.E.L., Lima, D.R.S., Gurgel, L.V.A., de Aquino, S.F., 2017. Methane and hydrogen production from anaerobic digestion of soluble fraction obtained by sugarcane bagasse ozonation. Ind. Crops Prod. 109, 288–299. https://doi.org/10.1016/j.indcrop.2017.08.040

Alatriste-Mondragón, F., Samar, P., Cox, H.H.J., Ahring, B.K., Iranpour, R., 2006. Anaerobic codigestion of municipal, farm, and industrial organic wastes: a survey of recent literature. Water Environ. Res. Res. Publ. Water Environ. Fed. 78, 607–636.

Alexandropoulou, M., Antonopoulou, G., Lyberatos, G., 2018. A novel approach of modeling continuous dark hydrogen fermentation. Bioresour. Technol. 250, 784–792. https://doi.org/10.1016/j.biortech.2017.12.005

Alhazmi, H., Loy, A.C.M., 2021. A review on environmental assessment of conversion of agriculture waste to bio-energy via different thermochemical routes: Current and future trends. Bioresour. Technol. Rep. 14, 100682. https://doi.org/10.1016/j.biteb.2021.100682

Alibardi, L., Astrup, T.F., Asunis, F., Clarke, W.P., De Gioannis, G., Dessì, P., Lens, P.N.L., Lavagnolo, M.C., Lombardi, L., Muntoni, A., Pivato, A., Polettini, A., Pomi, R., Rossi, A., Spagni, A., Spiga, D., 2020. Organic waste biorefineries: Looking towards implementation. Waste Manag. 114, 274–286. https://doi.org/10.1016/j.wasman.2020.07.010

Álvarez, J.A., Otero, L., Lema, J.M., 2010. A methodology for optimising feed composition for anaerobic co-digestion of agro-industrial wastes. Bioresour. Technol. 101, 1153–1158. https://doi.org/10.1016/j.biortech.2009.09.061

Amoah, J., Kahar, P., Ogino, C., Kondo, A., 2019. Bioenergy and Biorefinery: Feedstock, Biotechnological Conversion, and Products. Biotechnol. J. 14, 1800494. https://doi.org/10.1002/biot.201800494

An, X., Zuo, Y., Zhang, Q., Wang, J., 2009. Methanol Synthesis from CO2 Hydrogenation with a Cu/Zn/Al/Zr Fibrous Catalyst. Chin. J. Chem. Eng. 17, 88–94. https://doi.org/10.1016/S1004-9541(09)60038-0

Angelidaki, I., Ellegaard, L., Ahring, B.K., 1999. A comprehensive model of anaerobic bioconversion of complex substrates to biogas. Biotechnol. Bioeng. 63, 363–372. https://doi.org/10.1002/(SICI)1097-0290(19990505)63:3<363::AID-BIT13>3.0.CO;2-Z

Antonopoulou, G., Gavala, H.N., Skiadas, I.V., Lyberatos, G., 2012. Modeling of fermentative hydrogen production from sweet sorghum extract based on modified ADM1. Int. J. Hydrog. Energy, 11th China Hydrogen Energy Conference 37, 191–208. https://doi.org/10.1016/j.ijhydene.2011.09.081

Aregheore, E.M., 2002. Chemical evaluation and digestibility of cocoa (Theobroma cacao) byproducts fed to goats. Trop. Anim. Health Prod. 34, 339–348.

Argun, Hidayet & Dao, Siaka. (2015). Hydrogen gas production from waste peach pulp by dark fermentation and electrohydrolysis. International Journal of Hydrogen Energy. 41. 10.1016/j.ijhydene.2015.11.170.

Arifin, S., Chien, I.L., 2008. Design and Control of an Isopropyl Alcohol Dehydration Process via Extractive Distillation Using Dimethyl Sulfoxide as an Entrainer. Ind. Eng. Chem. Res. 47, 790–803. https://doi.org/10.1021/ie070996n

Ariunbaatar, J., Panico, A., Frunzo, L., Esposito, G., Lens, P.N.L., Pirozzi, F., 2014. Enhanced anaerobic digestion of food waste by thermal and ozonation pretreatment methods. J. Environ. Manage. 146, 142–149. https://doi.org/10.1016/j.jenvman.2014.07.042

Armor, J.N., 1999. The multiple roles for catalysis in the production of H2. Appl. Catal. Gen. 176, 159–176. https://doi.org/10.1016/S0926-860X(98)00244-0

Arora, A., Banerjee, J., Vijayaraghavan, R., MacFarlane, D., Patti, A.F., 2018. Process design and techno-economic analysis of an integrated mango processing waste biorefinery. Ind. Crops Prod. 116, 24–34. https://doi.org/10.1016/j.indcrop.2018.02.061

Astals, S., Ariso, M., Galí, A., Mata-Alvarez, J., 2011. Co-digestion of pig manure and glycerine: Experimental and modelling study. J. Environ. Manage. 92, 1091–1096. https://doi.org/10.1016/j.jenvman.2010.11.014

Astals, S., Musenze, R.S., Bai, X., Tannock, S., Tait, S., Pratt, S., Jensen, P.D., 2015. Anaerobic co-digestion of pig manure and algae: impact of intracellular algal products recovery on co-digestion performance. Bioresour. Technol. 181, 97–104. https://doi.org/10.1016/j.biortech.2015.01.039

Astals, S., Peces, M., Batstone, D.J., Jensen, P.D., Tait, S., 2018. Characterising and modelling free ammonia and ammonium inhibition in anaerobic systems. Water Res. 143, 127–135. https://doi.org/10.1016/j.watres.2018.06.021

Awasthi, S.K., Joshi, R., Dhar, H., Verma, S., Awasthi, M.K., Varjani, S., Sarsaiya, S., Zhang, Z., Kumar, S., 2018. Improving methane yield and quality via co-digestion of cow dung mixed with food waste. Bioresour. Technol. 251, 259–263. https://doi.org/10.1016/j.biortech.2017.12.063

Bab&aelig, E, A., Shayegan, J., Willems, E.M.M., Jablonska, B., Jan Ruig, G., Krikke, T., 2011. Effect of Organic Loading Rates (OLR) on Production of Methane from Anaerobic Digestion of Vegetables Waste.

Bai, J., Liu, H., Yin, B., Ma, H., 2015. Modeling of enhanced VFAs production from waste activated sludge by modified ADM1 with improved particle swarm optimization for parameters estimation. Biochem. Eng. J. 103, 22–31. https://doi.org/10.1016/j.bej.2015.06.015

Banerjee, S., Tiarks, J.A., Lukawski, M., Kong, S.-C., Brown, R.C., 2013. Technoeconomic Analysis of Biofuel Production and Biorefinery Operation Utilizing Geothermal Energy. Energy Fuels 27, 1381–1390. https://doi.org/10.1021/ef301898n

Bao, B., Ng, D.K.S., Tay, D.H.S., Jiménez-Gutiérrez, A., El-Halwagi, M.M., 2011. A shortcut method for the preliminary synthesis of process-technology pathways: An optimization approach and application for the conceptual design of integrated biorefineries. Comput. Chem. Eng., Energy & Sustainability 35, 1374–1383. https://doi.org/10.1016/j.compchemeng.2011.04.013

Barca, C., Ranava, D., Bauzan, M., Ferrasse, J.-H., Giudici-Orticoni, M.-T., Soric, A., 2016. Fermentative hydrogen production in an up-flow anaerobic biofilm reactor inoculated

with a co-culture of Clostridium acetobutylicum and Desulfovibrio vulgaris. Bioresour. Technol. 221, 526–533. https://doi.org/10.1016/j.biortech.2016.09.072

Barca, C., Soric, A., Ranava, D., Giudici-Orticoni, M.-T., Ferrasse, J.-H., 2015. Anaerobic biofilm reactors for dark fermentative hydrogen production from wastewater: A review. Bioresour. Technol. 185, 386–398. https://doi.org/10.1016/j.biortech.2015.02.063

Bastidas-Oyanedel, J.-R., Bonk, F., Thomsen, M.H., Schmidt, J.E., 2015. Dark fermentation biorefinery in the present and future (bio)chemical industry. Rev. Environ. Sci. Biotechnol. 14, 473–498. https://doi.org/10.1007/s11157-015-9369-3

Batstone, D.J., Keller, J., Angelidaki, I., Kalyuzhnyi, S.V., Pavlostathis, S.G., Rozzi, A., Sanders, W.T.M., Siegrist, H., Vavilin, V.A., 2002. The IWA Anaerobic Digestion Model No 1 (ADM1). Water Sci. Technol. J. Int. Assoc. Water Pollut. Res. 45, 65–73.

Batstone, D.J., Pind, P.F., Angelidaki, I., 2003. Kinetics of thermophilic, anaerobic oxidation of straight and branched chain butyrate and valerate. Biotechnol. Bioeng. 84, 195–204. https://doi.org/10.1002/bit.10753

Battista, F., Fino, D., Mancini, G., 2016. Optimization of biogas production from coffee production waste. Bioresour. Technol. 200, 884–890. https://doi.org/10.1016/j.biortech.2015.11.020

Benizri, D., Dietrich, N., Labeyrie, P., Hébrard, G., 2019. A compact, economic scrubber to improve farm biogas upgrading systems. Sep. Purif. Technol. 219, 169–179. https://doi.org/10.1016/j.seppur.2019.02.054

Bioenergy IEA, Task 40, 2006. Sustainable International Bioenergy Trade: Securing Supply and Demand Opportunities and barriers for sustainable international. URL https://www.bioenergytrade.org/iea-publications/task-40-library/ (accessed 6.22.21).

Bollon, J., Le-hyaric, R., Benbelkacem, H., Buffiere, P., 2011. Development of a kinetic model for anaerobic dry digestion processes: Focus on acetate degradation and moisture content. Biochem. Eng. J. 3, 212–218. https://doi.org/10.1016/j.bej.2011.06.011

Bruni, G., Rizzello, C., Santucci, A., Alique, D., Incelli, M., Tosti, S., 2019. On the energy efficiency of hydrogen production processes via steam reforming using membrane reactors. Int. J. Hydrog. Energy 44, 988–999. https://doi.org/10.1016/j.ijhydene.2018.11.095

C. von Enden, J., Calvert, K.C., 2010. Review of coffee wastewater characteristics and approaches to treatment.

Calderón Carreño, M.A., Garay Benítez, A.C., 2020. Inventario de ciclo de vida de la red de gas natural colombiana hacia tres centros de consumo del país.

Campos-Vega, R., Nieto-Figueroa, K.H., Oomah, B.D., 2018. Cocoa (Theobroma cacao L.) pod husk: Renewable source of bioactive compounds. Trends Food Sci. Technol. 81, 172–184. https://doi.org/10.1016/j.tifs.2018.09.022

Carotenuto, C., Guarino, G., D'Amelia, L.I., Morrone, B., Minale, M., 2020. The peculiar role of C/N and initial pH in anaerobic digestion of lactating and non-lactating water buffalo manure. Waste Manag. 103, 12–21. https://doi.org/10.1016/j.wasman.2019.12.008

Cebreiros, F., Guigou, M.D., Cabrera, M.N., 2017. Integrated forest biorefineries: Recovery of acetic acid as a by-product from eucalyptus wood hemicellulosic hydrolysates by solvent extraction. Ind. Crops Prod. 109, 101–108. https://doi.org/10.1016/j.indcrop.2017.08.012

Cesaro, A., 2021. The valorization of the anaerobic digestate from the organic fractions of municipal solid waste: Challenges and perspectives. J. Environ. Manage. 280, 111742. https://doi.org/10.1016/j.jenvman.2020.111742

Chanakya, H.N., De Alwis, A.A.P., 2004. Environmental Issues and Management in Primary Coffee Processing. Process Saf. Environ. Prot. 82, 291–300. https://doi.org/10.1205/095758204323162319

Chen, X.Y., Vinh-Thang, H., Ramirez, A.A., Rodrigue, D., Kaliaguine, S., 2015. Membrane gas separation technologies for biogas upgrading. RSC Adv. 5, 24399–24448. https://doi.org/10.1039/C5RA00666J

Chen, Y., Yin, Y., Wang, J., 2021. Recent advance in inhibition of dark fermentative hydrogen production. Int. J. Hydrog. Energy 46, 5053–5073. https://doi.org/10.1016/j.ijhydene.2020.11.096

Cinar, Z.Ö., Atanassova, M., Tumer, T.B., Caruso, G., Antika, G., Sharma, S., Sharifi-Rad, J., Pezzani, R., 2021. Cocoa and cocoa bean shells role in human health: An updated review. J. Food Compos. Anal. 103, 104115. https://doi.org/10.1016/j.jfca.2021.104115

Clauser, N.M., Felissia, F.E., Area, M.C., Vallejos, M.E., 2021. A framework for the design and analysis of integrated multi-product biorefineries from agricultural and forestry wastes. Renew. Sustain. Energy Rev. 139, 110687. https://doi.org/10.1016/j.rser.2020.110687

Clifford, M.N., 2012. Coffee: Botany, Biochemistry and Production of Beans and Beverage. Springer Science & Business Media.

Cvetković, S.M., Radoičić, T.K., Kijevčanin, M., Novaković, J.G., 2021. Life Cycle Energy Assessment of biohydrogen production via biogas steam reforming: Case study of biogas plant on a farm in Serbia. Int. J. Hydrog. Energy 46, 14130–14137. https://doi.org/10.1016/j.ijhydene.2021.01.181

Dai, L., Wang, Y., Liu, Y., Ruan, R., He, C., Yu, Z., Jiang, L., Zeng, Z., Tian, X., 2019. Integrated process of lignocellulosic biomass torrefaction and pyrolysis for upgrading bio-oil production: A state-of-the-art review. Renew. Sustain. Energy Rev. 107, 20–36. https://doi.org/10.1016/j.rser.2019.02.015

DANE, 2020. Departamento Administrativo Nacional de Estadística [WWW Document]. URL http://www.dane.gov.co/

Das, J., Rene, E.R., Dupont, C., Dufourny, A., Blin, J., van Hullebusch, E.D., 2019. Performance of a compost and biochar packed biofilter for gas-phase hydrogen sulfide removal. Bioresour. Technol. 273, 581–591. https://doi.org/10.1016/j.biortech.2018.11.052

Das, P., V.p., C., Mathimani, T., Pugazhendhi, A., 2021. A comprehensive review on the factors affecting thermochemical conversion efficiency of algal biomass to energy. Sci. Total Environ. 766, 144213. https://doi.org/10.1016/j.scitotenv.2020.144213

de Alcântara Pessôa Filho, P., Medeiros Hirata, G.A., Watanabe, É.O., Miranda, E.A., 2019. 2.49 - Precipitation and Crystallization☆, in: Moo-Young, M. (Ed.), Comprehensive Biotechnology (Third Edition). Pergamon, Oxford, pp. 725–738. https://doi.org/10.1016/B978-0-444-64046-8.00098-7

de Gracia, M., Grau, P., Huete, E., Gómez, J., García-Heras, J.L., Ayesa, E., 2009. New generic mathematical model for WWTP sludge digesters operating under aerobic and anaerobic conditions: Model building and experimental verification. Water Res. 43, 4626–4642. https://doi.org/10.1016/j.watres.2009.07.014

Demichelis, F., Fiore, S., Pleissner, D., Venus, J., 2018. Technical and economic assessment of food waste valorization through a biorefinery chain. Renew. Sustain. Energy Rev. 94, 38–48. https://doi.org/10.1016/j.rser.2018.05.064

Demirbas, A., 2010. Biorefineries - For Biomass Upgrading Facilities | Ayhan Demirbas | Springer. Springer-Verlag, London.

Dhar, H., Kumar, P., Kumar, S., Mukherjee, S., Vaidya, A.N., 2016. Effect of organic loading rate during anaerobic digestion of municipal solid waste. Bioresour. Technol., Special Issue on Bioenergy, Bioproducts and Environmental Sustainability 217, 56–61. https://doi.org/10.1016/j.biortech.2015.12.004

Dinesh, G.H., Nguyen, D.D., Ravindran, B., Chang, S.W., Vo, D.-V.N., Bach, Q.-V., Tran, H.N., Basu, M.J., Mohanrasu, K., Murugan, R.S., Swetha, T.A., Sivapraksh, G., Selvaraj, A., Arun, A., 2020. Simultaneous biohydrogen (H2) and bioplastic (poly-β-

hydroxybutyrate-PHB) productions under dark, photo, and subsequent dark and photo fermentation utilizing various wastes. Int. J. Hydrog. Energy, The 3rd International Conference on Alternative Fuels, Energy and Environment: Future and Challenges (ICAFEE2018) 45, 5840–5853. https://doi.org/10.1016/j.ijhydene.2019.09.036

Dinsdale, R.M., Hawkes, F.R., Hawkes, D.L., 1996. The mesophilic and thermophilic anaerobic digestion of coffee waste containing coffee grounds. Water Res. 30, 371–377. https://doi.org/10.1016/0043-1354(95)00157-3

Doassans-Carrère, N., Ferrasse, J.-H., Boutin, O., Mauviel, G., Lédé, J., 2014. Comparative Study of Biomass Fast Pyrolysis and Direct Liquefaction for Bio-Oils Production: Products Yield and Characterizations. Energy Fuels 28, 5103–5111. https://doi.org/10.1021/ef500641c

Donkoh, A., Atuahene, C.C., Wilson, B.N., Adomako, D., 1991. Chemical composition of cocoa pod husk and its effect on growth and food efficiency in broiler chicks. Anim. Feed Sci. Technol. 35, 161–169. https://doi.org/10.1016/0377-8401(91)90107-4

Donoso-Bravo, A., Mailier, J., Martin, C., Rodríguez, J., Aceves-Lara, C.A., Wouwer, A.V., 2011. Model selection, identification and validation in anaerobic digestion: A review. Water Res. 45, 5347–5364. https://doi.org/10.1016/j.watres.2011.08.059

Ebner, J.H., Labatut, R.A., Lodge, J.S., Williamson, A.A., Trabold, T.A., 2016. Anaerobic co-digestion of commercial food waste and dairy manure: Characterizing biochemical parameters and synergistic effects. Waste Manag. 52, 286–294. https://doi.org/10.1016/j.wasman.2016.03.046

Elbeshbishy, E., Dhar, B.R., Nakhla, G., Lee, H.-S., 2017. A critical review on inhibition of dark biohydrogen fermentation. Renew. Sustain. Energy Rev. 79, 656–668. https://doi.org/10.1016/j.rser.2017.05.075

Elgarahy, A.M., Hammad, A., El-Sherif, D.M., Abouzid, M., Gaballah, M.S., Elwakeel, K.Z., 2021. Thermochemical conversion strategies of biomass to biofuels, techno-economic and bibliometric analysis: A conceptual review. J. Environ. Chem. Eng. 9, 106503. https://doi.org/10.1016/j.jece.2021.106503

Energy Information Administration (EIA), 2020. Biomass explained - U.S. [WWW Document]. URL https://www.eia.gov/energyexplained/biomass/ (accessed 4.28.21).

Esposito, G., Frunzo, L., Panico, A., Pirozzi, F., 2011. Model calibration and validation for OFMSW and sewage sludge co-digestion reactors. Waste Manag. 31, 2527–2535. https://doi.org/10.1016/j.wasman.2011.07.024

Faheem, H.H., Tanveer, H.U., Abbas, Syed.Z., Maqbool, F., 2021. Comparative study of conventional steam-methane-reforming (SMR) and auto-thermal-reforming (ATR) with their hybrid sorption enhanced (SE-SMR & SE-ATR) and environmentally benign process models for the hydrogen production. Fuel 297, 120769. https://doi.org/10.1016/j.fuel.2021.120769

Fallot, A., Saint-Andre, L., le Maire, G., Laclau, J.-P., Nouvellon, Y., Marsden, C., Jean-Pierre, B., Silva, T., Piketty, M.-G., Hamel, O., 2009. Biomass sustainability, availability and productivity. Rev. Metall.-Cah. Inf. Tech. - REV Met.-CAH INF TECH 106, 410–418. https://doi.org/10.1051/metal/2009072

Faraji, M., Saidi, M., 2021. Hydrogen-rich syngas production via integrated configuration of pyrolysis and air gasification processes of various algal biomass: Process simulation and evaluation using Aspen Plus software. Int. J. Hydrog. Energy. https://doi.org/10.1016/j.ijhydene.2021.03.047

Fedebiocombustibles - COL, 2021. Federación Nacional de Biocombustibles de Colombia [WWW Document]. URL http://www.fedebiocombustibles.com/v3/main-index.htm (accessed 6.18.21).

Fedecacao - Federación Nacional de Cacaoteros [WWW Document], 2020. URL http://www.fedecacao.com.co/portal/index.php/es/

Federación Nacional de cafeteros [WWW Document], 2020. URL https://www.federaciondecafeteros.org/

Fedorovich, V., Lens, P., Kalyuzhnyi, S., 2003. Extension of Anaerobic Digestion Model No. 1 with processes of sulfate reduction. Appl. Biochem. Biotechnol. 109, 33–45. https://doi.org/10.1385/abab:109:1-3:33

Fernández-Polanco, D., Tatsumi, H., 2016. Optimum energy integration of thermal hydrolysis through pinch analysis. Renew. Energy, Special Issue: Biogas as a Renewable Fuel 96, 1093–1102. https://doi.org/10.1016/j.renene.2016.01.038

Fezzani, B., Cheikh, R., 2008. Implementation of IWA anaerobic digestion model No. 1 (ADM1) for simulating the thermophilic anaerobic co-digestion of olive mill wastewater with olive mill solid waste in a semi-continuous tubular digester. Chem. Eng. J. 141, 75–88. https://doi.org/10.1016/j.cej.2007.10.024

Fezzani, B., Cheikh, R.B., 2009. Extension of the anaerobic digestion model No. 1 (ADM1) to include phenolic compounds biodegradation processes for the simulation of anaerobic co-digestion of olive mill wastes at thermophilic temperature. J. Hazard. Mater. 162, 1563–1570. https://doi.org/10.1016/j.jhazmat.2008.06.127

Flores-Alsina, X., Solon, K., Kazadi Mbamba, C., Tait, S., Gernaey, K.V., Jeppsson, U., Batstone, D.J., 2016. Modelling phosphorus (P), sulfur (S) and iron (Fe) interactions for dynamic simulations of anaerobic digestion processes. Water Res. 95, 370–382. https://doi.org/10.1016/j.watres.2016.03.012

Fonoll, X., Astals, S., Dosta, J., Mata-Alvarez, J., 2015. Anaerobic co-digestion of sewage sludge and fruit wastes: Evaluation of the transitory states when the co-substrate is changed. Chem. Eng. J. 262, 1268–1274. https://doi.org/10.1016/j.cej.2014.10.045

Fountoulakis, M.S., Stamatelatou, K., Batstone, D.J., Lyberatos, G., 2006. Simulation of DEHP biodegradation and sorption during the anaerobic digestion of secondary sludge. Water Sci. Technol. J. Int. Assoc. Water Pollut. Res. 54, 119–128. https://doi.org/10.2166/wst.2006.533

Frunzo, L., Fermoso, F.G., Luongo, V., Mattei, M.R., Esposito, G., 2019. ADM1-based mechanistic model for the role of trace elements in anaerobic digestion processes. J. Environ. Manage. 241, 587–602. https://doi.org/10.1016/j.jenvman.2018.11.058

Galí, A., Benabdallah, T., Astals, S., Mata-Alvarez, J., 2009. Modified version of ADM1 model for agro-waste application. Bioresour. Technol. 100, 2783–2790. https://doi.org/10.1016/j.biortech.2008.12.052

Gao, Y., Zhao, J., Qin, C., Yuan, Q., Zhu, J., Sun, Y., Lu, C., 2021. Evaluating the effect of fluoxetine on mesophilic anaerobic dark biohydrogen fermentation of excess sludge. Bioresour. Technol. 336, 125320. https://doi.org/10.1016/j.biortech.2021.125320

Garfí, M., Ferrer-Martí, L., Perez, I., Flotats, X., Ferrer, I., 2011. Codigestion of cow and guinea pig manure in low-cost tubular digesters at high altitude. Ecol. Eng. 37, 2066–2070. https://doi.org/10.1016/j.ecoleng.2011.08.018

Gargalo, C.L., Carvalho, A., Gernaey, K.V., Sin, G., 2017. Optimal Design and Planning of Glycerol-Based Biorefinery Supply Chains under Uncertainty. Ind. Eng. Chem. Res. 56, 11870–11893. https://doi.org/10.1021/acs.iecr.7b02882

Garritano, A.N., Faber, M. de O., De Sá, L.R.V., Ferreira-Leitão, V.S., 2018. Palm oil mill effluent (POME) as raw material for biohydrogen and methane production via dark fermentation. Renew. Sustain. Energy Rev. 92, 676–684. https://doi.org/10.1016/j.rser.2018.04.031

Geraili, A., Romagnoli, J.A., 2015. A multiobjective optimization framework for design of integrated biorefineries under uncertainty. AIChE J. 61, 3208–3222. https://doi.org/10.1002/aic.14849

Ghimire, A., Frunzo, L., Pirozzi, F., Trably, E., Escudie, R., Lens, P.N.L., Esposito, G., 2015a. A review on dark fermentative biohydrogen production from organic biomass: Process parameters and use of by-products. Appl. Energy 144, 73–95. https://doi.org/10.1016/j.apenergy.2015.01.045

Ghimire, A., Frunzo, L., Pontoni, L., d'Antonio, G., Lens, P.N.L., Esposito, G., Pirozzi, F., 2015b. Dark fermentation of complex waste biomass for biohydrogen production by pretreated thermophilic anaerobic digestate. J. Environ. Manage. 152, 43–48. https://doi.org/10.1016/j.jenvman.2014.12.049

Goffé, J., Ferrasse, J.-H., 2019. Stoichiometry impact on the optimum efficiency of biomass conversion to biofuels. Energy 170, 438–458. https://doi.org/10.1016/j.energy.2018.12.137

Gomes, S.D., Fuess, L.T., Penteado, E.D., Lucas, S.D.M., Gotardo, J.T., Zaiat, M., 2015. The application of an innovative continuous multiple tube reactor as a strategy to control the specific organic loading rate for biohydrogen production by dark fermentation. Bioresour. Technol. 197, 201–207. https://doi.org/10.1016/j.biortech.2015.08.077

Gonçalves, M.R., Costa, J.C., Pereira, M.A., Abreu, A.A., Alves, M.M., 2014. On the independence of hydrogen production from methanogenic suppressor in olive mill wastewater. Int. J. Hydrog. Energy 39, 6402–6406. https://doi.org/10.1016/j.ijhydene.2014.02.056

Gong, J., You, F., 2015. Value-Added Chemicals from Microalgae: Greener, More Economical, or Both? ACS Sustain. Chem. Eng. 3, 82–96. https://doi.org/10.1021/sc500683w

Gong, J., You, F., 2014a. Optimal Design and Synthesis of Algal Biorefinery Processes for Biological Carbon Sequestration and Utilization with Zero Direct Greenhouse Gas Emissions: MINLP Model and Global Optimization Algorithm. Ind. Eng. Chem. Res. 53, 1563–1579. https://doi.org/10.1021/ie403459m

Gong, J., You, F., 2014b. Global optimization for sustainable design and synthesis of algae processing network for CO2 mitigation and biofuel production using life cycle optimization. AIChE J. 60, 3195–3210. https://doi.org/10.1002/aic.14504

Guo, X., Zhang, Y., Guo, Q., Zhang, R., Wang, C., Yan, B., Lin, F., Chen, G., Hou, L., 2021. Evaluation on energetic and economic benefits of the coupling anaerobic digestion and gasification from agricultural wastes. Renew. Energy 176, 494–503. https://doi.org/10.1016/j.renene.2021.05.097

Guo, X.M., Trably, E., Latrille, E., Carrere, H., Steyer, J.-P., 2014. Predictive and explicative models of fermentative hydrogen production from solid organic waste: Role of butyrate and lactate pathways. Int. J. Hydrog. Energy 39, 7476–7485. https://doi.org/10.1016/j.ijhydene.2013.08.079

Hajjaji, N., Martinez, S., Trably, E., Steyer, J.-P., Helias, A., 2016. Life cycle assessment of hydrogen production from biogas reforming. Int. J. Hydrog. Energy 41, 6064–6075. https://doi.org/10.1016/j.ijhydene.2016.03.006

Hansen, K.H., Angelidaki, I., Ahring, B.K., 1999. Improving thermophilic anaerobic digestion of swine manure. Water Res. 33, 1805–1810. https://doi.org/10.1016/S0043-1354(98)00410-2

Harris, K., Grim, R.G., Huang, Z., Tao, L., 2021. A comparative techno-economic analysis of renewable methanol synthesis from biomass and CO2: Opportunities and barriers to commercialization. Appl. Energy 303, 117637. https://doi.org/10.1016/j.apenergy.2021.117637

Hernandez, M., González, A., Suárez, F., Ochoa, C., Candela, A., Cabeza, I., 2018. Assessment of the Biohydrogen Production Potential of Different Organic Residues In Colombia: Cocoa Waste, Pig Manure and Coffee Mucilage. Chem. Eng. Trans. 65. https://doi.org/10.3303/CET1865042

Hernández, M., Rodríguez, M., 2013. Hydrogen production by anaerobic digestion of pig manure: Effect of operating conditions. Renew. Energy 53, 187–192. https://doi.org/10.1016/j.renene.2012.11.024

Hernández, M.A., Rodríguez Susa, M., Andres, Y., 2014. Use of coffee mucilage as a new substrate for hydrogen production in anaerobic co-digestion with swine manure.

Bioresour. Technol., Special Issue on Advance Biological Treatment Technologies for Sustainable Waste Management (ICSWHK2013) 168, 112–118. https://doi.org/10.1016/j.biortech.2014.02.101
Hierholtzer, A., Akunna, J.C., 2012. Modelling sodium inhibition on the anaerobic digestion process. Water Sci. Technol. J. Int. Assoc. Water Pollut. Res. 66, 1565–1573. https://doi.org/10.2166/wst.2012.345
Humberto Escalante Hernández, Janneth Orduz Prada, Henry Josué Zapata Lesmes, María Cecilia Cardona Ruiz, Martha Duarte Ortega, 2011. Atlas del potencial energético de la biomasa residual en Colombia.
ICA, 2018. Instituto Colombiano Agropecuario [WWW Document]. URL https://www.ica.gov.co/
IEA, 2021. Task 42 | Biorefining in a Circular Economy. URL https://task42.ieabioenergy.com/ (accessed 5.27.21).
IEA, 2020. International Energy Statistics - U.S. Energy Information Administration [WWW Document]. URL https://www.iea.org/
Inc, M.& E., Tchobanoglous, G., Burton, F.L., Stensel, H.D., 2002. Wastewater Engineering: Treatment and Reuse, 4th edition. ed. McGraw Hill Higher Education, Boston, Mass.
Jerry Murphy, Peter Weiland, Arthur Wellinger, Rudolf Braun, 2011. Biogas from Crop Digestion. IEA Bioenergy 24.
Ji, M., Wang, J., 2021. Review and comparison of various hydrogen production methods based on costs and life cycle impact assessment indicators. Int. J. Hydrog. Energy 46, 38612–38635. https://doi.org/10.1016/j.ijhydene.2021.09.142
Jiang, J., He, S., Kang, X., Sun, Y., Yuan, Z., Xing, T., Guo, Y., Li, L., 2020. Effect of Organic Loading Rate and Temperature on the Anaerobic Digestion of Municipal Solid Waste: Process Performance and Energy Recovery. Front. Energy Res. 8. https://doi.org/10.3389/fenrg.2020.00089
Jung, S., Lee, J., Moon, D.H., Kim, K.-H., Kwon, E.E., 2021. Upgrading biogas into syngas through dry reforming. Renew. Sustain. Energy Rev. 143, 110949. https://doi.org/10.1016/j.rser.2021.110949
Kampioti, Anastasia & Komilis, Dimitrios. (2022). Anaerobic co-digestion of coffee waste with other organic substrates: A mixture experimental design. Chemosphere. 297. 134124. 10.1016/j.chemosphere.2022.134124.
Karki, R., Chuenchart, W., Surendra, K.C., Shrestha, S., Raskin, L., Sung, S., Hashimoto, A., Kumar Khanal, S., 2021. Anaerobic co-digestion: Current status and perspectives. Bioresour. Technol. 330, 125001. https://doi.org/10.1016/j.biortech.2021.125001
Katakojwala, R., Mohan, S.V., 2021. A critical view on the environmental sustainability of biorefinery systems. Curr. Opin. Green Sustain. Chem. 27, 100392. https://doi.org/10.1016/j.cogsc.2020.100392
Kelloway, A., Daoutidis, P., 2014. Process Synthesis of Biorefineries: Optimization of Biomass Conversion to Fuels and Chemicals. Ind. Eng. Chem. Res. 53, 5261–5273. https://doi.org/10.1021/ie4018572
Khoshnoodi, M., Lim, Y.S., 1997. Simulation of partial oxidation of natural gas to synthesis gas using ASPEN PLUS. Fuel Process. Technol. 50, 275–289. https://doi.org/10.1016/S0378-3820(96)01079-X
Kim, S.-H., Han, S.-K., Shin, H.-S., 2004a. Feasibility of biohydrogen production by anaerobic co-digestion of food waste and sewage sludge. Int. J. Hydrog. Energy 29, 1607–1616. https://doi.org/10.1016/j.ijhydene.2004.02.018
Kim, S.-H., Han, S.-K., Shin, H.-S., 2004b. Feasibility of biohydrogen production by anaerobic co-digestion of food waste and sewage sludge. Int. J. Hydrog. Energy 29, 1607–1616. https://doi.org/10.1016/j.ijhydene.2004.02.018

Kiss, A.A., Pragt, J.J., Vos, H.J., Bargeman, G., de Groot, M.T., 2016. Novel efficient process for methanol synthesis by CO2 hydrogenation. Chem. Eng. J. 284, 260–269. https://doi.org/10.1016/j.cej.2015.08.101

Kleerebezem, R., van Loosdrecht, M.C.M., 2006. Critical analysis of some concepts proposed in ADM1. Water Sci. Technol. J. Int. Assoc. Water Pollut. Res. 54, 51–57.

Klein, B.C., Chagas, M.F., Junqueira, T.L., Rezende, M.C.A.F., Cardoso, T. de F., Cavalett, O., Bonomi, A., 2018. Techno-economic and environmental assessment of renewable jet fuel production in integrated Brazilian sugarcane biorefineries. Appl. Energy 209, 290–305. https://doi.org/10.1016/j.apenergy.2017.10.079

Kongjan, P., O-Thong, S., Angelidaki, I., 2011. Performance and microbial community analysis of two-stage process with extreme thermophilic hydrogen and thermophilic methane production from hydrolysate in UASB reactors. Bioresour. Technol. 102, 4028–4035. https://doi.org/10.1016/j.biortech.2010.12.009

Kovalovszki, A., Alvarado-Morales, M., Fotidis, I.A., Angelidaki, I., 2017. A systematic methodology to extend the applicability of a bioconversion model for the simulation of various co-digestion scenarios. Bioresour. Technol. 235, 157–166. https://doi.org/10.1016/j.biortech.2017.03.101

Kumar, N., Dixit, A., 2021. Chapter 4 - Management of biomass, in: Kumar, N., Dixit, A. (Eds.), Nanotechnology for Rural Development, Micro and Nano Technologies. Elsevier, pp. 97–140. https://doi.org/10.1016/B978-0-12-824352-7.00004-9

Lamnatou, Chr., Nicolaï, R., Chemisana, D., Cristofari, C., Cancellieri, D., 2019. Biogas production by means of an anaerobic-digestion plant in France: LCA of greenhouse-gas emissions and other environmental indicators. Sci. Total Environ. 670, 1226–1239. https://doi.org/10.1016/j.scitotenv.2019.03.211

Lar, J.S., Li, R., Li, X., 2010. The Influence of Calcium and Iron Supplementation on the Methane Yield of Biogas Treating Dairy Manure. Energy Sources Part Recovery Util. Environ. Eff. 32, 1651–1658. https://doi.org/10.1080/15567030902842269

Larragoiti-Kuri, J., Rivera-Toledo, M., Cocho-Roldán, J., Maldonado-Ruiz Esparza, K., Le Borgne, S., Pedraza-Segura, L., 2017. Convenient Product Distribution for a Lignocellulosic Biorefinery: Optimization through Sustainable Indexes. Ind. Eng. Chem. Res. 56, 11388–11397. https://doi.org/10.1021/acs.iecr.7b02101

Lay, J.-J., Lee, Y.-J., Noike, T., 1999. Feasibility of biological hydrogen production from organic fraction of municipal solid waste. Water Res. 33, 2579–2586. https://doi.org/10.1016/S0043-1354(98)00483-7

Lee, B., Lee, H., Lim, D., Brigljević, B., Cho, W., Cho, H.-S., Kim, C.-H., Lim, H., 2020. Renewable methanol synthesis from renewable H2 and captured CO2: How can power-to-liquid technology be economically feasible? Appl. Energy 279, 115827. https://doi.org/10.1016/j.apenergy.2020.115827

Li, D., Lee, I., Kim, H., 2021. Application of the linearized ADM1 (LADM) to lab-scale anaerobic digestion system. J. Environ. Chem. Eng. 9, 105193. https://doi.org/10.1016/j.jece.2021.105193

Li, D., Liu, S., Mi, L., Li, Z., Yuan, Y., Yan, Z., Liu, X., 2015. Effects of feedstock ratio and organic loading rate on the anaerobic mesophilic co-digestion of rice straw and pig manure. Bioresour. Technol. 187, 120–127. https://doi.org/10.1016/j.biortech.2015.03.040

Li, G., Wang, S., Zhao, J., Qi, H., Ma, Z., Cui, P., Zhu, Z., Gao, J., Wang, Y., 2020. Life cycle assessment and techno-economic analysis of biomass-to-hydrogen production with methane tri-reforming. Energy 199, 117488. https://doi.org/10.1016/j.energy.2020.117488

Li, H., Chen, Z., Fu, D., Wang, Y., Zheng, Y., Li, Q., 2020. Improved ADM1 for modelling C, N, P fates in anaerobic digestion process of pig manure and optimization approaches to biogas production. Renew. Energy 146, 2330–2336. https://doi.org/10.1016/j.renene.2019.08.086

Li, Y., Jin, Y., Borrion, A., Li, J., 2018. Influence of feed/inoculum ratios and waste cooking oil content on the mesophilic anaerobic digestion of food waste. Waste Manag. 73, 156–164. https://doi.org/10.1016/j.wasman.2017.12.027

Li, Y., Qi, C., Zhang, Y., Li, Yanming, Wang, Y., Li, G., Luo, W., 2021. Anaerobic digestion of agricultural wastes from liquid to solid state: Performance and environ-economic comparison. Bioresour. Technol. 332, 125080. https://doi.org/10.1016/j.biortech.2021.125080

Liu, S., Abrahamson, L.P., Scott, G.M., 2012. Biorefinery: Ensuring biomass as a sustainable renewable source of chemicals, materials, and energy. Biomass Bioenergy, Biorefinery 39, 1–4. https://doi.org/10.1016/j.biombioe.2010.12.042

Liu, X., Gao, X., Wang, W., Zheng, L., Zhou, Y., Sun, Y., 2012. Pilot-scale anaerobic co-digestion of municipal biomass waste: Focusing on biogas production and GHG reduction. Renew. Energy 44, 463–468. https://doi.org/10.1016/j.renene.2012.01.092

Logan, M., Ravishankar, H., Tan, L.C., Lawrence, J., Fitzgerald, D., Lens, P.N.L., 2021. Anaerobic digestion of dissolved air floatation slurries: Effect of substrate concentration and pH. Environ. Technol. Innov. 21, 101352. https://doi.org/10.1016/j.eti.2020.101352

López, D.E.B., 2013. Guía ambiental para el cultivo de cacao 127.

Lora, E.E.S., Nascimento, M.A.R., 2004. .. Thermoelectric generation: Planning, Project and Operation 19–40.

Łukajtis, R., Hołowacz, I., Kucharska, K., Glinka, M., Rybarczyk, P., Przyjazny, A., Kamiński, M., 2018. Hydrogen production from biomass using dark fermentation. Renew. Sustain. Energy Rev. 91, 665–694. https://doi.org/10.1016/j.rser.2018.04.043

Lundgren, J., Ekbom, T., Hulteberg, C., Larsson, M., Grip, C.-E., Nilsson, L., Tunå, P., 2013. Methanol production from steel-work off-gases and biomass based synthesis gas. Appl. Energy 112, 431–439. https://doi.org/10.1016/j.apenergy.2013.03.010

Luongo Malave', A.C., Bernardi, M., Fino, D., Ruggeri, B., 2015. Multistep anaerobic digestion (MAD) as a tool to increase energy production via H2 + CH4. Int. J. Hydrog. Energy 40, 5050–5061. https://doi.org/10.1016/j.ijhydene.2015.02.068

Ma, H., Guo, Y., Qin, Y., Li, Y.-Y., 2018. Nutrient recovery technologies integrated with energy recovery by waste biomass anaerobic digestion. Bioresour. Technol. 269, 520–531. https://doi.org/10.1016/j.biortech.2018.08.114

Madeira, J.G.F., Boloy, R.A.M., Delgado, A.R.S., Lima, F.R., Coutinho, E.R., Pereira Filho, R. de C., 2017a. Ecological analysis of hydrogen production via biogas steam reforming from cassava flour processing wastewater. J. Clean. Prod. 162, 709–716. https://doi.org/10.1016/j.jclepro.2017.06.076

Madeira, J.G.F., Delgado, A.R.S., Boloy, R.A.M., Coutinho, E.R., Loures, C.C.A., 2017b. Exergetic and economic evaluation of incorporation of hydrogen production in a cassava wastewater plant. Appl. Therm. Eng. 123, 1072–1078. https://doi.org/10.1016/j.applthermaleng.2017.05.153

Madeira, J.G.F., Oliveira, E.M., Springer, M.V., Cabral, H.L., Barbeito, D.F. do C., Souza, A.P.G., Moura, D.A. da S., Delgado, A.R.S., 2021. Hydrogen production from swine manure biogas via steam reforming of methane (SRM) and water gas shift (WGS): A ecological, technical, and economic analysis. Int. J. Hydrog. Energy 46, 8961–8971. https://doi.org/10.1016/j.ijhydene.2021.01.015

Mairet, F., Bernard, O., Ras, M., Lardon, L., Steyer, J.-P., 2011. Modeling anaerobic digestion of microalgae using ADM1. Bioresour. Technol. 102, 6823–6829. https://doi.org/10.1016/j.biortech.2011.04.015

Manish, S., Banerjee, R., 2008. Comparison of biohydrogen production processes. Int. J. Hydrog. Energy, IWHE 2006 33, 279–286. https://doi.org/10.1016/j.ijhydene.2007.07.026

Martínez, R., Torres, P., Meneses, M.A., Figueroa, J.G., Pérez-Álvarez, J.A., Viuda-Martos, M., 2012. Chemical, technological and in vitro antioxidant properties of cocoa

(Theobroma cacao L.) co-products. Food Res. Int. 49, 39–45. https://doi.org/10.1016/j.foodres.2012.08.005
Masoudi Soltani, S., Lahiri, A., Bahzad, H., Clough, P., Gorbounov, M., Yan, Y., 2021. Sorption-enhanced Steam Methane Reforming for Combined CO2 Capture and Hydrogen Production: A State-of-the-Art Review. Carbon Capture Sci. Technol. 1, 100003. https://doi.org/10.1016/j.ccst.2021.100003
Meegoda, J.N., Li, B., Patel, K., Wang, L.B., 2018. A Review of the Processes, Parameters, and Optimization of Anaerobic Digestion. Int. J. Environ. Res. Public. Health 15. https://doi.org/10.3390/ijerph15102224
Mendieta, O., Castro, L., Rodríguez, J., Escalante, H., 2020. Synergistic effect of sugarcane scum as an accelerant co-substrate on anaerobic co-digestion with agricultural crop residues from non-centrifugal cane sugar agribusiness sector. Bioresour. Technol. 303, 122957. https://doi.org/10.1016/j.biortech.2020.122957
Meng, Y., Luan, F., Yuan, H., Chen, X., Li, X., 2017. Enhancing anaerobic digestion performance of crude lipid in food waste by enzymatic pretreatment. Bioresour. Technol. 224, 48–55. https://doi.org/10.1016/j.biortech.2016.10.052
MinMinas - COL, 2021. Ministerio de Minas y Energía - MinMinas GM [WWW Document]. URL https://www.minenergia.gov.co/inicio (accessed 6.18.21).
Möller, K., Müller, T., 2012. Effects of anaerobic digestion on digestate nutrient availability and crop growth: A review. Eng. Life Sci. 12, 242–257. https://doi.org/10.1002/elsc.201100085
Moncada B., J., Aristizábal M., V., Cardona A., C.A., 2016. Design strategies for sustainable biorefineries. Biochem. Eng. J., Advances on Biorefinery Engineering and Food Supply Chain Waste Valorisation 116, 122–134. https://doi.org/10.1016/j.bej.2016.06.009
Moncada, J., El-Halwagi, M.M., Cardona, C.A., 2013. Techno-economic analysis for a sugarcane biorefinery: Colombian case. Bioresour. Technol. 135, 533–543. https://doi.org/10.1016/j.biortech.2012.08.137
Morais, A.R.C., da Costa Lopes, A.M., Bogel-Łukasik, R., 2015. Carbon Dioxide in Biomass Processing: Contributions to the Green Biorefinery Concept. Chem. Rev. 115, 3–27. https://doi.org/10.1021/cr500330z
Mortensen, P.M., Dybkjær, I., 2015. Industrial scale experience on steam reforming of CO2-rich gas. Appl. Catal. Gen. 495, 141–151. https://doi.org/10.1016/j.apcata.2015.02.022
Mosquera, J., Varela, L., Santis, A., Villamizar, S., Acevedo, P., Cabeza, I., 2020. Improving anaerobic co-digestion of different residual biomass sources readily available in Colombia by process parameters optimization. Biomass Bioenergy 142, 105790. https://doi.org/10.1016/j.biombioe.2020.105790
Motazedi, K., Salkuyeh, Y.K., Laurenzi, I.J., MacLean, H.L., Bergerson, J.A., 2021. Economic and environmental competitiveness of high temperature electrolysis for hydrogen production. Int. J. Hydrog. Energy 46, 21274–21288. https://doi.org/10.1016/j.ijhydene.2021.03.226
Munir, M.T., Mansouri, S.S., Udugama, I.A., Baroutian, S., Gernaey, K.V., Young, B.R., 2018. Resource recovery from organic solid waste using hydrothermal processing: Opportunities and challenges. Renew. Sustain. Energy Rev. 96, 64–75. https://doi.org/10.1016/j.rser.2018.07.039
Myint, M., Nirmalakhandan, N., Speece, R.E., 2007. Anaerobic fermentation of cattle manure: modeling of hydrolysis and acidogenesis. Water Res. 41, 323–332. https://doi.org/10.1016/j.watres.2006.10.026
Nami, H., Ranjbar, F., Yari, M., 2019. Methanol synthesis from renewable H2 and captured CO2 from S-Graz cycle – Energy, exergy, exergoeconomic and exergoenvironmental (4E) analysis. Int. J. Hydrog. Energy 44, 26128–26147. https://doi.org/10.1016/j.ijhydene.2019.08.079

Nassirpour, M., Khademi, M.H., 2020. Evaluation of different cooling technologies for industrial methanol synthesis reactor in terms of energy efficiency and methanol yield: An economic-optimization. J. Taiwan Inst. Chem. Eng. 113, 302–314. https://doi.org/10.1016/j.jtice.2020.08.029

National Institute for Public Health and the Environment, 2021. LCIA: the ReCiPe model | RIVM [WWW Document]. URL https://www.rivm.nl/en/life-cycle-assessment-lca/recipe (accessed 6.21.21).

Neshat, S.A., Mohammadi, M., Najafpour, G.D., Lahijani, P., 2017. Anaerobic co-digestion of animal manures and lignocellulosic residues as a potent approach for sustainable biogas production. Renew. Sustain. Energy Rev. 79, 308–322. https://doi.org/10.1016/j.rser.2017.05.137

Neu, A.-K., Pleissner, D., Mehlmann, K., Schneider, R., Puerta-Quintero, G.I., Venus, J., 2016. Fermentative utilization of coffee mucilage using Bacillus coagulans and investigation of down-stream processing of fermentation broth for optically pure l(+)-lactic acid production. Bioresour. Technol. 211, 398–405. https://doi.org/10.1016/j.biortech.2016.03.122

NGO Committee on Education, 1987. Report of the World Commission on Environment and Development: Our Common Future [WWW Document]. URL http://www.un-documents.net/wced-ocf.htm (accessed 5.27.21).

Nigam, P.S., Singh, A., 2014. Cocoa and Coffee Fermentations, in: Batt, C.A., Tortorello, M.L. (Eds.), Encyclopedia of Food Microbiology (Second Edition). Academic Press, Oxford, pp. 485–492. https://doi.org/10.1016/B978-0-12-384730-0.00074-4

Niu, J., Guo, F., Ran, J., Qi, W., Yang, Z., 2020. Methane dry (CO2) reforming to syngas (H2/CO) in catalytic process: From experimental study and DFT calculations. Int. J. Hydrog. Energy 45, 30267–30287. https://doi.org/10.1016/j.ijhydene.2020.08.067

Noorain, R., Kindaichi, T., Ozaki, N., Aoi, Y., Ohashi, A., 2019. Biogas purification performance of new water scrubber packed with sponge carriers. J. Clean. Prod. 214, 103–111. https://doi.org/10.1016/j.jclepro.2018.12.209

O'Callaghan, K., 2016. Technologies for the utilisation of biogenic waste in the bioeconomy. Food Chem. 198, 2–11. https://doi.org/10.1016/j.foodchem.2015.11.030

Ochoa, C., Hernández, M.A., Bayona, O.L., Camargo, H.A., Cabeza, I.O., Candela, A.M., 2021. Phosphorus recovery by struvite from anaerobic co-digestion effluents during residual biomass treatment. Biomass Convers. Biorefinery 11, 261–274. https://doi.org/10.1007/s13399-020-01146-6

Ondze, F., Ferrasse, J.-H., Boutin, O., Ruiz, J.-C., Charton, F., 2018. Process simulation and energetic analysis of different supercritical water gasification systems for the valorisation of biomass. J. Supercrit. Fluids 133, 114–121. https://doi.org/10.1016/j.supflu.2017.10.002

Page, D.I., Hickey, K.L., Narula, R., Main, A.L., Grimberg, S.J., 2008. Modeling anaerobic digestion of dairy manure using the IWA Anaerobic Digestion Model no. 1 (ADM1). Water Sci. Technol. 58, 689–695. https://doi.org/10.2166/wst.2008.678

Palatsi, J., Illa, J., Prenafeta-Boldú, F.X., Laureni, M., Fernandez, B., Angelidaki, I., Flotats, X., 2010. Long-chain fatty acids inhibition and adaptation process in anaerobic thermophilic digestion: batch tests, microbial community structure and mathematical modelling. Bioresour. Technol. 101, 2243–2251. https://doi.org/10.1016/j.biortech.2009.11.069

Palmeros Parada, M., Osseweijer, P., Posada Duque, J.A., 2017. Sustainable biorefineries, an analysis of practices for incorporating sustainability in biorefinery design. Ind. Crops Prod., Challenges in Building a Sustainable Biobased Economy 106, 105–123. https://doi.org/10.1016/j.indcrop.2016.08.052

Parker, W.J., Wu, G.H., 2006. Modifying ADM1 to include formation and emission of odourants. Water Sci. Technol. J. Int. Assoc. Water Pollut. Res. 54, 111–117. https://doi.org/10.2166/wst.2006.532

Pastor-Poquet, V., Papirio, S., Steyer, J.-P., Trably, E., Escudié, R., Esposito, G., 2018. High-solids anaerobic digestion model for homogenized reactors. Water Res. 142, 501–511. https://doi.org/10.1016/j.watres.2018.06.016

Patterson, T., Esteves, S., Dinsdale, R., Guwy, A., 2011. An evaluation of the policy and techno-economic factors affecting the potential for biogas upgrading for transport fuel use in the UK. Energy Policy 39, 1806–1816. https://doi.org/10.1016/j.enpol.2011.01.017

Peiris, B.R.H., Rathnasiri, P.G., Johansen, J.E., Kuhn, A., Bakke, R., 2006. ADM1 simulations of hydrogen production. Water Sci. Technol. J. Int. Assoc. Water Pollut. Res. 53, 129–137. https://doi.org/10.2166/wst.2006.243

Penumathsa, B.K.V., Premier, G.C., Kyazze, G., Dinsdale, R., Guwy, A.J., Esteves, S., Rodríguez, J., 2008. ADM1 can be applied to continuous bio-hydrogen production using a variable stoichiometry approach. Water Res. 42, 4379–4385. https://doi.org/10.1016/j.watres.2008.07.030

Perera, K.R.J., Ketheesan, B., Arudchelvam, Y., Nirmalakhandan, N., 2012. Fermentative biohydrogen production II: Net energy gain from organic wastes. Int. J. Hydrog. Energy, 11th China Hydrogen Energy Conference 37, 167–178. https://doi.org/10.1016/j.ijhydene.2011.09.042

Phyllis2, 2020. Database for (treated) biomass, algae, feedstocks for biogas production and biochaECN Phyllis classification [WWW Document]. URL https://phyllis.nl/

Porté, H., Kougias, P.G., Alfaro, N., Treu, L., Campanaro, S., Angelidaki, I., 2019. Process performance and microbial community structure in thermophilic trickling biofilter reactors for biogas upgrading. Sci. Total Environ. 655, 529–538. https://doi.org/10.1016/j.scitotenv.2018.11.289

Posada, J.A., Patel, A.D., Roes, A., Blok, K., Faaij, A.P.C., Patel, M.K., 2013. Potential of bioethanol as a chemical building block for biorefineries: Preliminary sustainability assessment of 12 bioethanol-based products. Bioresour. Technol., Biorefineries 135, 490–499. https://doi.org/10.1016/j.biortech.2012.09.058

Postels, S., Abánades, A., von der Assen, N., Rathnam, R.K., Stückrad, S., Bardow, A., 2016. Life cycle assessment of hydrogen production by thermal cracking of methane based on liquid-metal technology. Int. J. Hydrog. Energy 41, 23204–23212. https://doi.org/10.1016/j.ijhydene.2016.09.167

Puerta-Quintero, G.I., Ríos-Arias, S., 2011. COMPOSICIÓN QUÍMICA DEL MUCÍLAGO DE CAFÉ, SEGÚN EL TIEMPO DE FERMENTACIÓN Y REFRIGERACIÓN 18.

Puig-Gamero, M., Argudo-Santamaria, J., Valverde, J.L., Sánchez, P., Sanchez-Silva, L., 2018. Three integrated process simulation using aspen plus®: Pine gasification, syngas cleaning and methanol synthesis. Energy Convers. Manag.

Puig-Gamero, M., Pio, D.T., Tarelho, L.A.C., Sánchez, P., Sanchez-Silva, L., 2021. Simulation of biomass gasification in bubbling fluidized bed reactor using aspen plus®. Energy Convers. Manag. 235, 113981. https://doi.org/10.1016/j.enconman.2021.113981

Qi, C., Zhang, Y., Jia, S., Wang, R., Han, Y., Luo, W., Li, G., Li, Y., 2021. Effects of digestion duration on energy efficiency, compost quality, and carbon flow during solid state anaerobic digestion and composting hybrid process. Sci. Total Environ. 151363. https://doi.org/10.1016/j.scitotenv.2021.151363

Qu, J., Sun, Y., Awasthi, M.K., Liu, Y., Xu, X., Meng, X., Zhang, H., 2021. Effect of different aerobic hydrolysis time on the anaerobic digestion characteristics and energy consumption analysis. Bioresour. Technol. 320, 124332. https://doi.org/10.1016/j.biortech.2020.124332

Rajendran, K., Kankanala, H.R., Lundin, M., Taherzadeh, M.J., 2014. A novel process simulation model (PSM) for anaerobic digestion using Aspen Plus. Bioresour. Technol. 168, 7–13. https://doi.org/10.1016/j.biortech.2014.01.051

Rajesh Banu, J., Kavitha, S., Yukesh Kannah, R., Bhosale, R.R., Kumar, G., 2020a. Industrial wastewater to biohydrogen: Possibilities towards successful biorefinery route. Bioresour. Technol. 298, 122378. https://doi.org/10.1016/j.biortech.2019.122378

Rajesh Banu, J., Kavitha, S., Yukesh Kannah, R., Dinesh Kumar, M., Preethi, Atabani, A.E., Kumar, G., 2020b. Biorefinery of spent coffee grounds waste: Viable pathway towards circular bioeconomy. Bioresour. Technol. 302, 122821. https://doi.org/10.1016/j.biortech.2020.122821

Rakmak, Nirattisai & Noynoo, Laddawan & Jijai, Sunwanee & Siripatana, Chairat. (2019). Monod-Type Two-Substrate Models for Batch Anaerobic Co-Digestion.

Ramirez, I., Mottet, A., Carrère, H., Déléris, S., Vedrenne, F., Steyer, J.-P., 2009. Modified ADM1 disintegration/hydrolysis structures for modeling batch thermophilic anaerobic digestion of thermally pretreated waste activated sludge. Water Res. 43, 3479–3492. https://doi.org/10.1016/j.watres.2009.05.023

Rangel, C.J., Hernández, M.A., Mosquera, J.D., Castro, Y., Cabeza, I.O., Acevedo, P.A., 2021. Hydrogen production by dark fermentation process from pig manure, cocoa mucilage, and coffee mucilage. Biomass Convers. Biorefinery 11, 241–250. https://doi.org/10.1007/s13399-020-00618-z

Renó, M.L.G., Lora, E.E.S., Palacio, J.C.E., Venturini, O.J., Buchgeister, J., Almazan, O., 2011. A LCA (life cycle assessment) of the methanol production from sugarcane bagasse. Energy, ECOS 2009 36, 3716–3726. https://doi.org/10.1016/j.energy.2010.12.010

Rezaei, E., Dzuryk, S., 2019. Techno-economic comparison of reverse water gas shift reaction to steam and dry methane reforming reactions for syngas production. Chem. Eng. Res. Des. 144, 354–369. https://doi.org/10.1016/j.cherd.2019.02.005

Rivero, M., Solera, R., Perez, M., 2014. Anaerobic mesophilic co-digestion of sewage sludge with glycerol: Enhanced biohydrogen production. Int. J. Hydrog. Energy 39, 2481–2488. https://doi.org/10.1016/j.ijhydene.2013.12.006

Rodríguez, J., Lema, J.M., van Loosdrecht, M.C.M., Kleerebezem, R., 2006. Variable stoichiometry with thermodynamic control in ADM1. Water Sci. Technol. J. Int. Assoc. Water Pollut. Res. 54, 101–110. https://doi.org/10.2166/wst.2006.531

Bouaita, Rokaya & Kerroum, Derbal & Panico, Antonio & Floriana, Iasimone & Pontoni, Ludovico & Fabbricino, Massimiliano & Pirozzi, Francesco. (2022). Methane production from anaerobic co-digestion of orange peel waste and organic fraction of municipal solid waste in batch and semi-continuous reactors. Biomass and Bioenergy. 160. 106421. 10.1016/j.biombioe.2022.106421.

Ruiz, H.A., Galbe, M., Garrote, G., Ramirez-Gutierrez, D.M., Ximenes, E., Sun, S.-N., Lachos-Perez, D., Rodríguez-Jasso, R.M., Sun, R.-C., Yang, B., Ladisch, M.R., 2021. Severity factor kinetic model as a strategic parameter of hydrothermal processing (steam explosion and liquid hot water) for biomass fractionation under biorefinery concept. Bioresour. Technol. 342, 125961. https://doi.org/10.1016/j.biortech.2021.125961

Saady, N.M.C., 2013. Homoacetogenesis during hydrogen production by mixed cultures dark fermentation: Unresolved challenge. Int. J. Hydrog. Energy 38, 13172–13191. https://doi.org/10.1016/j.ijhydene.2013.07.122

Santamaría-Fernández, M., Molinuevo-Salces, B., Lübeck, M., Uellendahl, H., 2017. Biogas potential of green biomass after protein extraction in an organic biorefinery concept for feed, fuel and fertilizer production. Renew. Energy. https://doi.org/10.1016/j.renene.2017.03.012

Santibañez-Aguilar, J.E., Morales-Rodriguez, R., González-Campos, J.B., Ponce-Ortega, J.M., 2016. Stochastic design of biorefinery supply chains considering economic and environmental objectives. J. Clean. Prod., PRES'15: Cleaner energy planning,

management and technologies 136, 224–245. https://doi.org/10.1016/j.jclepro.2016.03.168
Sawatdeenarunat, C., Nguyen, D., Surendra, K.C., Shrestha, S., Rajendran, K., Oechsner, H., Xie, L., Khanal, S.K., 2016. Anaerobic biorefinery: Current status, challenges, and opportunities. Bioresour. Technol. 215, 304–313. https://doi.org/10.1016/j.biortech.2016.03.074
Seider, W.D., Seader, J.D., Lewin, D.R., Widagdo, S., 2008. Product and Process Design Principles: Synthesis, Analysis and Design.
Sekoai, P.T., Ghimire, A., Ezeokoli, O.T., Rao, S., Ngan, W.Y., Habimana, O., Yao, Y., Yang, P., Yiu Fung, A.H., Yoro, K.O., Daramola, M.O., Hung, C.-H., 2021. Valorization of volatile fatty acids from the dark fermentation waste Streams-A promising pathway for a biorefinery concept. Renew. Sustain. Energy Rev. 143, 110971. https://doi.org/10.1016/j.rser.2021.110971
Şenol, H., 2019. Biogas potential of hazelnut shells and hazelnut wastes in Giresun City. Biotechnol. Rep. 24, e00361. https://doi.org/10.1016/j.btre.2019.e00361
Seo, M.W., Lee, S.H., Nam, H., Lee, D., Tokmurzin, D., Wang, S., Park, Y.-K., 2022. Recent advances of thermochemical conversion processes for biorefinery. Bioresour. Technol. 343, 126109. https://doi.org/10.1016/j.biortech.2021.126109
Serrano, R.P., 2010. Biogas Process Simulation using Aspen Plus.
Sharma, D., Espinosa-Solares, T., Huber, D.H., 2013. Thermophilic anaerobic co-digestion of poultry litter and thin stillage. Bioresour. Technol. 136, 251–256. https://doi.org/10.1016/j.biortech.2013.03.005
Shen, X., Zeng, J., Zhang, D., Wang, F., Li, Y., Yi, W., 2020. Effect of pyrolysis temperature on characteristics, chemical speciation and environmental risk of Cr, Mn, Cu, and Zn in biochars derived from pig manure. Sci. Total Environ. 704, 135283. https://doi.org/10.1016/j.scitotenv.2019.135283
Shimada, T., Zilles, J., Raskin, L., Morgenroth, E., 2007. Carbohydrate storage in anaerobic sequencing batch reactors. Water Res. 41, 4721–4729. https://doi.org/10.1016/j.watres.2007.06.052
Shin, H.-S., Youn, J.-H., Kim, S.-H., 2004. Hydrogen production from food waste in anaerobic mesophilic and thermophilic acidogenesis. Int. J. Hydrog. Energy 29, 1355–1363. https://doi.org/10.1016/j.ijhydene.2003.09.011
Siegrist, H., Renggli, D., Gujer, W., 1993. Mathematical Modelling of Anaerobic Mesophilic Sewage Sludge Treatment. Water Sci. Technol. 27, 25–36. https://doi.org/10.2166/wst.1993.0070
Singhania, R.R., Patel, A.K., Christophe, G., Fontanille, P., Larroche, C., 2013. Biological upgrading of volatile fatty acids, key intermediates for the valorization of biowaste through dark anaerobic fermentation. Bioresour. Technol., Special Issue: IBS 2012 & Special Issue: IFIBiop 145, 166–174. https://doi.org/10.1016/j.biortech.2012.12.137
Smith, J.M., Ness, H.C.V., Abbott, M.M., 2007. Introduction to Chemical Engineering Thermodynamics, 7th Edition, 7th edition. ed. McGraw Hill Higher Education, Boston, Mass.
Soares, J.F., Confortin, T.C., Todero, I., Mayer, F.D., Mazutti, M.A., 2020. Dark fermentative biohydrogen production from lignocellulosic biomass: Technological challenges and future prospects. Renew. Sustain. Energy Rev. 117, 109484. https://doi.org/10.1016/j.rser.2019.109484
Sun, H., Yang, Z., Zhao, Q., Kurbonova, M., Zhang, R., Liu, G., Wang, W., 2021. Modification and extension of anaerobic digestion model No.1 (ADM1) for syngas biomethanation simulation: From lab-scale to pilot-scale. Chem. Eng. J. 403, 126177. https://doi.org/10.1016/j.cej.2020.126177
Surendra, K. c., Sawatdeenarunat, C., Shrestha, S., Sung, S., Khanal, S.K., 2015. Anaerobic Digestion-Based Biorefinery for Bioenergy and Biobased Products. Ind. Biotechnol. 11, 103–112. https://doi.org/10.1089/ind.2015.0001

Surra, E., Esteves, I.A.A.C., Lapa, N., 2021. Life cycle analysis of a biorefinery for activated carbon and biomethane production. Biomass Bioenergy 149, 106080. https://doi.org/10.1016/j.biombioe.2021.106080

Sy, C.L., Ubando, A.T., Aviso, K.B., Tan, R.R., 2018. Multi-objective target oriented robust optimization for the design of an integrated biorefinery. J. Clean. Prod. 170, 496–509. https://doi.org/10.1016/j.jclepro.2017.09.140

Taherzadeh, M.J., Karimi, K., 2008. Pretreatment of Lignocellulosic Wastes to Improve Ethanol and Biogas Production: A Review. Int. J. Mol. Sci. 9, 1621–1651. https://doi.org/10.3390/ijms9091621

Tan, Y.L., Abdullah, A.Z., Hameed, B.H., 2017. Fast pyrolysis of durian (Durio zibethinus L) shell in a drop-type fixed bed reactor: Pyrolysis behavior and product analyses. Bioresour. Technol. 243, 85–92. https://doi.org/10.1016/j.biortech.2017.06.015

Torres-Moreno, M., Torrescasana, E., Salas-Salvadó, J., Blanch, C., 2015. Nutritional composition and fatty acids profile in cocoa beans and chocolates with different geographical origin and processing conditions. Food Chem. 166, 125–132. https://doi.org/10.1016/j.foodchem.2014.05.141

Tugtas, A.E., Tezel, U., Pavlostathis, S.G., 2006. An extension of the Anaerobic Digestion Model No. 1 to include the effect of nitrate reduction processes. Water Sci. Technol. J. Int. Assoc. Water Pollut. Res. 54, 41–49. https://doi.org/10.2166/wst.2006.524

Uddin, M.N., Siddiki, S.Y.A., Mofijur, M., Djavanroodi, F., Hazrat, M.A., Show, P.L., Ahmed, S.F., Chu, Y.-M., 2021. Prospects of Bioenergy Production From Organic Waste Using Anaerobic Digestion Technology: A Mini Review. Front. Energy Res. 9. https://doi.org/10.3389/fenrg.2021.627093

Ullah Khan, I., Hafiz Dzarfan Othman, M., Hashim, H., Matsuura, T., Ismail, A.F., Rezaei-DashtArzhandi, M., Wan Azelee, I., 2017. Biogas as a renewable energy fuel – A review of biogas upgrading, utilisation and storage. Energy Convers. Manag. 150, 277–294. https://doi.org/10.1016/j.enconman.2017.08.035

UPME [WWW Document], 2020. URL https://www1.upme.gov.co/Paginas/default.aspx (accessed 8.19.21).

Valderrama, A., 2013. Biodegradación de residuos sólidos agropecuarios y uso de bioabono como acondicionador del suelo (Thesis).

Valdez-Vazquez, I., Ríos-Leal, E., Esparza-García, F., Cecchi, F., Poggi-Varaldo, H.M., 2005. Semi-continuous solid substrate anaerobic reactors for H2 production from organic waste: Mesophilic versus thermophilic regime. Int. J. Hydrog. Energy 30, 1383–1391. https://doi.org/10.1016/j.ijhydene.2004.09.016

Valente, A., Iribarren, D., Dufour, J., 2021. Comparative life cycle sustainability assessment of renewable and conventional hydrogen. Sci. Total Environ. 756, 144132. https://doi.org/10.1016/j.scitotenv.2020.144132

Varjani, S., Shah, A.V., Vyas, S., Srivastava, V.K., 2021. Processes and prospects on valorizing solid waste for the production of valuable products employing bio-routes: A systematic review. Chemosphere 282, 130954. https://doi.org/10.1016/j.chemosphere.2021.130954

Vavilin, V.A., Vasiliev, V.B., Ponomarev, A.V., Rytow, S.V., 1994. Simulation model 'methane' as a tool for effective biogas production during anaerobic conversion of complex organic matter. Bioresour. Technol. 48, 1–8. https://doi.org/10.1016/0960-8524(94)90126-0

Wang, W., Lee, D.-J., 2021. Valorization of anaerobic digestion digestate: A prospect review. Bioresour. Technol. 323, 124626. https://doi.org/10.1016/j.biortech.2020.124626

Wang, Y., Li, G., Chi, M., Sun, Y., Zhang, J., Jiang, S., Cui, Z., 2018. Effects of co-digestion of cucumber residues to corn stover and pig manure ratio on methane production in solid state anaerobic digestion. Bioresour. Technol. 250, 328–336. https://doi.org/10.1016/j.biortech.2017.11.055

Weinrich, S., Nelles, M., 2021. Systematic simplification of the Anaerobic Digestion Model No. 1 (ADM1) – Model development and stoichiometric analysis. Bioresour. Technol. 333, 125124. https://doi.org/10.1016/j.biortech.2021.125124

Wett, B., Eladawy, A., Ogurek, M., 2006. Description of nitrogen incorporation and release in ADM1. Water Sci. Technol. J. Int. Assoc. Water Pollut. Res. 54, 67–76. https://doi.org/10.2166/wst.2006.527

Willquist, K., Nkemka, V.N., Svensson, H., Pawar, S., Ljunggren, M., Karlsson, H., Murto, M., Hulteberg, C., van Niel, E.W.J., Liden, G., 2012. Design of a novel biohythane process with high H2 and CH4 production rates. Int. J. Hydrog. Energy 37, 17749–17762. https://doi.org/10.1016/j.ijhydene.2012.08.092

Wu, Q., Wang, H., Zheng, X., Liu, F., Wang, A., Zou, D., Yuan, J., Xiao, Z., 2020. Thermochemical liquefaction of pig manure: Factors influencing on oil. Fuel 264, 116884. https://doi.org/10.1016/j.fuel.2019.116884

Wu, W., Pai, C.-T., Viswanathan, K., Chang, J.-S., 2021. Comparative life cycle assessment and economic analysis of methanol/hydrogen production processes for fuel cell vehicles. J. Clean. Prod. 300, 126959. https://doi.org/10.1016/j.jclepro.2021.126959

Xie, S., Hai, F.I., Zhan, X., Guo, W., Ngo, H.H., Price, W.E., Nghiem, L.D., 2016. Anaerobic co-digestion: A critical review of mathematical modelling for performance optimization. Bioresour. Technol. 222, 498–512. https://doi.org/10.1016/j.biortech.2016.10.015

Yasui, H., Goel, R., Li, Y.Y., Noike, T., 2008. Modified ADM1 structure for modelling municipal primary sludge hydrolysis. Water Res. 42, 249–259. https://doi.org/10.1016/j.watres.2007.07.004

Ye, J., Li, D., Sun, Y., Wang, G., Yuan, Z., Zhen, F., Wang, Y., 2013. Improved biogas production from rice straw by co-digestion with kitchen waste and pig manure. Waste Manag. 33, 2653–2658. https://doi.org/10.1016/j.wasman.2013.05.014

Yoneyama, F., Yamamoto, M., Hashimoto, W., Murata, K., 2015. Production of polyhydroxybutyrate and alginate from glycerol by Azotobacter vinelandii under nitrogen-free conditions. Bioengineered 6, 209–217. https://doi.org/10.1080/21655979.2015.1040209

Yue, L., Cheng, J., Hua, J., Dong, H., Zhou, J., Li, Y.-Y., 2020. Improving fermentative methane production of glycerol trioleate and food waste pretreated with ozone through two-stage dark hydrogen fermentation and anaerobic digestion. Energy Convers. Manag. 203, 112225. https://doi.org/10.1016/j.enconman.2019.112225

Zaher, U., Li, R., Jeppsson, U., Steyer, J.-P., Chen, S., 2009. GISCOD: General Integrated Solid Waste Co-Digestion model. Water Res. 43, 2717–2727. https://doi.org/10.1016/j.watres.2009.03.018

Zhang, C., Su, H., Baeyens, J., Tan, T., 2014. Reviewing the anaerobic digestion of food waste for biogas production. Renew. Sustain. Energy Rev. 38, 383–392. https://doi.org/10.1016/j.rser.2014.05.038

Zhang, Q., Zeng, L., Fu, X., Pan, F., Shi, X., Wang, T., 2021. Comparison of anaerobic co-digestion of pig manure and sludge at different mixing ratios at thermophilic and mesophilic temperatures. Bioresour. Technol. 337, 125425. https://doi.org/10.1016/j.biortech.2021.125425

Zhang, R., El-Mashad, H.M., Hartman, K., Wang, F., Liu, G., Choate, C., Gamble, P., 2007. Characterization of food waste as feedstock for anaerobic digestion. Bioresour. Technol. 98, 929–935. https://doi.org/10.1016/j.biortech.2006.02.039

Zhang, T., He, X., Deng, Y., Tsang, D.C.W., Jiang, R., Becker, G.C., Kruse, A., 2020. Phosphorus recovered from digestate by hydrothermal processes with struvite crystallization and its potential as a fertilizer. Sci. Total Environ. 698, 134240. https://doi.org/10.1016/j.scitotenv.2019.134240

Zhang, Y., Piccard, S., Zhou, W., 2015. Improved ADM1 model for anaerobic digestion process considering physico-chemical reactions. Bioresour. Technol. 196, 279–289. https://doi.org/10.1016/j.biortech.2015.07.065

Zhao, X., Joseph, B., Kuhn, J., Ozcan, S., 2020. Biogas Reforming to Syngas: A Review. iScience 23, 101082. https://doi.org/10.1016/j.isci.2020.101082

Zheng, Z., Cai, Y., Zhang, Y., Zhao, Y., Gao, Y., Cui, Z., Hu, Y., Wang, X., 2021. The effects of C/N (10–25) on the relationship of substrates, metabolites, and microorganisms in “inhibited steady-state” of anaerobic digestion. Water Res. 188, 116466. https://doi.org/10.1016/j.watres.2020.116466

Zhou, X., Lu, Y., Huang, L., Zhang, Q., Wang, X., Zhu, J., 2021. Effect of pH on volatile fatty acid production and the microbial community during anaerobic digestion of Chinese cabbage waste. Bioresour. Technol. 336, 125338. https://doi.org/10.1016/j.biortech.2021.125338

Zhu, H., Parker, W., Basnar, R., Proracki, A., Falletta, P., Béland, M., Seto, P., 2008. Biohydrogen production by anaerobic co-digestion of municipal food waste and sewage sludges. Int. J. Hydrog. Energy, TMS07: Symposium on Materials in Clean Power Systems 33, 3651–3659. https://doi.org/10.1016/j.ijhydene.2008.04.040

.

ANNEXES

I. UNTREATED EXPERIMENTAL RESULTS

Table 32 Methane production in the anaerobic digestion process and hydrogen production in the dark fermentation, in the experimental step.

AD			DF								
Blend	Total methane production (ml)	Days (d)	Blend	Total hydrogen production (ml)	Days (d)	Blend	Total hydrogen production (ml)	Days (d)	Blend	Total hydrogen production (ml)	Days (d)
M1	333.20	15	**C1**	94.5	9	**C6**	79.00	8	**C10**	214.00	8
M1	227.00	16	**C1**	84.00	7	**C6**	101.50	8	**C10**	187.00	7
M1	201.50	10	**C1**	112.00	6	**C6**	74.00	7	**C10**	211.00	8
M2	178.50	17	**C1**	118.50	6	**C6**	102.00	6	**C10**	287.00	8
M2	229.00	14	**C1**	84.50	6	**C6**	87.00	6	**C10**	191.00	7
M2	388.50	17	**C1**	143.00	8	**C6**	91.33	6	**C10**	265.00	8
M3	753.00	16	**C1**	96.00	6	**C6**	174.00	10	**C10**	230.00	9
M3	783.50	17	**C1**	82.00	7	**C6**	98.00	10	**C11**	168.00	8
M3	839.00	17	**C1**	121.50	9	**C6**	151.00	8	**C11**	61.50	7
M4	604.00	16	**C1**	145.60	9	**C6**	174.90	10	**C11**	62.00	7
M4	444.50	14	**C2**	91.50	8	**C6**	81.00	9	**C11**	117.00	6
M4	834.00	17	**C2**	115.50	10	**C6**	50.00	10	**C11**	126.50	6
M5	264.00	16	**C2**	96.00	10	**C6**	61.00	11	**C11**	75.50	6
M5	308.00	18	**C2**	61.00	5	**C6**	36.00	8	**C11**	93.00	7
M5	535.00	18	**C2**	91.00	6	**C7**	66.00	8	**C11**	163.00	6
M6	510.00	17	**C2**	82.67	6	**C7**	76.00	8	**C11**	101.00	6
M6	525.00	18	**C2**	204.00	8	**C7**	138.00	6	**C11**	75.20	9
M6	398.00	18	**C2**	82.00	6	**C7**	93.50	6	**C11**	85.30	11
M6	296.00	12	**C2**	138.00	8	**C7**	132.00	7	**C12**	327.00	8
M6	169.00	12	**C2**	117.65	8	**C7**	104.75	10	**C12**	200.00	6
M7	379.00	17	**C2**	114.35	8	**C7**	73.25	10	**C12**	236.00	7
M7	345.00	16	**C3**	247.00	8	**C7**	68.00	9	**C12**	329.00	8
M7	498.00	17	**C3**	331.00	10	**C7**	149.00	10	**C12**	241.00	9
M8	417.00	17	**C3**	296.00	10	**C8**	83.50	9	**C12**	168.50	8
M8	431.00	11	**C3**	302.00	11	**C8**	74.00	6	**C12**	228.00	9
M8	429.00	17	**C3**	220.00	11	**C8**	105.00	8	**C12**	132.80	9
M8	374.00	12	**C3**	307.20	12	**C8**	63.00	6	**C12**	250.30	11
M8	274.00	12	**C4**	158.00	8	**C8**	70.00	6	**C13**	185.00	8
M9	220.00	16	**C4**	109.67	8	**C8**	53.00	5	**C13**	84.00	7
M9	146.00	14	**C4**	121.00	6	**C8**	96.00	6	**C13**	105.50	6
M9	160.00	12	**C4**	218.00	10	**C8**	52.00	6	**C13**	218.00	9
M10	561.00	15	**C4**	147.00	10	**C8**	66.60	7	**C13**	221.50	10
M10	708.00	17	**C4**	229.00	9	**C8**	94.85	9	**C13**	177.50	9
M10	819.00	14	**C4**	244.13	11	**C8**	101.80	8	**C13**	109.50	11
M11	125.40	17	**C4**	215.80	9	**C8**	112.00	10	**C13**	99.30	10
M11	122.00	16	**C5**	62.25	7	**C8**	159.00	8	**C13**	211.00	9

M11	203.00	17	**C5**	55.25	8	**C8**	48.00	10	**C13**	168.00	10
M12	351.00	15	**C5**	78.00	10	**C9**	64.25	8	**C13**	70.00	9
M12	753.00	17	**C5**	73.00	10	**C9**	63.00	6	**C14**	179.00	8
M12	577.00	16	**C5**	119.75	10	**C9**	78.00	6	**C14**	174.00	8
M13	278.00	14	**C5**	146.50	9	**C9**	71.50	10	**C14**	232.00	8
M13	306.00	19	**C5**	72.00	9	**C9**	90.00	10	**C14**	201.00	11
M13	286.00	14	**C5**	60.30	9	**C9**	71.00	10	**C14**	203.00	10
M13	208.00	12				**C9**	72.60	10	**C14**	196.55	12
M13	209.00	12				**C9**	74.20	11	**C14**	193.00	12
M14	324.00	20							**C15**	238.00	10
M14	196.00	16							**C15**	185.00	10
M14	293.00	19							**C15**	105.50	9
M15	391.00	20							**C15**	221.50	11
M15	278.00	18									
M15	335.00	19									

II. UNTREATED SIMULATION STREAMS RESULTS

Table 33 Input values of initial load (biomass) for sensitivity analysis in five representative departments of Colombia.

	ton COD/yr			kg/d	MJ/kg	MJ/d
	Cocoa mucilage	Coffee mucilage	Swine manure	Dry biomass input	LHV Biomass	Biomass energy
Antioquia	325.875	2,184.506	150,381.585	338,812.787	33.028	11,190,175.261
Boyacá	208.663	70.846	15,621.900	35,248.881	33.025	1,164,109.799
Cundinamarca	64.436	165.352	42,063.459	93,526.544	33.222	3,107,096.924
Meta	108.736	2.062	19,365.545	43,072.703	33.224	1,431,040.094
Santander	1,527.908	605.367	8,032.940	23,385.140	29.842	697,854.946

Table 34 Calculation of biogas, residue and total energy yield for the ADF process as a function of the variation of the initial load concentration.

	g COD/L	MJ/d Heat process	kg/d Biogas (dry)	MJ/kg LHV Biogas	MJ/d Biogas energy	kg/d Residue (dry)	MJ/kg LHV Residue	MJ/d Residue energy	TOTAL INPUT	TOTAL OUTPUT	*n_gas*	*n_residue*	*n_total*	*Difference*
Antioquia	2	66670261.351	280872.998	19.983	5612638.724	130189.074	17.714	2306184.927	77,860,436.61	7,918,823.65	*7.21%*	*2.96%*	*10%*	
	5	26719523.402	281024.489	20.007	5622380.123	129960.935	17.710	2301597.490	37,909,698.66	7,923,977.61	*14.83%*	*6.07%*	*21%*	*10.7%*
	8	16709328.198	280874.581	20.024	5624309.233	129965.415	17.709	2301537.345	27,899,503.46	7,925,846.58	*20.16%*	*8.25%*	*28%*	*7.5%*
	11	12155344.714	280672.387	20.041	5624922.293	130010.686	17.708	2302251.274	23,345,519.98	7,927,173.57	*24.09%*	*9.86%*	*34%*	*5.5%*
	14	9570844.085	280377.167	20.056	5623183.442	130149.962	17.707	2304517.560	20,761,019.35	7,927,701.00	*27.09%*	*11.10%*	*38%*	*4.2%*
	17	7891848.481	280234.748	20.070	5624299.301	130155.061	17.707	2304629.702	19,082,023.74	7,928,929.00	*29.47%*	*12.08%*	*42%*	*3.4%*
	20	6714615.063	280153.383	20.070	5622673.023	130225.216	17.706	2305767.049	17,904,790.32	7,928,440.07	*31.40%*	*12.88%*	*44%*	*2.7%*
	23	5845912.468	280033.923	20.069	5619956.205	130338.303	17.705	2307591.485	17,036,087.73	7,927,547.69	*32.99%*	*13.55%*	*47%*	*2.3%*
	26	5177372.916	279995.391	20.069	5619233.409	130368.314	17.704	2308104.335	16,367,548.18	7,927,337.74	*34.33%*	*14.10%*	*48%*	*1.9%*
Boyacá	2	6934291.271	29206.190	19.989	583816.212	13556.530	17.698	239918.510	8,098,401.07	823,734.72	*7.21%*	*2.96%*	*10%*	
	5	2773743.433	29238.965	20.001	584808.868	13528.636	17.693	239368.891	3,937,853.23	824,177.76	*14.85%*	*6.08%*	*21%*	*10.8%*
	8	1735802.078	29232.492	20.007	584846.390	13531.378	17.692	239397.515	2,899,911.88	824,243.91	*20.17%*	*8.26%*	*28%*	*7.5%*
	11	1265789.339	29186.730	20.047	585092.189	13537.696	17.692	239503.884	2,429,899.14	824,596.07	*24.08%*	*9.86%*	*34%*	*5.5%*
	14	975907.593	29211.227	20.017	584723.896	13541.904	17.690	239561.733	2,140,017.39	824,285.63	*27.32%*	*11.19%*	*39%*	*4.6%*
	17	801714.646	29194.161	20.021	584495.570	13553.643	17.689	239751.576	1,965,824.44	824,247.15	*29.73%*	*12.20%*	*42%*	*3.4%*
	20	679822.718	29184.635	20.026	584457.650	13557.255	17.689	239812.028	1,843,932.52	824,269.68	*31.70%*	*13.01%*	*45%*	*2.8%*
	23	589790.064	29171.688	20.031	584329.416	13564.533	17.688	239931.818	1,753,899.86	824,261.23	*33.32%*	*13.68%*	*47%*	*2.3%*
	26	523435.388	29116.512	20.074	584498.618	13574.899	17.688	240112.372	1,687,545.19	824,610.99	*34.64%*	*14.23%*	*49%*	*1.9%*
Cundinamarca	2	18417529.142	77203.200	20.034	1546727.138	36323.488	17.705	643124.206	21,524,626.07	2,189,851.34	*7.19%*	*2.99%*	*10%*	
	5	7342577.995	77283.158	20.045	1549129.589	36258.382	17.701	641811.500	10,449,674.92	2,190,941.09	*14.82%*	*6.14%*	*21%*	*10.8%*
	8	4574457.116	77274.906	20.051	1549400.847	36258.029	17.700	641760.569	7,681,554.04	2,191,161.42	*20.17%*	*8.35%*	*29%*	*7.6%*
	11	3308730.383	77251.505	20.055	1549288.776	36269.769	17.699	641936.411	6,415,827.31	2,191,225.19	*24.15%*	*10.01%*	*34%*	*5.6%*
	14	2595068.133	77207.790	20.059	1548685.807	36301.057	17.697	642437.849	5,702,165.06	2,191,123.66	*27.16%*	*11.27%*	*38%*	*4.3%*
	17	2131731.154	77162.506	20.062	1548022.989	36333.882	17.696	642968.270	5,238,828.08	2,190,991.26	*29.55%*	*12.27%*	*42%*	*3.4%*
	20	1816662.906	77024.373	20.114	1549241.427	36335.913	17.697	643039.210	4,923,759.83	2,192,280.64	*31.46%*	*13.06%*	*45%*	*2.7%*
	23	1568055.087	77128.945	20.072	1548137.895	36338.319	17.696	643051.626	4,675,152.01	2,191,189.52	*33.11%*	*13.75%*	*47%*	*2.3%*
	26	1383889.069	77086.863	20.075	1547537.875	36367.499	17.695	643525.678	4,490,985.99	2,191,063.55	*34.46%*	*14.33%*	*49%*	*1.9%*
Meta	2	8493551.599	35546.450	20.037	712260.121	16736.702	17.699	296227.651	9,924,591.69	1,008,487.77	*7.18%*	*2.98%*	*10%*	
	5	3385681.236	35583.409	20.048	713368.912	16706.638	17.695	295621.530	4,816,721.33	1,008,990.44	*14.81%*	*6.14%*	*21%*	*10.8%*
	8	2103711.949	35579.624	20.053	713494.492	16706.461	17.694	295597.588	3,534,752.04	1,009,092.08	*20.19%*	*8.36%*	*29%*	*7.6%*
	11	1525626.809	35568.545	20.058	713440.721	16712.024	17.693	295681.240	2,956,666.90	1,009,121.96	*24.13%*	*10.00%*	*34%*	*5.6%*
	14	1195054.494	35548.813	20.062	713165.135	16726.255	17.691	295909.186	2,626,094.59	1,009,074.32	*27.16%*	*11.27%*	*38%*	*4.3%*
	17	981685.537	35527.989	20.065	712859.758	16741.367	17.690	296153.323	2,412,725.63	1,009,013.08	*29.55%*	*12.27%*	*42%*	*3.4%*
	20	832384.809	35524.446	20.071	712993.939	16737.948	17.690	296100.714	2,263,424.90	1,009,094.65	*31.50%*	*13.08%*	*45%*	*2.8%*
	23	722019.575	35504.593	20.074	712707.696	16751.928	17.689	296327.998	2,153,059.67	1,009,035.69	*33.10%*	*13.76%*	*47%*	*2.3%*
	26	637342.629	35484.489	20.077	712412.112	16766.153	17.688	296559.491	2,068,382.72	1,008,971.60	*34.44%*	*14.34%*	*49%*	*1.9%*

Continue...

	MJ/d	kg/d	MJ/kg	MJ/d	kg/d	MJ/kg	MJ/d

	g COD/L	Heat process	Biogas (dry)	LHV Biogas	Biogas energy	Residue (dry)	LHV Residue	Residue energy	TOTAL INPUT	TOTAL OUTPUT	n_gas	n_residue	n_total	Difference
Santander	2	4423970.56	23385.137	19.139	447577.388	7643.867	17.856	136486.151	5,121,825.51	584,063.54	8.74%	2.66%	11%	
	5	1764663.74	20564.755	19.331	397530.909	7553.681	17.635	133205.472	2,462,518.69	530,736.38	16.14 %	5.41%	22%	10.1%
	8	1104754.87	20477.545	19.450	398278.660	7557.359	17.635	133277.725	1,802,609.82	531,556.39	22.09 %	7.39%	29%	7.9%
	11	798462.085	20537.484	19.369	397796.792	7554.959	17.634	133220.891	1,496,317.03	531,017.68	26.59 %	8.90%	35%	6.0%
	14	626221.265	20516.276	19.386	397734.682	7562.969	17.632	133352.777	1,324,076.21	531,087.46	30.04 %	10.07%	40%	4.6%
	17	514854.600	20502.028	19.405	397842.170	7563.629	17.633	133368.024	1,212,709.55	531,210.19	32.81 %	11.00%	44%	3.7%
	20	436962.221	20484.904	19.423	397868.813	7567.502	17.633	133435.044	1,134,817.17	531,303.86	35.06 %	11.76%	47%	3.0%
	23	379522.118	20464.663	19.439	397808.189	7574.896	17.632	133558.717	1,077,377.06	531,366.91	36.92 %	12.40%	49%	2.5%
	26	335327.420	20444.512	19.455	397742.045	7582.409	17.631	133684.769	1,033,182.37	531,426.81	38.50 %	12.94%	51%	2.1%

III. RESULTS SUMMARY MODELS IN ASPEN PLUS

Table 35 Heaters results summary - models, biorefinery No. 1

Name	E101	E102
Property method	SRK	SRK
Henry's component list ID		
Electrolyte chemistry ID		
Use true species approach for electrolytes	YES	YES
Free-water phase properties method	STEAM-TA	STEAM-TA
Water solubility method	3	3
Specified pressure [Pa]	101325	101325
Specified temperature [C]	35	54
Specified vapor fraction		
Specified heat duty [Watt]		
EO Model components		
Calculated pressure [N/sqm]	101325	101325
Calculated temperature [K]	308.15	327.15
Calculated vapor fraction	3.49883E-05	1
Calculated heat duty [Watt]	669840.547	7277.13686
Temperature change [K]		
Degrees of superheating [K]		
Degrees of subcooling [K]		
Pressure-drop correlation parameter	2	
Net duty [Watt]	669840.547	7277.13686
First liquid / total liquid	1	
Total feed stream CO2e flow [kg/day]	0	176332.198
Total product stream CO2e flow [kg/day]	0	176332.198
Net stream CO2e production [kg/day]	0	0
Utility CO2e production [kg/day]	0	0
Total CO2e production [kg/day]	0	0
Utility usage		
Utility cost		
Utility ID		

Table 36 Separators results summary - models, biorefinery No. 1

Name	S1A	S1B	S101	S102	S103	S104
Property method	SRK	SRK	SRK	SRK	SRK	SRK
Henry's component list ID						
Electrolyte chemistry ID						
Use true species approach for electrolytes	YES	YES	YES	YES	YES	YES
Free-water phase properties method	STEAM-TA	IDEAL	STEAM-TA	STEAM-TA	STEAM-TA	STEAM-TA
Water solubility method	3	3	3	3	3	3
Inlet flash pressure [Pa]	101325	0	101325	30	30	30
First outlet flash temperature [C]	35	35		38	35	35

First outlet flash pressure [Pa]	101325			30		30
First outlet flash temperature change [K]						
First outlet flash vapor fraction						
First outlet flash temperature estimate [K]						
First outlet flash pressure estimate [N/sqm]					30	
Second outlet flash temperature [C]	35	35				
Second outlet flash pressure [N/sqm]						
Second outlet flash temperature change [K]						
Second outlet flash vapor fraction						
Second outlet flash temperature estimate [K]						
Second outlet flash pressure estimate [N/sqm]						
EO Model components						
Heat duty [Watt]	-1582139.94	-1620307.04	-5.38470628	-996.471679	-339.372308	-8.41475088
Total feed stream CO2e flow [kg/day]	3784.96572	172547.232	176332.198	176332.198	176332.198	150453.327
Total product stream CO2e flow [kg/day]	3784.96572	172547.232	176332.198	176332.198	176332.198	150453.327
Net stream CO2e production [kg/day]	0	0	0	0	0	0
Utility CO2e production [kg/day]	0	0	0	0	0	0
Total CO2e production [kg/day]	0	0	0	0	0	0
Utility usage						
Utility cost						
Utility ID						

Table 37 Compressors results summary - models, biorefinery No. 1

Name	C1
Property method	SRK
Henry's component list ID	
Electrolyte chemistry ID	
Use true species approach for electrolytes	YES
Free-water phase properties method	STEAM-TA
Water solubility method	3
Number of stages	2
Fix discharge pressure from last stage [atm]	30
Feed stream stage	
Product stream stage	
No. of performance maps	
Number of curves	
Outlet pressure [N/sqm]	3039750
Total work [Watt]	154900.006
Total cooling duty [Watt]	-166306.744
Net work required [Watt]	154900.006
Net cooling duty [Watt]	-166306.744
Total feed stream CO2e flow [kg/day]	176332.198
Total product stream CO2e flow [kg/day]	176332.198
Net stream CO2e production [kg/day]	0
Utility CO2e production [kg/day]	0
Total CO2e production [kg/day]	0

Table 38 Reactors Stoic results summary - models, biorefinery No. 1

Name	R101-HOM	R101-HY	R102-HY

Property method	NRTL	SRK	SRK
Henry's component list ID			
Electrolyte chemistry ID			
Use true species approach for electrolytes	YES	YES	YES
Free-water phase properties method	STEAM-TA	STEAM-TA	STEAM-TA
Water solubility method	3	3	3
Specified pressure [Pa]	101325	102300	101325
Specified temperature [C]	35	35	35
Specified vapor fraction			
Specified heat duty [Watt]			
EO Model components			
Outlet temperature [K]	308.15	308.15	308.15
Outlet pressure [N/sqm]	101325	102300	101325
Calculated heat duty [Watt]	1465.05681	44441.6812	-171237.329
Net heat duty [Watt]	1465.05681	44441.6812	-171237.329
Calculated vapor fraction	0.970430812	0.000455889	0.002589182
First liquid / total liquid	1	1	1
Total feed stream CO2e flow [kg/day]	766.701159	0	0
Total product stream CO2e flow [kg/day]	461.747453	532.89123	23153.2159
Net stream CO2e production [kg/day]	-304.953706	532.89123	23153.2159
Utility CO2e production [kg/day]	0	0	0
Total CO2e production [kg/day]	-304.953706	532.89123	23153.2159
Utility usage			
Utility cost			
Utility ID			

Table 39 Reactors RCSTR results summary - models, biorefinery No. 1

Name	R101-DF	R102-AD
Property method	IDEAL	IDEAL
Henry's component list ID		
Electrolyte chemistry ID		
Use true species approach for electrolytes	YES	YES
Free-water phase properties method	IDEAL	IDEAL
Water solubility method	3	3
Specified pressure [N/sqm]	101325	101325
Specified temperature [C]	35	35
Specified heat duty [Watt]		
Reactor volume [cum]		
Reactor residence time [day]	10	20
Phase volume [cum]		
Phase volume frac	0.8	0.8
Phase residence time [day]	10	15
EO Model components		
Outlet temperature [K]	308.15	308.15
Calculated heat duty [Watt]	1634116.21	1777362.62
Net heat duty [Watt]	1634116.21	1777362.62
Reactor volume [cum]	52990.7093	274900.832
Vapor phase volume [cum]	10598.1419	253603.107
Liquid phase volume [cum]	42392.5675	21297.7258
Liquid 1 phase volume		

Salt phase volume		
Condensed phase volume [cum]	42392.5675	21297.7258
Reactor residence time [sec]	868973.154	1738418.9
Vapor phase residence time [sec]	218038.85	1738418.9
Condensed phase residence time [sec]	3425892.21	1738418.9
Total feed stream CO2e flow [kg/day]	532.89123	23153.2159
Total product stream CO2e flow [kg/day]	4089.91942	172547.232
Net stream CO2e production [kg/day]	3557.02819	149394.016
Utility CO2e production [kg/day]	0	0
Total CO2e production [kg/day]	3557.02819	149394.016
Utility usage		
Utility cost		
Utility ID		

Table 40 Mixer results summary - models, biorefinery No. 1

Name	B10	M101
Property method	SRK	SRK
Henry's component list ID		
Electrolyte chemistry ID		
Use true species approach for electrolytes	YES	YES
Free-water phase properties method	STEAM-TA	STEAM-TA
Water solubility method	3	3
Specified pressure [N/sqm]	0	100000
Temperature estimate [C]	35	
EO Model components		
Outlet temperature [K]	308.101101	296.584514
Calculated outlet pressure [N/sqm]	101325	100000
Vapor fraction	1	3.68728E-05
First liquid /Total liquid	1	1
Total feed stream CO2e flow [kg/day]	176332.198	0
Total product stream CO2e flow [kg/day]	176332.198	0
Net stream CO2e production [kg/day]	0	0

Table 41 Model specifications results summary - models, biorefinery No. 2

Name	**B6**	**RELACCIO**
Specification	**H2O/CH4**	**RELA**
Specification target	**3**	**3**
Specification tolerance	**0.5**	**1**
Lower bound	**20**	**298.15**
Upper bound	**55**	**308.15**

Table 42 Mixer results summary - models, biorefinery No. 2

Name	B3	B10	B18	MIX
Property method	SRK	SRK	SRK	SRK
Henry's component list ID				
Electrolyte chemistry ID				

Use true species approach for electrolytes	YES	YES	YES	YES
Free-water phase properties method	STEAM-TA	STEAM-TA	STEAM-TA	STEAM-TA
Water solubility method	3	3	3	3
Specified pressure [atm]	30	0	101325	100000
Temperature estimate [K]		35	25	
EO Model components				
Outlet temperature [K]	486.891215	302.347087	289.449157	296.577108
Calculated outlet pressure [N/sqm]	3039750	101325	101325	100000
Vapor fraction	0.9107471071		1	3.72525E-05
First liquid /Total liquid	1	1	1	1
Total feed stream CO2e flow [kg/day]	147410.406	178039.514	30629.1084	0
Total product stream CO2e flow [kg/day]	147410.406	178039.514	30629.1084	0
Net stream CO2e production [kg/day]	0	0	0	0

Table 43 Reactors CSTR results summary - models, biorefinery No. 2

Name	AD	DF
Property method	IDEAL	NRTL
Henry's component list ID		
Electrolyte chemistry ID		
Use true species approach for electrolytes	YES	YES
Free-water phase properties method	IDEAL	IDEAL
Water solubility method	3	3
Specified pressure [N/sqm]	101325	101325
Specified temperature [C]	35	35
Specified heat duty [Watt]		
Reactor volume [cum]		
Reactor residence time [day]	20	10
Phase volume [cum]		
Phase volume frac	0.8	0.8
Phase residence time [day]	15	10
EO Model components		
Outlet temperature [K]	308.15	308.15
Calculated heat duty [Watt]	1777109.03	1580652.43
Net heat duty [Watt]	1777109.03	1580652.43
Reactor volume [cum]	272655.797	52260.6779
Vapor phase volume [cum]	251485.568	10452.1356
Liquid phase volume [cum]	21170.2285	41808.5423
Liquid 1 phase volume		
Salt phase volume		
Condensed phase volume [cum]	21170.2285	41808.5423
Reactor residence time [sec]	1728019.92	863999.998
Vapor phase residence time [sec]	1728019.92	217232.754
Condensed phase residence time [sec]	1728019.92	3379292.65
Total feed stream CO2e flow [kg/day]	23153.1933	532.89123
Total product stream CO2e flow [kg/day]	172181.384	4089.91809
Net stream CO2e production [kg/day]	149028.191	3557.02686
Utility CO2e production [kg/day]	0	0
Total CO2e production [kg/day]	149028.191	3557.02686
Utility usage		
Utility cost		

Utility ID	

Table 44 Reactors RGibbs results summary - models, biorefinery No. 2

Name	R103
Property method	IDEAL
Henry's component list ID	
Electrolyte chemistry ID	
Use true species approach for electrolytes	YES
Free-water phase properties method	STEAM-TA
Water solubility method	3
Specified pressure [atm]	2
Specified temperature [C]	800
Specified heat duty [Watt]	
EO Model components	
Outlet temperature [K]	1073.15
Outlet pressure [N/sqm]	202650
Calculated heat duty [Watt]	1193941.68
Net heat duty [Watt]	1193941.68
Vapor fraction	1
Number of fluid phases	1
Maximum number of pure solids	0
Total feed stream CO2e flow [kg/day]	147395.877
Total product stream CO2e flow [kg/day]	2025.62873
Net stream CO2e production [kg/day]	-145370.249
Utility CO2e production [kg/day]	0
Total CO2e production [kg/day]	-145370.249
Utility usage	
Utility cost	
Utility ID	

Table 45 Reactors RStoic results summary - models, biorefinery No. 2

Name	HOMOACET	HYD-1A	HYD-1B
Property method	NRTL	SRK	SRK
Henry's component list ID			
Electrolyte chemistry ID			
Use true species approach for electrolytes	YES	YES	YES
Free-water phase properties method	STEAM-TA	STEAM-TA	STEAM-TA
Water solubility method	3	3	3
Specified pressure [Pa]	101325	102300	101325
Specified temperature [C]	35	35	35
Specified vapor fraction			
Specified heat duty [Watt]			
EO Model components			
Outlet temperature [K]	308.15	308.15	308.15
Outlet pressure [N/sqm]	101325	102300	101325
Calculated heat duty [Watt]	6140.50839	44440.3919	-171245.282
Net heat duty [Watt]	6140.50839	44440.3919	-171245.282
Calculated vapor fraction	0.974837255	0.000455888	0.002588171
First liquid / total liquid	1	1	1

Total feed stream CO2e flow [kg/day]	257.416504	0	0
Total product stream CO2e flow [kg/day]	0	532.89123	23153.1933
Net stream CO2e production [kg/day]	-257.416504	532.89123	23153.1933
Utility CO2e production [kg/day]	0	0	0
Total CO2e production [kg/day]	-257.416504	532.89123	23153.1933
Utility usage			
Utility cost			
Utility ID			

Table 46 Compressors results summary - models, biorefinery No. 2

Name	C101
Property method	SRK
Henry's component list ID	
Electrolyte chemistry ID	
Use true species approach for electrolytes	YES
Free-water phase properties method	STEAM-TA
Water solubility method	3
Number of stages	2
Fix discharge pressure from last stage [atm]	30
Feed stream stage	
Product stream stage	
No. of performance maps	
Number of curves	
Outlet pressure [N/sqm]	3039750
Total work [Watt]	436688.588
Total cooling duty [Watt]	-456205.62
Net work required [Watt]	436688.588
Net cooling duty [Watt]	-456205.62
Total feed stream CO2e flow [kg/day]	178039.514
Total product stream CO2e flow [kg/day]	178039.514
Net stream CO2e production [kg/day]	0
Utility CO2e production [kg/day]	0
Total CO2e production [kg/day]	0

Table 47 Valves results summary - models, biorefinery No. 2

Name	B9	B12	B13	B14	B17
Property method	SRK	SRK	SRK	SRK	SRK
Henry's component list ID					
Electrolyte chemistry ID					
Use true species approach for electrolytes	YES	YES	YES	YES	YES
Free-water phase properties method	STEAM-TA	STEAM-TA	STEAM-TA	STEAM-TA	STEAM-TA
Water solubility method	3	3	3	3	3
Specified outlet pressure [Pa]	101325	101325	101325	101325	101325
Specified pressure drop [N/sqm]					
Valve operating specification: % operating					
Valve operating specification: flow coef					
Cv at 100% opening					

Valve pressure drop ratio factor					
Valve pressure recovery factor					
Valve inlet diameter [meter]					
Calculation type	ADIAB-FLASH	ADIAB-FLASH	ADIAB-FLASH	ADIAB-FLASH	ADIAB-FLASH
Valve pressure specification (design mode)	P-OUT	P-OUT	P-OUT	P-OUT	P-OUT
EO Model components					
Valve pressure specification (rating mode)	VAL-POSN	VAL-POSN	VAL-POSN	VAL-POSN	VAL-POSN
Calculated outlet pressure [N/sqm]	101325	101325	101325	101325	101325
Calculated pressure drop [N/sqm]	2938425	2938425	2938425	0	2938425
Calculated valve % operating					
Checked outlet pressure					
Cavitation index					
Pressure drop ratio factor					
Pressure recovery factor					
Piping geometry factor	1	1	1	1	1
Total feed stream CO2e flow [kg/day]	0	27421.747	1426.96621	0	1780.39514
Total product stream CO2e flow [kg/day]	0	27421.747	1426.96621	0	1780.39514
Net stream CO2e production [kg/day]	0	0	0	0	0

Table 48 Heaters results summary - models, biorefinery No. 2

Name	B5	E103	E104	E105	E106	E107	EXCH1
Property method	SRK	SRK	SRK	SRK	SRK	SRK	SRK
Henry's component list ID							
Electrolyte chemistry ID							
Use true species approach for electrolytes	YES	YES	YES	YES	YES	YES	YES
Free-water phase properties method	STEAM-TA	STEAM-TA	STEAM-TA	STEAM-TA	STEAM-TA	STEAM-TA	STEAM-TA
Water solubility method	3	3	3	3	3	3	3
Specified pressure [Pa]	101325	1	30	101325	101325	101325	101325
Specified temperature [C]	54	130	500	25	25	25	35
Specified vapor fraction							
Specified heat duty [Watt]							
EO Model components							
Calculated pressure [N/sqm]	101325	100000	3000000	101325	101325	101325	101325
Calculated temperature [K]	327.15	403.15	773.15	298.15	298.15	298.15	308.15
Calculated vapor fraction	1	1	1	0.705295796	1	1	3.49909E-05
Calculated heat duty [Watt]	22060.9239	638804.824	263559.544	-996356.512	-605.074835	-5868.087	669841.873
Temperature change [K]							
Degrees of superheating [K]							
Degrees of subcooling [K]							
Pressure-drop correlation parameter							2
Net duty [Watt]	22060.9239	638804.824	263559.544	-996356.512	-605.074835	-5868.087	669841.873
First liquid / total liquid				1			1
Total feed stream CO2e flow [kg/day]	178039.514	0	147410.406	2025.62873	0	0	0
Total product stream CO2e flow [kg/day]	178039.514	0	147395.877	2025.62873	0	0	0
Net stream CO2e production [kg/day]	0	0	-14.5286379	0	0	0	0
Utility CO2e production [kg/day]	0	0	0	0	0	0	0
Total CO2e production [kg/day]	0	0	-14.5286379	0	0	0	0
Utility usage							

Utility cost	
Utility ID	

Table 49 Separators results summary - models, biorefinery No. 2

Name	S1A	S1B	S101	S102	S103	S104	S105	S106
Property method	SRK	SRK	SRK	SRK	SRK	SRK	SRK	SRK
Henry's component list ID								
Electrolyte chemistry ID								
Use true species approach for electrolytes	YES	YES	YES	YES	YES	YES	YES	YES
Free-water phase properties method	STEAM-TA	IDEAL	STEAM-TA	STEAM-TA	STEAM-TA	STEAM-TA	STEAM-TA	STEAM-TA
Water solubility method	3	3	3	3	3	3	3	3
Inlet flash pressure [N/sqm]	0	0	101325	30	30	30	30	101325
First outlet flash temperature [C]	35	35		38		35	35	
First outlet flash pressure [N/sqm]				30			30	
First outlet flash temperature change [K]								
First outlet flash vapor fraction								
First outlet flash temperature estimate [K]								
First outlet flash pressure estimate [N/sqm]						30		
Second outlet flash temperature [C]	35	35						
Second outlet flash pressure [N/sqm]								
Second outlet flash temperature change [K]								
Second outlet flash vapor fraction								
Second outlet flash temperature estimate [K]								
Second outlet flash pressure estimate [N/sqm]								
EO Model components								
Heat duty [Watt]	-1528886.45	-1620278.91	-13.27022871	-650.2210477	-1.594539319	-15835381.51	-6668721124.22	-34
Total feed stream CO2e flow [kg/day]	3832.501581	72181.38417	8039.514178	039.514178039	.514176259	.119148837	.372202	5.62873
Total product stream CO2e flow [kg/day]	3832.501581	72181.38417	8039.514178	039.514178039	.514176259	.119148837	.372202	5.62873
Net stream CO2e production [kg/day]	0	0	0	0	0	0	0	0
Utility CO2e production [kg/day]	0	0	0	0	0	0	0	0
Total CO2e production [kg/day]	0	0	0	0	0	0	0	0
Utility usage								
Utility cost								
Utility ID								

Table 50 Heaters results summary - models, biorefinery No. 3

Name	E101	E102	E103	E104	E105	E106	E107	E108
Property method	SRK	SRK	SRK	SRK	SRK	SRK	SRK	SRK
Henry's component list ID								
Electrolyte chemistry ID								
Use true species approach for	YES	YES	YES	YES	YES	YES	YES	YES

electrolytes								
Free-water phase properties method	STEAM-TA	STEAM-TA	STEAM-TA	STEAM-TA	STEAM-TA	STEAM-TA	STEAM-TA	STEAM-TA
Water solubility method	3	3	3	3	3	3	3	3
Specified pressure [Pa]	101325	101325	100000	3000000	101325	101325	5066250	101325
Specified temperature [C]	35	54	130	850	25	25	250	25
Specified vapor fraction								
Specified heat duty [Watt]								
EO Model components								
Calculated pressure [N/sqm]	101325	101325	100000	3000000	101325	101325	5066250	101325
Calculated temperature [K]	308.15	327.15	403.15	1123.15	298.15	298.15	523.15	298.15
Calculated vapor fraction	3.49883E-05	1	1	1	0.738106511	1	1	0.996628193
Calculated heat duty [Watt]	669840.547	211059.144	638691.151	574501.501	-1002555.41	-613.687391	443287.142	-388060.167
Temperature change [K]								
Degrees of superheating [K]								
Degrees of subcooling [K]								
Pressure-drop correlation parameter	2							
Net duty [Watt]	669840.547	211059.144	638691.151	574501.501	-1002555.41	-613.687391	443287.142	-388060.167
First liquid / total liquid	1				1			1
Total feed stream CO2e flow [kg/day]	0	492554.528	0	163062.452	1967.928	0	35769.4928	29858.7094
Total product stream CO2e flow [kg/day]	0	492554.528	0	163062.452	1967.928	0	35769.4928	29858.7094
Net stream CO2e production [kg/day]	0	0	0	0	0	0	0	0
Utility CO2e production [kg/day]	0	0	0	0	0	0	0	0
Total CO2e production [kg/day]	0	0	0	0	0	0	0	0
Utility usage								
Utility cost								
Utility ID								

Table 51 Separators results summary - models, biorefinery No. 3

Name	S1A	S1B	S101	S102	S103	S104	S105	S106	S107	S108
Property method	SRK	SRK	SRK	SRK	SRK	SRK	SRK	IDEAL	SRK	SRK
Henry's component list ID										
Electrolyte chemistry ID										
Use true species approach for electrolytes	YES	YES	YES	YES	YES	YES	YES	YES	YES	YES
Free-water phase properties method	STEAM-TA	IDEAL	STEAM-TA	STEAM-TA	STEAM-TA	STEAM-TA	STEAM-TA	STEAM-TA	STEAM-TA	STEAM-TA
Water solubility method	3	3	3	3	3	3	3	3	3	3
Inlet flash pressure [N/sqm]	0	0	101325	30	30	30	30	101325	0	0
First outlet flash temperature [C]	35	35		38		35	35			
First outlet flash pressure [N/sqm]				30			30			
First outlet flash temperature change [K]										
First outlet flash vapor fraction										

First outlet flash temperature estimate [K]										
First outlet flash pressure estimate [N/sqm]						30				
Second outlet flash temperature [C]	35	35								
Second outlet flash pressure [N/sqm]										
Second outlet flash temperature change [K]										
Second outlet flash vapor fraction										
Second outlet flash temperature estimate [K]										
Second outlet flash pressure estimate [N/sqm]										
EO Model components										
Heat duty [Watt]	-1528826.57	-1514366.61	5.354584	24068.90	18274.47	466.1975	798.8096	14647.04	59481.89	817.0867
Total feed stream CO2e flow [kg/day]	3832.501 58	172151.081	492554.528	492554.528	492554.528	487628.983	193906.399	1967.928	29858.7094	0
Total product stream CO2e flow [kg/day]	3832.501 58	172151.081	492554.528	492554.528	492554.528	487628.983	193906.399	1967.928	29858.7094	0
Net stream CO2e production [kg/day]	0	0	0	0	0	0	0	0	0	0
Utility CO2e production [kg/day]	0	0	0	0	0	0	0	0	0	0
Total CO2e production [kg/day]	0	0	0	0	0	0	0	0	0	0
Utility usage										
Utility cost										
Utility ID										

Table 52 Compressors A results summary - models, biorefinery No. 3

Name	C102
Property method	SRK
Henry's component list ID	
Electrolyte chemistry ID	
Use true species approach for electrolytes	YES
Free-water phase properties method	STEAM-TA
Water solubility method	3
Model Type	ISENTROPIC
Specified discharge pressure [atm]	60
Specified pressure increase [N/sqm]	
Specified pressure ratio	
Specified power required [Watt]	
Isentropic efficiency	
Mechanical efficiency	
Polytropic efficiency	
EO Model components	
Indicated horsepower [Watt]	73063.9491
Calculated brake horsepower [Watt]	73063.9491

Net work required [Watt]	73063.9491
Power loss [Watt]	0
Efficiency (polytropic / isentropic) used	0.72
Calculated discharge pressure [N/sqm]	6079500
Calculated pressure change [N/sqm]	1013250
Calculated pressure ratio	1.2
Outlet temperature [K]	558.64595
Isentropic outlet temperature [K]	548.681528
Vapor fraction	1
Displacement	
Volumetric efficiency	
Head developed [J/kg]	54740.7074
Isentropic power requirement [Watt]	52606.0433
Inlet heat capacity ratio	1.36216895
Inlet volumetric flow rate [l/day]	4797252.16
Outlet volumetric flow rate [l/day]	4282847.33
Inlet compressibility factor	1.01926935
Outlet compressibility factor	1.0225744
Compressor percent above surge	
Percent below stonewall	
Surge volume flow rate	
Stonewall volume flow rate	
Shaft speed	
Specific speed	
Inlet Mach number	
Total feed stream CO2e flow [kg/day]	35769.4928
Total product stream CO2e flow [kg/day]	35769.4928
Net stream CO2e production [kg/day]	0
Utility CO2e production [kg/day]	0
Total CO2e production [kg/day]	0
Utility usage	
Utility cost	
Utility ID	

Table 53 Compressors B results summary - models, biorefinery No. 3

Name	C101
Property method	SRK
Henry's component list ID	
Electrolyte chemistry ID	
Use true species approach for electrolytes	YES
Free-water phase properties method	STEAM-TA
Water solubility method	3
Number of stages	2
Fix discharge pressure from last stage [atm]	30
Feed stream stage	
Product stream stage	
No. of performance maps	
Number of curves	

Outlet pressure [N/sqm]	3039750
Total work [Watt]	2243871.42
Total cooling duty [Watt]	-2409958.66
Net work required [Watt]	2243871.42
Net cooling duty [Watt]	-2409958.66
Total feed stream CO2e flow [kg/day]	492554.528
Total product stream CO2e flow [kg/day]	492554.528
Net stream CO2e production [kg/day]	0
Utility CO2e production [kg/day]	0
Total CO2e production [kg/day]	0

Table 54 Valves results summary - models, biorefinery No. 3

Name	B9	B12	B14
Property method	SRK	SRK	SRK
Henry's component list ID			
Electrolyte chemistry ID			
Use true species approach for electrolytes	YES	YES	YES
Free-water phase properties method	STEAM-TA	STEAM-TA	STEAM-TA
Water solubility method	3	3	3
Specified outlet pressure [atm]	1	101325	101325
Specified pressure drop [N/sqm]			
Valve operating specification: % operating			
Valve operating specification: flow coef			
Cv at 100% opening			
Valve pressure drop ratio factor			
Valve pressure recovery factor			
Valve inlet diameter [meter]			
Calculation type	ADIAB-FLASH	ADIAB-FLASH	ADIAB-FLASH
Valve pressure specification (design mode)	P-OUT	P-OUT	P-OUT
EO Model components			
Valve pressure specification (rating mode)	VAL-POSN	VAL-POSN	VAL-POSN
Calculated outlet pressure [N/sqm]	101325	101325	101325
Calculated pressure drop [N/sqm]	4964925	2938425	0
Calculated valve % operating			
Checked outlet pressure			
Cavitation index			
Pressure drop ratio factor			
Pressure recovery factor			
Piping geometry factor	1	1	1
Total feed stream CO2e flow [kg/day]	29858.7094	293722.583	0
Total product stream CO2e flow [kg/day]	29858.7094	293722.583	0
Net stream CO2e production [kg/day]	0	0	0

Table 55 Reactors RStoic results summary - models, biorefinery No. 3

Name	R101-HOM	R101-HY	R102-HY
Property method	NRTL	SRK	SRK

Henry's component list ID			
Electrolyte chemistry ID			
Use true species approach for electrolytes	YES	YES	YES
Free-water phase properties method	STEAM-TA	STEAM-TA	STEAM-TA
Water solubility method	3	3	3
Specified pressure [Pa]	101325	102300	101325
Specified temperature [C]	35	35	35
Specified vapor fraction			
Specified heat duty [Watt]			
EO Model components			
Outlet temperature [K]	308.15	308.15	308.15
Outlet pressure [N/sqm]	101325	102300	101325
Calculated heat duty [Watt]	6081.53775	44441.6812	-171246.403
Net heat duty [Watt]	6081.53775	44441.6812	-171246.403
Calculated vapor fraction	0.974030688	0.000455889	0.002588119
First liquid / total liquid	1	1	1
Total feed stream CO2e flow [kg/day]	257.416504	0	0
Total product stream CO2e flow [kg/day]	0	532.89123	23153.1933
Net stream CO2e production [kg/day]	-257.416504	532.89123	23153.1933
Utility CO2e production [kg/day]	0	0	0
Total CO2e production [kg/day]	-257.416504	532.89123	23153.1933
Utility usage			
Utility cost			
Utility ID			

Table 56 Reactors REquil results summary - models, biorefinery No. 3

Name	R104
Property method	SRK
Henry's component list ID	
Electrolyte chemistry ID	
Use true species approach for electrolytes	YES
Free-water phase properties method	STEAM-TA
Water solubility method	3
Specified pressure [atm]	50
Specified temperature [C]	220
Specified vapor fraction	
Specified heat duty [Watt]	
Products generation: molar extent [kmol/hr]	
Temperature approach [C]	220
EO Model components	
Outlet temperature [K]	493.15
Outlet pressure [N/sqm]	5066250
Calculated heat duty [Watt]	-79885.2597
Net heat duty [Watt]	-79885.2597
Calculated vapor fraction	1
Total feed stream CO2e flow [kg/day]	35769.4928
Total product stream CO2e flow [kg/day]	29858.7094
Net stream CO2e production [kg/day]	-5910.78344

Utility CO2e production [kg/day]	0
Total CO2e production [kg/day]	-5910.78344
Utility usage	
Utility cost	
Utility ID	

Table 57 Reactors RGibbs results summary - models, biorefinery No. 3

Name	R103
Property method	IDEAL
Henry's component list ID	
Electrolyte chemistry ID	
Use true species approach for electrolytes	YES
Free-water phase properties method	STEAM-TA
Water solubility method	3
Specified pressure [bar]	30
Specified temperature [C]	800
Specified heat duty [Watt]	
EO Model components	
Outlet temperature [K]	1073.15
Outlet pressure [N/sqm]	3000000
Calculated heat duty [Watt]	1005659.61
Net heat duty [Watt]	1005659.61
Vapor fraction	1
Number of fluid phases	1
Maximum number of pure solids	0
Total feed stream CO2e flow [kg/day]	163062.452
Total product stream CO2e flow [kg/day]	1967.928
Net stream CO2e production [kg/day]	-161094.524
Utility CO2e production [kg/day]	0
Total CO2e production [kg/day]	-161094.524
Utility usage	
Utility cost	
Utility ID	

Table 58 Reactors CSTR results summary - models, biorefinery No. 3

Name	R101-DF	R102-AD
Property method	NRTL	NRTL
Henry's component list ID		
Electrolyte chemistry ID		
Use true species approach for electrolytes	YES	YES
Free-water phase properties method	IDEAL	IDEAL
Water solubility method	3	3
Specified pressure [N/sqm]	101325	101325
Specified temperature [C]	35	35
Specified heat duty [Watt]		
Reactor volume [cum]		

Reactor residence time [day]	10	20
Phase volume [cum]		
Phase volume frac	0.8	0.8
Phase residence time [day]	10	15
EO Model components		
Outlet temperature [K]	308.15	308.15
Calculated heat duty [Watt]	1580652.46	1671172.04
Net heat duty [Watt]	1580652.46	1671172.04
Reactor volume [cum]	52260.6519	232484.54
Vapor phase volume [cum]	10452.1304	211940.977
Liquid phase volume [cum]	41808.5216	20543.5629
Liquid 1 phase volume		
Salt phase volume		
Condensed phase volume [cum]	41808.5216	20543.5629
Reactor residence time [sec]	863999.569	1673428.04
Vapor phase residence time [sec]	217232.646	1673428.04
Condensed phase residence time [sec]	3379290.97	1673428.04
Total feed stream CO2e flow [kg/day]	532.89123	23153.1933
Total product stream CO2e flow [kg/day]	4089.91809	172151.081
Net stream CO2e production [kg/day]	3557.02686	148997.888
Utility CO2e production [kg/day]	0	0
Total CO2e production [kg/day]	3557.02686	148997.888
Utility usage		
Utility cost		
Utility ID		

Table 59 Mixer results summary - models, biorefinery No. 3

Name	B10	M102	M103	MIX
Property method	SRK	SRK	SRK	SRK
Henry's component list ID				
Electrolyte chemistry ID				
Use true species approach for electrolytes	YES	YES	YES	YES
Free-water phase properties method	STEAM-TA	STEAM-TA	STEAM-TA	STEAM-TA
Water solubility method	3	3	3	3
Specified pressure [N/sqm]	0	30	30	100000
Temperature estimate [C]	35			
EO Model components				
Outlet temperature [K]	284.540447	485.212373	304.277152	296.584514
Calculated outlet pressure [N/sqm]	101325	3039750	3039750	100000
Vapor fraction	1	0.909341075	0.997444588	3.68728E-05
First liquid /Total liquid	1	1	1	1
Total feed stream CO2e flow [kg/day]	492575.191	163062.452	35769.4928	0
Total product stream CO2e flow [kg/day]	492554.528	163062.452	35769.4928	0
Net stream CO2e production [kg/day]	-20.6628228	0	0	0

Table 60 FSplit results summary - models, biorefinery No. 3

Name	M104	M105
Property method	SRK	SRK
Henry's component list ID		
Electrolyte chemistry ID		
Use true species approach for electrolytes	YES	YES
Free-water phase properties method	STEAM-TA	STEAM-TA
Water solubility method	3	3
First outlet stream	0.3	
First specified split fraction	0.3	
First calculated split fraction	0.3	0.881422973
First actual volume flow [l/day]		
First limit flow [kg/day]		
First volume limit flow [l/day]		
First cum limit flow [kg/day]		
First cum volume limit flow [l/day]		
First residual fraction		
Second outlet stream		0.2
Second specified split fraction		0.2
EO Model components		
Second calculated split fraction	0.7	0.118577027
Second actual volume flow [l/day]		
Second limit flow [kg/day]		
Second volume limit flow [l/day]		
Second cum limit flow [kg/day]		
Second cum volume limit flow [l/day]		
Second residual fraction		
Total feed stream CO2e flow [kg/day]	29858.7094	0
Total product stream CO2e flow [kg/day]	29858.7094	0
Net stream CO2e production [kg/day]	0	0

Table 61 Model specifications results summary - models, biorefinery No. 3

Name	B2	B6	RELACCIO
Specification	H2O/CH4	H2/CO2	RELA
Specification target	3	4	3
Specification tolerance	0.5	1	1
Lower bound	18	0.1	298.15
Upper bound	55	0.9	308.15

IV. BIOREFINERY LCA RESULTS

Table 62 LCA SimaPro results . Biorefinery scheme No. 1

category impact	Unit	STREAMS										
		ADOUTLIQ	L2	DF OUTGAS	AD OUTGAS	8	10	11	13	12	14	16
Global warming	kg CO2 eq	5.62E+03	9.90E+04	2.03E+06	1.32E+04	2.06E+06	2.06E+06	2.06E+06	1.82E+06	2.48E+05	1.84E+06	1.84E+06
Stratospheric ozone depletion	kg CFC11 eq	0.00119	0.0239	0.489	0.00278	0.496	0.496	0.496	0.437	0.0596	0.437	0.437
Ionizing radiation	kBq Co-60 eq	57.7	9.10E+03	1.85E+05	1.35E+02	1.87E+05	1.87E+05	1.87E+05	1.64E+05	2.24E+04	1.64E+05	1.64E+05
Ozone formation, Human health	kg NOx eq	7.22	118	2.43E+03	1.69E+01	2.46E+03	2.46E+03	2.46E+03	2.17E+03	296	2.17E+03	2.17E+03
Fine particulate matter formation	kg PM2.5 eq	5.57	345	7.03E+03	1.30E+01	7.11E+03	7.36E+04	7.36E+04	6.42E+03	8.76E+02	6.43E+03	6.43E+03
Ozone formation, Terrestrial ecosystems	kg NOx eq	7.4	121	2.49E+03	1.73E+01	2.53E+03	2.52E+03	2.53E+03	2.22E+03	303	2.22E+03	2.22E+03
Terrestrial acidification	kg SO2 eq	14.2	258	5.30E+03	3.32E+01	5.38E+03	5.49E+05	5.49E+05	6.08E+03	8.30E+02	6.11E+03	6.11E+03
Freshwater eutrophication	kg P eq	0.757	90.4	1.84E+03	1.77E+00	1.85E+03	1.85E+03	1.86E+03	1.63E+03	223	1.63E+03	1.63E+03
Marine eutrophication	kg N eq	0.0511	5.7	1.16E+02	0.12	117	117	117	103	14	103	103
Terrestrial ecotoxicity	kg 1,4-DCB	2.00E+04	1.33E+05	2.79E+06	4.69E+04	2.86E+06	2.85E+06	2.86E+06	2.51E+06	3.43E+05	2.52E+06	2.52E+06
Freshwater ecotoxicity	kg 1,4-DCB	53.1	8.27E+03	1.68E+05	1.24E+02	1.70E+05	1.69E+05	1.70E+05	1.49E+05	2.04E+04	1.49E+05	1.49E+05
Marine ecotoxicity	kg 1,4-DCB	79.7	1.05E+04	2.13E+05	1.86E+02	2.15E+05	2.15E+05	2.15E+05	1.89E+05	2.58E+04	1.89E+05	1.89E+05
Human carcinogenic toxicity	kg 1,4-DCB	57.7	4.68E+03	9.52E+04	1.35E+02	9.62E+04	9.62E+04	9.63E+04	8.47E+04	1.16E+04	8.47E+04	8.47E+04
Human non-carcinogenic toxicity	kg 1,4-DCB	1.98E+03	1.42E+05	2.89E+06	4.63E+03	2.92E+06	2.92E+06	2.92E+06	2.57E+06	3.51E+05	2.57E+06	2.57E+06
Land use	m2a crop eq	36.4	1.54E+03	3.13E+04	8.51E+01	3.17E+04	3.17E+04	3.17E+04	2.79E+04	3.81E+03	2.79E+04	2.79E+04
Mineral resource scarcity	kg Cu eq	2.63E+00	89.1	1.82E+03	6.15E+00	1.84E+03	1.84E+03	1.84E+03	1.62E+03	221	1.62E+03	1.62E+03
Fossil resource scarcity	kg oil eq	1.62E+03	3.00E+04	6.15E+05	3.79E+03	6.25E+05	6.24E+05	6.25E+05	5.50E+05	7.50E+04	5.50E+05	5.50E+05
Water consumption	m3	222	326	6.63E+03	5.20E+02	7.21E+03	7.16E+03	7.17E+03	6.35E+03	866	6.35E+03	6.35E+03

Table 63 LCA SimaPro results . Biorefinery scheme No. 2

Category Impact	Unit	STREAMS											
		AD LIQ	OUTL2	DF OUTGAS	AD OUTGAS	8	10	11	13	H2	H2	14	19
Global warming	kg CO2 eq	5.62E+03	9.90E+04	2.05E+06	1.31E+04	1.44E+08	1.90E+08	1.90E+08	9.52E+07	9.52E+07	1.90E+08	1.68E+08	1.68E+08
Stratospheric ozone depletion	kg CFC11 eq	0.00119	0.0239	4.94E-01	2.77E-03	5.39E+03	7.11E+03	7.11E+03	3.57E+03	3.57E+03	7.15E+03	6.29E+03	6.29E+03
Ionizing radiation	kBq Co-60 eq	57.7	9.10E+03	1.87E+05	1.35E+02	1.44E+06	1.80E+06	1.80E+06	9.03E+05	9.03E+05	1.81E+06	1.59E+06	1.59E+06
Ozone formation, Human health	kg NOx eq	7.22	118	2.45E+03	1.68E+01	1.53E+05	2.00E+05	2.00E+05	1.01E+05	1.01E+05	2.01E+05	1.77E+05	1.77E+05
Fine particulate matter formation	kg PM2.5 eq	5.57	345	7.09E+03	1.30E+01	7.68E+04	9.77E+04	9.77E+04	4.91E+04	4.91E+04	9.82E+04	8.64E+04	8.64E+04
Ozone formation, Terrestrial ecosystems	kg NOx eq	7.4	121	2.51E+03	1.73E+01	1.70E+05	2.23E+05	2.23E+05	1.12E+05	1.12E+05	2.24E+05	1.97E+05	1.97E+05
Terrestrial acidification	kg SO2 eq	14.2	258	5.35E+03	3.31E+01	1.83E+05	2.40E+05	2.40E+05	1.20E+05	1.20E+05	2.41E+05	2.12E+05	2.12E+05
Freshwater eutrophication	kg P eq	0.757	90.4	1.85E+03	1.77E+00	3.31E+03	3.38E+03	3.38E+03	1.70E+03	1.70E+03	3.41E+03	2.98E+03	2.98E+03
Marine eutrophication	kg N eq	0.0511	5.7	1.17E+02	1.19E-01	1.05E+03	1.32E+03	1.32E+03	6.65E+02	6.65E+02	1.33E+03	1.17E+03	1.17E+03
Terrestrial ecotoxicity	kg 1,4-DCB	2.00E+04	1.33E+05	2.81E+06	4.67E+04	1.60E+08	2.10E+08	2.10E+08	1.05E+08	1.05E+08	2.11E+08	1.86E+08	1.86E+08
Freshwater ecotoxicity	kg 1,4-DCB	53.1	8.27E+03	1.69E+05	1.24E+02	2.61E+06	3.35E+06	3.35E+06	1.68E+06	1.68E+06	3.37E+06	2.96E+06	2.96E+06
Marine ecotoxicity	kg 1,4-DCB	79.7	1.05E+04	2.15E+05	1.86E+02	3.34E+06	4.30E+06	4.30E+06	2.16E+06	2.16E+06	4.32E+06	3.80E+06	3.80E+06
Human carcinogenic toxicity	kg 1,4-DCB	57.7	4.68E+03	9.61E+04	1.35E+02	1.50E+06	1.93E+06	1.93E+06	9.68E+05	9.68E+05	1.94E+06	1.70E+06	1.70E+06
Human non-carcinogenic toxicity	kg 1,4-DCB	1.98E+03	1.42E+05	2.92E+06	4.61E+03	3.82E+07	4.88E+07	4.88E+07	2.45E+07	2.45E+07	4.91E+07	4.31E+07	4.31E+07
Land use	m2a crop eq	36.4	1.54E+03	3.16E+04	8.48E+01	-3.77E+06	-4.99E+06	-4.99E+06	-2.51E+06	-2.51E+06	-5.01E+06	-4.41E+06	-4.41E+06
Mineral resource scarcity	kg Cu eq	2.63	89.1	1.83E+03	6.13E+00	1.76E+05	2.31E+05	2.31E+05	1.16E+05	1.16E+05	2.32E+05	2.04E+05	2.04E+05
Fossil resource scarcity	kg oil eq	1.62E+03	3.00E+04	6.21E+05	3.78E+03	2.21E+07	2.88E+07	2.88E+07	1.45E+07	1.45E+07	2.89E+07	2.54E+07	2.54E+07
Water consumption	m3	222	326	6.69E+03	5.19E+02	6.21E+05	8.15E+05	8.15E+05	4.10E+05	4.10E+05	8.19E+05	7.21E+05	7.21E+05

Table 64 LCA SimaPro results . Biorefinery scheme No. 3

category impact	Unit	STREAMS									
		AD OUT LIQ	DF OUTGAS	AD OUTGAS	8	H2	12	13	27	12A	METHANOL
Global warming	kg CO2 eq	5.62E+03	2.05E+06	1.31E+04	1.68E+08	1.36E+07	1.14E+08	1.01E+08	1.09E+08	9.99E+07	1.10E+08
Stratospheric ozone depletion	kg CFC11 eq	0.00119	4.94E-01	2.77E-03	6.30E+03	512	4.26E+03	3.78E+03	4.09E+03	3.75E+03	4.14E+03
Ionizing radiation	kBq Co-60 eq	57.7	1.87E+05	1.35E+02	1.65E+06	1.29E+05	1.07E+06	9.50E+05	1.03E+06	9.44E+05	1.04E+06
Ozone formation, Human health	kg NOx eq	7.22	2.45E+03	1.68E+01	1.78E+05	1.44E+04	1.20E+05	1.06E+05	1.15E+05	1.06E+05	1.17E+05
Fine particulate matter formation	kg PM2.5 eq	5.57	7.09E+03	1.30E+01	8.88E+04	7.01E+03	5.84E+04	5.17E+04	5.61E+04	5.14E+04	5.66E+04
Ozone formation, Terrestrial ecosystems	kg NOx eq	7.4	2.51E+03	1.73E+01	1.98E+05	1.60E+04	1.33E+05	1.18E+05	1.28E+05	1.17E+05	1.30E+05
Terrestrial acidification	kg SO2 eq	14.2	5.35E+03	3.31E+01	2.13E+05	1.72E+04	1.43E+05	1.27E+05	1.38E+05	1.26E+05	1.39E+05
Freshwater eutrophication	kg P eq	0.757	1.85E+03	1.77E+00	3.63E+03	239	1.99E+03	1.75E+03	1.91E+03	1.75E+03	1.91E+03
Marine eutrophication	kg N eq	0.0511	1.17E+02	1.19E-01	1.21E+03	94.9	7.91E+02	700	759	6.96E+02	7.66E+02
Terrestrial ecotoxicity	kg 1,4-DCB	2.00E+04	2.81E+06	4.67E+04	1.87E+08	1.51E+07	1.26E+08	1.11E+08	1.21E+08	1.11E+08	1.22E+08
Freshwater ecotoxicity	kg 1,4-DCB	53.1	1.69E+05	1.24E+02	3.02E+06	2.40E+05	2.00E+06	1.78E+06	1.92E+06	1.76E+06	1.94E+06
Marine ecotoxicity	kg 1,4-DCB	79.7	2.15E+05	1.86E+02	3.88E+06	3.09E+05	2.57E+06	2.28E+06	2.47E+06	2.26E+06	2.49E+06
Human carcinogenic toxicity	kg 1,4-DCB	57.7	9.61E+04	1.35E+02	1.74E+06	1.38E+05	1.15E+06	1.02E+06	1.11E+06	1.01E+06	1.12E+06
Human non-carcinogenic toxicity	kg 1,4-DCB	1.98E+03	2.92E+06	4.61E+03	4.42E+07	3.50E+06	2.92E+07	2.59E+07	2.80E+07	2.57E+07	2.83E+07
Land use	m2a crop eq	36.4	3.16E+04	8.48E+01	-4.40E+06	-3.59E+05	-2.99E+06	-2.65E+06	-2.87E+06	-2.63E+06	-2.90E+06
Mineral resource scarcity	kg Cu eq	2.63	1.83E+03	6.13E+00	2.05E+05	1.66E+04	1.38E+05	1.23E+05	1.33E+05	1.22E+05	1.34E+05
Fossil resource scarcity	kg oil eq	1.62E+03	6.21E+05	3.78E+03	2.57E+07	2.07E+06	1.72E+07	1.53E+07	1.65E+07	1.52E+07	1.67E+07
Water consumption	m3	222	6.69E+03	5.19E+02	7.24E+05	5.86E+04	4.88E+05	4.33E+05	4.69E+05	4.30E+05	4.74E+05

V. SCIENTIST PRODUCTION

CONFERENCES

Rendimiento total de recuperación de energía en función de la carga orgánica de entrada para la simulación de bioprocesos de digestión anaeróbica y fermentación oscura, IV Foro Internacional en Nuevos Materiales y Energías Alternativas – GINMEA "Apuestas por una Recuperación Verde". Evento organizado por el grupo de Investigación GINMEA. 2021, Bucaramanga, Colombia.

ORAL PRESENTATION

ICheaP15 – The 15th International Conference on CHEMICAL and PROCESS ENGINEERING Technical and Environmental Analysis of Large-Scale Pig Manure Digestion Through Process Simulation and Life Cycle Assessment. Italy, 2021.

28ème congrès de l'école doctorale Sciences de l'Environnement d'Aix Marseille Université - Total energy recovery yield as a function of inlet organic load for anaerobic digestion and dark fermentation bioprocesses. France, 2021.

14° CONGRESO INTERAMERICANO DE COMPUTACIÓN APLICADA A LA INDUSTRIA DE PROCESOS Technical and environmental assessment of large-scale pig manure digestion through process simulation and life cycle assessment (LCA). ISBN: 978-612-48025-3-9 Peru, 2019.

POSTER

2nd Biorestec Conference Bioenergy and metabolites from residual biomass through anaerobic digestion and dark fermentation processes in biorefinery schemes. Spain, 2018.

PUBLICATIONS

Amado, M., Barca, C., Hernández, M. A., & Ferrasse, J.-H. (2021). Evaluation of energy recovery potential by anaerobic digestion and dark fermentation of residual biomass in Colombia. Frontiers in Energy Research, 9. https://doi.org/10.3389/fenrg.2021.690161

Amado, M., Carrasco, J., Ochoa, L. D., Rangel, C. J., Becerra, A. P., Cabeza, I. O., & Acevedo, P. A. (2021). Technical and Environmental Analysis of Large-scale Pig Manure Digestion Through Process Simulation and Life Cycle Assessment. Chemical Engineering Transactions, 87, 439–444. https://doi.org/10.3303/CET2187074